205 pages

12825

dsL 9492249

(NASA-CR-172127) ANALYSIS OF DIRECT AND
NEARBY LIGHTNING STRIKE DATA FOR AIRCRAFT
Final Report (LuTech, Inc.) 205 p
HC A10/MF A01   CSCL 04B

N86-27855

Unclas
G3/47 43301

Analysis of Direct and Nearby Lightning Strike Data for Aircraft

D.V.Giri,R.S.Noss
D.B.Phuoc and F.M.Tesche

LuTech, Inc.
3516 Breakwater Court
Hayward, CA   94545

NASA

National Aeronautics and
Space Administration

Langley Research Center
Hampton, Virginia 23665

Review for general release (3 yrs. from report date)

TABLE OF CONTENTS

LIST OF TABLES

LIST OF FIGURES

SECTION I

INTRODUCTION

The effects of lightning on aircraft have been of interest for many years, not only from the aspect of personnel safety, but also from that of system reliability. Because newer aircraft often use poorly conducting advanced composite materials, the natural electrical protection usually provided by the skin of the aircraft is not present. Furthermore, with the increasing use of microelectronic circuitry in airborne systems, the damage or susceptibility levels of the components are being drastically reduced, resulting in a higher probability of system failure in the event of a lightning strike. As illustrated in Figure 1, such a lightning strike may be nearby the aircraft, in which case the radiated electromagnetic fields induce currents on the conducting portions of the aircraft, or it may be a direct strike in which the bolt current is injected directly onto the aircraft.

As a result of this change in aircraft design, it is desirable to understand the effects of lightning on aircraft as accurately as possible, so as to take countermeasures against damage or upset. To this end NASA has initiated a test program for the acquisition of direct and nearby strike lightning data for an aircraft. The hope of this effort is that the acquired data will provide a better understanding of the fundamental nature of lightning itself, as well as an indication of how lightning interacts with the aircraft.

This report documents the efforts of investigators at LuTech, Inc. in analyzing the lightning data acquired by NASA in the test programs described in references [1] and [2], and in the area of modeling lightning/aircraft interactions. Other research groups have also been involved in similar analysis and measurement programs. Reference [3] describes a finite difference approach for modeling lightning interaction with an aircraft, and proposes several interpretations of the measured 1980 and 1981 data. Extensive calculations are performed in this report for the case of a nearby lightning strike exciting the F-106 aircraft.

In addition, an experimental scale model study has been undertaken in an attempt to simulate the aircraft response undergoing a direct

Direct
Strike

Aircraft Current
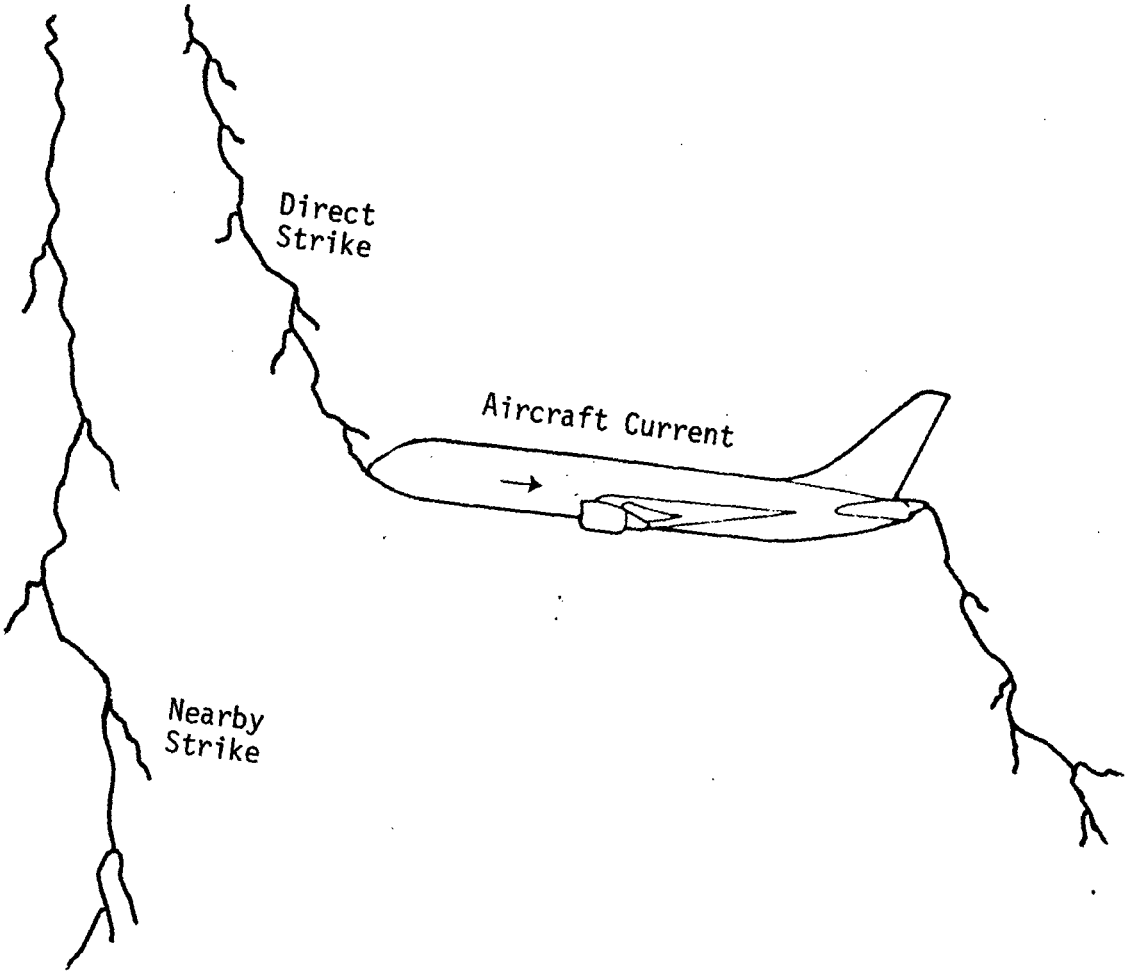
Nearby
Strike

Figure 1. Aircraft Current Induced by Direct or
Nearby Lightning Strikes.

lightning strike (Reference [4]). The data obtained from these measurements are useful in determining the natural resonant frequencies of the F-106 test aircraft, and in understanding how they change with an attachment of the lightning channel.

In Section II of this report, the theoretical basis for interpreting aircraft-measured lightning data is discussed. These concepts involve the use of relatively simple transmission line models of the aircraft and lightning channel. Section III discusses the determination of the resonances of an isolated aircraft, and then applies this to the specific F-106 aircraft used by NASA. In Section IV, the methods used for extracting the aircraft resonances from the measured data are presented, and a direct strike and a nearby strike data record are processed to illustrate the data processing techniques on real data. Section V then discusses various experimental aspects of lightning measurements. In Section VI a summary of this work is given and conclusions made, and finally in the Appendix, the 1981 lightning data are presented, along with their spectral (FFT) and pole, residue (Prony) representations.

SECTION II

THEORETICAL CONSIDERATIONS FOR DIRECT STRIKE
LIGHTNING DATA ANALYSIS AND INTERPRETATION

A. Overview

One of the difficulties in attempting to interpret measured
lightning data from an aircraft by using a finite difference
calculational model [3] is it is relatively time-consuming and costly,
when compared with alternate approaches. Although a reasonable degree of
accuracy may be obtained by using finite difference computational
techniques for modeling EMP and LEMP excitation, it requires a large
computer facility to perform the calculation. Furthermore, the addition
of the lightning channel in a finite difference code is not
straightforward, since it must extend outside of the computational mesh,
and it also has a non-zero impedance (whose value is presently not well
understood.)

In an attempt to circumvent some of these computational problems
for the purpose of understanding the NASA direct-strike lightning data,
an alternate calculational approach has been investigated by LuTech, Inc.
This involves utilizing a transmission line model for both the lightning
channel and the aircraft. As an example, consider the isolated lightning
discharge shown in Figure 2a. In the absence of the aircraft, a
cloud-to-ground potential initiates a discharge through the channel,
which may be described by a generalized time-varying surge impedance and
propagation velocity. The bolt current at any point along the channel
length, $i_b(t)$, may be determined from the solution of the appropriate
equations for the transmission line model of the channel shown in Figure
2b.

The fact that the channel impedance varies with time adds some
complexity in determining the bolt current. One useful approximation is
to assume that the channel impedance is constant and this results in a
simple solution for the current. The problem is, of course, that the time
dependence of the excitation voltage source in this model is not known,
and hence, it is difficult to calculate the lightning bolt current from
first principles.

Cloud

$i_b(t)$

+ + +   Ground

a.

L

V(t) Z_c , v $i_b(t)$
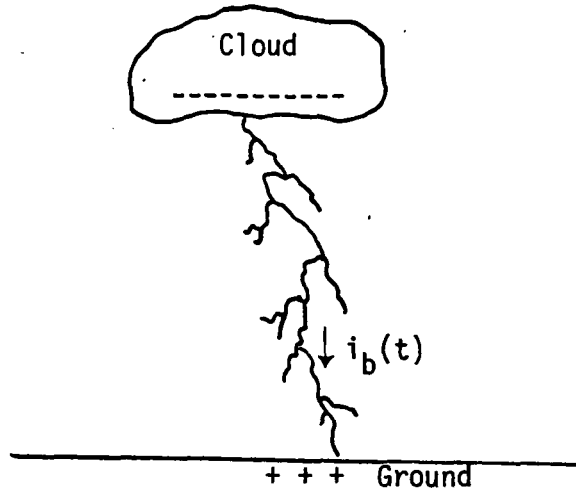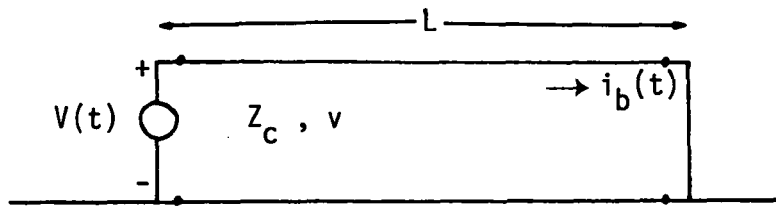
b.

Figure 2.   Cloud-to-Ground Lightning Discharge and Electrical
Propagation Model.

With the addition of an aircraft in the lightning channel, it is possible to make measurements of local aircraft currents and charges in an attempt to determine experimentally the lightning bolt current. As illustrated in Figure 3a, the lightning channel and the aircraft may be regarded as a suitable collection of intersecting wires or "sticks". The behavior of the channel current and the current on the aircraft structure depends on the transmission line properties of each of the sticks, as well as on the channel impedance. Figure 3b shows a detailed transmission line model for this case.

The presence of the fuselage, wing, and stabilizer wires in the lightning/aircraft model serves to contaminate the measured response of the bolt current with the exterior resonant frequencies of the aircraft. Such natural frequencies for an isolated aircraft are reasonably well understood and have been determined for several different aircraft through integral equation solutions [5] involving the moment method [6,7] or by transmission line methods of analysis [8]. However, with the lightning channel attached, it is expected that the resonant behavior of the aircraft will be modified. As may be noted from Figure 3b, if the surge impedance of the lightning channel is significantly larger than that of the conductors comprising the aircraft, it will be expected that the observed natural resonances will be similar to those of the isolated aircraft.

As discussed in references [9,10], the characteristic impedance of a segment of conductor of length L and radius a may be approximated as

$$Z \cong \frac{Z_0}{\pi} \ln (L/a) \tag{1}$$

where Z_0 is the impedance of free space. This impedance may be utilized in the transmission line model for the lightning/aircraft interaction. In most instances, it is expected that the lightning channel is rather long and thin, so that the impedance as given by Eq. (1) is relatively high compared with that computed for the shorter, thicker wire segments of the aircraft model.

Another consideration in interpreting measured lightning data is that of the location of the electromagnetic field sensors on the aircraft, relative to the points of channel attachment and detachment.
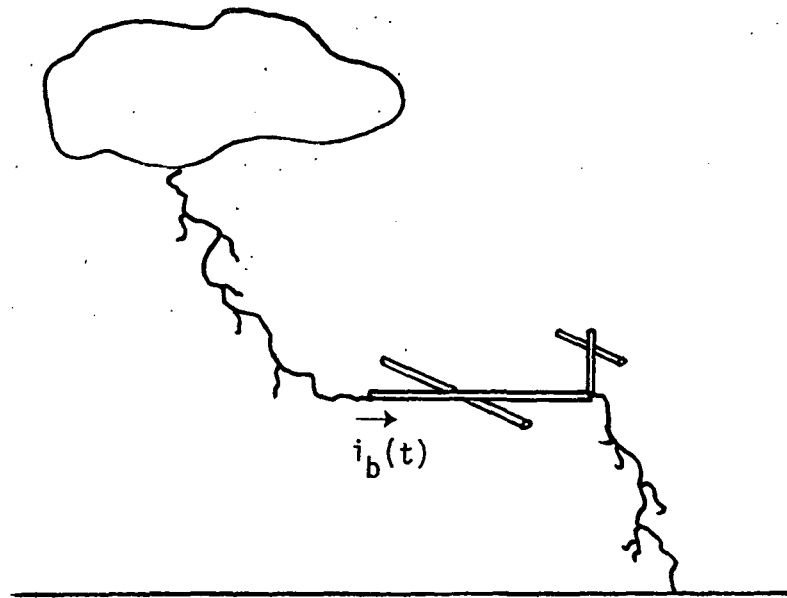
a.
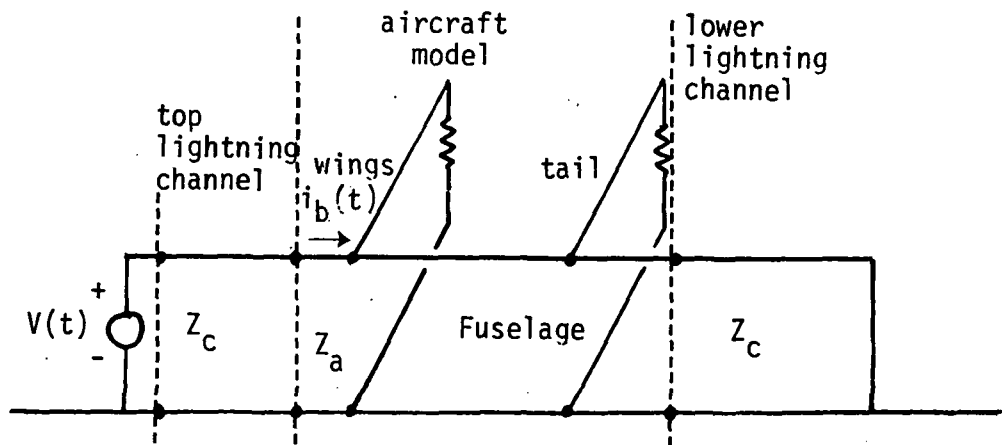
b.

Figure 3.   Direct Strike of Lightning with Aircraft and
Corresponding Transmission Line Model.

For example, the B-dot sensor labeled "A" in Figure 4a will be strongly influenced by the total channel current passing through the aircraft, especially at times after the local aircraft resonances have died out and only the lightning channel current is flowing. However, sensor "B" is not as strongly excited and may not provide a true measure of the bolt current.

On the other hand, if the lightning detaches from a wing as indicated in Figure 4b, the roles of sensors A and B are reversed. This illustrates the fact that for proper interpretation of measured direct-strike lightning data, it is imperative to know the geometrical locations of the attachment and detachment points on the aircraft, as well as having information on the individual time histories of the measured sensor data.

B. Representation of Lightning Responses

From concepts developed from the singularity expansion method (SEM) [11], it is possible to obtain an approximate understanding of the unperturbed lightning characteristics from the measured aircraft current responses. In the following discussions it will be assumed that any derivative sensor measurements (i.e., B-dot) have been integrated and converted to a total current quantity by multiplying by the circumference of the fuselage.

One model for the lightning channel is a two wire transmission line of length L and excited by a zero impedance voltage source as illustrated in Figure 5a. The load impedance is taken to be zero and the characteristic impedance Z_c and propagation constant γ_c are related to the electrical properties of the channel. In the actual channel, the propagation constant is complex, with a propagation velocity significantly less than the speed of light in free space. Similarly, the characteristic impedance may be complex.

The addition of an aircraft in the lightning channel is illustrated in Figure 5b. This is modeled as discontinuity in the transmission line with a length L_a and a different characteristic impedance and propagation constant. Of special interest is the current at some point on the section of transmission line representing the aircraft. This may be

a.

b.
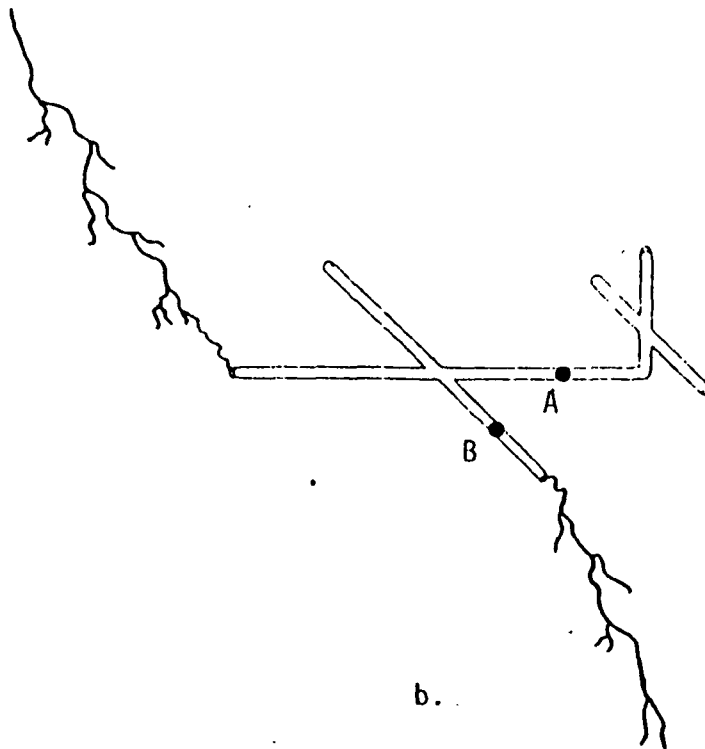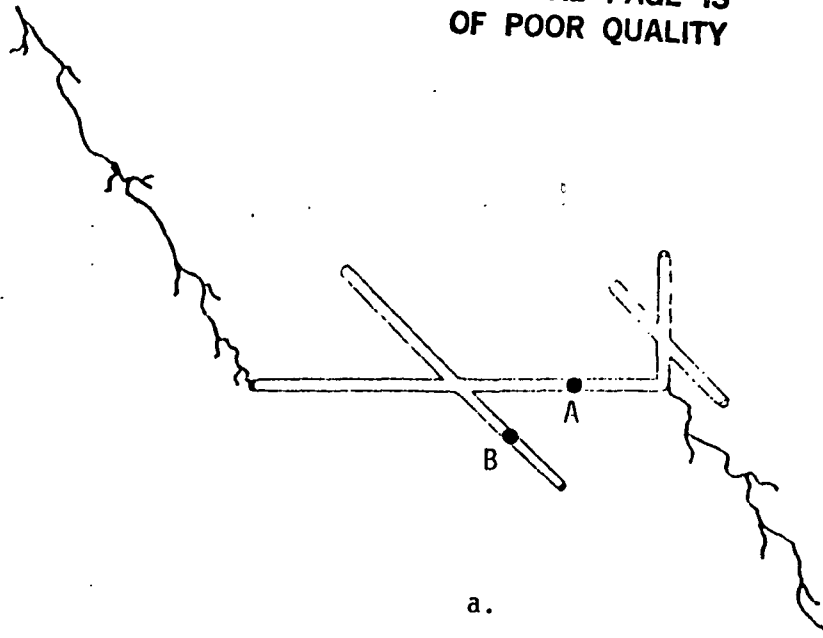
Figure 4. Direct Strike of Aircraft Strongly Exciting
Measurement Sensor A (a) and B (b).
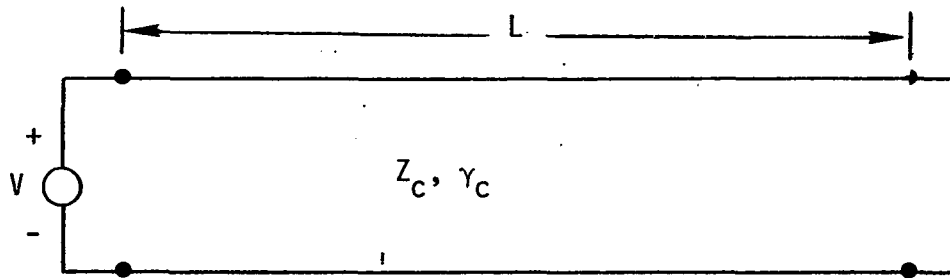
a. Unperturbed Lightning Channel.
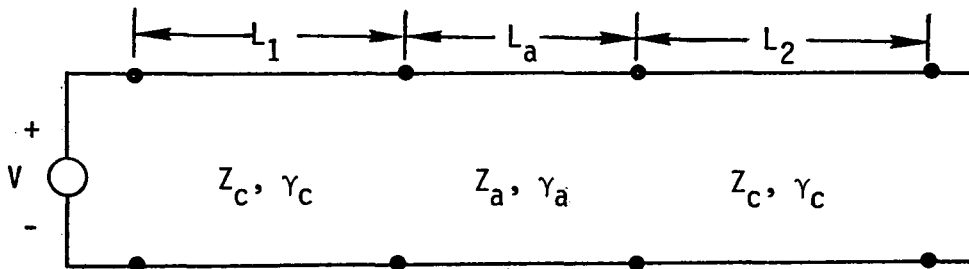
b. Lightning Attached To Aircraft.
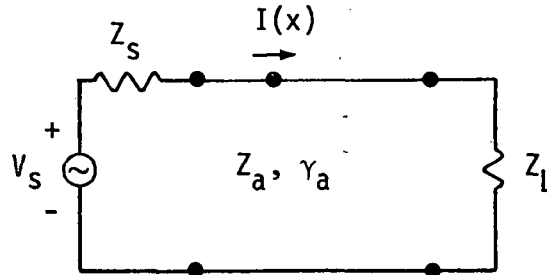
C. Equivalent Circuit For Aircraft.
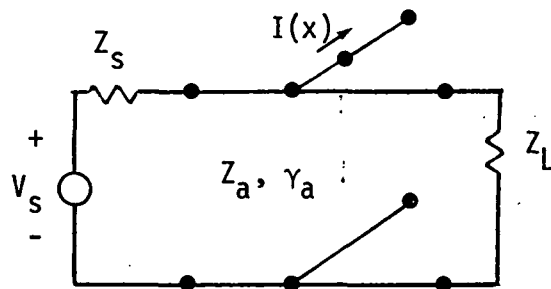
d. Equivalent Circuit for Aircraft with Sensor Point
    Not in Current Path.

Figure 5. Equivalent Circuits for Different Sensor Locations
           for Direct Strike Lightning Excitation of Aircraft
           in Figure 4a.

-10-

determined by transforming the source voltage and short circuit load through the lengths of transmission line denoted as L_1 and L_2 respectively, to yield the equivalent circuit in Figure 5c. In this figure, the excitation is provided by a Thevenin voltage source and the load is a lumped impedance element.

The current flowing on the aircraft at a position x can be expressed in simple terms as

$$I(x) = \frac{V}{2Z_a} (1-\rho_s) \frac{e^{-\gamma_a x} - \rho_L e^{\gamma_a(x-2L_a)}}{1 - \rho_s \rho_L e^{-2\gamma_a L}} \qquad (2)$$

where the reflection coefficients are given in terms of the load and source impedances as

$$\rho_L = (Z_L - Z_a)/(Z_L + Z_a) \qquad (3a)$$

and

$$\rho_s = (Z_s - Z_a)/(Z_s + Z_a) \qquad (3b)$$

In this equation, it is important to notice that there are a series of resonances in the current response at those frequencies where the denominator goes to zero. These frequencies are clearly a function of the reflection coefficients at each end of the aircraft transmission line section and as a result depend on the electrical parameters of the lightning channel.

In addition, note that the voltage source exciting the line is itself a function of the line parameters, and varies with frequency. If the aircraft were absent from the channel, the current flowing in the channel at this point would be given by $I_b = V/(Z_L + Z_s)$, a fact which may be verified from Eq.(2) by setting $L = 0$.

It is known from SEM that the current on the aircraft can be expressed as a sum of complex pole terms as

$$I = \sum_\alpha \frac{R_\alpha}{s - s_\alpha} \qquad (4)$$

where s_α are the complex natural resonances and R_α are the complex residues. As may be noted from linear system theory, the natural frequencies s_α are either due to resonances of current on the aircraft/channel set of conductors, or are due to the time variation of the excitation source. As a result, it is possible to write Eq.(4) in two terms as

$$I = I_b + \sum_{\substack{\text{structure} \\ \text{poles}}} \frac{R_\alpha}{s-s_\alpha} \tag{5}$$

where the first part I_b represents the contributions from the lightning excitation and the second is from the resonances on the aircraft.

It should be realized that the natural frequencies in Eq.(5) are those for the aircraft loaded by the lightning channel impedance, and not those for the isolated aircraft. This may be verified by looking at the denominator in Eq.(3) which clearly shows the dependence on the reflection coefficients. The resonant frequencies for the isolated aircraft are found with the relection coefficients equal to unity. Hence, it is expected that any measured resonances from the direct-strike lightning data will be different from those of the isolated aircraft. If, however, the channel impedance is significantly higher than the aircraft impedance, we expect that the measured resonances will be close to those for the isolated aircraft.

For the case of the sensor not in the primary current path on the aircraft, as illustrated for sensor B in Figure 4a, it becomes more difficult to determine the channel current using the expression discussed above. In this case, the transmission line model shown in Figure 5d is more appropriate. In this case, we expect that the response is dominated by resonance response of the aircraft, not by the injected current from the lightning channel.

C. Estimation of Lightning Current

For those direct stike data obtained with the electromagnetic sensor in the primary current path, it is possible to remove the influence of the aircraft in the measured data using the representation of the response as given by Eq. (4). Suppose that a time domain measurement of the current (or the time derivation of the current) is

made at the sensor location. If this waveform is transformed into the frequency domain, it will have a number of resonances related to the aircraft, and others related to the lightning bolt current. If the aircraft resonances and the corresponding residues are known, they may be subtracted from the total response, leaving only the contributions from the channel current.

One method of determining the resonant frequencies and residues of a measured time domain response is through the use of Prony's method [12,13]. This involves fitting a time domain function with a series of exponentially damped sinusoids whose amplitudes, frequencies, and damping constants are related to the excitation of the natural resonances of the aircraft and lightning channel. Ideally, one would like to process a particular time domain measurement, obtain the residues and natural frequencies, identify those resonances arising from the aircraft, and then subtract them from a response representation given by Eq.(4) to estimate the lightning current.

Unfortunately, this approach has several problems, which were studied in the course of this effort. The first, and perhaps most severe, is that although Prony's method is capable of representing a complicated time domain waveform in terms of poles and residues, there is no real guarantee that the Prony poles correspond to the physical poles of the problem. In other words, the Prony method will curve-fit the transient waveform with suitable damped sine waves, but they may not be the correct ones. A second problem is that it is often difficult to identify which resonances in a complex frequency representation of the aircraft current response are due to the aircraft, and which are due to the driving waveform.

Nothwithstanding these problems, the NASA acquired lightning data has been examined from this viewpoint in an attempt to determine if it is possible to extract a knowledge of the lightning current from the aircraft data. In the next section, a detailed discussion of the stick-wire aircraft model is presented in an attempt to get a better understanding of the nature of the natural resonances of the F-106 aircraft.

SECTION III

DETERMINATION OF AIRCRAFT RESONANCES

A. Overview

As previously discussed, the primary goals of this effort are analysis and interpretation of the in-flight test data and determination of lightning characteristics. In doing this, we assume that as lightning attaches to an aircraft and detaches from it, certain "natural resonances" are excited as currents flow along various segments of the aircraft. These segments include the fuselage, the wings, and the horizontal and vertical stabilizers, and may also combine into various other possible current channels. These "resonances" would then be present in the actual aircraft data and must be filtered out so that only the lightning characteristics remain.

From this basic assumption, we then proceed in two complementary directions. On the one hand, we seek to construct appropriate aircraft models in order to determine its "natural resonances". On the other hand, we wish to model the test traces correctly so that appropriate characteristics of the trace can be correlated with modeling predictions.

In this section, we discuss the development of three different aircraft models, leading to a determination of natural or free resonances of the aircraft. The results from the three models are compared with each other, as well as other available independent studies. Then, the problem of processing the test data using Prony analysis, so that the appropriate features of the measurement can be compared with model predictions, forms the subject of the following Section IV.

Current aircraft modeling methods in electromagnetic theory have essentially dealt with studying the behavior of current over an aircraft body. These methods range from the elaborate study of dynamic current behavior to the simple study of steady state current behavior. It is the latter approach that we have taken.

Our models are derived from initial work reported by Bedrosian [8], which attempts to model various aircrafts by considering the main structures, such as the fuselage, wings, horizontal and vertical stabilizers, as long, conducting wires, whence came the name "stick model". The main objective here is to determine the "natural resonances" of the current that would flow on these wires. This technique has proven to model quite well various aircraft with long wing spans, such as the B-1, B-52 and E-4. Bedrosian's work [8] is adapted here with some improvements, described in this section. This may be referred to as the "modified stick model". The other two models are named "wire-plate model" and "wire-mesh model". In the wire-plate model, the delta wing is approximated by a rectangular plate such that the portion of the main fuselage attached to it is subdivided into many individual wire segments. In the wire-mesh model, the delta wing is approximated by a wire-mesh, where each wire in the mesh assumes the same character as wires elsewhere.

The three models outlined above are discussed in detail in Sections IIIA, IIIB and IIIC. Later, in Section IIID, comparison of results from different models is carried out.

B. Modified Stick Model of Aircraft.

As was pointed out earlier, Bedrosian's work [8] employs a constant stick-parameter $\Omega = 2\,\ell n\,[2(\text{stick length})/(\text{stick radius})]$ for all of the six sticks used in modeling an aircraft. This results in the use of realistic lengths for individual sticks, but somewhat adjusted radii in order that the parameter Ω is the same for all sticks. The process of determining the natural frequencies also requires the satisfaction of the Kirchoff's current condition at all junctions, the end conditions and a condition on the charge densities at all junctions. Reference [8] uses the condition that the charge per unit length Q_i (not the surface charge density n_i) be continuous at the junction. In the present work, a frequency-dependent junction condition derived by Wu and King [14] has been employed. This condition is that the quantity $[\psi_i\, Q_i]$ is continuous at the junction with $\psi_i = 2\,[\ell n\{2/(ka_i)\} - \gamma]$. Unlike the continuity of the linear (Q_i) or the surface (n_i) density of charge, the condition used

here is frequency-dependent and is expected to yield more accurate results.

The modification of earlier work of Bedrosian [8] consists of letting each stick have its own radius and consequently, different Ω_i parameters. In view of this, the induced current on an individual stick by an incident plane wave is approximated by

$$I_{ind,n}(k, x, \Omega_i, \theta) = \frac{4\pi jE_o}{kZ_o\Omega_n\sin\theta} \exp(jkx\cos\theta) \qquad (6)$$

where (see Figure 6),

Ω_n = 2 ℓn [(nth stick length)/nth stick radius)]

k ≡ wave number of the incident field

x ≡ position along the stick

Z_o ≡ impedance of free space

E_o ≡ electric field strength of the incident wave

θ ≡ angle between $\vec{k}$ and $-\vec{1}_x$.

As in reference [8], the phase of the incident field is set to zero at $x = 0$ and $\vec{H}$ is polarized perpendicular to the stick. Note that the induced current of Eq.(6) is devoid of the end condition and that the lengths and radii of the six sticks modeling a general aircraft are specified in Figure 6.
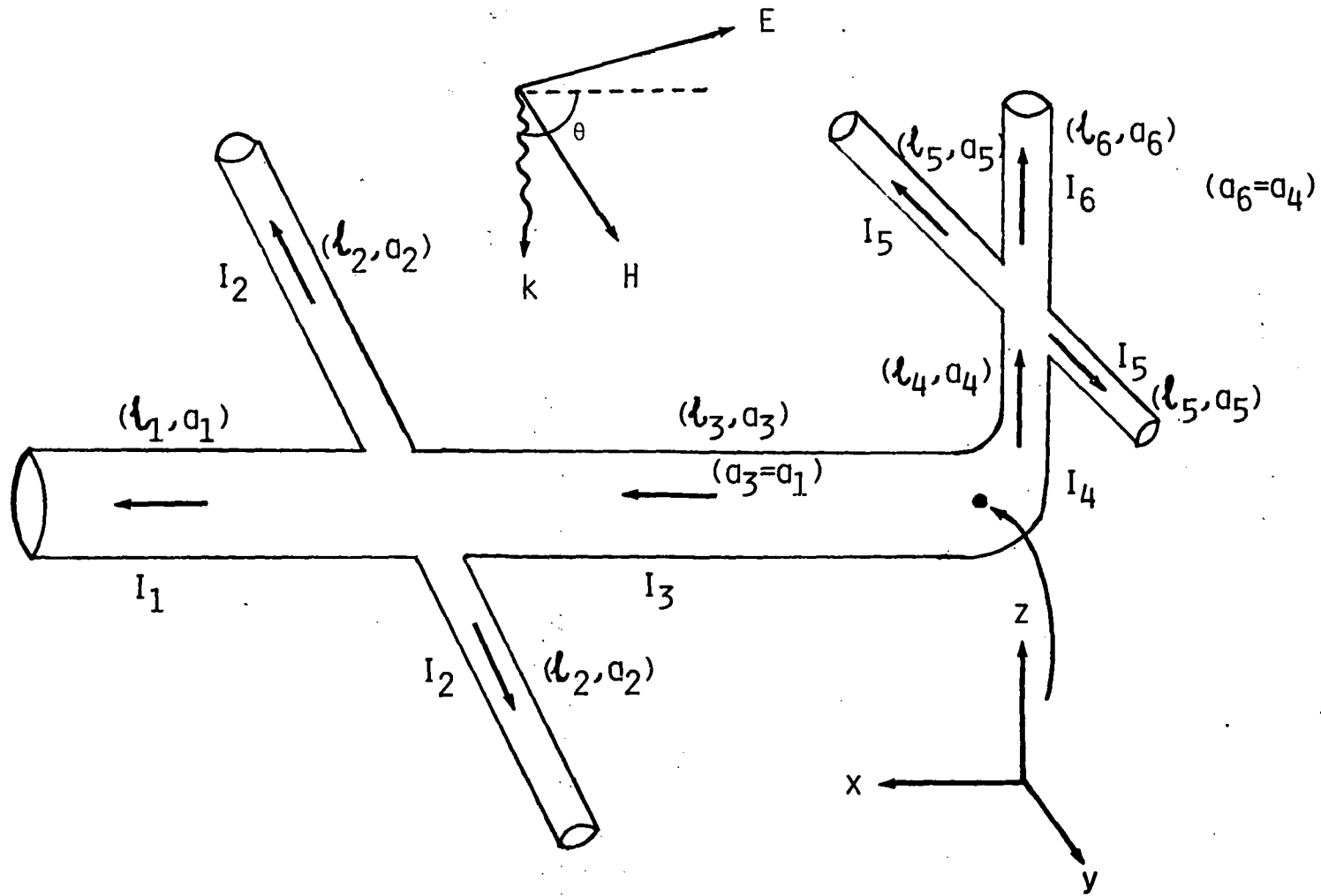
Figure 6. The Six-Stick Model with Different Radii.

To a first order in $(1/\Omega_n)$, the current on each stick can be written as a directly induced component plus a sine and a cosine component, as given by

$$I_n(\xi) = I_{ind,n}(k, \Omega_n, \xi, \theta) + S_n \sin[k(\xi - \ell_n)] + C_n \cos[k(\xi - \ell_n)] \qquad (7)$$

$$\text{for} \quad n = 1 \text{ to } 6$$

The constants S_n and C_n must be chosen to satisfy the free end conditions $I_n(\xi_{end}) = 0$ and the junction conditions of current and and charge. The free end conditions lead to the following expressions

$$I_1(x) = I_{ind,1}(k, \Omega, x, \theta) + S_1 \sin[k(x - \ell_1 - \ell_3)]$$
$$- I_{ind,1}(k, \Omega, \ell_1 + \ell_3, \theta) \cos[k(x - \ell_1 - \ell_3)]$$

$$I_2(y) = S_2 \sin[k(y - \ell_2)] \qquad (y > 0)$$

$$I_3(x) = I_{ind,3}(k, \Omega_3, x, \theta) + S_3 \sin[k(x - \ell_3)] + C_3 \cos[k(x - \ell_3)]$$

$$I_4(z) = -I_{ind,4}(k, \ell_4, z, \pi/2 - \theta) + S_4 \sin[k(z - \ell_4)] + C_4 \cos[k(z - \ell_4)]$$

$$I_5(y) = S_5 \sin[k(y - \ell_5)] \qquad (y > 0)$$

$$I_6(z) = -I_{ind,6}(k, \Omega_6, z, \pi/2 - \theta) + S_6 \sin[k(z - \ell_4 - \ell_6)]$$
$$+ I_{ind,6}(k, \Omega_6, \ell_4 + \ell_6, \pi/2 - \theta) \cos[k(z - \ell_4 - \ell_6)]$$

$$(8)$$

Equation (8) satisfies the following four end conditions:

$$I_1(\ell_1 + \ell_3) = 0 \qquad\qquad ; \quad x = (\ell_1 + \ell_3)$$

$$I_2(\ell_2) = 0 \qquad\qquad ; \quad y = \ell_2$$

$$I_5(\ell_5) = 0 \qquad\qquad ; \quad y = \ell_5 \qquad\qquad\qquad (9)$$

$$I_6(\ell_4 + \ell_6) = 0 \qquad\qquad ; \quad z = (\ell_4 + \ell_6)$$

The remaining eight unknowns in Eq. (6),

$$S_1, \; S_2, \; S_3, \; S_4, \; S_5, \; S_6, \; C_3, \; \text{and} \; C_4,$$

are determined from three Kirchoff's law equations and five equations of continuity at the stick junctions:

1) $\sum$ (currents) $= 0$ at $x = \ell_3, \; y = 0$

2) $\sum$ (currents) $= 0$ at $x = z = 0$

3) $\sum$ (currents) $= 0$ at $y = 0, \; z = \ell_4$

4) $Q_1 \psi_1 = Q_3 \psi_3$ & 5) $Q_2 \psi_2 = Q_3 \psi_3$ at $x = \ell_3$, $y = 0$

6) $Q_3 \psi_3 = Q_4 \psi_4$ at $x = z = 0$

7) $Q_4 \psi_4 = Q_5 \psi_5$ & 8) $Q_4 \psi_4 = Q_6 \psi_6$ at $z = \ell_4$, $y = 0$

where the charge per unit length Q_n and the expansion parameter ψ_n are given by

$$Q_n(\xi) = -\frac{1}{j\omega} \frac{dI_n(\xi)}{d\xi}, \quad \text{for } n = 1 \text{ to } 6 \tag{10}$$

$$\psi_n = 2 \left[\ell n \left(\frac{2}{ka_n}\right) - \gamma\right]; \quad \text{for } n = 1 \text{ to } 6 \tag{11}$$

with

$$k = \frac{\omega}{c} \; ; \; \omega = 2\pi f \; ; \; f = \text{frequency in Hz and}$$

$$c = \text{free space speed of light}$$

$$a_n = \text{radius of the nth wire}$$

$$\gamma = 0.577 \quad \text{Euler's constant}$$

Eight boundary conditions needed in solving for the eight unknowns are

(i) $\quad I_1 (x = \ell_3) + 2 I_2 (y = 0) = I_3 (x = \ell_3)$ $\hspace{3cm}$ (12)

(ii) $\quad I_3 (x = 0) + I_4 (z = 0) = 0$ $\hspace{3cm}$ (13)

(iii) $\quad I_6 (z = \ell_4) + 2 I_5 (y = 0) = I_4 (z = \ell_4)$ $\hspace{2cm}$ (14)

(iv) $\quad \dfrac{\partial I_1(x)}{\partial x}\bigg|_{x = \ell_3} \psi_1 = \dfrac{\partial I_3(x)}{\partial x}\bigg|_{x = \ell_3} \psi_3$ $\hspace{2.5cm}$ (15)

(v) $\quad \dfrac{\partial I_2(y)}{\partial y}\bigg|_{y = 0} \psi_2 = \dfrac{\partial I_3(x)}{\partial x}\bigg|_{x = \ell_3} \psi_3$ $\hspace{2.5cm}$ (16)

(vi) $\quad \dfrac{\partial I_3(x)}{\partial x}\bigg|_{x = 0} \psi_3 = \dfrac{\partial I_4(z)}{\partial z}\bigg|_{z = 0} \psi_4$ $\hspace{2.5cm}$ (17)

(vii) $\quad \dfrac{\partial I_4(z)}{\partial z}\bigg|_{z = \ell_4} \psi_4 = \dfrac{\partial I_5(y)}{\partial y}\bigg|_{y = 0} \psi_5$ $\hspace{2.5cm}$ (18)

(viii) $\quad \dfrac{\partial I_4(z)}{\partial z}\bigg|_{z = \ell_4} \psi_4 = \dfrac{\partial I_6(z)}{\partial z}\bigg|_{z = \ell_4} \psi_6$ $\hspace{2.5cm}$ (19)

After applying the above conditions, one gets the following matrix equation for the unknown quantities.

TABLE 1. Matrix Equation (20)

$$
\begin{bmatrix}
-\sin k\ell_1 & -2\sin k\ell_2 & 0 & -1 & 0 & 0 & 0 & 0 \\[2mm]
\cos k\ell_1 & 0 & -\dfrac{\psi_3}{\psi_1} & 0 & 0 & 0 & 0 & 0 \\[2mm]
0 & \cos k\ell_2 & -\dfrac{\psi_3}{\psi_2} & 0 & 0 & 0 & 0 & 0 \\[2mm]
0 & 0 & -\sin k\ell_3 & \cos k\ell_3 & \cos k\ell_4 & -\sin k\ell_4 & 0 & 0 \\[2mm]
0 & 0 & \cos k\ell_3 & \sin k\ell_3 & \dfrac{-\psi_4}{\psi_3}\sin k\ell_4 & -\cos k\ell_4 & 0 & 0 \\[2mm]
0 & 0 & 0 & 0 & 0 & -\dfrac{\psi_4}{\psi_3} & \cos k\ell_5 & 0 \\[2mm]
0 & 0 & 0 & 0 & 0 & -\dfrac{\psi_4}{\psi_6} & 0 & \cos k\ell_6 \\[2mm]
0 & 0 & 0 & 0 & -1 & 0 & -2\sin k\ell_6 & -\sin k\ell_6
\end{bmatrix}
\begin{bmatrix}
S_1 \\[2mm] S_2 \\[2mm] S_3 \\[2mm] C_3 \\[2mm] C_4 \\[2mm] S_4 \\[2mm] S_5 \\[2mm] S_6
\end{bmatrix}
=
\frac{4\pi j E_0}{kZ_0}
\begin{bmatrix}
\csc\theta\, e^{jk\ell_3\cos\theta}\left(\dfrac{1}{\Omega_3}-\dfrac{1}{\Omega_1}\right) + \dfrac{\cos k\ell_1}{\Omega_1}\csc\theta\, e^{jk(\ell_1+\ell_3)\cos\theta} \\[4mm]
e^{jk\ell_3\cos\theta}\, j(\cot\theta)\left(\dfrac{\psi_3}{\psi_1}\dfrac{1}{\Omega_3}-\dfrac{1}{\Omega_1}\right) + \dfrac{(\sin k\ell_1)(\csc\theta)}{\Omega_1}e^{jk(\ell_1+\ell_3)\cos\theta} \\[4mm]
+\, j\,\dfrac{\cot\theta}{\Omega_3}\,e^{jk\ell_3\cos\theta} \\[4mm]
\left(\dfrac{\sec\theta}{\Omega_4}-\dfrac{\csc\theta}{\Omega_3}\right) \\[4mm]
-j\left(\dfrac{\psi_4}{\psi_3}\dfrac{1}{\Omega_4}\tan\theta + \dfrac{1}{\Omega_3}\cot\theta\right) \\[4mm]
-j\,\dfrac{\tan\theta}{\Omega_4}\left(\dfrac{\psi_4}{\psi_5}\right)e^{jk\ell_4\sin\theta} \\[4mm]
-j\tan\theta\, e^{jk\ell_4\sin\theta}\left(\dfrac{1}{\Omega_4}\dfrac{\psi_4}{\psi_6}-\dfrac{1}{\Omega_6}\right) -\sin k\ell_6\,\dfrac{\sec\theta}{\Omega_6}\,e^{jk(\ell_4+\ell_6)\sin\theta} \\[4mm]
\sec\,e^{jk\ell_4\sin\theta}\,\dfrac{1}{\Omega_6}-\dfrac{1}{\Omega_4} -(\cos k\ell_6)\dfrac{\sec\theta}{\Omega_6}\,e^{jk(\ell_4+\ell_6)\sin\theta}
\end{bmatrix}
$$

It is observed that the present matrix equation (20) of Table I reduces identically to the matrix equation (4) of reference [8] in the case of $\psi_n = \psi$ and $\Omega_n = \Omega$ for n = 1 to 6.

The natural frequencies are found by setting the incident field amplitude $E_0 = 0$ and investigating Eq.(20) for nontrivial solutions. Setting the determinant equal to zero, one obtains

$$0 = 2\, c_1\, c_4\, c_5\, c_6\, s_2\, \psi_{32} - 2\, c_1\, c_3\, c_5\, s_2\, s_4\, s_6\, \psi_{32}\, \psi_{43}\, \psi_{46}$$

$$- 4\, c_1\, c_3\, c_6\, s_2\, s_4\, s_5\, \psi_{32}\, \psi_{43}\, \psi_{45} - 4\, c_1\, c_4\, c_6\, s_2\, s_3\, s_5\, \psi_{32}\, \psi_{45}$$

$$- 2\, c_1\, c_5\, c_6\, s_2\, s_3\, s_4\, \psi_{32} - 2\, c_1\, c_4\, c_5\, s_2\, s_3\, s_6\, \psi_{32}\, \psi_{46}$$

$$+ c_2\, c_3\, c_4\, c_5\, c_6\, s_1\, \psi_{31} - c_2\, c_3\, c_5\, s_1\, s_4\, s_6\, \psi_{31}\, \psi_{43}\, \psi_{46}$$

$$- 2\, c_2\, c_3\, c_6\, s_1\, s_4\, s_5\, \psi_{31}\, \psi_{43}\, \psi_{45} - 2\, c_2\, c_4\, c_6\, s_1\, s_3\, s_5\, \psi_{31}\, \psi_{45}$$

$$- c_2\, c_5\, c_6\, s_1\, s_3\, s_4\, \psi_{31} - c_2\, c_4\, c_5\, s_1\, s_3\, s_6\, \psi_{31}\, \psi_{46}$$

$$+ c_1\, c_2\, c_3\, c_4\, c_5\, s_6\, \psi_{46} + 2\, c_1\, c_2\, c_3\, c_4\, s_5\, \psi_{45}\, c_6$$

$$+ c_1\, c_2\, c_3\, c_5\, c_6\, s_4 + c_1\, c_2\, c_4\, c_5\, s_3\, c_6$$

$$- c_1\, c_2\, c_5\, s_3\, s_4\, s_6\, \psi_{43}\, \psi_{46} - 2\, c_1\, c_2\, c_6\, s_3\, s_4\, s_5\, \psi_{43}\, \psi_{45}$$

$$\tag{16}$$

where the following abbreviated notation is employed

$$c_i = \cos(k\ell_i) \quad ; \quad S_i = \sin(k\ell_i)$$

and $$\tag{17}$$

$$\psi_{ij} = \psi_i / \psi_j$$

It has also been verified that the above equation (21) reduces to equation (5) of reference [8] in the limit of $\psi_n = \Omega$ for n = 1 to 6. However, while in this limiting case of reference [8], the solution for the six constants in terms of one of the arbitrary constants can be written in closed form, such elegance is not possible in the present general case. The matrix equation has been solved numerically. The natural modes are then determined by substituting the matrix solution into equation (3).

The final task is to find the imaginary components of the natural frequencies. The procedure followed is same as in reference [8] and the temporal damping constant α_m is given by

$$\alpha_m = \frac{P_m}{4W_m} = \frac{ck_m \, P'_m}{D_m} \tag{23}$$

where P_m = average radiated power and W_m = stored magnetic energy per cycle. The denominator D_m is given by

$$D_m = \sum_{n=1}^{6} \int I_n^2 (\xi_n) \, d\xi_n \tag{24}$$

and the numerator factor P'_m is given by

$$P'_m = \int_{\text{sticks}'} \int_{\text{sticks}''} \left[P(',\, '') \, I(\xi') \, I(\xi'') \right.$$

$$\left. - \frac{1}{K_m^2} \left(\frac{\partial}{\partial \xi'} I(\xi') \right) \left(\frac{\partial}{\partial \xi''} I(\xi'') \right) \right] \frac{\sin[k_m |\vec{r}' - \vec{r}''|]}{|\vec{r}' - \vec{r}''|}$$

$$d\xi' \, d\xi'' \tag{25}$$

and,

$$P\,('\,,\,'') = \begin{cases} 0 \text{ if stick' is perpendicular to stick''} \\ 1 \text{ if stick' is parallel to stick''} \end{cases} \tag{26}$$

The modified stick model described above was initially used in computing the first several natural frequencies for other aircrafts e.g., B-1, E-4 and EC-135 for comparison with Bedrosian's [8] results. These example aircraft results are not reported here, since the present interest is in the F-106 aircraft.

C. Stick-Plate Model

In this model, the aircraft wing is modeled by a rectangular plate, while all other aircraft elements such as fuselage and stabilizers are approximated by wires as before. The model is shown in Figure 7. Similar to the stick model, the assumed current distributions in the different aircraft elements can be written as follows:

$$I_1(x) = I_{ind,1}(k, \Omega_1, x, \theta) + S_1 \sin[k(x-\ell_1)] + C_1 \cos[k(x-\ell_1)]$$

$$I_2(x) = F(x)$$

$$I_3(x) = I_{ind,3}(k, \Omega_3, x, \theta) + S_3 \sin[k(x-\ell_3)] + C_3 \cos[k(x-\ell_3)]$$

$$I_4(x, y) \cong G(x) \qquad \text{(on the wing, parallel to fuselage)}$$

$$I_5(x, y) = S(x) \cos k(y - a_2 - \ell) \qquad \text{(on the wing, orthogonal to fuselage)}$$

$$I_6(z) = I_{ind,6}(k, \Omega_6, z, \theta) + S_6 \sin[k(z-\ell_6)] + C_6 \cos[k(z-\ell_6)]$$

$$(27)$$

where the induced currents on wires 1, 3 and 6 are similar to what was employed in the stick model. The constants S_1, S_3, S_6 and C_1, C_3, C_6 are determined by application of end and junction conditions. The assumed functions $F(x)$, $G(x)$ and $S(x)$ are approximated by using a finite number (n) of points along the mid-fuselage. The end condition leads to vanishing currents at free ends of rods and wing plate edges. The junction condition includes the application of Kirchoff's current rule as well as both the frequency independent charge condition $[Q_i = Q_j]$ and the frequency dependent charge condition $[\psi_i Q_i = \psi_j Q_j]$. Once again, the results are deferred to Section IIID.
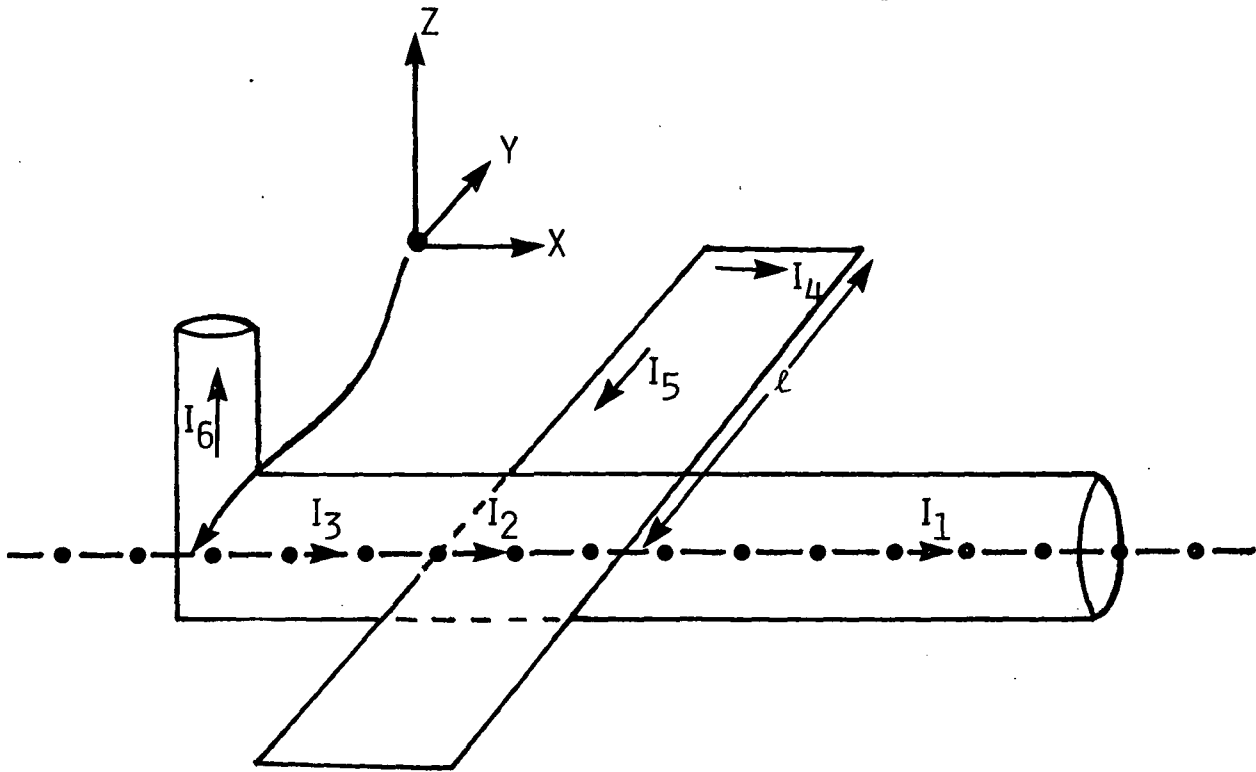
Figure 7. Wire-Plate Model of Aircraft.

D. Wire-Mesh Model

In this model, the aircraft wing is modeled by a wire-mesh rather than a plate as in the previous model. The model is schematically shown in Figure 8. Although Figure 8 is a line diagram, each wire is characterized by a certain length and radius and assumes the same character as wires elsewhere. Junction conditions are imposed at every wire intersection. The intersection or joining of wires is always at right angles, so that all of the wire segments are along one of the orthogonal coordinate axes. Thus it is seen that this model does not differ conceptually from the stick model described earlier, except that it gives rise to a similar and larger system of linear equations. Since the mathematical description of the model is identical to that of the stick model, it is not repeated here. In the following subsection, the results of the computations for all three models are presented and compared.

E. Numerical Results and Comparisons

Computer routines were written to determine the natural resonances of the aircraft, using all three models. We will first report the computed results, followed by a discussion of their interpretation.

1) Modified stick model

Figure 9, along with the accompanying tabulation, shows all of the eleven cases considered in this parametric study. For each case, the length and radius of each stick is tabulated. In the sets identified under the 'a' and 'c' group, only one cross member is used for the wing, while the 'b' group employs two cross wires to simulate the wing. Figure 10 plots the computed resonances for each of the eleven cases.
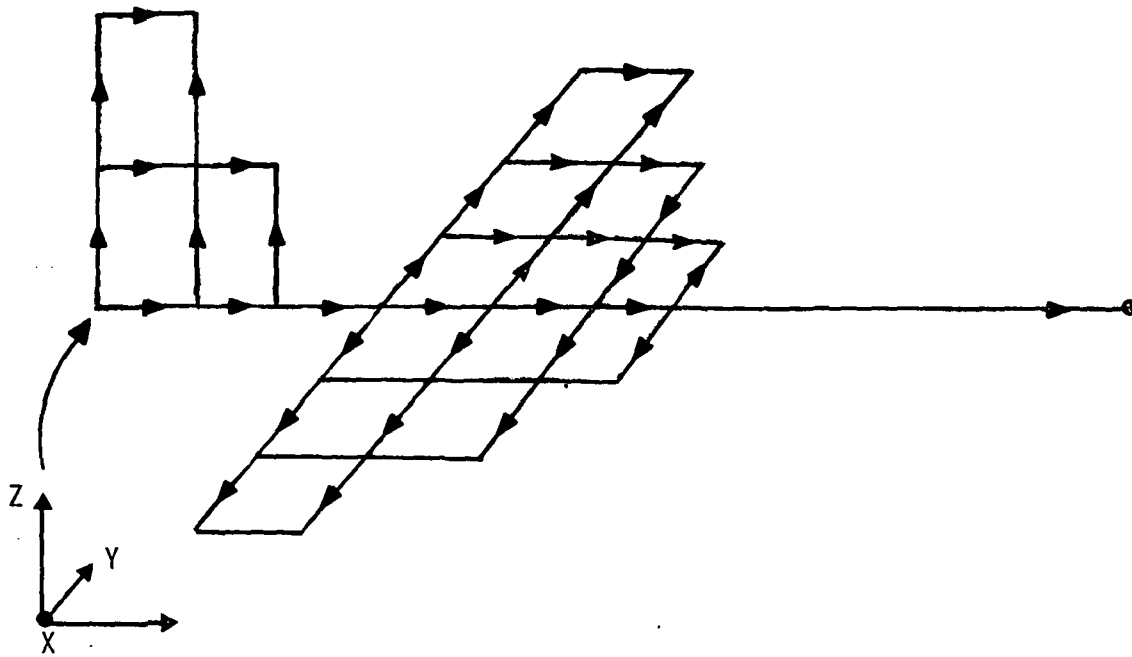
Figure 8. Wire-Mesh Model of Aircraft.

Model Length (Radius)	a_1	a_2	a_3	a_4	a_5	b_2	b_3	b_4	c_2	c_3	c_4
l_1 (1.00)	6.48	9.19	11.91	14.62	17.34	9.19	11.91	14.62	9.19	11.91	14.62
l_2 (0.25)	5.84	----	----	----	5.84	1.46	2.92	4.38	1.46	2.92	4.38
l_3 (1.00)	12.10	9.39	6.67	3.96	1.24	8.15	5.43	2.72	9.39	6.67	3.96
l_4 (1.48)	3.96	----	----	----	----	----	----	----	----	----	3.96
l_5 (0.25)						5.84	----	5.84			
l_6 (1.00)						1.24	----	1.24			
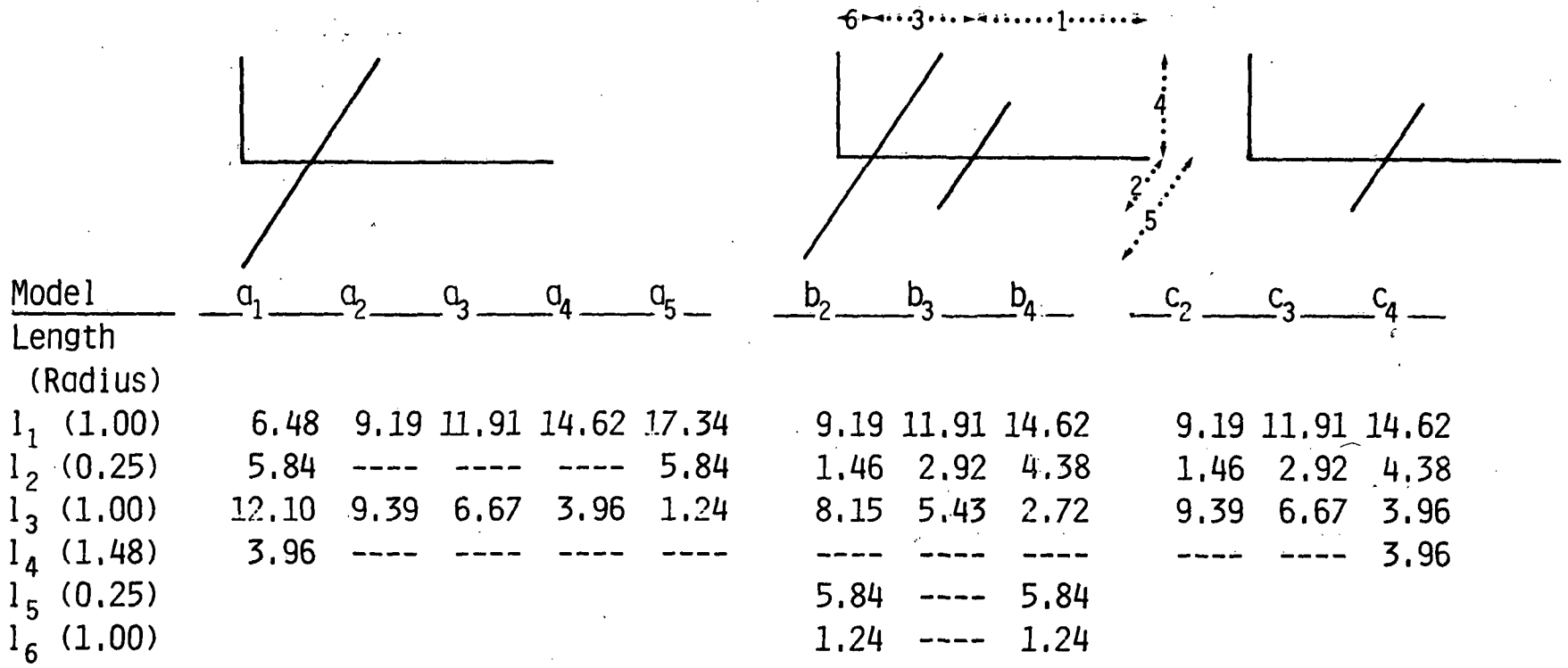
Figure 9. Modified Stick Model Parametric Values.
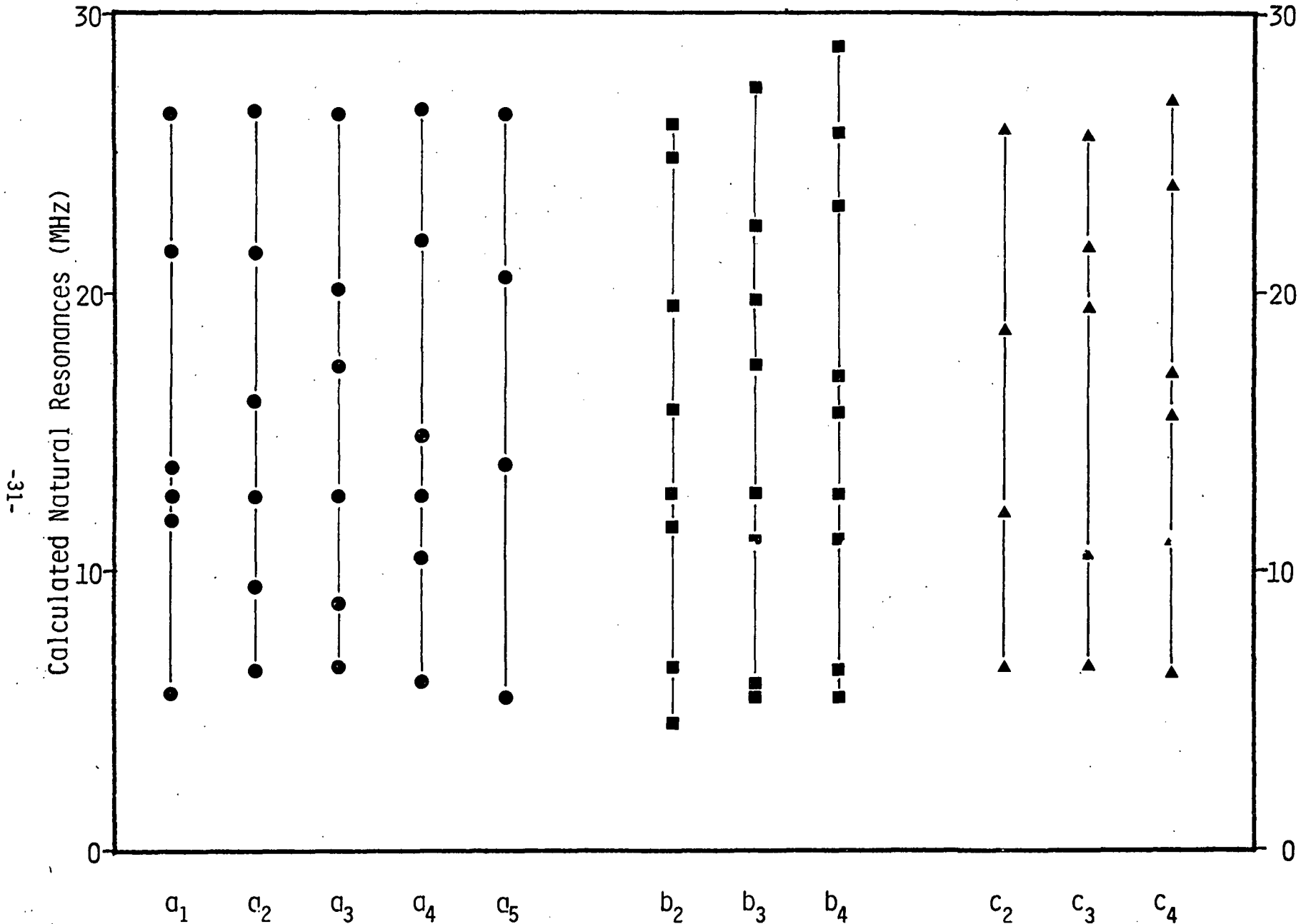
Figure 10. Resonances Corresponding to Modified Stick Models of Figure 9.

-31-

2) Wire-plate model

Figure 11, along with the accompanying tabulation, shows all the eleven cases considered in this parametric study. The lengths and radii of all sticks together with the plate dimensions are tabulated. The location and size of the plates are varied. Figure 12 plots the computed resonances for the various cases.

3) Wire-mesh model

Figure 13, along with the accompanying tabulation, shows the parametric values considered for this model. For each set of parameters, the resonances are computed two different ways employing (1) the simple continuity of charge at junction ($Q_i = Q_j$) and (2) the frequency-dependent junction condition ($\psi_i\, Q_i = \psi_j\, Q_j$) at the junction of conductors i and j. A plot of the results is shown in Figure 14.

In Figure 15 the resonances determined by scale model tests [12] are plotted for comparison. These show the fundamental fuselage resonance at approximately 7.5 MHz and its harmonics at approximately 15 MHz and 23 MHz. Other resonances occur around 12 and 19 MHz due to combination of aircraft element lengths. It is observed that all three analytical models described above also yield the fundamental resonances accurately and the harmonics approximately. However, there is a 2 MHz resonance appearing in the wire-plate model, corresponding to a 150m wavelength. The perimeter of the plate is approximately 35m suggesting a resonance occurring with the perimeter becoming a quarter-wavelength. This is only speculative, since the plate is in physical contact with a wire modeling the fuselage. More detailed work is required to interpret the 2 MHz resonance, which is the result of model topology and should not be present in the F-106 aircraft resonances.

In all three models, the computed resonances are seen to be quite sensitive to changes in lengths and radii. There is a certain amount of flexibility in choosing the appropriate values for lengths and radii starting with the known dimensions of the aircraft. Consequently, we have varied these values in this study.
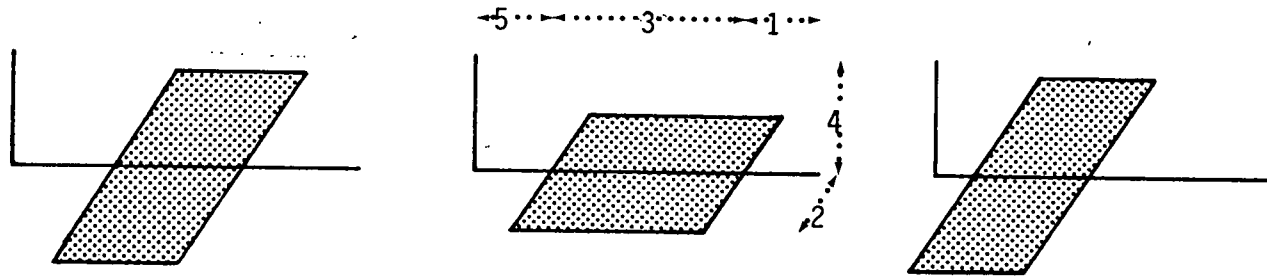
Model	X_3	X_4	X_5	Y_3	Y_4	Y_5	Z_3	Z_4	Z_5
Length (Radius)									
Points	3	4	5	3	4	5	3	4	5
l_1 (1.00)	9.20	----	9.20	6.48	----	6.48	11.92	----	11.92
l_2	5.84	----	5.84	2.92	----	2.92	5.84	----	5.84
l_3	5.43	----	5.43	10.86	----	10.86	5.43	----	5.43
l_4 (1.48)	3.96	----	----	----	----	----	----	----	3.96
l_5 (1.00)	4.72	----	4.72	2.00	----	----	----	----	2.00

Figure 11. Wire-Plate Model Parametric Values.
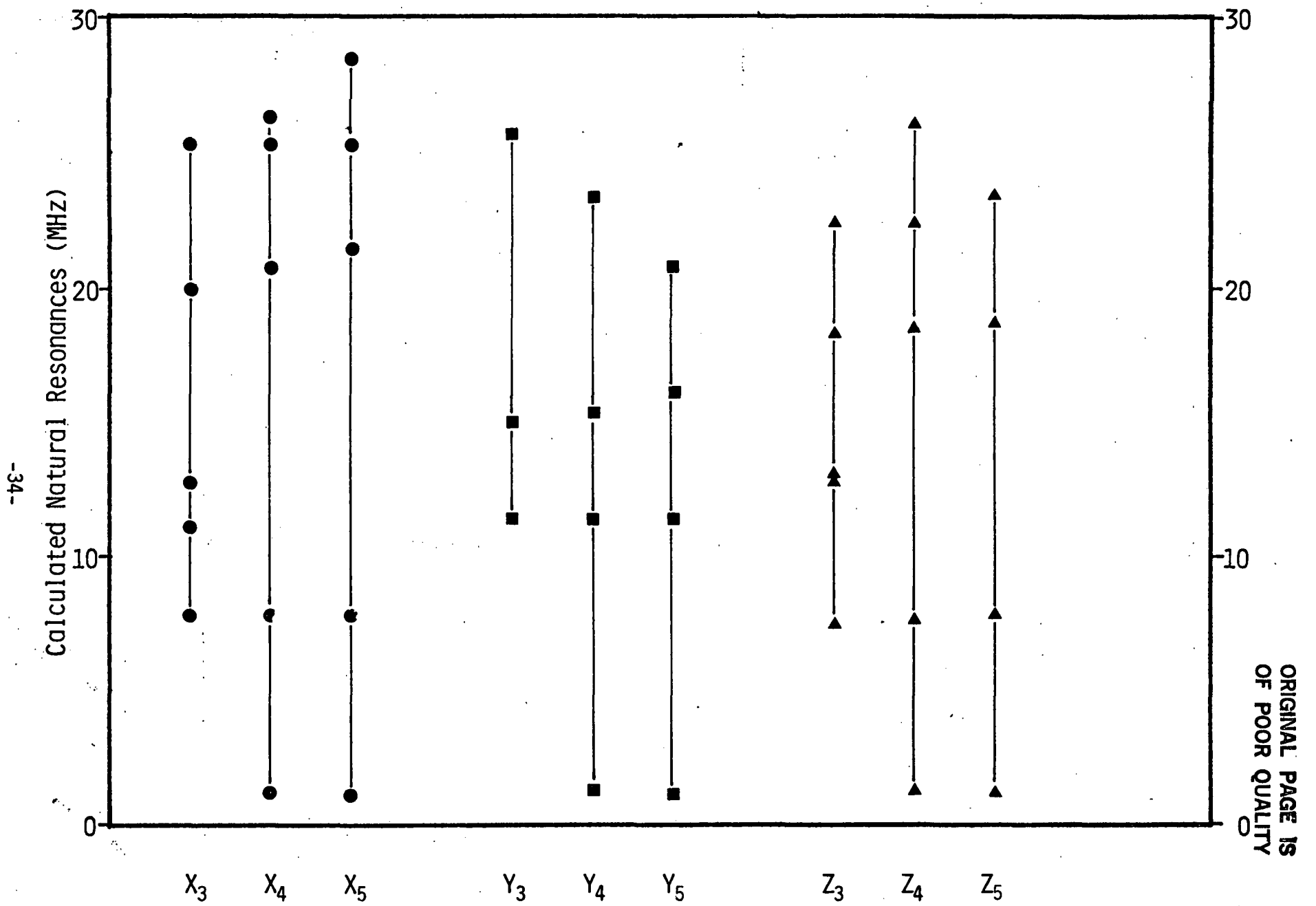
Figure 12.   Resonances Corresponding to Wire-Plate Models of Figure 11.
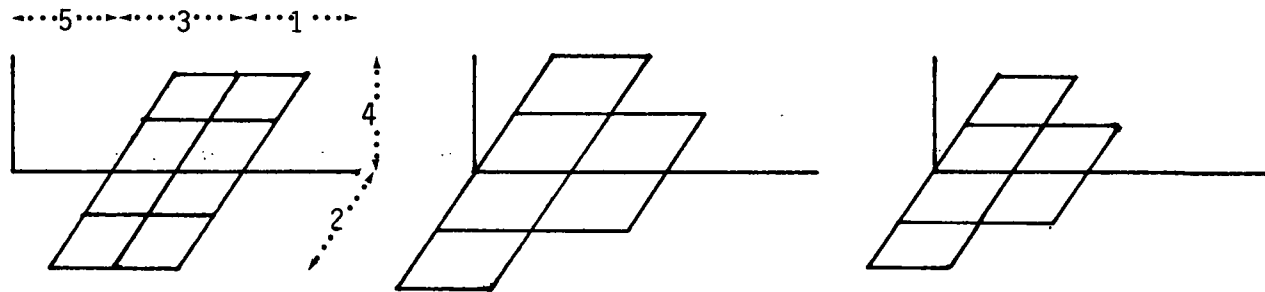
Model	A_1	A_2	B_1	B_2	C_1	C_2
Length (Radius)		*	#	*	#	*
Charge eqn		(4')	(4)	(4')	(4)	(4')
l_1 (1.00)		9.20	6.48		10.10	
l_2 (0.25)		5.84	5.84		3.89	
l_3 (0.25)		5.43	10.86		7.24	
(1.00)						
l_4 (1.48)		3.96	----		3.96	
l_5 (1.00)		4.72				

\# = simple charge junction condition $Q_i = Q_j$

* = frequency dependent charge condition $\Psi_i \, Q_i = \Psi_j \, Q_j$

Figure 13. Wire-Mesh Model Parametric Values.
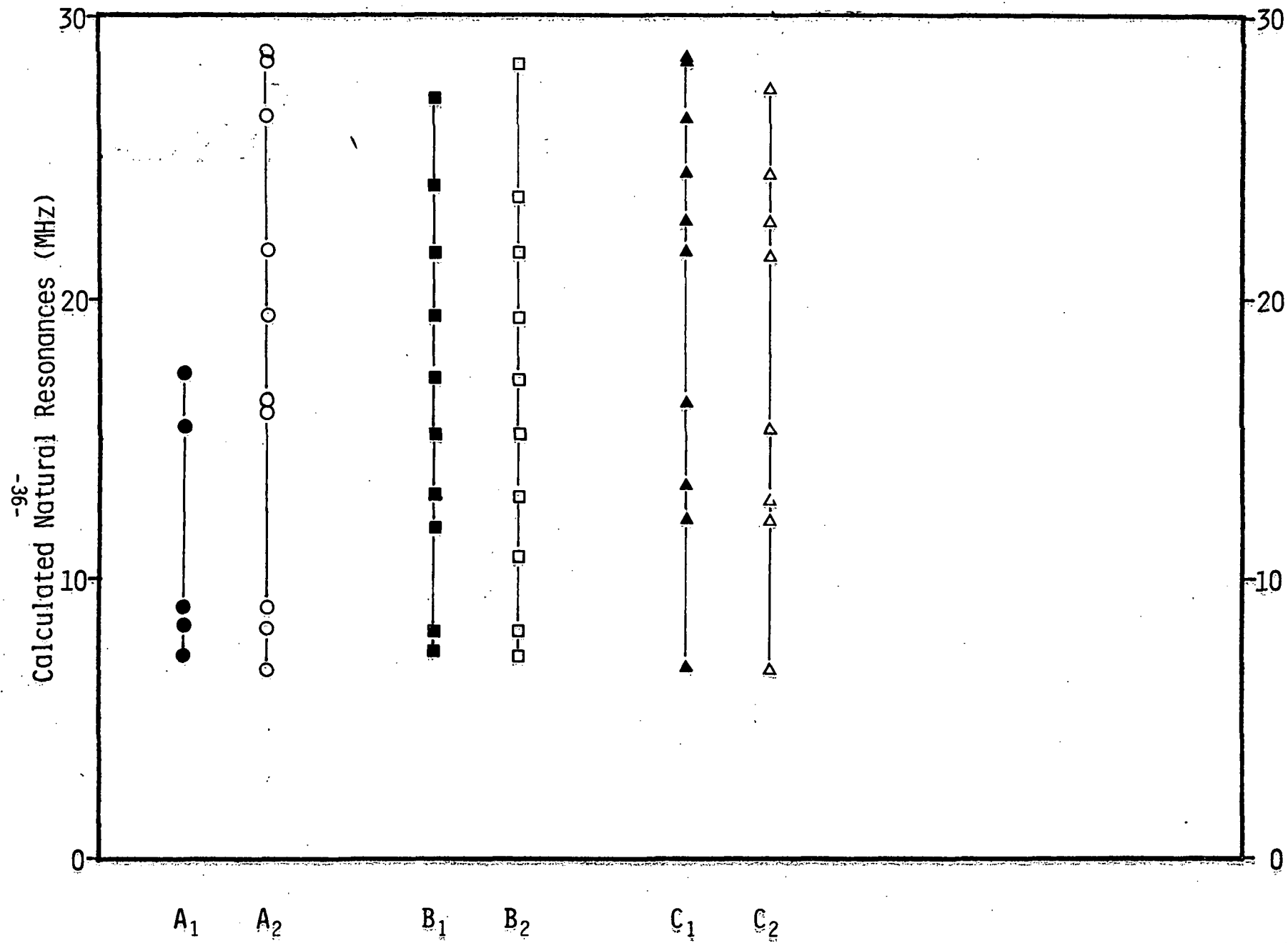
Figure 14. Resonances Corresponding to Wire-Mesh Models of Figure 13.

-36-

Calculated Natural Resonances (MHz)

30

Fuselage

Wings & Tail

20

Fuselage

Wings & Tail

10

Fuselage

0

-37-
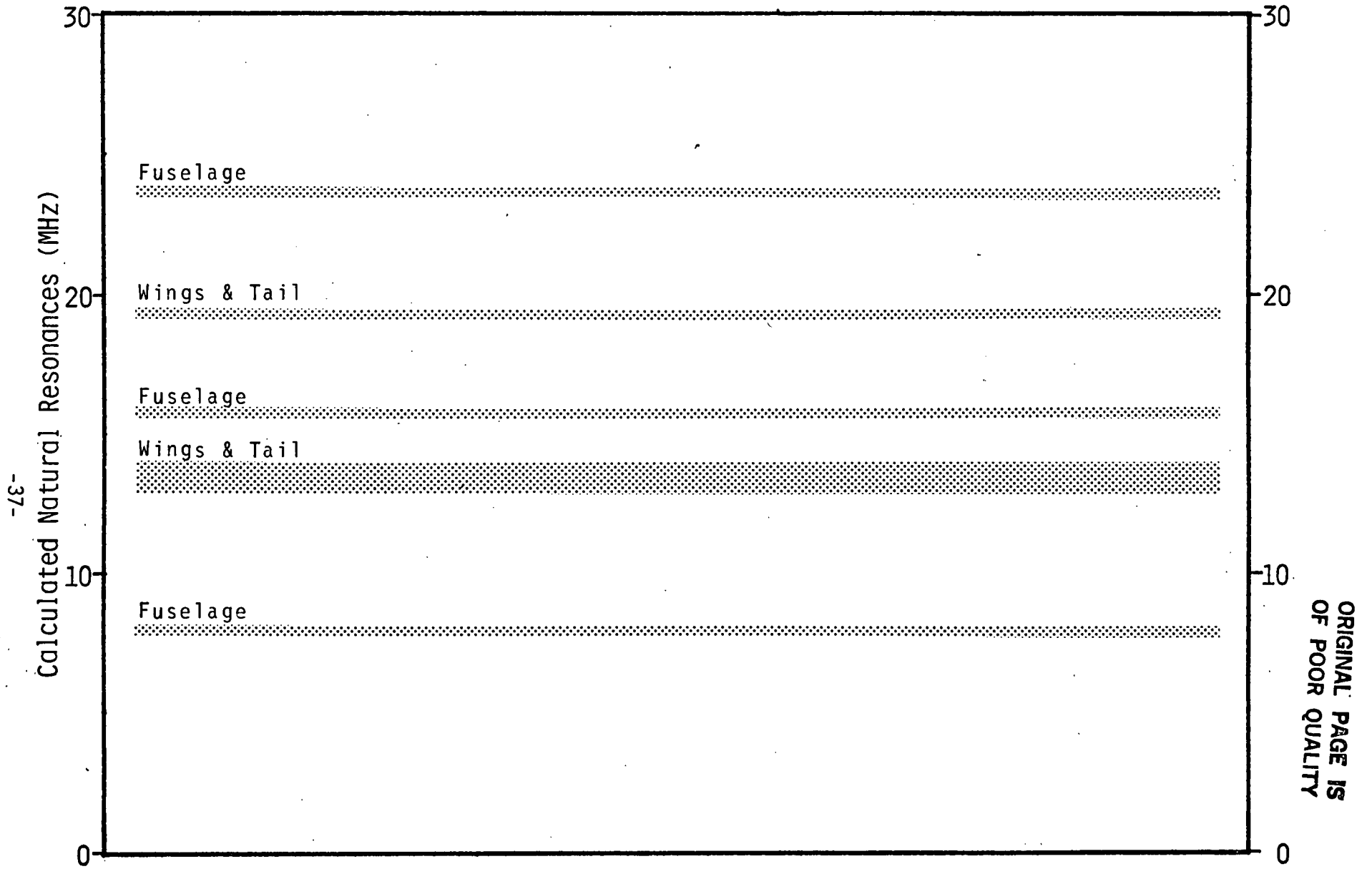
Figure 15.　Scale Model Data [Reference 13].

SECTION IV

DATA PROCESSING TECHNIQUES FOR LIGHTNING DATA INTERPRETATION

A. Overview

As mentioned earlier, the approach taken for the interpretation of direct strike lightning data is to first process the measured data, identify the natural resonances in the response which are due to the aircraft, and remove these from the data, with the remainder being a measure of the unperturbed lightning current. In this section, details of this procedure are discussed, and the feasibility of doing this with real lightning data is investigated. In addition, the processed 1981 data are presented in the Appendix.

B. Data Analysis Techniques

There are two methods useful for calculating the dominant frequencies of a lightning data record. They are the fast Fourier transform (FFT) [16] and the Prony algorithm [12,13]. The FFT performs a fast calculation of the spectral contribution F_k at a number of discrete frequencies of an N-point real data sequence f_n, using the formula

$$F_k = \sum_{n=0}^{N-1} f_n \, e^{-j2\pi nk/N} \qquad (k = 0, 1, \ldots, N-1) \qquad (28)$$

Frequently, zero-padding of the real data interpolates the spectral values and smoothes the appearance of the spectrum in frequency-domain. A peak in the spectrum indicates a dominant frequency, or pole, and the damping constant, σ, is related to the Q of the measured resonance. In most practical applications, it is fairly easy to determine the resonant frequency from the FFT spectral data, but the damping constant is more difficult to determine.

An alternate approach in treating the measured data is to use the Prony method. This analysis extracts both the resonant frequency and the damping constants of the data, but suffers from numerous disadvantages, most notably a failure to inspire confidence in the results. A more

-38-

complete discussion of Prony analysis may be found in the literature and
a brief review of the theory is presented here for completeness.

For analysis of measured data using the Prony method, the data is
assumed to be a uniformly spaced sampling

$$\left\{ (t_i, y_i) \mid t_i = i \cdot \Delta t, \; y_i = f(t_i), \; i=0,\ldots,m-1 \right\}$$

of a time-domain waveform composed of N damped sinusoids, written as

$$f(t) = \sum_{k=1}^{N} R_k e^{s_k t} = \sum_{k=1}^{N} R_k e^{\sigma_k t} (\cos \omega_k t + j \sin \omega_k t) \qquad (29)$$

where s_k and R_k are complex poles and residues to be determined. The
"Prony order", N, or the number of assumed poles in the data, is limited
to m/2 to derive an invertible matrix, as is discussed in reference [4].

By defining $z_k = e^{s_k t}$, the Prony algorithm has a concise matrix
representation. Multiplying both sides of the original non-linear system
of equations

$$\begin{bmatrix} 1 & 1 & \cdots & 1 \\ z_1 & z_2 & & z_N \\ z_z^2 & z_2^2 & & z_N^2 \\ \vdots & \vdots & \ddots & \vdots \\ z_1^{m-1} & z_2^{m-1} & \cdots & z_N^{m-1} \end{bmatrix} \begin{bmatrix} R_1 \\ R_2 \\ R_3 \\ \vdots \\ R_N \end{bmatrix} = \begin{bmatrix} y_0 \\ y_1 \\ y_2 \\ \vdots \\ y_{m-1} \end{bmatrix} \qquad (30)$$

by the N x 2N matrix

$$\begin{bmatrix} \alpha_0 & \alpha_1 & \alpha_2 & \cdots & \alpha_{N-2} & \alpha_{N-1} & \alpha_N & 0 & 0 & \cdots & 0 \\ 0 & \alpha_0 & \alpha_1 & \cdots & \alpha_{N-3} & \alpha_{N-2} & \alpha_{N-1} & \alpha_N & 0 & \cdots & 0 \\ 0 & 0 & \alpha_0 & \cdots & \alpha_{N-4} & \alpha_{N-3} & \alpha_{N-2} & \alpha_{N-1} & \alpha_N & \cdots & 0 \\ \vdots & \vdots & \vdots & & \vdots & \vdots & \vdots & \vdots & \vdots & \ddots & \vdots \\ 0 & 0 & 0 & \cdots & 0 & \alpha_0 & \alpha_1 & \alpha_2 & \alpha_3 & \cdots & \alpha_N \end{bmatrix} \qquad (31)$$

on the left yields the following matrix equation:

$$
\begin{bmatrix}
P(Z_1) & P(Z_2) & \cdots & P(Z_N) \\
Z_1 P(Z_1) & Z_2 P(Z_2) & \cdots & Z_N P(Z_N) \\
Z_1^2 P(Z_1) & Z_2^2 P(Z_2) & \cdots & Z_N^2 P(Z_N) \\
\vdots & \vdots & \ddots & \vdots \\
Z_1^{N-1} P(Z_1) & Z_2^{N-1} P(Z_2) & \cdots & Z_N^{N-1} P(Z_N)
\end{bmatrix}
\begin{bmatrix}
R_1 \\
R_2 \\
R_3 \\
\vdots \\
R_N
\end{bmatrix}
=
\begin{bmatrix}
\sum\limits_{K=0}^{N} \alpha_k y_k \\
\sum\limits_{K=0}^{N} \alpha_k y_{k+1} \\
\sum\limits_{K=0}^{N} \alpha_k y_{k+2} \\
\vdots \\
\sum\limits_{K=0}^{N} \alpha_k y_{k+N-1}
\end{bmatrix}
\tag{32}
$$

Since the z_k's are roots of a polynomial

$$
\begin{aligned}
P(z) &= (z-z_0)(z-z_1)..(z-z_{N-1}) \\
&= \alpha_N z^N + \alpha_{N-1} z^{N-1} + \ldots + \alpha_0
\end{aligned}
\tag{33}
$$

where $\alpha_N = 1$ without loss of generality, the left hand matrix vanishes, leaving the system of equations as

$$
\begin{bmatrix}
y_0 & y_1 & y_2 & \cdots & y_{N-1} \\
y_1 & y_2 & y_3 & \cdots & y_N \\
\vdots & \vdots & \vdots & \ddots & \vdots \\
y_{N-1} & y_N & y_{N+1} & \cdots & y_{2N-2}
\end{bmatrix}
\begin{bmatrix}
\alpha_0 \\
\alpha_1 \\
\vdots \\
\alpha_{N-1}
\end{bmatrix}
=
\begin{bmatrix}
y_N \\
y_{N+1} \\
\vdots \\
y_{2N-1}
\end{bmatrix}
\tag{34}
$$

which may be solved for the coefficients α_k. Once these are determined, the roots of Eq.(33) may be determined, and the poles and residues calculated.

The major drawback of the Prony algorithm is that several parameters must be chosen carefully to obtain "reliable" results. The assumed number of degrees of freedom (Prony order) N and sampling rate Δt determine a "window" of data points of width $2N\Delta t$. If this window is too small the waveform is not fairly represented by the data points. If the sampling rate Δt is less than twice the frequency of the highest pole then aliasing can occur, in the same manner as with the discrete Fourier transform. If the order is too small, the resulting poles are incorrect, but too large an order causes incorrect "curve-fitting" poles to be given.

Even if these parameters are varied until the poles are consistent, the only way to check them is by reconstruction of a waveform from its Prony representation, and then comparing the time domain response with the measured data. In some cases the inclusion of poles with positive real parts improves the reconstruction, despite their lack of physical significance. Such poles arise not only from assuming too large an order but also from the shape of the waveform in the window.

C. Selected Numerical Results

In order to assess the feasibility of using the Prony method in the analysis of the NASA lightning data, a computer program was written in BASIC to execute to perform the previously described calculations. This code used Gaussian elimination to solve for the coefficients α_k and residues R_k and the Muller algorithm to calculate the complex roots of the polynomial $P(z)$. This section discusses the processing performed on the various data records.

As an example of a typical data record, Figure 16a is the response of a D-dot sensor located at the forward fuselage of the aircraft, as illustrated in reference [2]. This particular record was for Flight 81-026, Record 10, which was excited by a nearby lightning strike on 7/1/81. As a result, it is expected that the aircraft resonances in the measured data will be those of the isolated aircraft. Figure 16b shows the corresponding frequency domain spectrum for this data record as calculated by the FFT. Note that there are several resonances which are
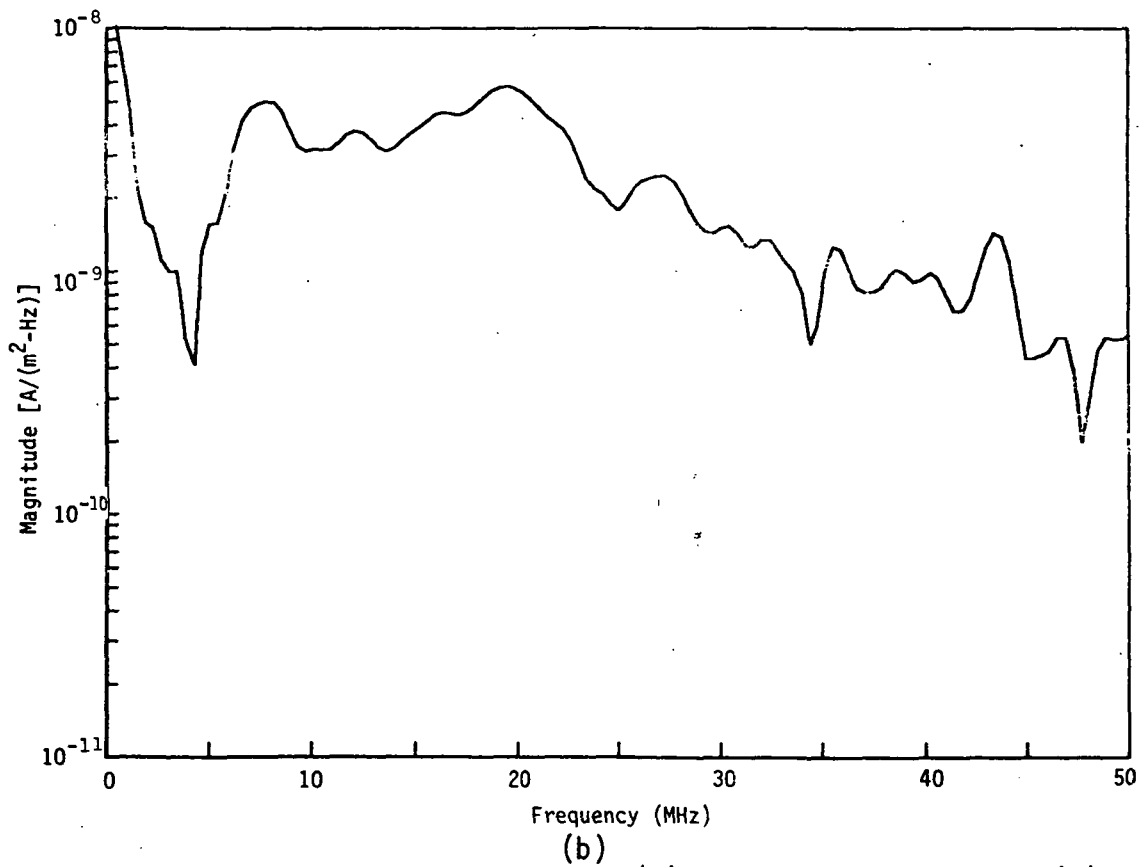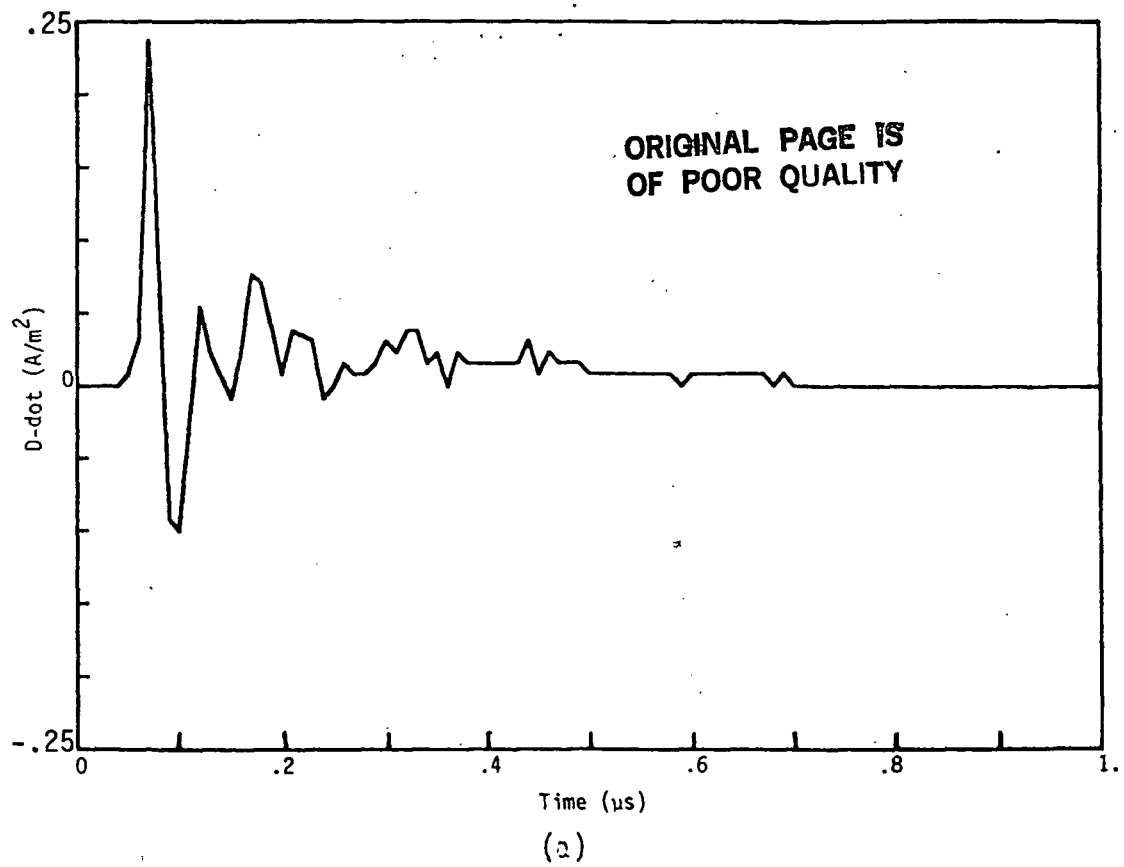
Figure 16. Plot of Time History (a) and Fourier Transform (b) of D-dot Response for Flight 81-026-10.

in the 6 to 20 Mhz region and which correspond to the aircraft resonances.

Table II illustrates the various resonant frequencies for this data record as determined from an examination of the spectral response. Note that this table shows the various peak values in increasing frequency, as well as ordered according to their magnitudes. The resonances at 7.8, 12.1, 16.4, and 19.5 Mhz appear to agree reasonably well with those given in reference [4] for the nearby strike excitation.

For the Prony processing of the lightning data, a sliding window technique was used to help identify aircraft resonances. Poles which appear in several different windows are more likely due to aircraft resonance than to the lightning. The amount of interpolation, movement and size of the window, and Prony order were varied for each data trace. Since the order is unknown for lightning data (but limited by computer time and memory) a maximum of 30 poles was requested. Initially the window was located after the largest spike, and was backed up to include it. As an example, Table III presents the Prony poles and residues for the sample data record presented in Figure 16a. It is to be noted that these data include both the physical (aircraft) poles, as well as the nonphysical, curve-fitting poles. In order to reduce the number of Prony poles in the data, the order was decreased until the calculated poles appeared to lose physical significance (see criteria below).

For low frequencies, the Laplace transform of the assumed form of the measured response along the $j\omega$ axis is given by

$$F(j\omega) = \sum \frac{R_k}{-j\omega - s_k} \qquad (35)$$

and at low frequencies, this becomes

$$F(j\omega) \cong -\sum \frac{R_k}{s_k} \qquad (36)$$

A measure of the importance of the contribution of any pole to the response is thus given by the magnitude of the ratio R_k/s_k. The prony poles were thus ranked according to this ratio.

TABLE II
PEAK VALUES OF FFT SPECTRUM FOR DATA RECORD 81-026-10

* Relative peak height for this run -- .01 *
* Bounds set for this run : 2 to 50 Mhz *
* Min pt --   47.66 MHz , 2.00E-03 amplitude *

* Increasing frequency representation *

* # *	* MHz *	* amplitude *
1	3.52	1.00E-02
2	7.81	5.04E-02
3	10.16	3.21E-02
4	12.11	3.81E-02
5	16.41	4.53E-02
6	19.53	5.79E-02
7	27.34	2.49E-02
8	30.47	1.55E-02
9	32.03	1.36E-02
10	35.55	1.28E-02
11	38.67	1.03E-02
12	40.23	9.89E-03
13	43.36	1.45E-02
14	46.88	5.39E-03
15	48.83	5.41E-03
16	50.00	5.43E-03

* Decreasing amplitude representation *
* the 10 highest peaks *

* # *	* MHz *	* amplitude *	* % *
1	19.53	5.79E-02	100.00
2	7.81	5.04E-02	87.02
3	16.41	4.53E-02	78.24
4	12.11	3.81E-02	65.78
5	10.16	3.21E-02	55.36
6	27.34	2.49E-02	43.06
7	30.47	1.55E-02	26.73
8	43.36	1.45E-02	25.06
9	32.03	1.36E-02	23.42
10	35.55	1.28E-02	22.05

TABLE III
PRONY POLES AND RESIDUES FOR DATA RECORD 81-026-10

#	POLES damping	freq(MHz)	RESIDUES real	imag	RES/POL	%
1	-2.056	0.000	0.341	0.000	1.66E-01	100.00
2	-19.586	-0.000	-0.374	-0.000	1.91E-02	11.51
3	-8.703	7.490	0.476	-0.288	1.16E-02	7.01
4	-8.703	-7.490	0.476	0.288	1.16E-02	7.01
5	-14.873	-19.959	-0.593	-1.027	9.39E-03	5.66
6	-14.873	19.959	-0.593	1.027	9.39E-03	5.66
7	-16.513	10.401	0.484	0.207	7.82E-03	4.71
8	-16.513	-10.401	0.484	-0.207	7.82E-03	4.71
9	-9.458	26.314	-0.028	0.203	1.24E-03	0.75
10	-9.458	-26.314	-0.028	-0.203	1.24E-03	0.75
11	-12.318	-41.188	-0.179	-0.009	6.90E-04	0.42
12	-12.318	41.188	-0.179	0.009	6.90E-04	0.42
13	-4.583	-13.286	-0.019	-0.054	6.80E-04	0.41
14	-4.583	13.286	-0.019	0.054	6.80E-04	0.41
15	-3.992	-43.414	-0.077	0.078	4.00E-04	0.24
16	-3.992	43.414	-0.077	-0.078	4.00E-04	0.24
17	-2.795	16.949	-0.000	0.026	2.46E-04	0.15
18	-2.795	-16.949	-0.000	-0.026	2.46E-04	0.15
19	3.652	-2.846	0.003	0.000	1.92E-04	0.12
20	3.652	2.846	0.003	-0.000	1.92E-04	0.12
21	-2.562	33.929	-0.028	-0.003	1.34E-04	0.08
22	-2.562	-33.929	-0.028	0.003	1.34E-04	0.08
23	-1.866	22.036	-0.007	0.017	1.32E-04	0.08
24	-1.866	-22.036	-0.007	-0.017	1.32E-04	0.08
25	-1.285	28.838	-0.009	-0.007	6.30E-05	0.04
26	-1.285	-28.838	-0.009	0.007	6.30E-05	0.04
27	-0.949	47.079	-0.005	0.015	5.36E-05	0.03
28	-0.949	-47.079	-0.005	-0.015	5.36E-05	0.03
29	1.048	-36.284	-0.002	0.007	3.14E-05	0.02
30	1.048	36.284	-0.002	-0.007	3.14E-05	0.02

The poles must be purely real or occur in conjugate pairs, but the Prony algorithm is very sensitive to noise in the data [12,13], so that poles which were not precisely complex conjugates were noted in some cases. Poles in the tabulated data were rejected if they met any of the following criteria:

Criterion	Reasons
1. Real part of pole positive	No physical significance
2. Complex conjugates not found	Numerical error, noise, and curve-fitting
3. Frequency $\omega/2\pi$ too high	Aliasing
4. Residue-to-pole ratio too small	Contribution to F(s) insignificant

Table IV presents the selected Prony poles and residues for the data record of Figure 16. Note that the complex conjugate poles are not listed explicitly in this table. The pole pairs 3, 4, 5 and 8 correspond approximately to those aircraft resonances identified in the FFT spectrum.

As previously mentioned, it is useful to observe the convergence of the numerically constructed Prony response as a function of the number of poles taken in the response. Figure 17a shows the reconstructed time domain response for the data record corresponding to Flight 81-026, Record 10. This reconstruction involves the first two real poles and the first complex pole pair tabulated in Table IV. Figure 17b presents the reconstructed waveform for 8 poles, and Figure 17c shows similar results for 18 poles. Figure 18 presents an overlay of the original time domain measured data with the Prony reconstruction of the data. As may be noted, the agreement is reasonable.

The reconstructed Fourier spectrum of this data is shown in Figure 19. Note that Prony reconstruction compares reasonably well with the FFT calculated spectrum, with the exception of the high frequency response. The poor comparison at the high frequencies is possibly due to the effects of aliasing in the FFT calculation. In the aircraft resonance region, however, the two calculations agree well.

TABLE IV
FILTERED PRONY POLES AND RESIDUES FOR DATA RECORD 81-026-10

* Filename --- d8102610 * dt =0.010 *
* Window 0 * 30 poles * t = .04 to .64 μs *

Pole Pair	Prony damp.	Pole freq(MHz)	Prony real	Residue imag	Residue pole	%
1	-2.06	0.0	0.341	0.0000	0.166	100.00
2	-19.59	0.0	-0.374	0.0000	0.019	11.51
3	-8.70	7.5	0.476	-0.2885	0.012	7.01
4	-14.87	20.0	-0.593	1.0272	0.009	5.66
5	-16.51	10.4	0.484	0.2070	0.008	4.71
6	-9.46	26.3	-0.028	0.2033	0.001	0.75
7	-12.32	41.2	-0.179	0.0093	0.001	0.42
8	-4.58	13.3	-0.019	0.0538	0.001	0.41
9	-3.99	43.4	-0.077	-0.0778	0.000	0.24

* 14 of 30 poles rejected.

Figure 17.   Reconstruction of D-dot Data Using Various Numbers
of Prony Poles.
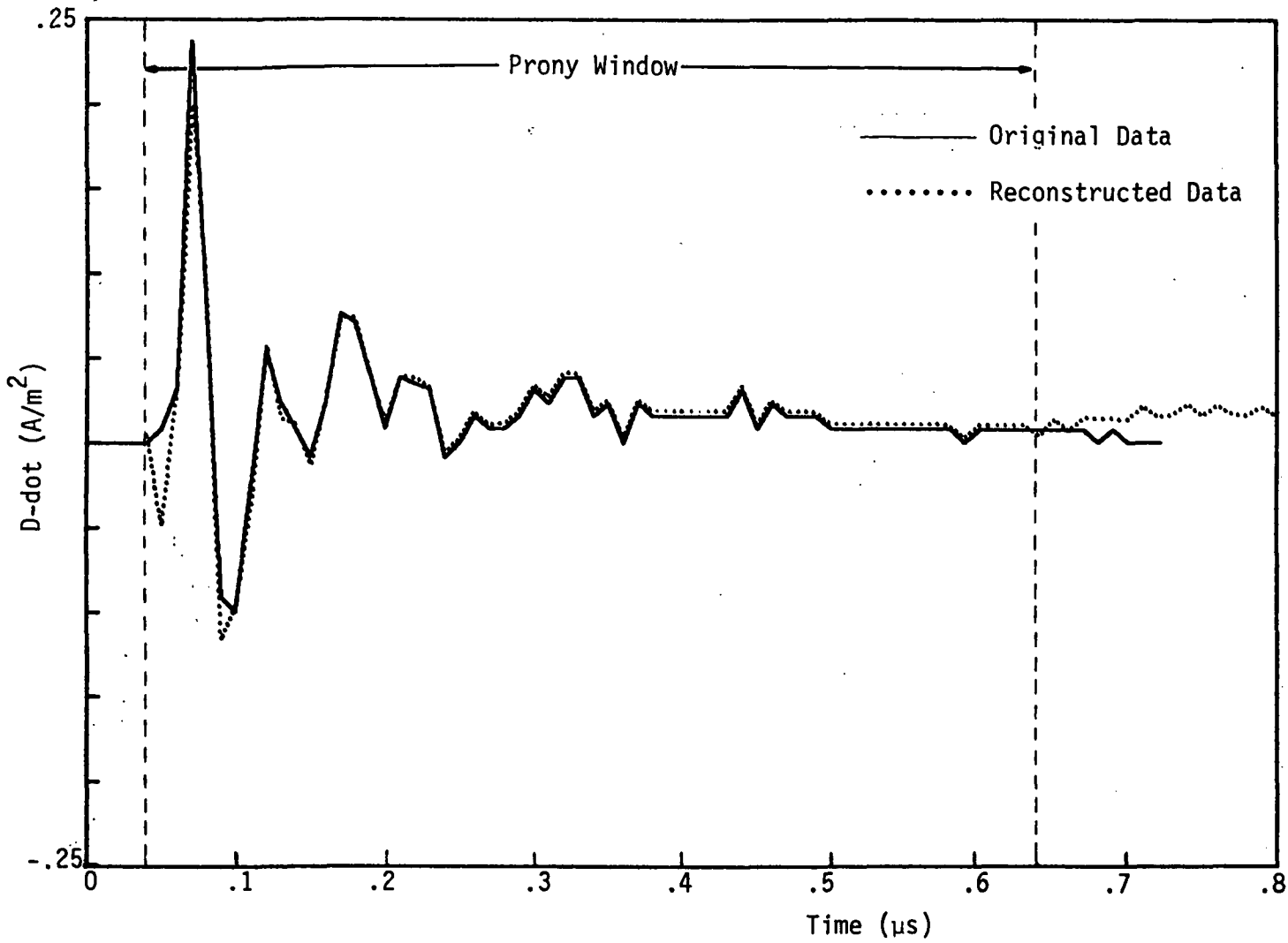
Figure 18.   Comparison of Reconstructed D-dot Data with Measured Data.
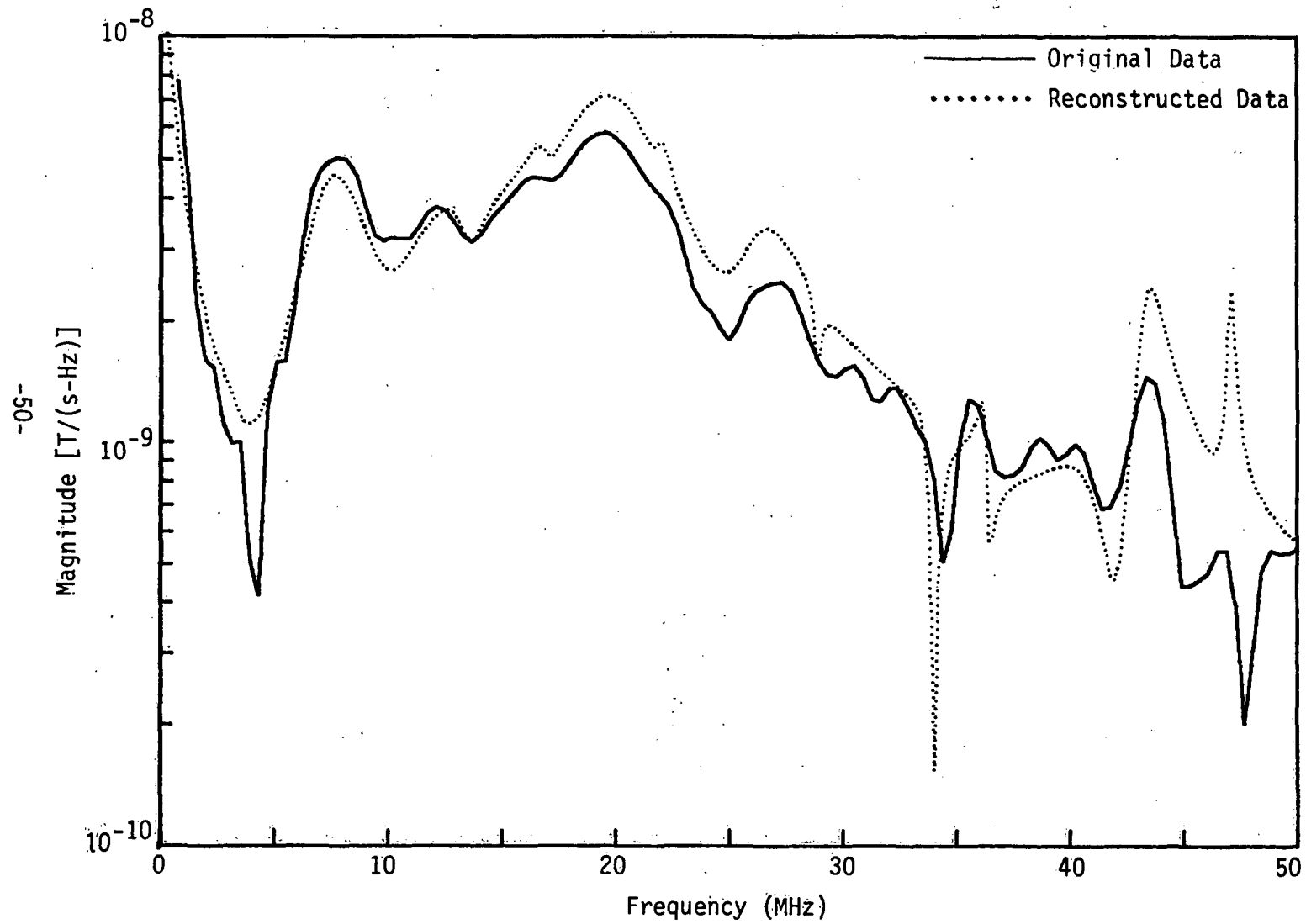
Figure 19. Comparison of Reconstructed D-dot Spectral Response with FFT Response

Figure 20a illustrates another type of data obtained in the NASA direct strike program. This is a B-dot measurement for Flight 81-043, Record 2, performed at the mid-fuselage position of the aircraft, and oriented in such a way that the sensor measures the longitudinal current. Furthermore, this particular data record involved a direct strike to the aircraft.

Figure 20b shows the corresponding FFT spectrum for this direct strike data record. It may be observed that several of the lowest resonances have shifted downward in frequency when compared with the spectrum in Figure 16b, a fact that is attributable to the addition of the lightning channel to the aircraft. For this data record, the various peaks in the FFT spectrum are presented in Table V.

The application of the Prony processing techniques to this data set provides the poles and residues shown in Table VI. Upon suitable filtering in order to remove the unphysical poles, the pole pairs presented in Table VII remain, and may be identified as arising from the lightning current and the aircraft resonances.

From the Prony pole data presented for the nearby strike D-dot measurement in Table IV and those for the direct strike B-dot measurement in Table VII, it is possible to infer the behavior of the unperturbed lightning by identifying the aircraft resonances and removing them from the reconstructed response. For example, if we assume that all oscillatory contributions in the response arise from the aircraft, it is possible to remove them, and reconstruct the responses shown in Figures 21 and 22. Note that the D-dot response for the nearby excitation shown in Figure 21 is not as large as is that for the B-dot response for the direct strike shown in Figure 22. This is presumably due to the fact that there is much more of a contribution of the lightning characteristics in the direct strike data.

ORIGINAL PAGE IS
OF POOR QUALITY
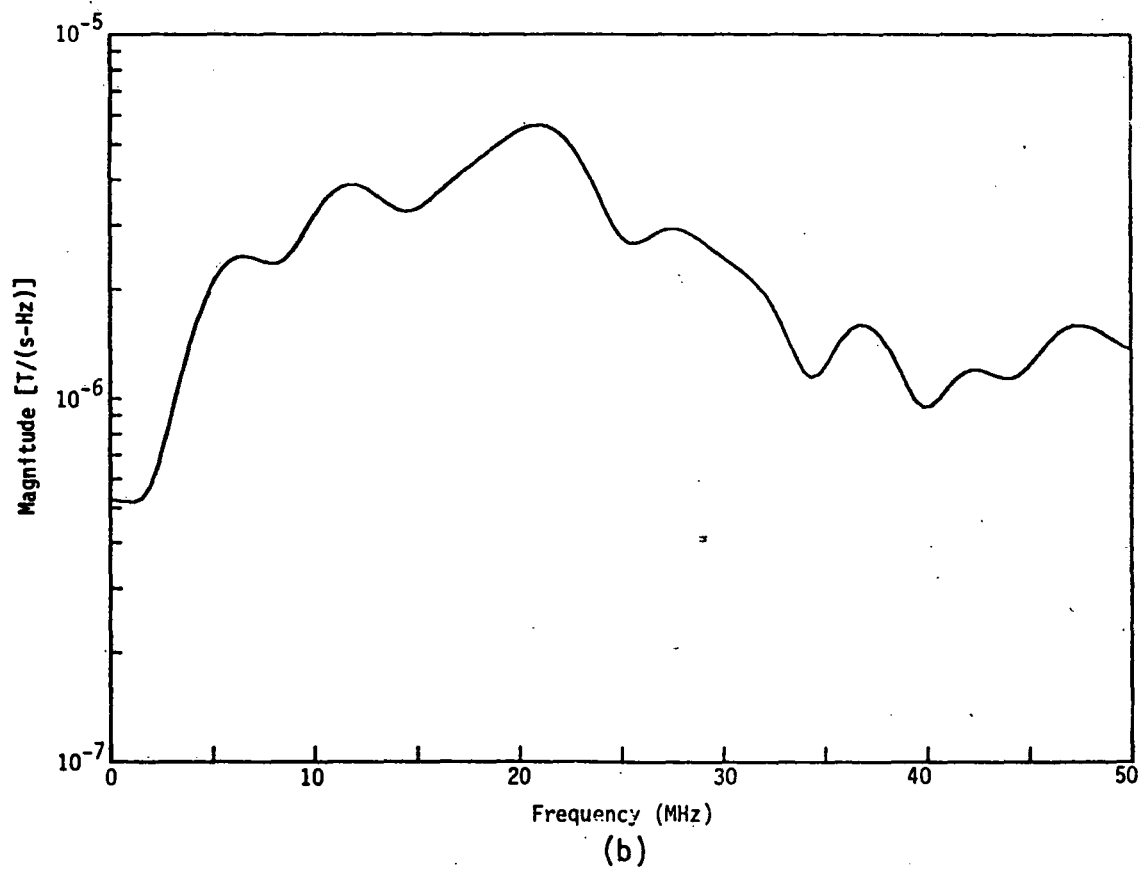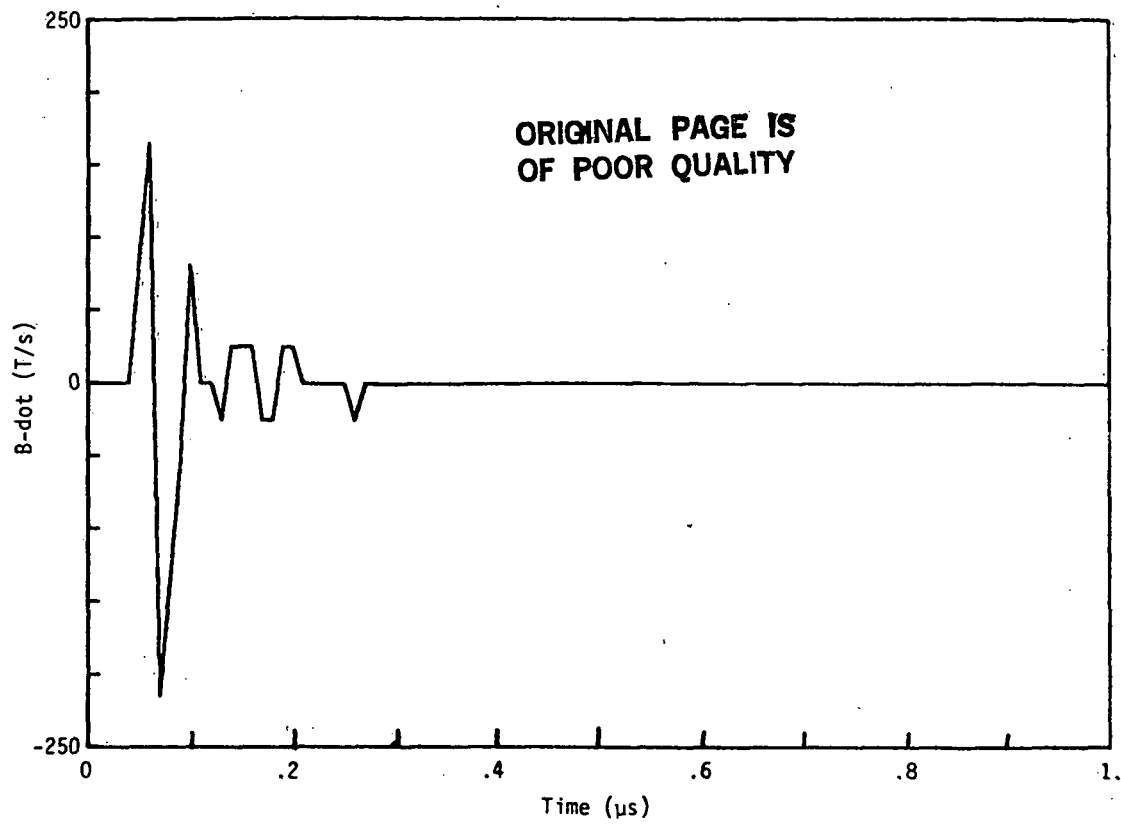
Figure 20. Plot of Time History (a) and Fourier Transform (b)
of B-dot Response for Flight 81-043-02.

TABLE V
PEAK VALUES OF FFT SPECTRUM FOR DATA RECORD 81-043-02

* Relative peak height for this run -- .01 *
  * Bounds set for this run : 0 to 50 Mhz *
* Min pt --   1.17 MHz , 5.17E-01 amplitude *

* Increasing frequency representation *

* # *	* MHz *	* amplitude *
1	0.00	5.25E-01
2	6.64	2.46E+00
3	11.72	3.88E+00
4	21.09	5.65E+00
5	27.73	2.93E+00
6	36.72	1.59E+00
7	42.19	1.20E+00
8	47.27	1.59E+00
9	50.00	1.37E+00

* Decreasing amplitude representation *
* the 9 highest peaks *

* # *	* MHz *	* amplitude *	* % *
1	21.09	5.65E+00	100.00
2	11.72	3.88E+00	68.68
3	27.73	2.93E+00	51.87
4	6.64	2.46E+00	43.56
5	36.72	1.59E+00	28.17
6	47.27	1.59E+00	28.17
7	50.00	1.37E+00	24.19
8	42.19	1.20E+00	21.20
9	0.00	5.25E-01	9.30

TABLE VI
PRONY POLES AND RESIDUES FOR DATA RECORD 81-043-02

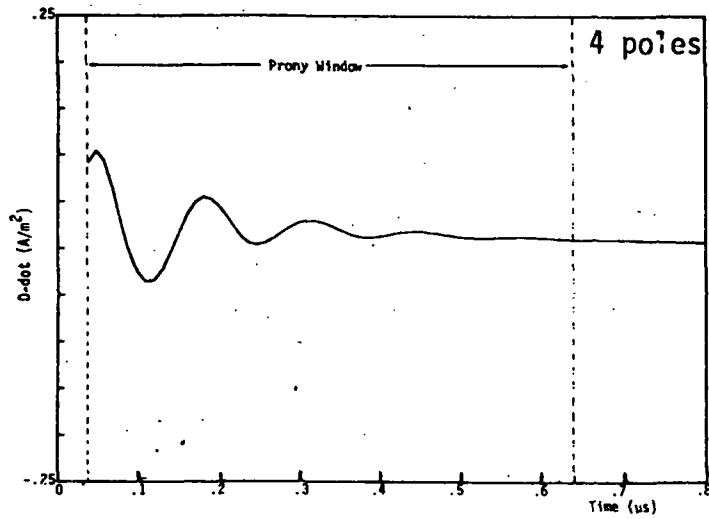| #	POLES damping	freq(MHz)	RESIDUES real	imag	RES/POL	%
1	-34.479	0.000	100.820	-0.000	2.92E+00	100.00
2	-27.138	-5.793	-19.314	-114.907	2.57E+00	87.77
3	-27.138	5.793	-19.314	114.907	2.57E+00	87.77
4	-17.256	-21.306	-55.921	99.674	8.47E-01	28.96
5	-17.256	21.306	-55.921	-99.674	8.47E-01	28.96
6	-13.906	-49.103	48.477	42.336	2.08E-01	7.13
7	-13.906	49.103	48.477	-42.336	2.08E-01	7.13
8	-13.619	28.138	-25.078	-17.827	1.74E-01	5.93
9	-13.619	-28.138	-25.078	17.827	1.74E-01	5.93
10	0.298	10.825	2.621	3.903	6.91E-02	2.36
11	0.298	-10.825	2.621	-3.903	6.91E-02	2.36
12	6.223	-36.407	-1.194	-0.219	5.30E-03	0.18
13	6.223	36.407	-1.194	0.219	5.30E-03	0.18

TABLE VII
FILTERED PRONY POLES AND RESIDUES FOR DATA RECORD 81-043-02

* Filename --- b810432 * dt =0.010 *
* Window 0 * 13 poles * t = .04 to .3 us *

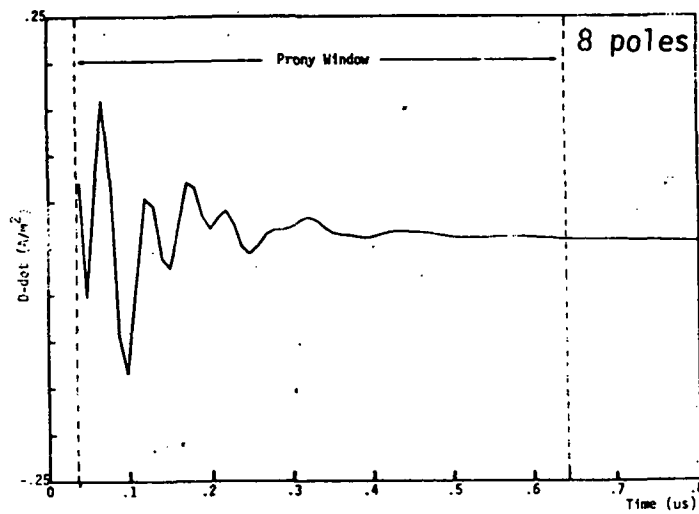| Pole Pair	Prony damp.	Pole freq(MHz)	Prony real	Residue imag	Residue pole	%
1	-34.48	0.0	100.820	-0.000	2.924	100.00
2	-27.14	5.8	-19.314	114.907	2.566	87.77
3	-17.26	21.3	-55.921	-99.674	0.847	28.96
4	-13.91	49.1	48.477	-42.336	0.208	7.13
5	-13.62	28.1	-25.078	-17.827	0.174	5.93

* 4 of 13 poles rejected. *

Figure 21. Processed D-dot Data for Flight 81-026-10.
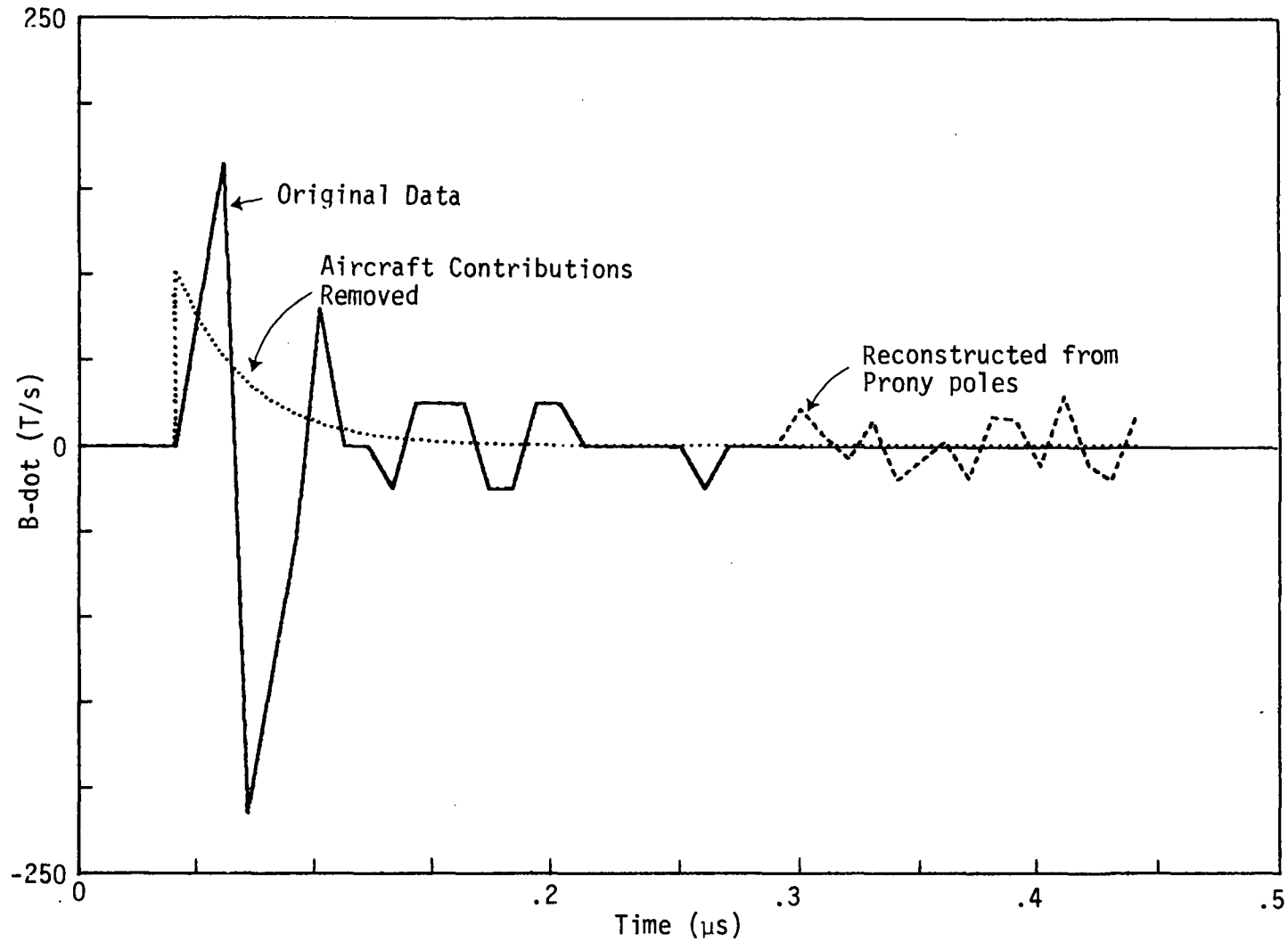
Figure 22. Processed B-dot Data for Flight 81-043-02.

D. Description of Processed Data

The above discussion has described a technique for analyzing the NASA lightning data for the purpose of determining the characteristics of the exciting lightning bolt. As may be seen from the B-dot and D-dot examples, it is necessary to identify which of the Prony poles in the measured response arise from the aircraft interaction, and which are inherent in the lightning response. In the examples, it was assumed that all of the oscillatory resonances were from the aircraft, but it is not clear that this is correct. It is possible to conceive of having oscillations in the lightning channel as well.

Furthermore, the accurate analysis of data of this type requires a better knowledge of the response transfer impedance as discussed in Section II. For nearby strikes, this implies needing to know where the strike occurred in relation to the aircraft. For the direct strike case, a knowledge of the attachment and detachment points is similarly needed. In much of the present lightning data, the required details of the strikes are not available for further analysis. However, the 1981 lightning data have been processed to yield the pertinent pole and residue data which describe their behavior. These data are presented in the Appendix.

Appendix A presents the time domain measurements for 1981. These data have been digitized, and processed with an FFT algorithm, with the results also being displayed. Note that no attempt has been made to integrate these data to provide B or D information. Along with each data trace, the peak values in the frequency domain for the FFT data are given. These were computed by simply searching the FFT records for the various peaks and ranking them by frequency and magnitude. The results of the Prony processing of these data are also presented in this Appendix. Note that the poles and residues for several different sliding time windows are presented, and any unphysical poles have been filtered out using the previously discussed criteria.

SECTION V
EXPERIMENTAL CONSIDERATIONS

The F-106 aircraft was instrumented to measure B-dot and D-dot for both the direct attachment and nearby lightning phenomena. Some of the in-flight data have been processed in the previous section IV and the "free" resonances computed in Section III. In this section, we describe a full scale experimental procedure, in which the aircraft was excited by a two-wire transmission line field with the objective of determining its natural resonances.

During the week of March 29, 1982, a ground lightning simulation test was performed by MCAIR with the assistance of LuTech personnel. One of the objectives of this series of experiments was to attempt the simulation of a nearby lightning stroke on an aircraft. Since the precise spatial and spectral or temporal characteristics of the lightning phenomenon are not well understood, our approach was to excite the isolated F-106B aircraft with a known electromagnetic field and experimentally obtain its response with D-dot sensors placed at several locations on the aircraft. From these measurements, one can extract the natural frequencies of the aircraft. The natural frequencies are independent of the nature of the incident or the exciting field in this case, since the source of the electromagnetic field and the aircraft as a scattering object are physically removed from each other. This is in contrast with the simulation of the direct strike with hardwired attachment, where in effect the source and the scatterer are physically connected. Such a configuration where the source and scatterer are in contact significantly impacts the natural frequencies of the scatterer.

Consequently, with the intent to obtain the natural frequencies of the aircraft and thus provide an experimental verification of prior calculations reported in Section III, a two-wire transmission line was designed. The aircraft, parked on ground is excited by the transmission line field and data is collected using the D-dot sensors and the data acquisition instrumentation. The raw time domain data has been transformed into the frequency domain by using a fast Fourier transform (FFT) software package, built into the data acquisition system. The FFT results give a reasonable indication of the aircraft natural resonances.

A. Design Considerations and Description of the Experimental Setup.

Basically, the experiment consisted of a two-wire transmission line above ground. The transmission line was oriented such that the principal electric field was horizontal and parallel to the fuselage of the F-106B aircraft parked on ground. The two-wire transmission line is schematically shown in Figure 23. The wires have a diameter d, separated by a distance D, and both are above ground at a height h. The line was excited by a Marx generator at one end and terminated by a load resistance at the far end. In order to avoid the aircraft responding to the reflected wave after the main forward wave had traversed the width of the aircraft, it was essential to terminate the line in its matched or characteristic impedance. An unterminated or open circuited line would be prohibitively long to discriminate between the forward and reflected waves in the simulator. The characteristic impedance of the two-wire transmission line of Figure 23 is given by

$$Z_c = 276 \ \text{Log}_{10} \left\{ \frac{2D}{d} \bigg/ \left[1 + \left(\frac{D}{2h} \right)^2 \right]^{\frac{1}{2}} \right\}$$

$$= 120 \ \ln \left\{ \frac{2D}{d} \bigg/ \left[1 + \left(\frac{D}{2h} \right)^2 \right]^{\frac{1}{2}} \right\} \quad , \ \text{for} \ d << D, h \tag{37}$$

The parameter values used here, determined mainly by practical considerations, were

$$D = 40m \ , \quad h = 3.58m \ , \quad d = 2.4 \times 10^{-3}m \quad (12 \ \text{gauge})$$

These values yield a characteristic impedance of about 1060 Ohms. However, if one neglects the effects of the ground, a simpler formula for Z_c is given by

$$Z_c = 120 \ \ell n \ (2D/d) = 1250 \ \text{Ohms} \tag{38}$$
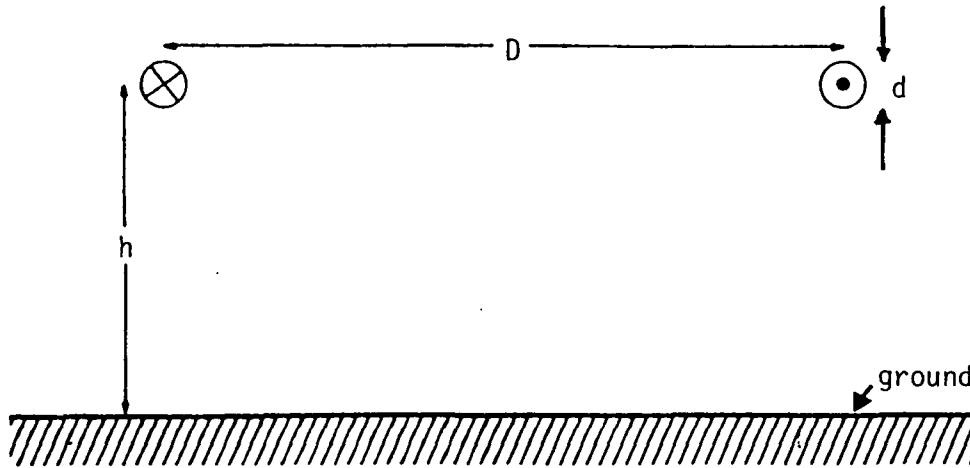
Figure 23. Two-wire transmission line above ground.

A resistor having this value was used and the resistance was constructed using a graphite fiber material. The fiber resistor was approximately 180 feet long with a resistance of about 7 ohms/foot. The same Marx generator employed in direct attachment simulation testing was used here. The two wires that form the transmission line were supported on wooden stands roughly 10 feet above ground. The wires were 12 gauge, multistranded and plastic coated. The effect of the plastic insulation was considered negligible. The 40m between the wires was about twice the aircraft length and insured a reasonably uniform excitation of the aircraft. Also, estimates were made of the expected levels of sensor pick up voltages given the Marx parameters. This indicated that one can record data with a reasonable signal to noise ratios.

B. Experimental Results

This section contains the complete set of experimental raw data collected, as indexed in Table VIII. The shot numbers are identified by the date (4/2/82) and a letter code (A, B, C, D ...). They are also identifiable by the track and file number for the cassette storage. If additional inductance is added to the Marx output for wave shaping, it is indicated in the index. The sensor type, location and attenuation are also indicated. The quantities measured are mainly D-dot at various locations and I-dot or I(t) from the Marx generator. In the section which follows the compilation of the raw data, we have examined the FFT data of selected shots.

TABLE VIII. INDEX OF EXPERIMENTAL DATA

Change Voltage - 45kV/stage
6 stages

F-106 TEST
DATE: 4/2/82

SHOT NO. TRK - FILE	ADDED INDUCTANCE	OUTPUT	TYPE	SENSORS MONITORED LOCATION		ATTN. - COMMENTS
4/2 CAL	RADIATED		$\dot{E}_M$			No signal
(actually 4/2A)	DOORS OPEN		--			
1-9			$\dot{D}_N$	L. WING	1x	The magnitudes for
			$\dot{D}_N$	R. WING	1x	these 3 sensors are
			$\dot{D}_N$	LF FUS.	2x	not calibrated exactly, but they should be close.
4/2 CAL 1-10	CALIBRATION					
4/2 CAL	RADIATED		$\dot{D}_N$	L. WING	1x	Memory Dropout
(actually 4/2B)	DOORS OPEN		--			
1-11			E_M	Near L. WING	25x	
			$\dot{D}_N$	R. WING	1x	Batteries Going Down
			$\dot{D}_N$	FUS.	2x	
4/2 C, D	RADIATED		$\dot{D}_N$	L. WING	1x	Memory Dropout
	DOORS OPEN		--			
1-12, 13			E_M	Near L. WING	25x	
			$\dot{D}_N$	R. WING	1x	Batteries
			$\dot{D}_N$	FUS.	2x	
4/2 E, F	RADIATED		--			Grounding Plug
	DOORS OPEN		--			attached to plane
0-0, 1			E_M	Near L. WING	25x	on these two shots,
			$\dot{D}_N$	R. WING	1x	and possibly, all shots
			$\dot{D}_N$	FUS.	2x	previous to this.
4/2 G	RADIATED		--			
	DOORS OPEN		--			
0-2			E_M	Near L. WING	25x	
			$\dot{D}_N$	R. WING	.5x	Changed from .2 to .1 Input Range
			$\dot{D}_N$	FUS.	1x	Changed from .2 to .1 Input Range

-63-

TABLE VIII. INDEX OF EXPERIMENTAL DATA (cont.)

ORIGINAL PAGE IS
OF POOR QUALITY

F-106 TEST

DATE: 4/2/82

SHOT NO. TRK - FILE	ADDED INDUCTANCE	OUTPUT	TYPE	SENSORS MONITORED		
				LOCATION	ATTN. -	COMMENTS
4/2 T-7 0-3	Replaced Transmitter 9 with Tran.			-7 - Stored a triangle wave to scale t		
4/2 H, I, J	RADIATED		--			
	DOORS OPEN		--			
0-4, 5, 6			E_M	Near L. WING	25x	
			$\dot{D}_N$	R. WING	.5x	
			$\dot{D}_N$	FUS.	1x	
4/2 K, L, M	RADIATED		--			
	DOORS CLOSED		--			
0-7, 8, 9			E_M	Near L. WING	25x	
			$\dot{D}_N$	R. WING	.5x	
			$\dot{D}_N$	FUS.	1x	
4/2 NF 0-10	Started using Nanofast fiber optic system on channel 3. Did not recalibrate. Stored a triangle wave to scale to. (.1V 0→ pk)					
4/2 N, O, P	RADIATED		--			
	DOORS OPEN		--			
0-11, 12, 13			$\dot{I}_M$		50x - 100x - 100x All saturated	
			$\dot{D}_N$	L. WING	.5x	
			$\dot{D}_N$	TAIL	1x	
4/2 Q, R, S, T	RADIATED		--			
	DOORS CLOSED		--			
0-14 1-0, 1, 2	(Second shot R didn't sound quite as loud as the rest. Generator problem)		$\dot{I}_M$ $\dot{D}_N$ $\dot{D}_N$	L. WING TAIL	500x .5x 1x	
4/2 U, V, W, X, Y	RADIATED		--			
	DOORS CLOSED		--			
1-3, 4, 5, 6, 7			$\dot{I}_M$ $\dot{D}_N$ $\dot{D}_N$	PCT - OUTPUT L. WING TAIL	50x .5x 1x	Current measured at generator output.

ABBREVIATIONS

Subscript N with sensor type means NASA sensor.

Subscript M with sensor type means MACAIR sensor.

$\dot{D}_N$ R. WING	-	NASA $\dot{D}$ sensor beneath right wing.
$\dot{D}_N$ L. WING	-	NASA $\dot{D}$ sensor beneath left wing.
$\dot{D}_N$ FUS.	-	NASA $\dot{D}$ sensor on lower forward fuselage.
$\dot{D}_N$ LF FUS.	-	Same as $\dot{D}_N$ FUS.
$\dot{D}_N$ TAIL	-	NASA $\dot{D}$ sensor on vertical stabilator.
$\dot{I}_M$	-	MACAIR $\dot{I}$ sensor.
$\dot{E}_M$	-	MACAIR E-field sensor.
DOORS OPEN	-	Cockpit and Bombay doors open.
DOORS CLOSED	-	Cockpit and Bombay doors closed.
I_M	-	MACAIR I sensor.
PCT	-	Pearson Current Transformer (This is the I_M).

SENSOR INFORMATION

NASA $\dot{D}$ sensors:

$$V_{OUT} = R \; Aeq \; \dot{D}$$

$$R = 50\Omega$$

$$Aeq = 4.1 \times 10^{-2} \; m^2 \text{ for NASA TAIL and FUS.}$$
$$\dot{D} \text{ sensors}$$

$$Aeq = 2.7 \times 10^{-2} \; m^2 \text{ for NASA L.WING and}$$
$$\text{R.WING } \dot{D} \text{ sensors}$$

MACAIR $\dot{I}$ sensor:

EG&G $V_{OUT} = M\dot{I}$

CPM-1A

I-DOT PROBE $M = 10^{-2} \; \mu H$

MACAIR I sensor:

PEARSON CURRENT TRANSFORMER
MODEL 3025

CALIBRATION: .025F/Amp
used into 50Ω input as in this test it becomes;
.0125V/Amp

MACAIR E-FIELD sensor:

CALIBRATION: 100 V/m/VOLT OUTPUT OF SENSOR

RADIATED // DOORS OPEN

Test: 4/2 Cal (A)
TRK File: 1-9
Notes
_____
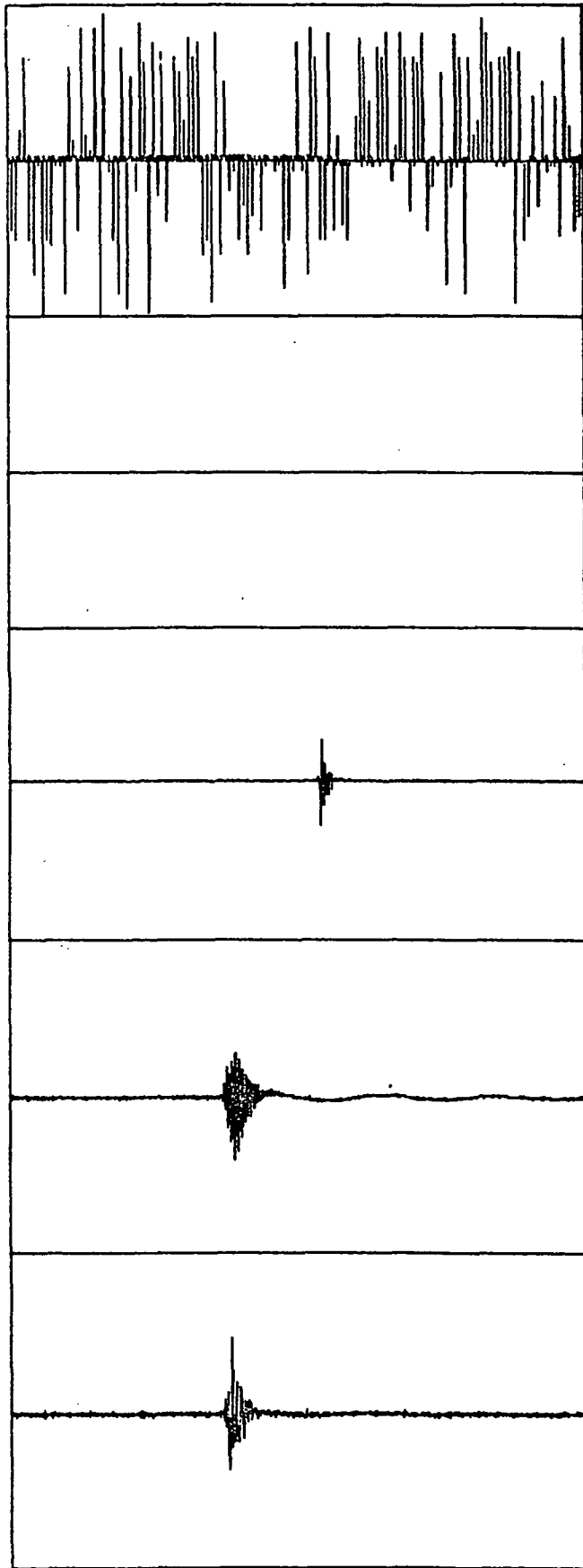
Type: E
Loc :
Attn: 250x
x   : 0 - 0   µs
y   : +/- 0.53   V
 min: V
 max: V

Type:
Loc :
Attn:
x   : 0 -   µs
y   : +/-   V
 min: V
 max: V

Type: D_N
Loc : L. Wing
Attn: 1x
x   : 0 - 0   µs
y   : +/- 0   V
 min: V
 max: V

Type: D_N
Loc : R. Wing
Attn: 1x
x   : 0 - 20   µs
y   : +/- 0.56   V
 min: -0.22   V
 max: 0.15   V

Type: D_N
Loc : Fus.
Attn: 2x
x   : 0 - 20   µs
y   : +/- 0.51   V
 min: -0.38   V
 max: 0.46   V

We probably had
calibrated at least
one time before this
shot but had not
stored it. (Else
the no. wouldn't
have come out in
this range.)
But I don't know
if the same trans-
mitters were left
in or if they might
have been adjusted.
Therefore, these
members are probably
in the right ballpark,
but I wouldn't
entirely trust them.

Test: 4/2 Cal (A)
TRK File: 1-10
Notes _____
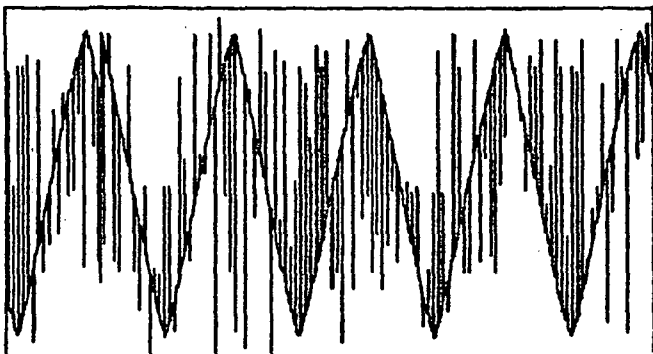
Type: T-1, R-3
Loc :
Attn:
x   : 0 - 0   μs
y   : +/- 0.53   V
 min: -0.53   V
 max: 0.50   V
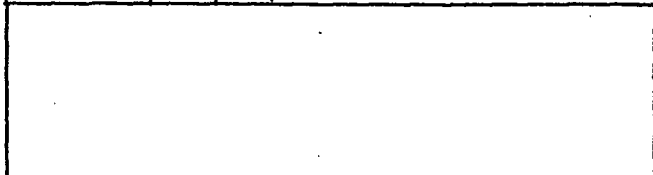
Type:
Loc :
Attn:
x   : 0 -   μs
y   : +/-   V
 min: V
 max: V
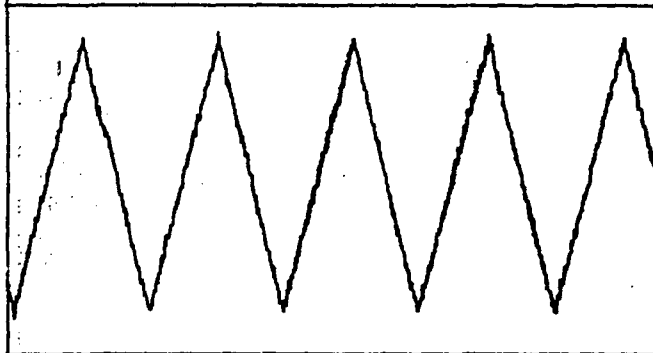
Type: T-4, R-1
Loc :
Attn:
x   : 0 - 100   μs
y   : +/- 0.10   V
 min: -.078   V
 max: .084   V

Cal. w/50Ω input.

Ran w/high impedance
input.
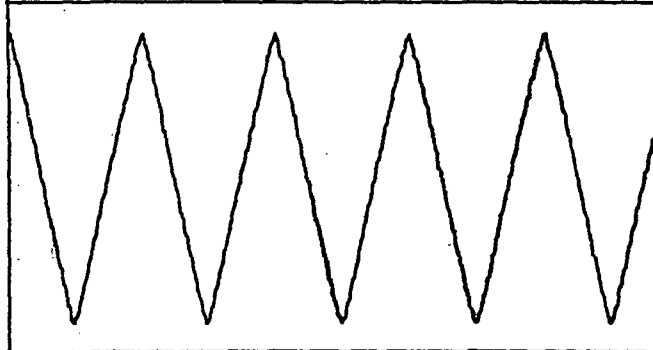
Type: T-5, R-4
Loc :
Attn:
x   : 0 - 100   μs
y   : +/- 0.60   V
 min: -0.51   V
 max: 0.50   V
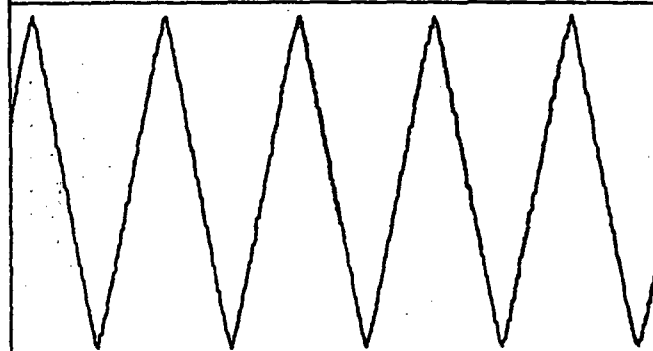
Type: T-9, R-5
Loc :
Attn:
x   : 0 - 100   μs
y   : +/- 0.54   V
 min: -0.52   V
 max: 0.50   V

Test: 4/2 Cal (B)
TRK File: 1-11
Notes
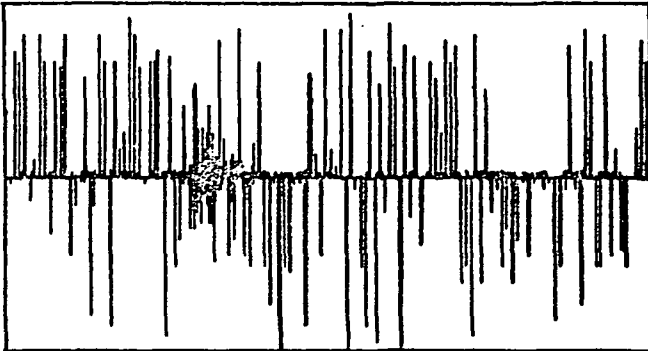
Type: D_N
Loc : L. Wing
Attn: 1x
x   : 0 - 20   μs
y   : +/- 0.53   V
 min: -0.53   V
 max: 0.50   V

Type:
Loc :
Attn:
x   : 0 -   μs
y   : +/-   V
 min: V
 max: V
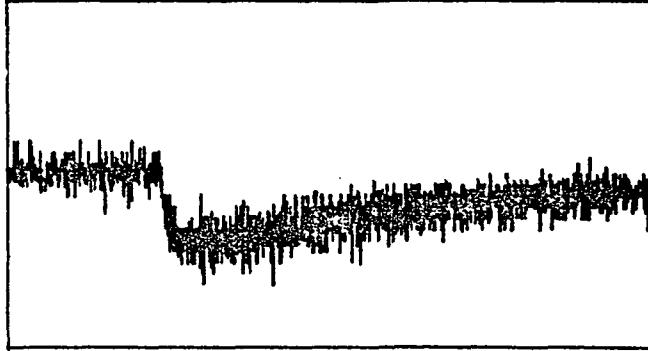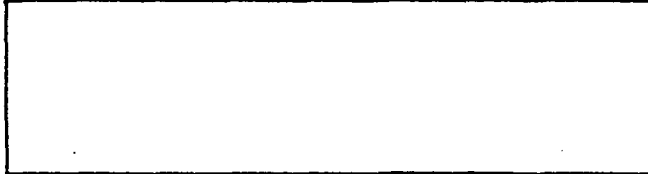
Type: E_M
Loc :
Attn: 25x
x   : 0 - 20   μs
y   : +/- 2.50   V
 min: -1.60   V
 max: 0.45   V

250x at E-field
sensor.

Ran Biomation on
.1 Input Range.

∴ 25x Attn.

Type: D_N
Loc : R. Wing
Attn: 1x
x   : 0 - 10   μs
y   : +/- 0.60   V
 min: -0.13   V
 max: 0.07   V

Batteries going
dead.

Type: D_N
Loc : Fus.
Attn: 2x
x   : 0 - 10   μs
y   : +/- 1.08   V
 min: -0.66   V
 max: 0.32   V

RADIATED // DOORS OPEN

Test: 4/2 C
TRK File: 1-12
Notes
_____
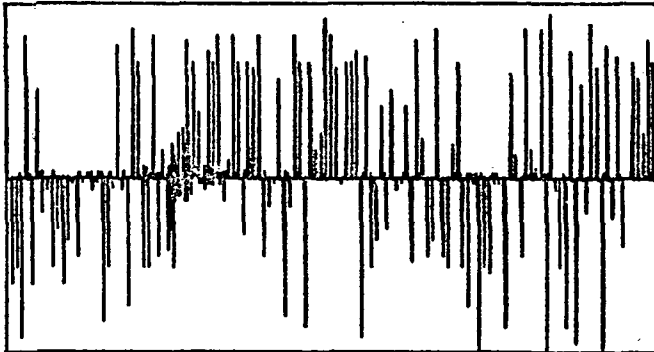
Type: D_N
Loc : L. Wing
Attn: 1x
x   : 0 - 20   μs
y   : +/- 0.53   V
 min: -0.53   V
 max: 0.50   V
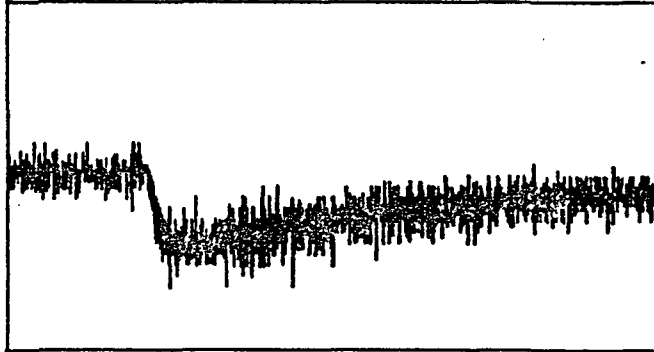
Type:
Loc :
Attn:
x   : 0 -   μs
y   : +/-   V
 min: V
 max: V

Type: E
Loc : Mac
Attn: 25x
x   : 0 - 20   μs
y   : +/- 2.50   V
 min: -1.70   V
 max: 0.50   V

Type: D_N
Loc : R. Wing
Attn: 1x
x   : 0 - 10   μs
y   : +/- 0.60   V
 min: -0.08   V
 max: 0.04   V

Batteries

Type: D_N
Loc : Fus.
Attn: 2x
x   : 0 - 10   μs
y   : +/- 1.08   V
 min: -0.33   V
 max: 0.28   V

-70-

RADIATED // DOORS OPEN

Type: $\dot{D}_N$
Loc : L. Wing
Attn: 1x
x   : 0 - 20   µs
y   : +/- 0.53   V
 min: -0.53   V
 max: 0.50   V

Type:
Loc :
Attn:
x   : 0 -   µs
y   : +/-   V
 min: V
 max: V
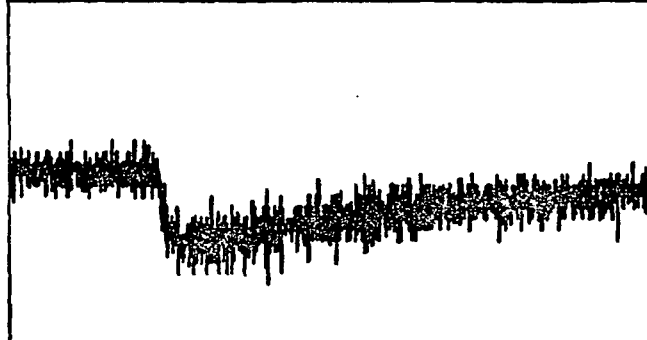
Type: E
Loc : Mac
Attn: 25x
x   : 0 - 20   µs
y   : +/-2.50   V
 min: -1.70   V
 max: 0.50   V
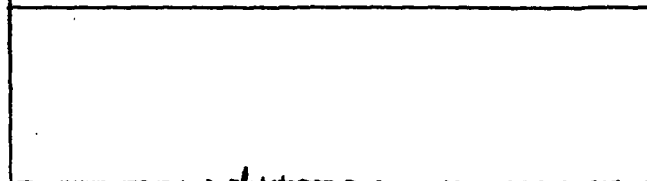
Type: $\dot{D}_N$
Loc : R. Wing
Attn: 1x
x   : 0 -10   µs
y   : +/-0.60   V
 min: -0.05   V
 max: 0.05   V
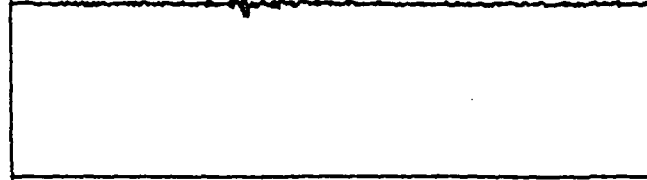
Type: $\dot{D}_N$
Loc : Fus.
Attn: 2x
x   : 0 - 10   µs
y   : +/- 1.08   V
 min: -0.38   V
 max: 0.48   V
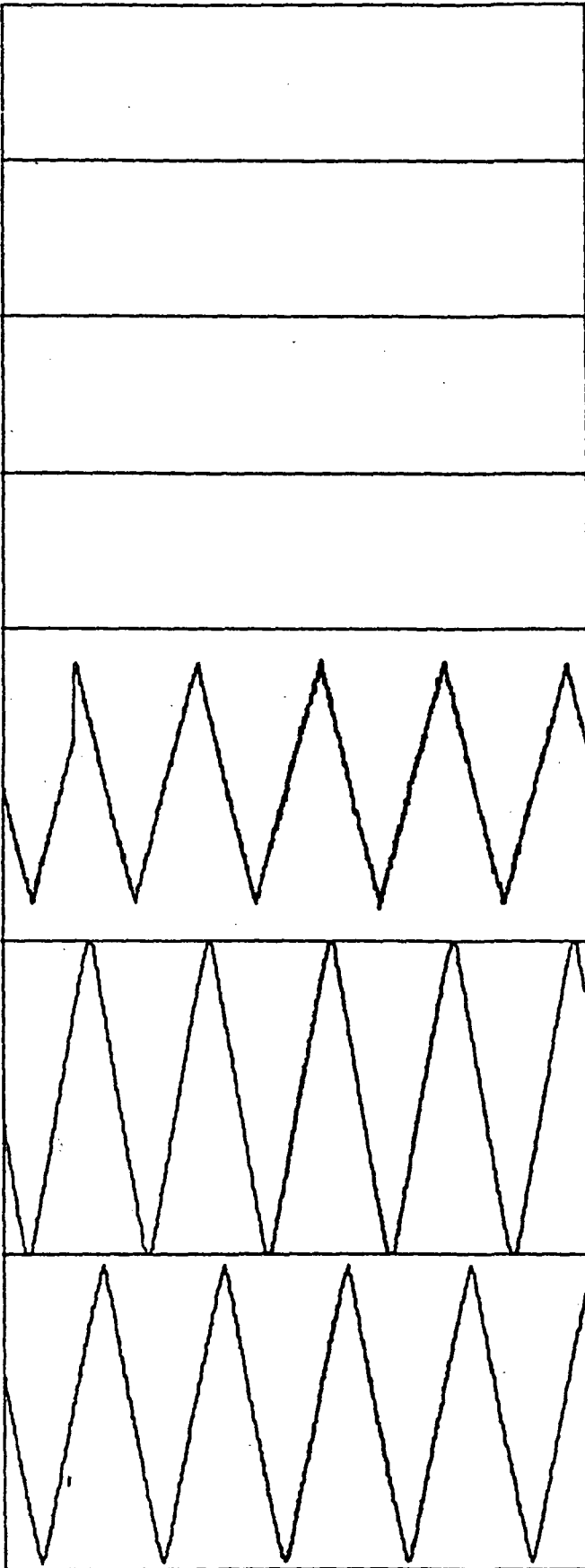
Batteries

RADIATED // DOORS OPEN

Type:
Loc :
Attn:
x   : 0 -   μs
y   : +/-   V
 min: V
 max: V

Type:
Loc :
Attn:
x   : 0 -   μs
y   : +/-   V
 min: V
 max: V

Type:T-4, R-1
Loc :
Attn:
x   : 0 -100   μs
y   : +/-0.12   V
 min: -0.094   V
 max: 0.096   V

Cal   50Ω input.

Ran w/high impedance
input.

Type:T-1, R-4
Loc :
Attn:
x   : 0 -100   μs
y   : +/-0.50   V
 min: -0.50   V
 max: 0.50   V

Type:T-9, R-5
Loc :
Attn:
x   : 0 -100   μs
y   : +/-0.53   V
 min: -0.51   V
 max: 0.50   V

Test: 4/2 E
TRK File: 0-0
Notes

Ground Plus attached
to plane.
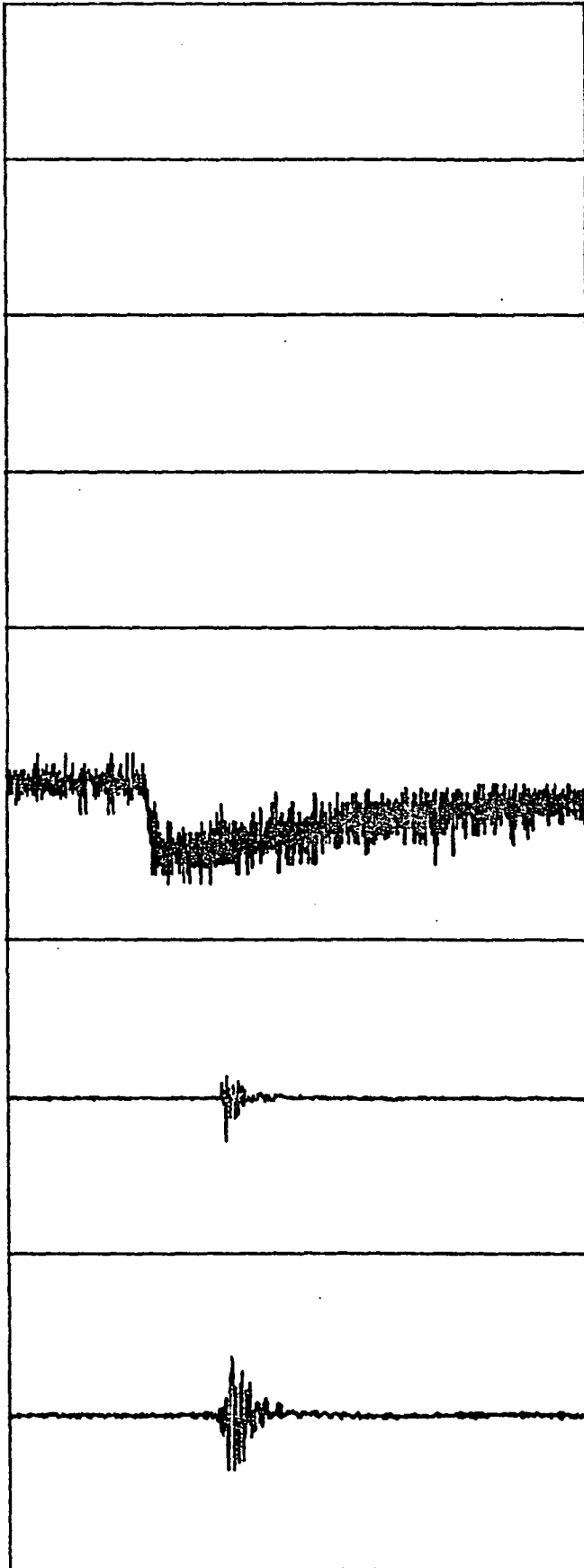
Type:
Loc :
Attn:
x : 0 -   µs
y : +/-   V
min: V
max: V

Type:
Loc :
Attn:
x : 0 -   µs
y : +/-   V
min: V
max: V

Type: E
Loc : Mac
Attn: 25x
x : 0 - 20   µs
y : +/- 3.10   V
min: -1.96   V
max: 0.58   V

Type: D_N
Loc : R. Wing
Attn: 1x
x : 0 - 10   µs
y : +/- 0.50   V
min: -0.14   V
max: 0.07   V

Type: D_N
Loc : Fus.
Attn: 2x
x : 0 - 10   µs
y : +/- 1.07   V
min: -0.39   V
max: 0.38   V

-73-

ORIGINAL PAGE IS
OF POOR QUALITY

Ground Plug attached
to plane
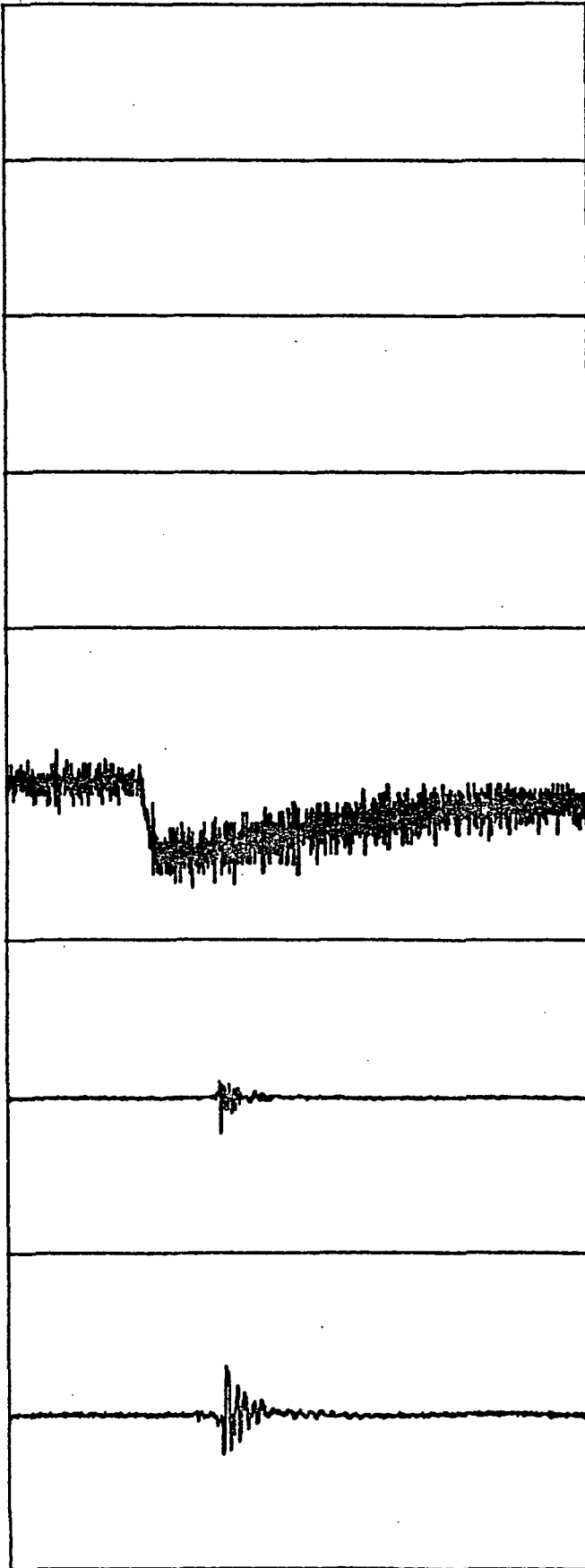
Type:
Loc :
Attn:
x   : 0 -   μs
y   : +/-   V
 min: V
 max: V

Type:
Loc :
Attn:
x   : 0 -   μs
y   : +/-   V
 min: V
 max: V

Type: E
Loc : Mac
Attn: 25x
x   : 0 - 20   μs
y   : +/- 3.10   V
 min: -2.04   V
 max: 0.66   V

Type: D_N
Loc : R. Wing
Attn: 1x
x   : 0 - 10   μs
y   : +/- 0.50   V
 min: -0.12   V
 max: 0.05   V

Type: D_N
Loc : Fus.
Attn: 2x
x   : 0 - 10   μs
y   : +/- 1.07   V
 min: -0.30   V
 max: 0.31   V

Test: 4/2 G
TRK File: 0-2
Notes

Type:
Loc :
Attn:
x   : 0 -   µs
y   : +/-   V
 min: V
 max: V

Type:
Loc :
Attn:
x   : 0 -   µs
y   : +/-   V
 min: V
 max: V

Type: E
Loc : Mac
Attn: 25x
x   : 0 - 20   µs
y   : +/- 3.10   V
 min: -1.96   V
 max: 0.58   V

Type: D_N
Loc : R. Wing
Attn: 0.5x
x   : 0 - 10   µs
y   : +/- 0.252   V
 min: -0.085   V
 max: 0.055   V

Type: D_N
Loc : Fus.
Attn: 1x
x   : 0 - 10   µs
y   : +/- 0.54   V   Batteries
 min: -0.08   V
 max: 0.05   V

RADIATED // DOORS OPEN

Test: 4/2 T-7
TRK File: 0-3
Notes _____

Type:
Loc :
Attn:
x   : 0 -   µs
y   : +/-   V
 min: V
 max: V

Type:
Loc :
Attn:
x   : 0 -   µs
y   : +/-   V
 min: V
 max: V

Type:
Loc :
Attn:
x   : 0 -   µs
y   : +/-   V
 min: V
 max: V

Type:
Loc :
Attn:
x   : 0 -   µs
y   : +/-   V
 min: V
 max: V

.5V

0 V

Type: T-7
Loc :
Attn:
x   : 0 - 80   µs
y   : +/- 0.37   V
 min: -0.37   V
 max: 0.37   V

Replaced T-9 with
T-7
_____

Did not Recalibrate.
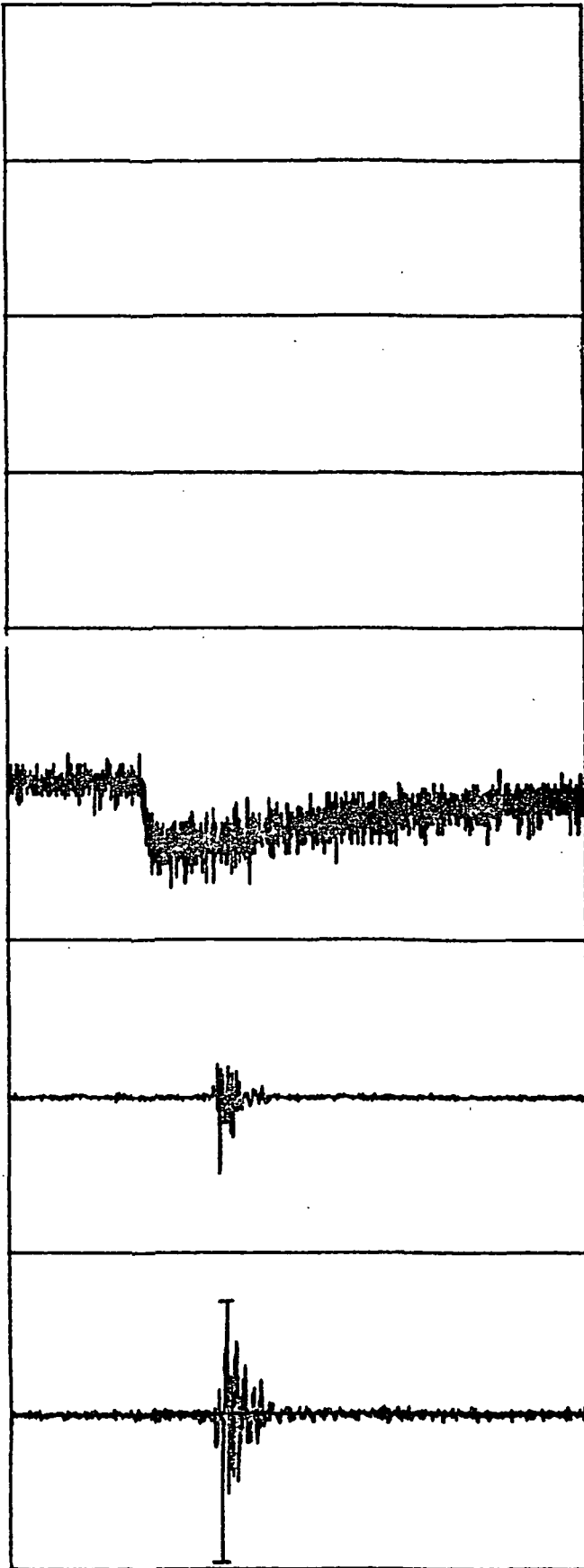
RADIATED // DOORS OPEN

Type:
Loc :
Attn:
x   : 0 -   µs
y   : +/-   V
 min: V
 max: V

Type:
Loc :
Attn:
x   : 0 -   µs
y   : +/-   V
 min: V
 max: V

Type: E
Loc : Mac
Attn: 25x
x   : 0 - 20   µs
y   : +/- 3.10   V
 min: -2.04   V
 max: 0.58   V

Type: D_N
Loc : R. Wing
Attn: 0.5x
x   : 0 - 10   µs
y   : +/-0.252   V
 min: -0.122   V
 max: 0.051   V

Type:D_N
Loc :Fus.
Attn:1x
x   : 0 -10   µs
y   : +/-0.37   V
 min: -0.35   V
 max: 0.26   V

-77-
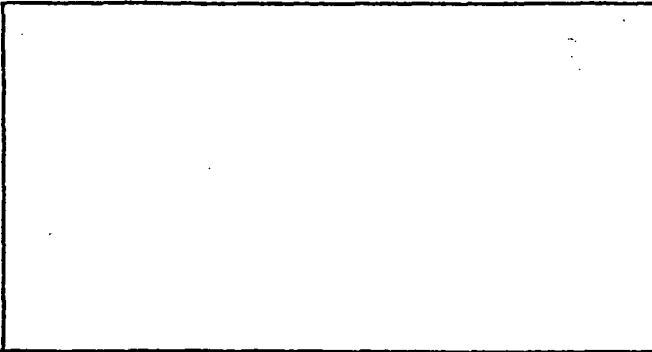
Type:
Loc :
Attn:
x   : 0 -   µs
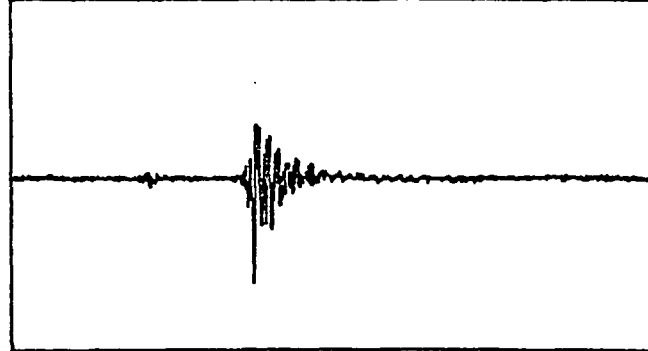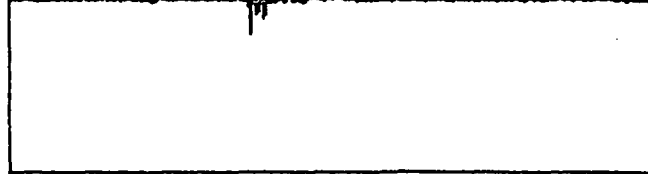y   : +/-   V
 min: V
 max: V
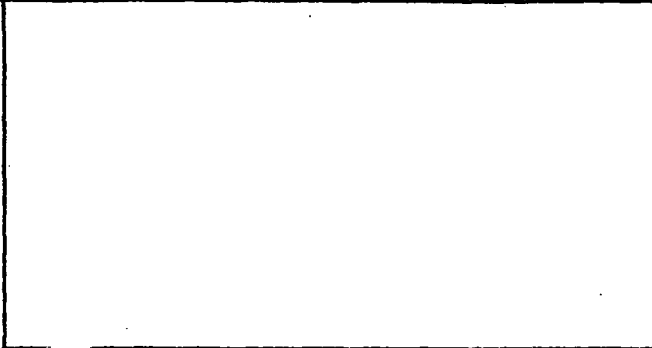
Type:
Loc :
Attn:
x   : 0 -   µs
y   : +/-   V
 min: V
 max: V

Type: E
Loc : Mac
Attn: 25x
x   : 0 - 20   µs.
y   : +/- 3.10   V
 min: -1.94   V
 max: 0.56   V

Type: D_N
Loc : R. Wing
Attn: 0.5x
x   : 0 - 10   µs
y   : +/- 0.252 V
 min: -0.106   V
 max: 0.053   V
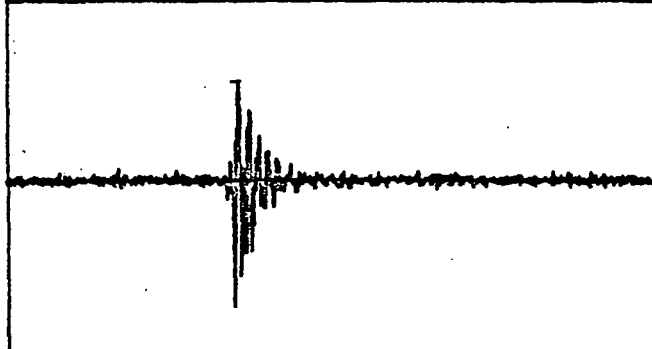
Type: D_N
Loc : Fus.
Attn: 1x
x   : 0 - 10   µs
y   : +/- 0.37   V
 min: -0.26   V
 max: 0.21   V

RADIATED // DOORS OPEN

Test: 4/2 J
TRK File: 0-6
Notes _____
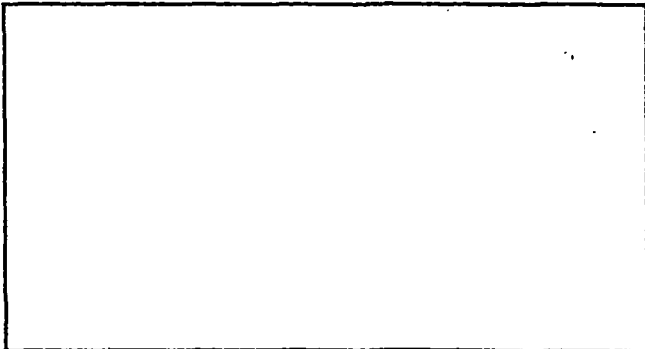
Type:
Loc :
Attn:
x   : 0 -   µs
y   : +/-   V
 min: V
 max: V
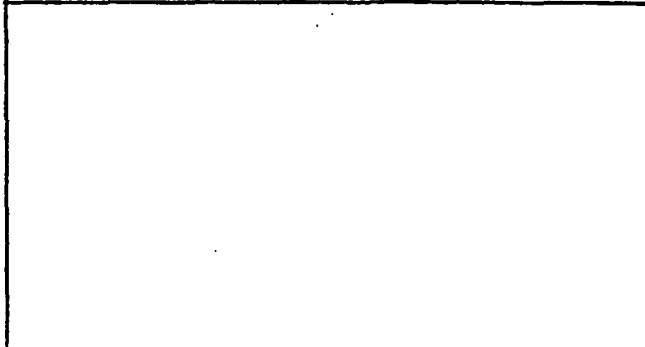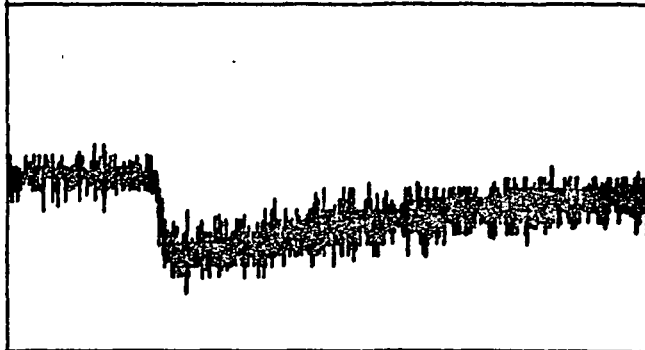
Type:
Loc :
Attn:
x   : 0 -   µs
y   : +/-   V
 min: V
 max: V

Type: E
Loc : Mac
Attn: 25x
x   : 0 - 20   µs
y   : +/- 3.10   V
 min: -2.04   V
 max: 0.58   V

Type: D_N
Loc : R. Wing
Attn: 0.5x
x   : 0 - 10   µs
y   : +/- 0.252   V
 min: -0.102   V
 max: 0.032   V
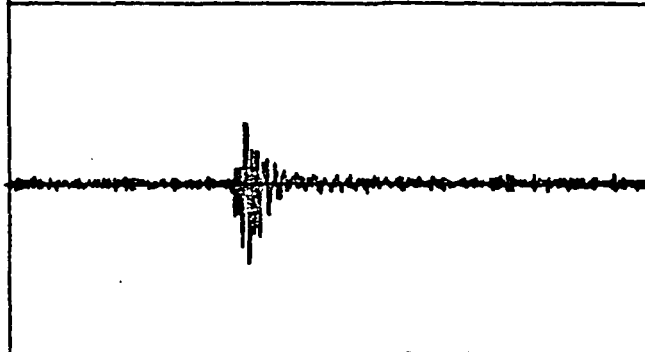
Type: D_N
Loc : Fus.
Attn: 1x
x   : 0 - 10   µs
y   : +/- 0.37   V
 min: -0.16   V
 max: 0.13   V
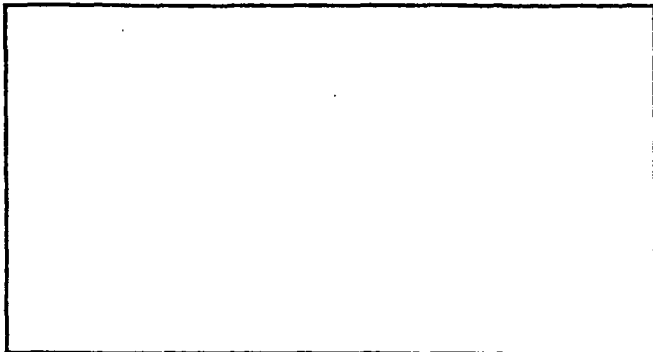
RADIATED // DOORS CLOSED
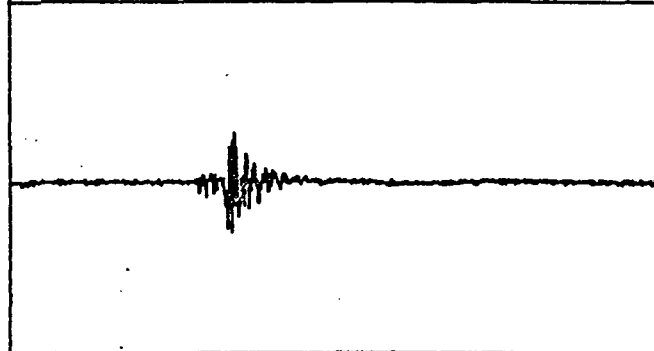
Test: 4/2 K
.TRK File: 0-7
Notes _____

Type:
Loc :
Attn:
x   : 0 -   μs
y   : +/-   V
 min: V
 max: V
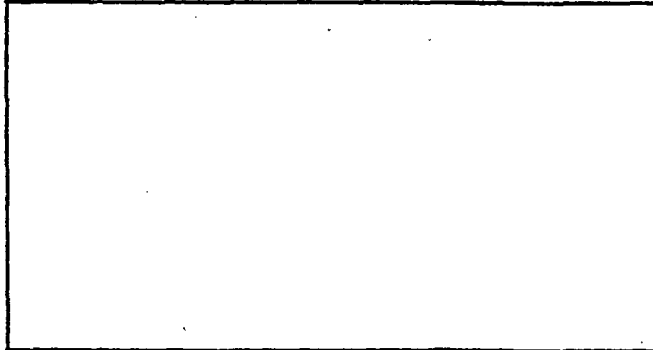
Type:
Loc :
Attn:
x   : 0 -   μs
y   : +/-   V
 min: V
 max: V

Type: E
Loc : Mac
Attn: 25x
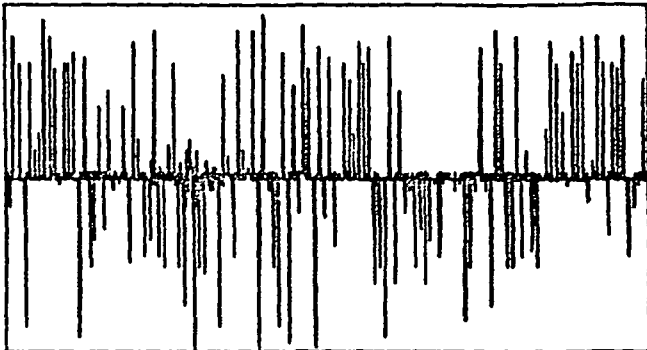x   : 0 - 20   μs
y   : +/- 3.10   V
 min: -2.14   V
 max: 0.76   V
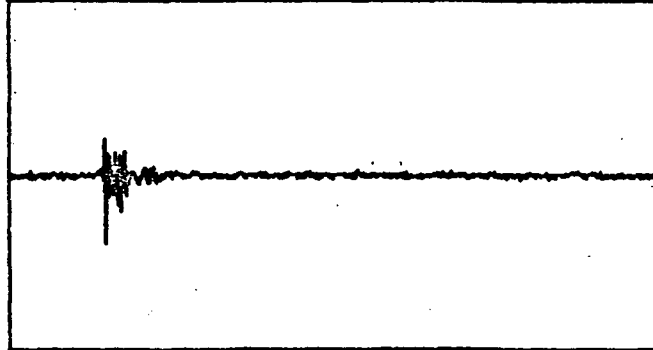
Type: D_N
Loc : R. Wing
Attn: 0.5x
x   : 0 - 10   μs
y   : +/- 0.252   V
 min: -0.096   V
 max: 0.051   V
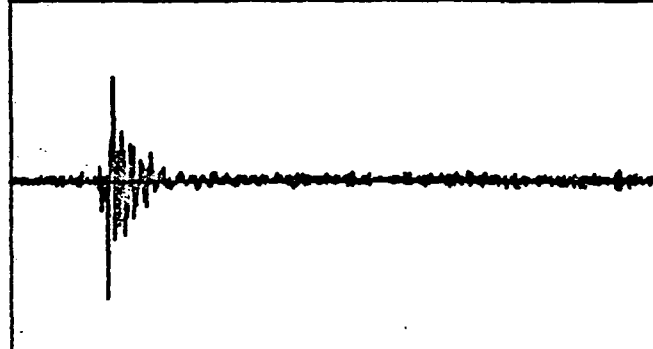
Type: D_N
Loc : Fus.
Attn: 1x
x   : 0 - 10   μs
y   : +/- 0.37   V
 min: -0.24   V
 max: 0.22   V

Test: 4/2 L
TRK File: 0-8
Notes

Type:
Loc :
Attn:
x   : 0 -   µs
y   : +/-   V
 min: V
 max: V
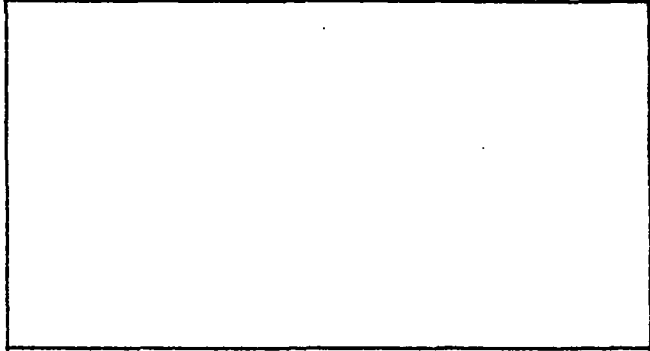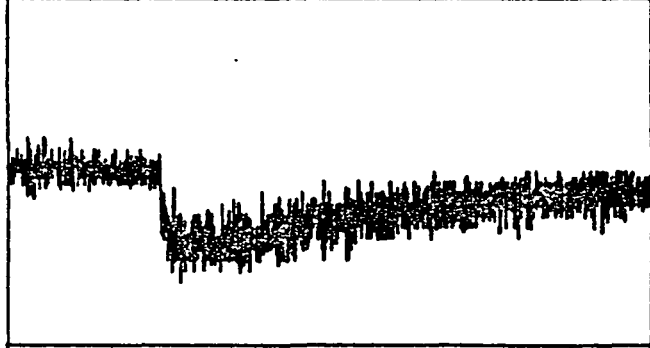
Type:
Loc :
Attn:
x   : 0 -   µs
y   : +/-   V
 min: V
 max: V

Type: E
Loc : Mac
Attn: 25x
x   : 0 - 20   µs
y   : +/- 3.10   V
 min: -1.96   V
 max: 0.58   V
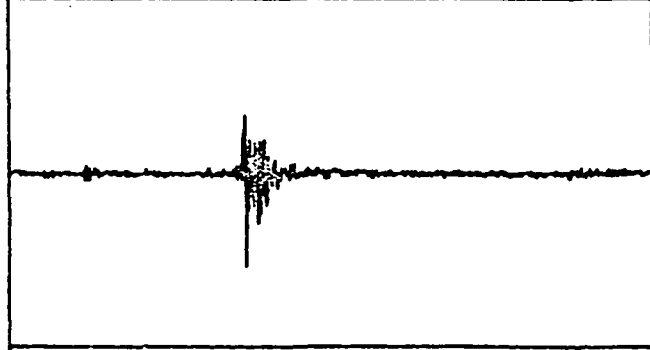
Type: D_N
Loc : R. Wing
Attn: 0.5x
x   : 0 - 10   µs
y   : +/- 0.252   V
 min: -0.134   V
 max: 0.081   V
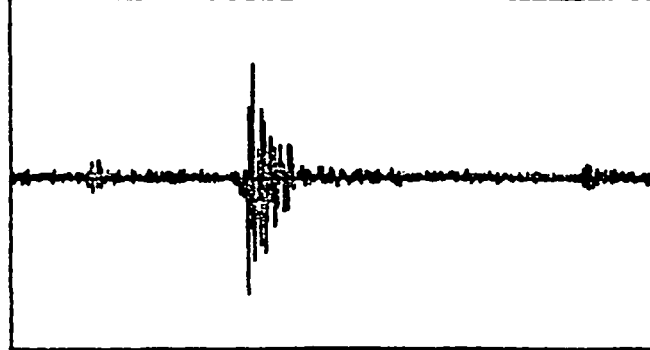
Type: D_N
Loc : Fus.
Attn: 1x
x   : 0 - 10   µs
y   : +/- 0.37   V
 min: -0.25   V
 max: 0.24   V
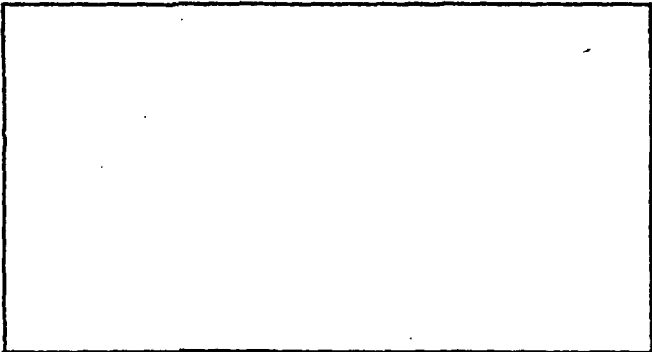
RADIATED // DOORS CLOSED

Type:
Loc :
Attn:
x   : 0 -   μs
y   : +/-   V
 min: V
 max: V

Type:
Loc :
Attn:
x   : 0 -   μs
y   : +/-   V
 min: V
 max: V
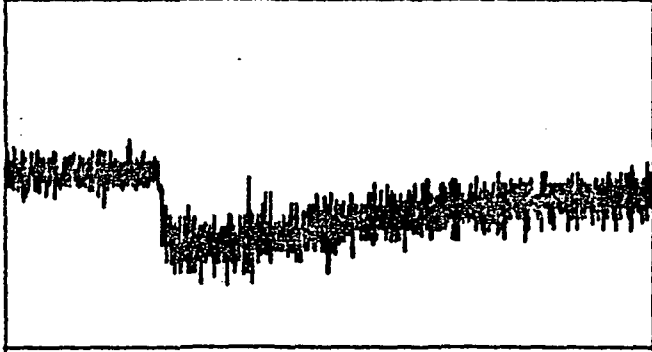
Type: E
Loc : Mac
Attn: 25x
x   : 0 - 20   μs
y   : +/- 3.10   V
 min: -1.96   V
 max: 0.56   V
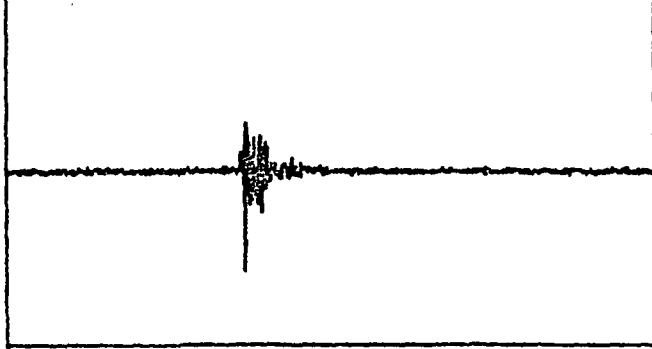
Type: $\dot{D}_N$
Loc : R. Wing
Attn: 0.5x
x   : 0 - 10   μs
y   : +/- 0.252   V
 min: -0.144   V
 max: 0.065   V
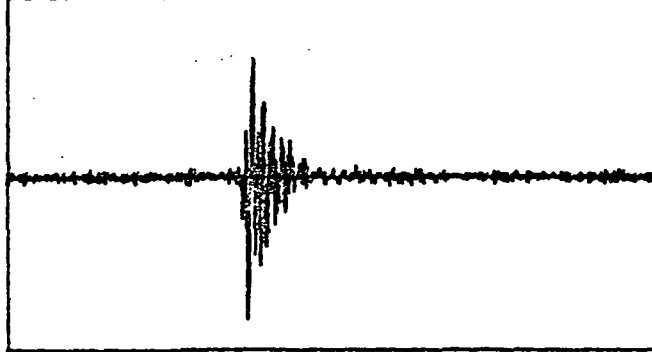
Type: $\dot{D}_N$
Loc : Fus.
Attn: 1x
x   : 0 - 10   μs
y   : +/- 0.37   V
 min: -0.30   V
 max: 0.25   V

Test: 4/2 NF
TRK File: 0-10
Notes _____
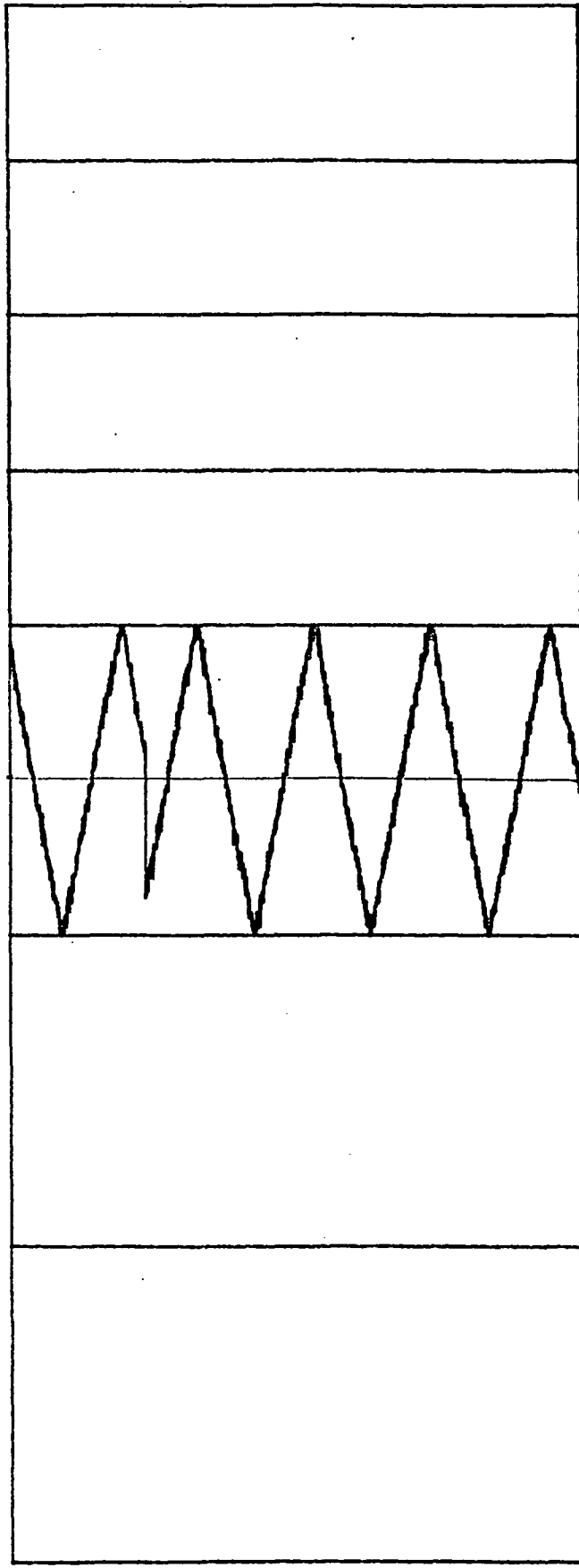
Type:
Loc :
Attn:
x   : 0 -   µs
y   : +/-   V
 min: V
 max: V

Type:
Loc :
Attn:
x   : 0 -   µs
y   : +/-   V
 min: V
 max: V

Type: Replaced Transmitter
Loc :   No. 4 with Nanofast
Attn: system.
x   : 0 - 100   µs
y   : +/- 0.10   V   Triangle wave to
 min: -0.10   V   scale to for Nanofast
 max: 0.10   V   Fiber Optic System.

Type:
Loc :
Attn:
x   : 0 -   µs
y   : +/-   V
 min: V
 max: V

Type:
Loc :
Attn:
x   : 0 -   µs
y   : +/-   V
 min: V
 max: V

RADIATED // DOORS CLOSED

Test: 4/2 N
TRK File: 0-11
Notes
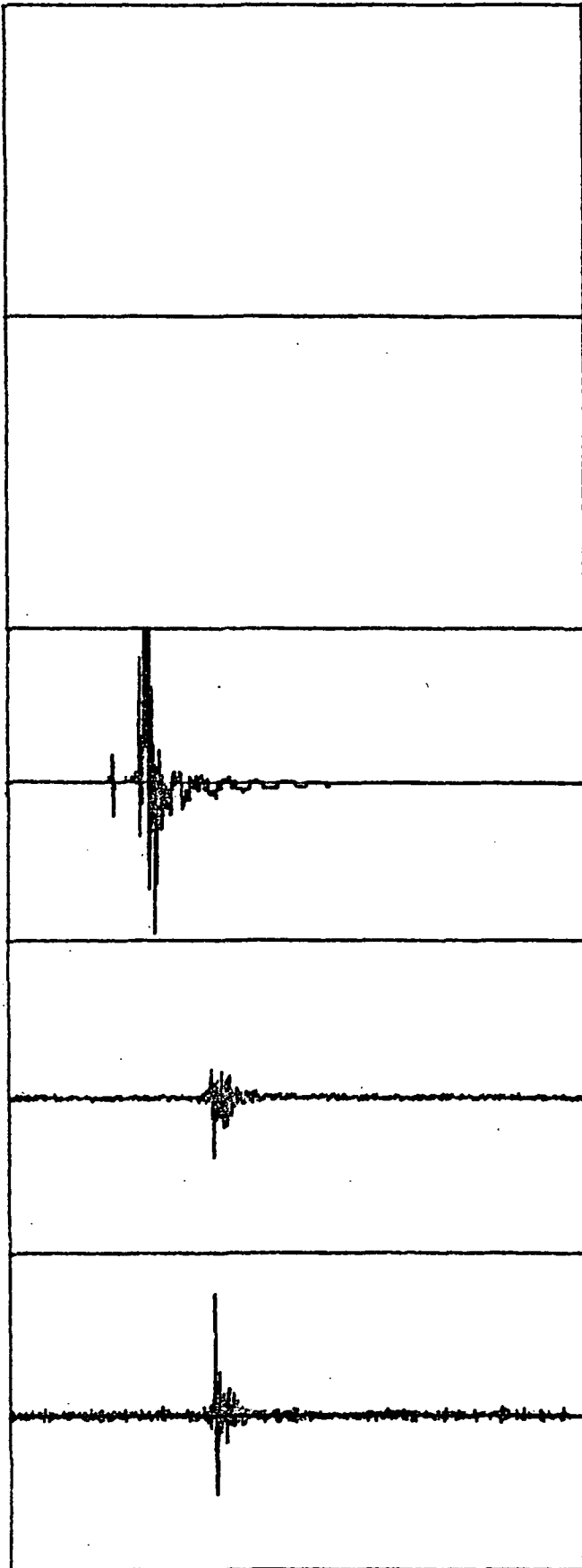
Type:
Loc :
Attn:
x   : 0 -   µs
y   : +/-   V
 min: V
 max: V

Type:
Loc :
Attn:
x   : 0 -   µs
y   : +/-   V
 min: V
 max: V

Type: I
Loc :
Attn: 50x
x   : 0 - 20   µs
y   : +/- 5.00   V
 min: -4.75   V
 max: >5.   V

Type: D_N
Loc : L. Wing
Attn: 0.5x
x   : 0 - 10   µs
y   : +/- 0.252   V
 min: -0.096   V
 max: 0.045   V

Type: D_N
Loc : Tail
Attn: 1x
x   : 0 - 10   µs
y   : +/- 0.37   V
 min: -0.19   V
 max: 0.29   V

RADIATED // DOORS CLOSED
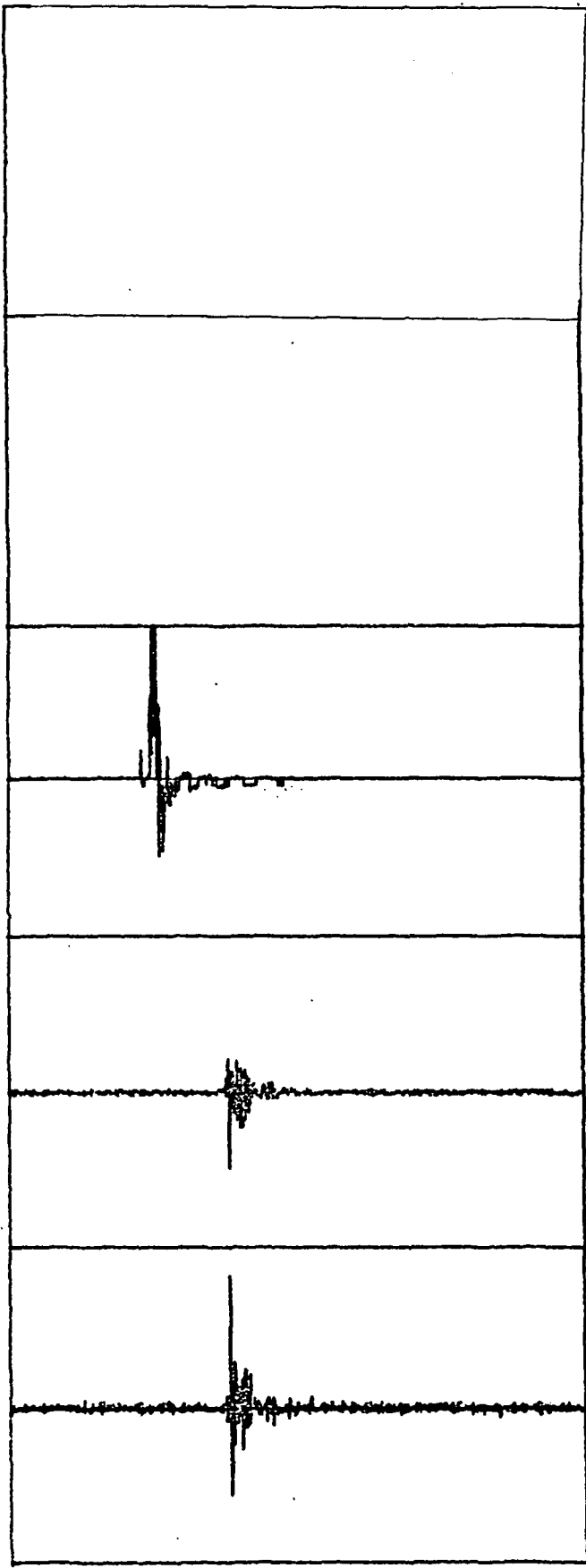
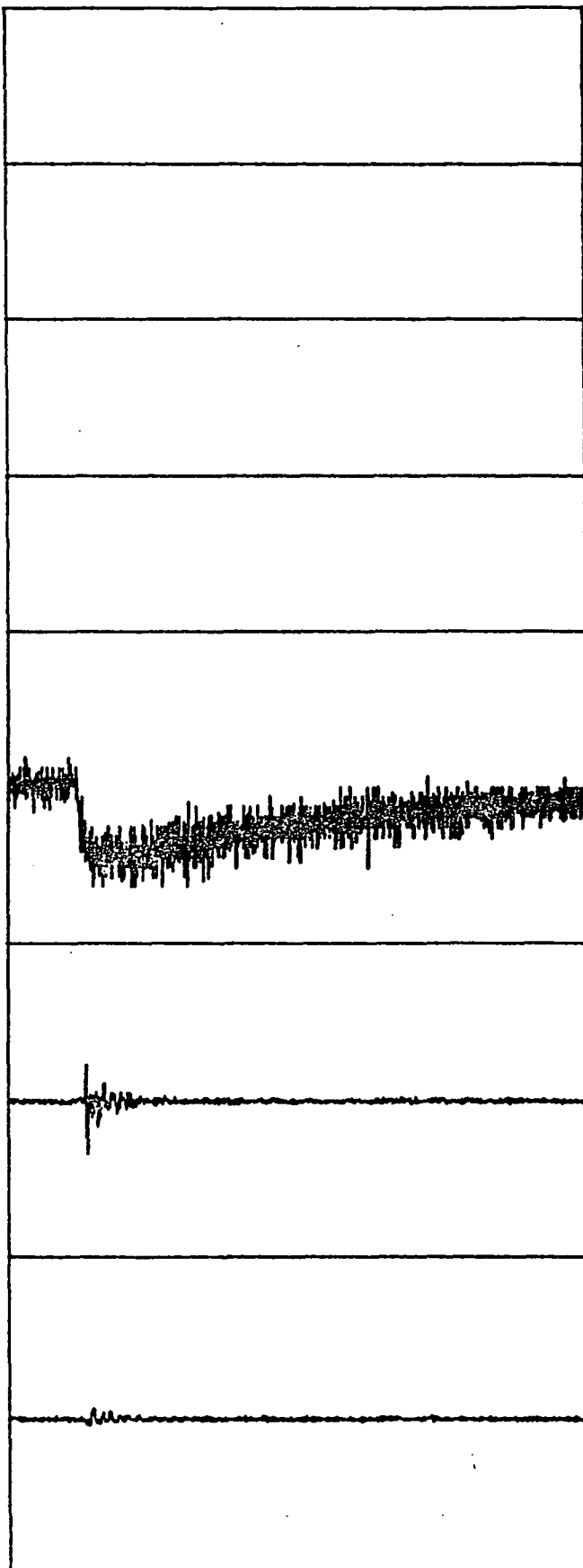Type:
Loc :
Attn:
x : 0 -   μs
y : +/-   V
 min: V
 max: V

Type:
Loc :
Attn:
x : 0 -   μs
y : +/-   V
 min: V
 max: V

Type: I
Loc :
Attn: 100x
x : 0 - 20   μs
y : +/- 10.00   V
 min: -5.00   V
 max: >10.   V

Type: $\dot{D}_N$
Loc : L. Wing
Attn: 0.5x
x : 0 - 10   μs
y : +/-0.252   V
 min: -0.120   V
 max: 0.053   V

Type: $\dot{D}_N$
Loc : Tail
Attn: 1x
x : 0 - 10   μs
y : +/- 0.37   V
 min: -0.20   V
 max: 0.32   V
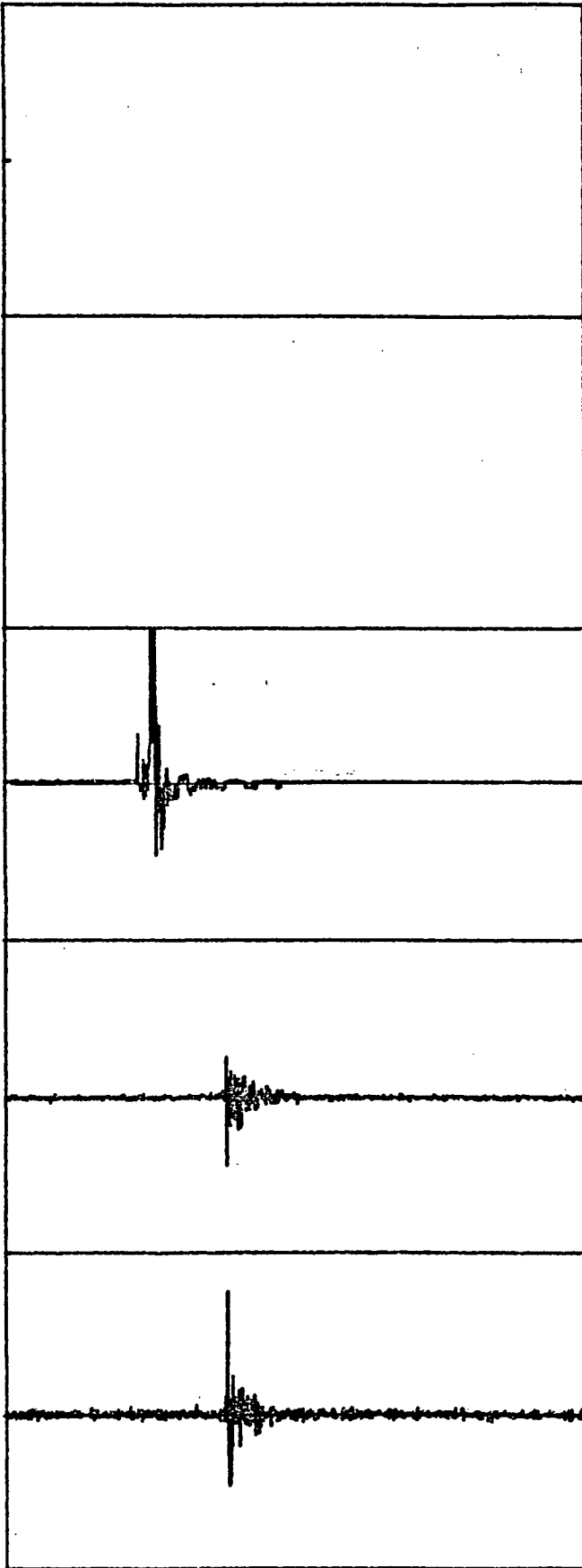
RADIATED // DOORS CLOSED

Type:
Loc :
Attn:
x   : 0 -   µs
y   : +/-   V
 min: V
 max: V

Type:
Loc :
Attn:
x   : 0 -   µs
y   : +/-   V
 min: V
 max: V

Type: I
Loc :
Attn: 100x
x   : 0 - 20   µs
y   : +/- 10.   V
 min: -4.5   V
 max: >10.   V

Type: D_N
Loc : L. Wing
Attn: 0.5x
x   : 0 - 10   µs
y   : +/- 0.252 V
 min: -0.108 V
 max: 0.063 V

Type: D_N
Loc : Tail
Attn: 1x
x   : 0 - 10   µs
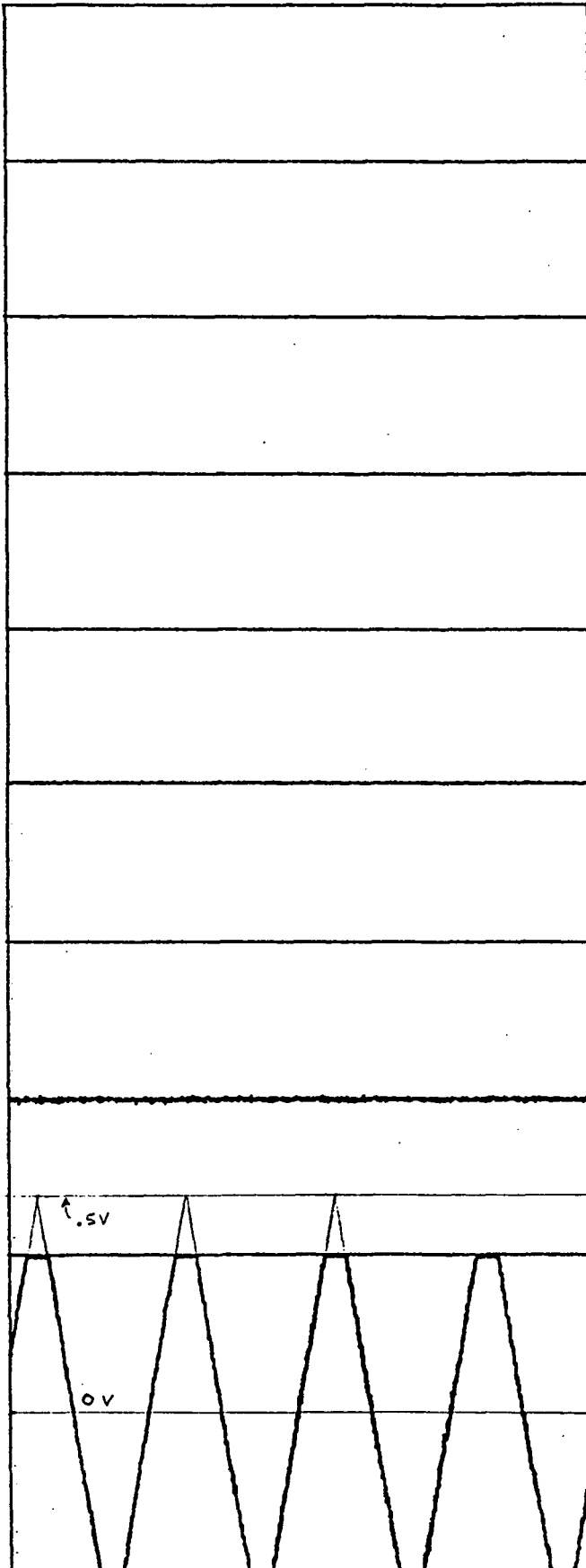y   : +/- 0.37 V
 min: -0.17   V
 max: 0.30   V
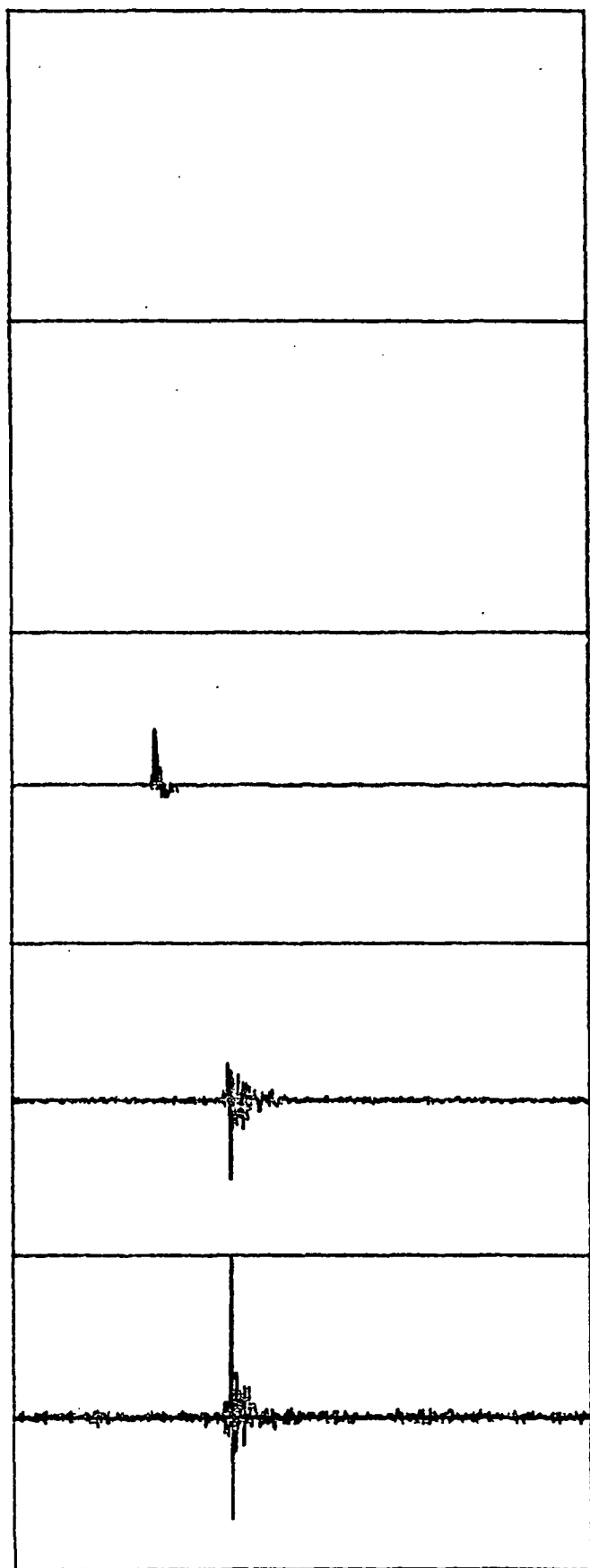
RADIATED // DOORS CLOSED

Type:
Loc :
Attn:
x   : 0 -   µs
y   : +/-   V
 min: V
 max: V

Type:
Loc :
Attn:
x   : 0 -   µs
y   : +/-   V
 min: V
 max: V

Type: I
Loc :
Attn: 500x
x   : 0 - 20   µs
y   : +/- 50.   V
 min: -3.75   V
 max: 18.75   V

Type: $\dot{D}_N$
Loc : L. Wing
Attn: 0.5x
x   : 0 - 10   µs
y   : +/- 0.252   V
 min: -0.126   V
 max: 0.059   V

Type: $\dot{D}_N$
Loc : Tail
Attn: 1x
x   : 0 - 10   µs
y   : +/- 0.37   V
 min: -0.24   V
 max: >0.37   V

RADIATED // DOORS CLOSED
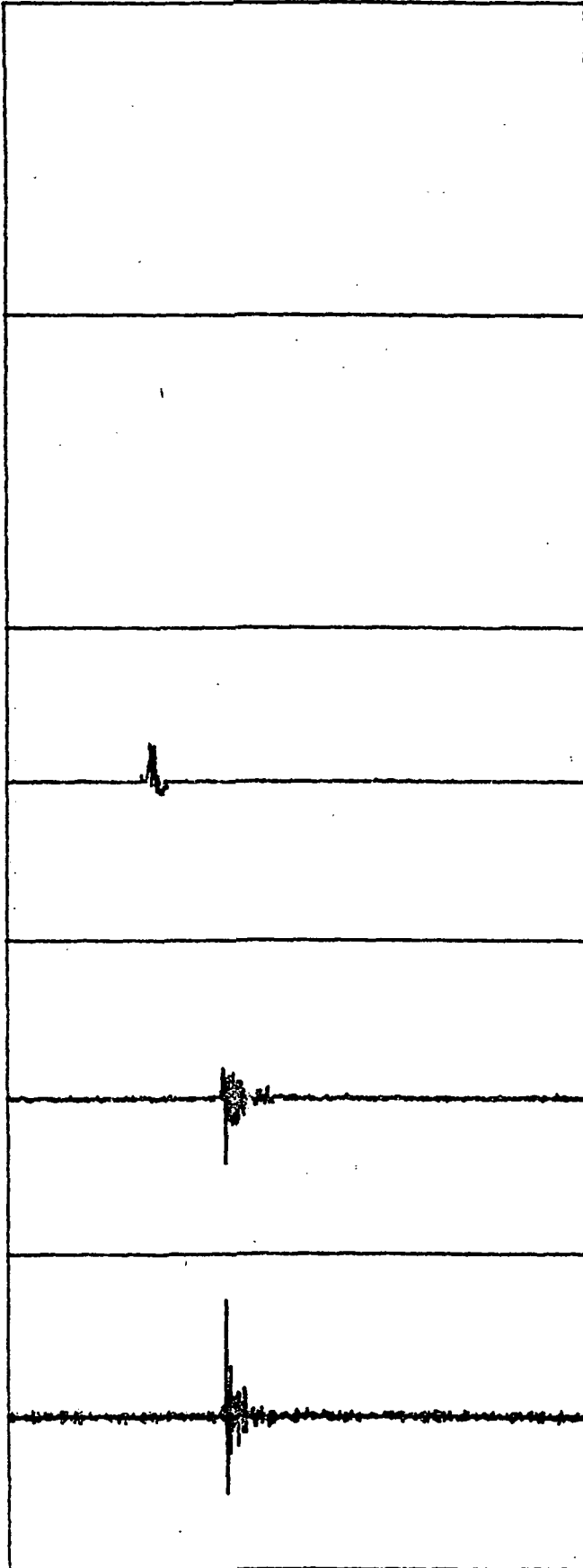
Type:
Loc :
Attn:
x   : 0 -   μs
y   : +/-   V
 min: V
 max: V

Type:
Loc :
Attn:
x   : 0 -   μs
y   : +/-   V
 min: V
 max: V

Type: I
Loc :
Attn: 500x
x   : 0 - 20   μs
y   : +/- 50.   V
 min: -5.   V
 max: 12.50   V

Type: D_N
Loc : L. Wing
Attn: 0.5x
x   : 0 -10   μs
y   : +/-0.252   V
 min: -0.106   V
 max: 0.045   V

Type: D_N
Loc : Tail
Attn: 1x
x   : 0 -10   μs
y   : +/-0.37   V
 min: -0.18   V
 max: 0.27   V

RADIATED // DOORS CLOSED

Test: 4/2 S
TRK File: 1-1
Notes
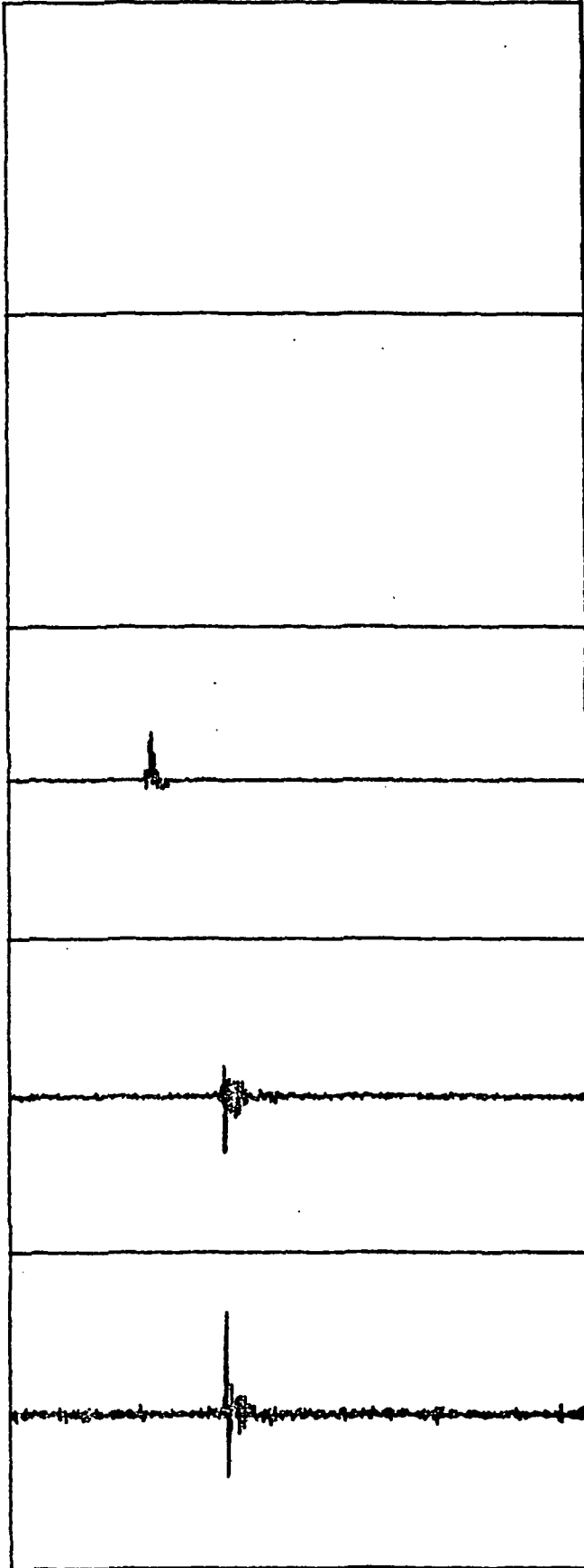
Type:
Loc :
Attn:
x   : 0 -   µs
y   : +/-   V
 min: V
 max: V

Type:
Loc :
Attn:
x   : 0 -   µs
y   : +/-   V
 min: V
 max: V

Type: I
Loc :
Attn: 500x
x   : 0 - 20   µs
y   : +/- 50   V
 min: -3.75   V
 max: 16.25   V

Type: D_N
Loc : L. Wing
Attn: 0.5x
x   : 0 - 10   µs
y   : +/- 0.252 V
 min: -0.089   V
 max: 0.047   V

Type: D_N
Loc : Tail
Attn: 1x
x   : 0 - 10   µs
y   : +/- 0.37   V
 min: -0.15   V
 max: 0.24   V

RADIATED // DOORS CLOSED

Test: 4/2 T
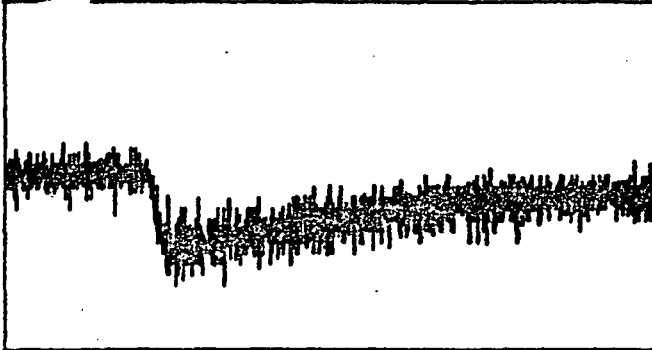TRK File: 1-2
Notes
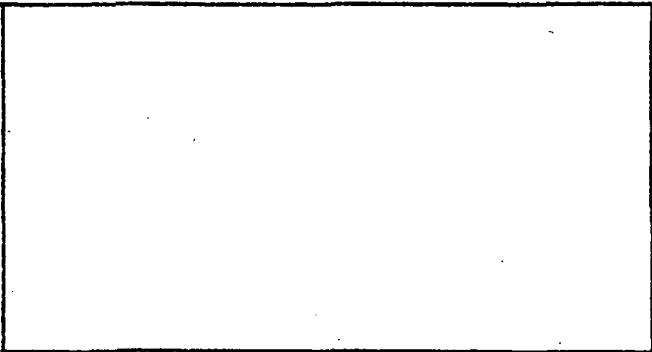
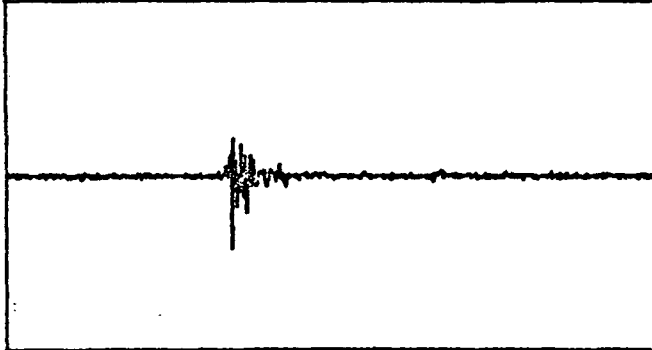Type:
Loc :
Attn:
x   : 0 -   µs
y   : +/-   V
 min: V
 max: V
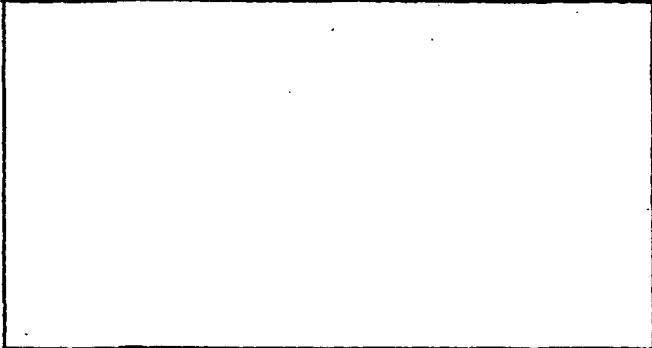
Type:
Loc :
Attn:
x   : 0 -   µs
y   : +/-   V
 min: V
 max: V
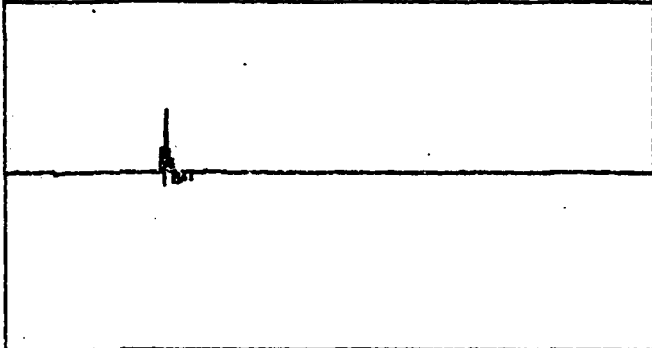
Type: I
Loc :
Attn: 500x
x   : 0 - 20   µs
y   : +/- 50   V
 min: -4.38   V
 max: 18.75   V
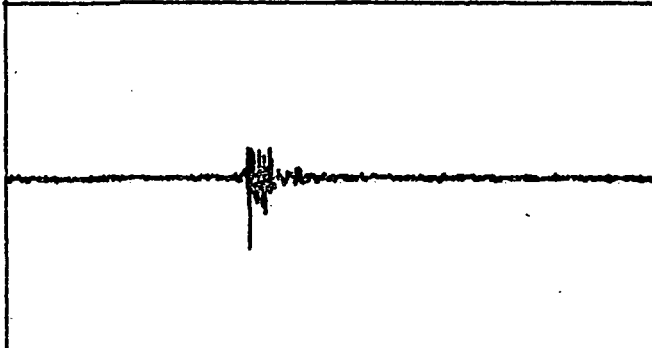
Type: D_N
Loc : L. Wing
Attn: 0.5x
x   : 0 - 10   µs
y   : +/- 0.252 V
 min: -0.102   V
 max: 0.041   V
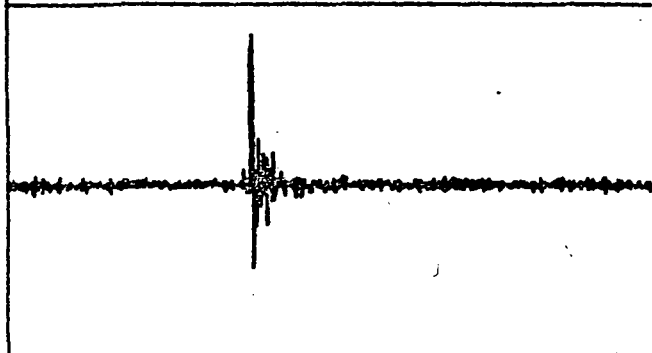
Type: D_N
Loc : Tail
Attn: 1x
x   : 0 - 10   µs
y   : +/- 0.37   V
 min: -0.18   V
 max: 0.31   V

RADIATED // DOORS CLOSED

Test: 4/2 U
TRK File: 1-3
Notes _____

Type:
Loc :
Attn:
x   : 0 -   µs
y   : +/-   V
 min: V
 max: V

Type:
Loc :
Attn:
x   : 0 -   µs
y   : +/-   V
 min: V
 max: V

Type: I
Loc : PCT, at Gen. Output
Attn: 50x
x   : 0 - 100   µs
y   : +/- 5.0   V
 min: -5.0   V
 max: V

Type: $\dot{D}_N$
Loc : L. Wing
Attn: 0.5x
x   : 0 - 10   µs
y   : +/-0.252   V
 min: -0.102   V
 max: 0.041   V

Type: $\dot{D}_N$
Loc : Tail
Attn: 1x
x   : 0 - 10   µs
y   : +/-0.37   V
 min: -0.17   V
 max: 0.32   V

-91-

RADIATED // DOORS CLOSED

Test: 4/2 V
TRK File: 1-4
Notes
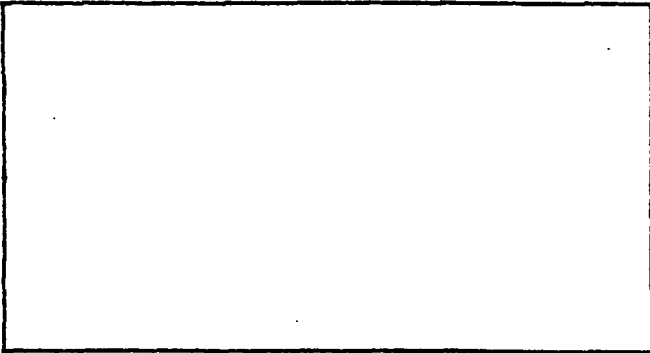
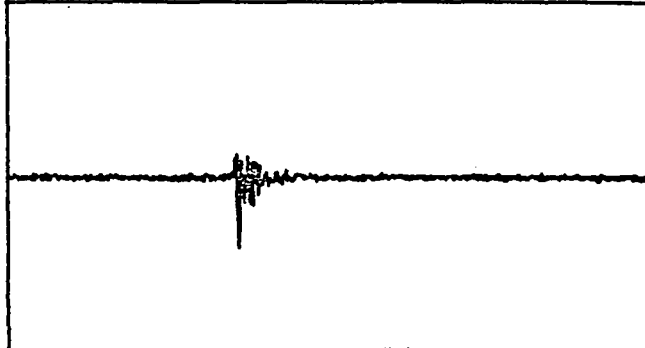
Type:
Loc :
Attn:
x   : 0 -   µs
y   : +/-   V
 min: V
 max: V

Type:
Loc :
Attn:
x   : 0 -   µs
y   : +/-   V
 min: V
 max: V

Type: I
Loc : PCT, at Gen Output
Attn: 50x
x   : 0 - 20   µs
y   : +/- 5.0   V
 min: -4.0   V
 max: V

Type: D_N
Loc : L. Wing
Attn: 0.5x
x   : 0 -10   µs
y   : +/- 0.252 V
 min: -0.102   V
 max: 0.041   V
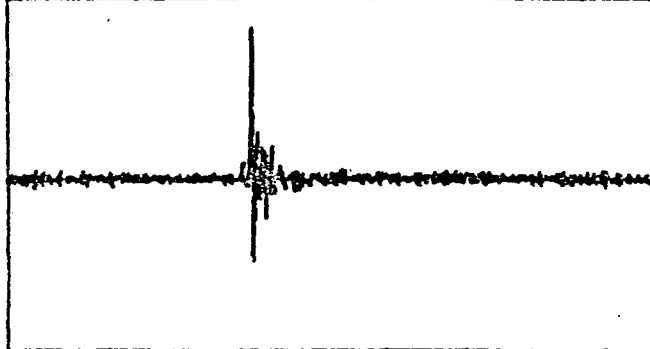
Type: D_N
Loc : Tail
Attn: 1x
x   : 0 -10   µs
y   : +/- 0.37   V
 min: -0.18   V
 max: 0.31   V

-92-

RADIATED // DOORS CLOSED
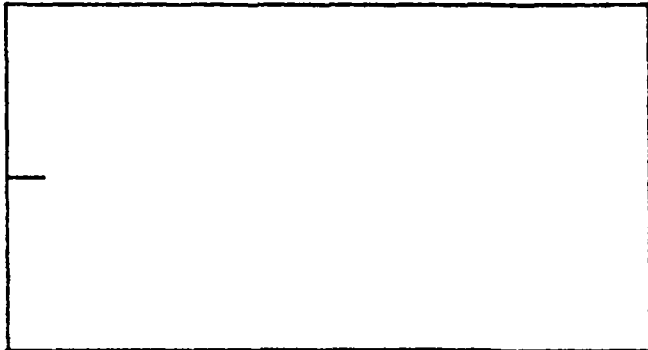
Type:
Loc :
Attn:
x   : 0 -   µs
y   : +/-   V
 min: V
 max: V
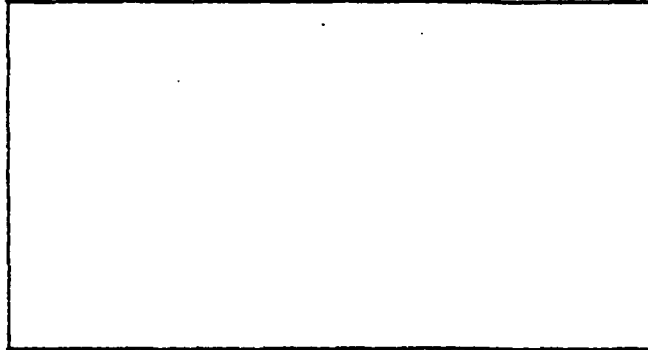
Type:
Loc :
Attn:
x   : 0 -   µs
y   : +/-   V
 min: V
 max: V
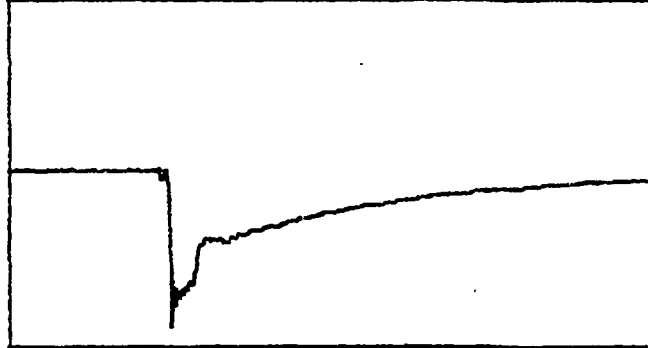
Type: I
Loc : PCT, at Gen. Ouput
Attn: 50x
x   : 0 - 20   µs
y   : +/- 5.   V
 min: -4.63   V
 max: V

Type: $\dot{D}_N$
Loc : L. Wing
Attn: 0.5x
x   : 0 - 10   µs
y   : +/- 0.252   V
 min: -0.102   V
 max: 0.041   V
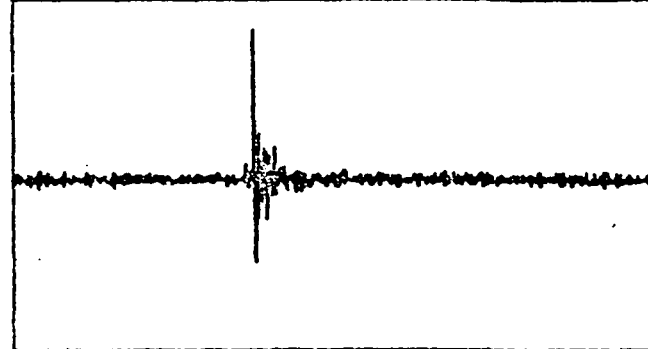
Type: $\dot{D}_N$
Loc : Tail
Attn: 1x
x   : 0 - 10   µs
y   : +/- 0.37   V
 min: -0.17   V
 max: 0.32   V

-93-

C-2

RADIATED // DOORS CLOSED
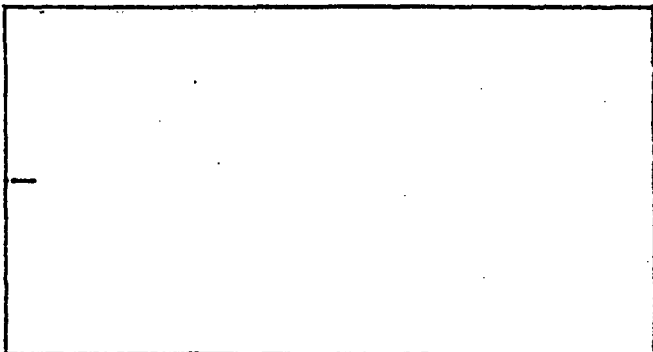
Type:
Loc :
Attn:
x   : 0 -   µs
y   : +/-   V
 min: V
 max: V
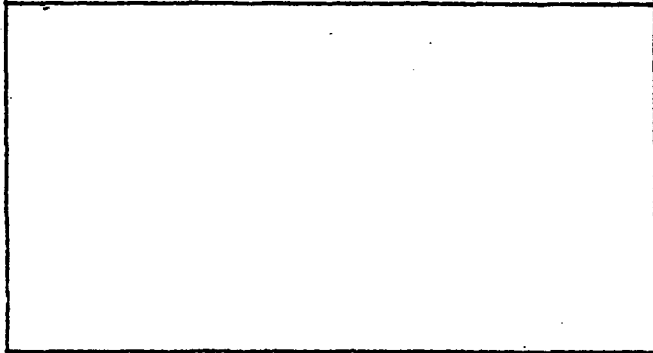
Type:
Loc :
Attn:
x   : 0 -   µs
y   : +/-   V
 min: V
 max: V
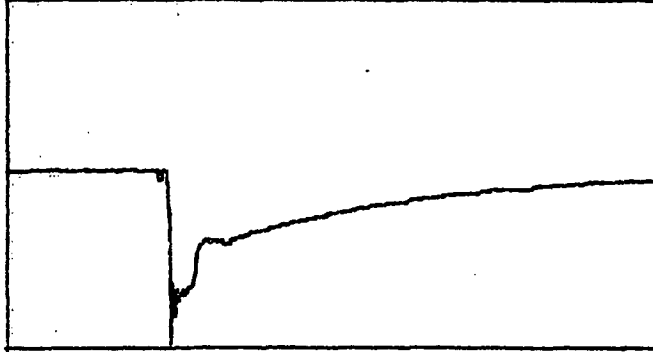
Type: I
Loc : PCT, at Gen. Output
Attn: 50x
x   : 0 - 20   µs
y   : +/- 5.0   V
 min: -5.0   V
 max: V

Type: D_N
Loc : 1. Wing
Attn: 0.5x
x   : 0 - 10   µs
y   : +/- 0.252   V
 min: -0.102   V
 max: 0.041   V
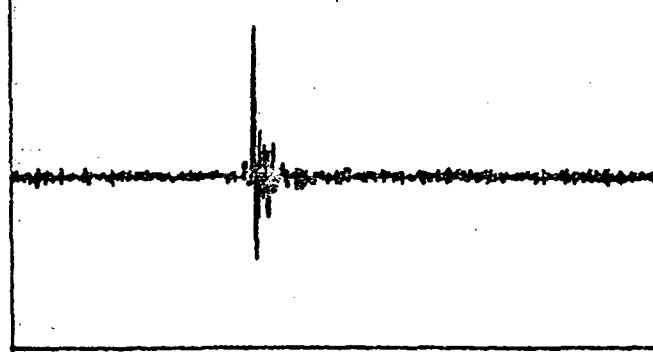
Type: D_N
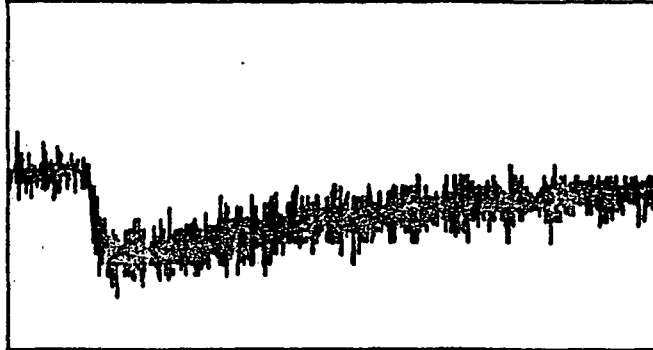Loc : Tail
Attn: 1x
x   : 0 - 10   µs
y   : +/- 0.37   V
 min: -0.17   V
 max: -0.32   V

Type:
Loc :
Attn:
x   : 0 -   μs
y   : +/-   V
 min: V
 max: V
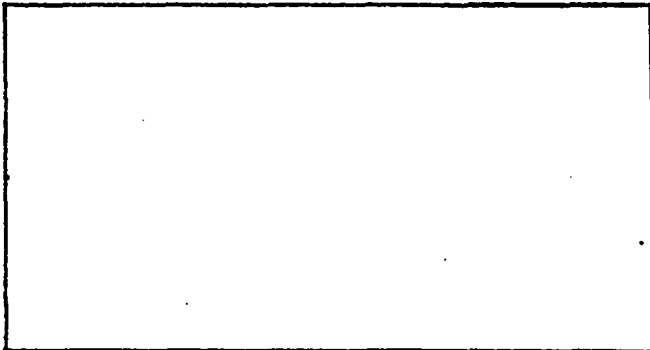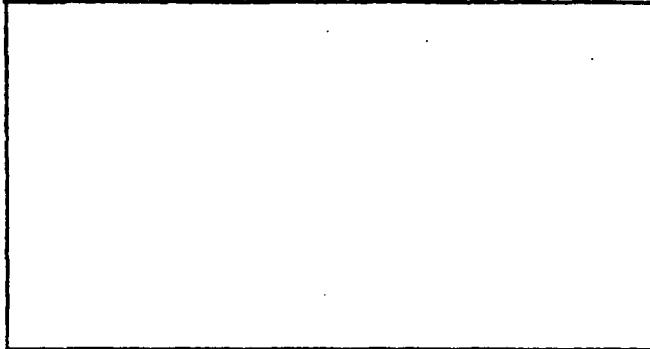
Type:
Loc :
Attn:
x   : 0 -   μs
y   : +/-   V
 min: V
 max: V
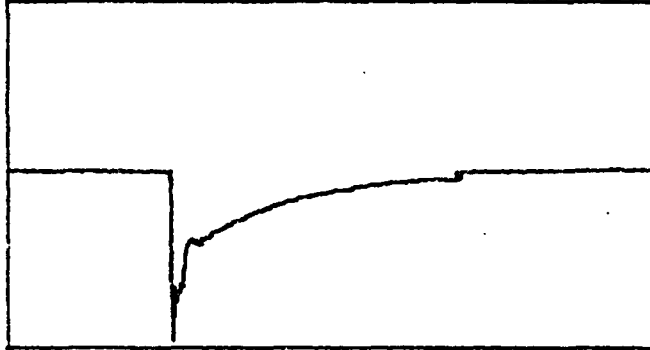
Type: I
Loc : PCT, at Gen. Output
Attn:
x   : 0 - 40   μs
y   : +/- 5.0   V
 min: -4.95   V
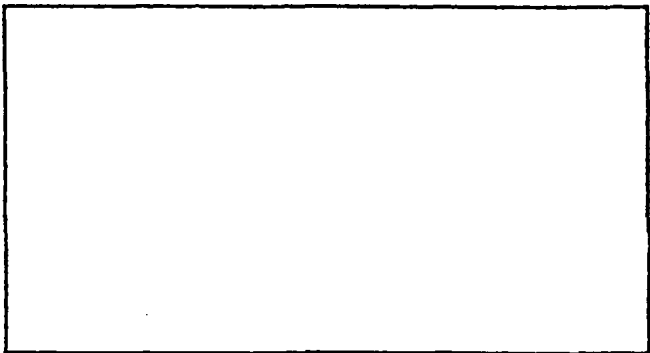 max: V

Type: D_N
Loc : L. Wing
Attn: 0.5x
x   : 0 - 10   μs
y   : +/- 0.252   V
 min: -0.102   V
 max: 0.041   V
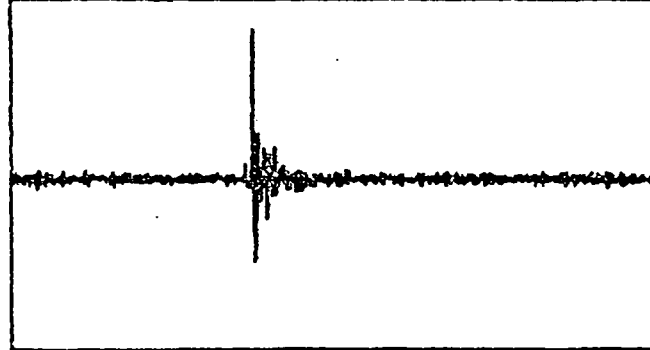
Type: D_N
Loc : Tail
Attn: 1x
x   : 0 - 10   μs
y   : +/- 0.37   V
 min: -0.17   V
 max: 0.32   V

C. Interpretation of Experimental Data

Out of all the raw data presented, the following representative samples were selected and FFT data obtained:

TABLE IX. SELECTED DATA FOR ANALYSIS

Bomb-bay and Cockpit OPEN

Shot No.	Qty.	Location	FFT range
4/2 H	$\dot{D}_N$	R. Wing	(0 to 50 MHz.)
4/2 H	$\dot{D}_N$	Fuselage	(0 to 50 MHz)
4/2 P	$\dot{D}_N$	L. Wing	(0 to 50 MHz)
4/2 P	$\dot{D}_N$	Tail	(0 to 50 MHz)
4/2 P	$\dot{I}_M$		(0 to 50 MHz.)

Bomb-bay and Cockpit CLOSED

Shot No.	Qty.	Location	FFT range
4/2 L	$\dot{D}_N$	R. Wing	(0 to 50 MHz)
4/2 L	$\dot{D}_N$	Fuselage	(0 to 50 MHz)
4/2 Q	$\dot{D}_N$	L. Wing	(0 to 50 MHz)
4/2 Q	$\dot{D}_N$	Tail	(0 to 50 MHz)
4/2 Q	$\dot{I}_M$		(0 to 50 MHz)

It is noted that the amplitude scale on the FFT data is a linear but arbitrary scale. Furthermore, the FFT data presented here are the magnitudes of the transforms of derivative data. To get the transform or the spectral content of the D-dot or I-dot traces, one needs to divide the FFT's presented here by a factor of $2\pi f$, where f is the frequency. This explains why the higher harmonics appear to have a larger amplitude in the FFT curves. The main aircraft resonance corresponding to fuselage = $\lambda_{res}/2$, is about 7.5 MHz. This resonance is identifiable in all of the data, in addition to the generator resonance of approximately 0.35 MHz.* This value also compares well with the results of aircraft models described in Section III. The higher harmonics of principal resonance are seen in addition to more complicated resonances, e.g., forward fuselage plus one wing, aft fuselage plus one wings, etc.

Comparisons can be made between FFT's at the same locations with the bomb bay door and cockpit canopy open and closed indicating differences due to field penetration. In this experimental configuration, since the electric field is mainly in the plane of the aircraft, the difference between doors open and closed is much less than a situation where the entire aircraft is immersed in an electromagnetic field.

Finally, it is observed that the main current I (Pearson Current Transformer) (see Shot 4/2 x 1-6 for example) has a notch roughly 600ns after the start of the pulse. This is the time of arrival of the reflected pulse at the measurement location. The reflected pulse, although not significant, could have been reduced by lowering the termination resistance from the 1250 ohms used in the experiment. This refinement was not done in the time spent on this phase of the overall lightning simulation study.

* This number for the generator resonance was supplied by MACAIR.

DOORS OPEN   Test: 4/2 H

0   FREQ. MHZ.   50.0

DOORS CLOSED   Test: 4/2 L

0   FREQ. MHZ.   50.0

RADIATED // FOURIER TRANSFORM
Type: D_N Location: Fus.

DOORS OPEN   Test: 4/2 H

0   FREQ. MHZ.   50.0

DOORS CLOSED   Test: 4/2 L

0   FREQ. MHZ.   50.0

DOORS OPEN   Test: 4/2 P

0   FREQ. MHZ.   50.0

DOORS CLOSED   Test: 4/2 Q

0   FREQ. MHZ.   50.0

ORIGINAL PAGE IS
OF POOR QUALITY

DOORS OPEN   Test: 4/2 P

0   FREQ. MHZ.   50.0

DOORS CLOSED   Test: 4/2 Q

0   FREQ. MHZ.   50.0

DOORS OPEN   Test: 4/2 P

0   FREQ. MHZ.   50.0

DOORS CLOSED   Test: 4/2 Q

0   FREQ. MHZ.   50.0
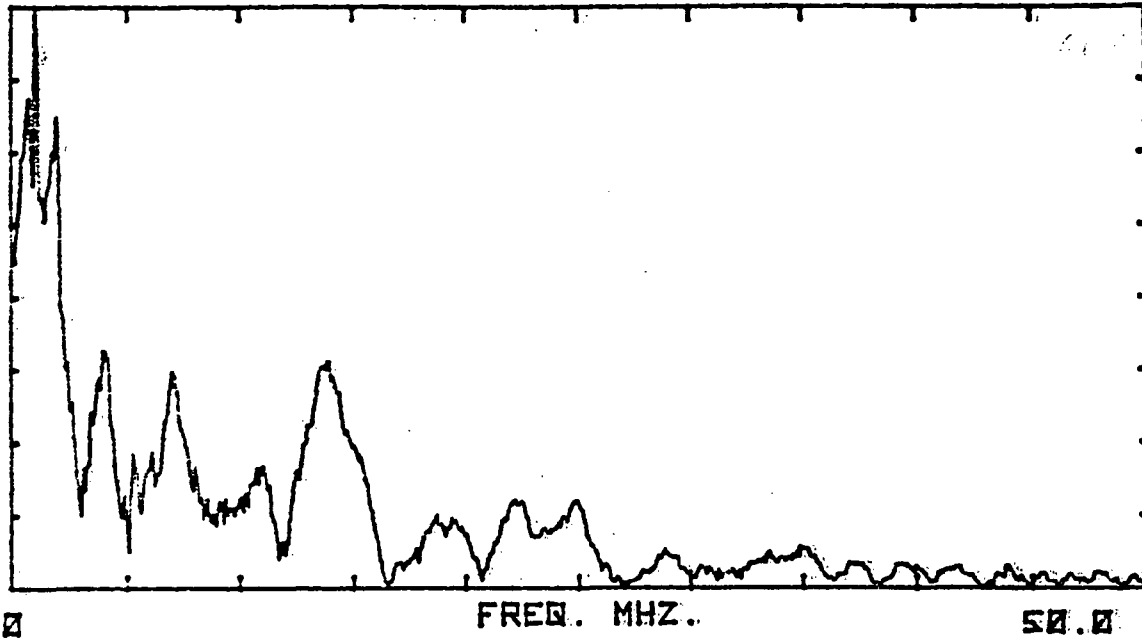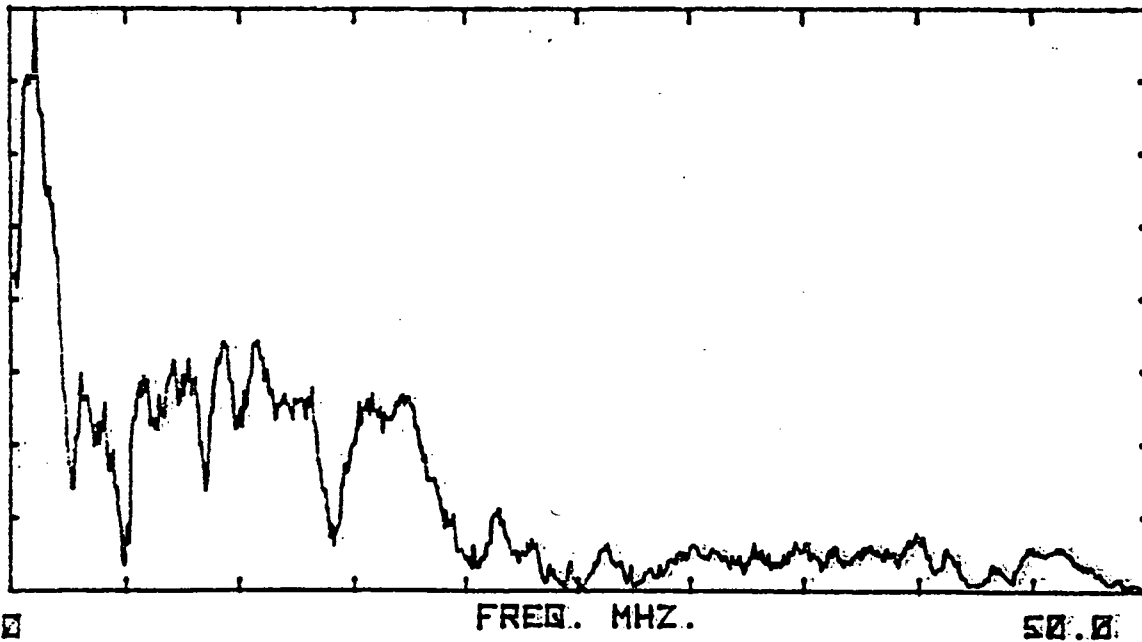
SECTION VI

SUMMARY AND CONCLUSIONS

This report has discussed a transmission line model useful for interpreting nearby and direct strike lightning data measured on aircraft. The basic approach is to process the measured transient data in order to determine a knowledge of the natural resonances of the aircraft, and then remove these from the data. The data processed in this manner is thus a more accurate representation of the actual lightning excitation of the aircraft.

In doing this, there are several uncertainties which arise. First, the process of extracting the natural resonances or poles by the Prony method or by an FFT calculation may not be accurate. Furthermore, once this is done, it is difficult to identify which poles are due to the aircraft, and which arise from the time domain dependence of the exciting source.

In an attempt to determine the sensitivity of the aircraft poles to the modeling of the aircraft and channel, a series of stick wire calculations have been performed. These indicate that there can be a significant variation of pole location in the complex frequency plane with the calculational model used, thereby adding to difficulty in identifying which poles should be extracted from the measured data. Finally, the effect of the lightning channel on the measured data was seen to reduce the resonant frequencies of the aircraft, and otherwise add more difficulty in interpreting the lightning data.

Notwithstanding these difficulties, the data processing technique suggested in this report is illustrated by processing several data records for the 1981 flight test. This is done by removing all oscillatory poles and the remaining data appear to be that of one or more exponential functions. The corrected response for the case of a direct strike excitation of the aircraft is seen to be significantly larger than the response of the nearby strike, as expected.

The 1981 measured data has been processed to yield the FFT and Prony poles and residues, and these are presented in this report.

Unfortunately, time does not permit a more detailed analysis of the pole data in this effort. It would be particularly useful to divide the data into nearby and direct strike categories, and study the statistical distributions of the Prony pole locations in order to obtain a more detailed knowledge of the effects of the lightning channel on the aircraft response.

In addition, in the theoretical development in Section II, the effects of the transfer function on the aircraft have been discussed, but not calculated explicitly due to the fact that knowledge of the angle of incidence of the nearby strikes, and the attachment and detachment points for the direct strike case were not always available. It would be useful in future efforts to have a better understanding of these quantities, so that this type of data analysis can be used.

REFERENCES

[1] Pitts, F.L., and M.E. Thomas, "1980 Direct Strike Lightning Data", NASA Technical Memorandum 81946, February, 1981.

[2] Pitts, F.L., and M.E. Thomas, "1981 Direct Strike Lightning Data", NASA Technical Memorandum 83273, March, 1982.

[3] Ruldolph, T., and R.A. Perala, "Interpretation Methodology and Analysis of In-Flight Lightning Data", NASA Contractor Report 3590, October, 1982.

[4] Turner, C.D., and T.F. Trost, "Laboratory Modeling and Analysis of Aircraft-Lightning Interactions", NASA Contractor Report 169455, August, 1982.

[5] Taylor, C.D., "External Interaction of the Nuclear EMP with Aircraft and Missiles", IEEE Trans. EMC, Vol. MEC-20, No. 1, February, 1978, pp. 64-76.

[6] Harrington, R.F., FIELD COMPUTATION BY MOMENT METHODS, reprinted by the author, 1968.

[7] Poggio, A.J., and E.K. Miller, "Integral Equation Solutions of Three Dimensional Scattering Problems," COMPUTER TECHNIQUES FOR ELECTROMAGNETICS, R. Mittra, Ed. Permagon, 1973, Ch. 4.

[8] Bedrosian, G., "Stick-Model Characterization of the Natural Frequencies and Natural Modes of the Aircraft", AFWL EMP Interaction Note 326, September 14, 1977.

[9] Baum, C.E., "Resistively Loaded Radiating Dipole Based on a Transmission Line Model for the Antenna", AFWL EMP Sensor and Simulation Notes, Note SSN 81, April 7, 1969.

[10] Prewitt, J.F., and D.L. Wright, "Transmission Line Model of a Radiating Dipole with Special Form of Impedance Loading", AFWL EMP Sensor and Simulation Notes, Note SSN 185, September, 1973.

[11] Baum, C.E., "The Singularity Expansion Method", TRANSIENT ELECTROMAGNETIC FIELDS, L.B. Felsen, Ed., Springer-Verlag, 1975, Ch. 3.

[12] Poggio, A.J., M.L. Van Blaricum, E.K. Miller, and R. Mittra, "Evaluation of a Processing Technique for Transient Data", IEEE Trans. A.P., Vol AP-26, No.1, January, 1978, pp. 165-182.

[13] Scrivner, G.L., "Prony Analysis in the Presence of Noise", AFWL Mathmatics Notes, Note 67, October, 1977.

[14] Wu, T.T., and R.W.P. King, "The Tapered Antenna and its Application to the Junction Problem for Thin Wires", IEEE Trans. A.P., Vol. AP-24, No. 1, January, 1976, pp. 42-45.

[15] Trost, T.F., and F.L. Pitts, "Analysis of Electromagnetic Fields on an F-106B Aircraft During Lightning Strikes," International Aerospace Conference on Lightning and Static Electricity, Oxford (1982).

[16] Cooley, J.W., and J.W. Tukey, "An Algorithm for the Machine Computation of Complex Fourier Series", Math. Comp., Vol. 19, April, 1965, pp. 297-301

APPENDIX

This appendix presents the measured 1981 lightning data acquired by NASA on the F-106 aircraft. In addition to the raw B-dot or D-dot data which is reproduced here for completeness, the FFT transformed data is also plotted. Following these, the peak values (resonances) in the spectral domain are tabulated, as are the Prony poles and residues. The following table summarizes the individual data records and the pages in which these data are found.

TABLE X

INDEX OF PROCESSED 1981

IN-FLIGHT LIGHTNING DATA

Page	Figure	Strike #	Record #	Type	Notes
109	A1	81-026	1	D nearby	
112	A2	81-026	2A	D nearby	2 excitations for this record.
116	A3	81-026	2B	D nearby	2nd followed 1st by $\cong$ 4 µs
118	A4	81-026	3	D nearby	
121	A5	81-026	4	D nearby	
124	A6	81-026	5	D nearby	
128	A7	81-026	5	B nearby	
132	A8	81-026	6	D nearby	
135	A9	81-026	7	D nearby	
139	A10	81-026	8	D nearby	
143	A11	81-026	8	B nearby	
146	A12	81-026	9	D nearby	
149	A13	81-026	9	B nearby	
153	A14	81-026	10	D nearby	
159	A15	81-026	10	B nearby	
163	A16	81-041	1	B nearby	
166	A17	81-041	2	B nearby	
171	A18	81-042		B direct	no record # given
174	A19	81-043	1	B direct	
177	A20	81-043	2	B direct	
180	A21	81-043	3	B direct	
185	A22	81-043	4	B direct	
189	A23	81-045	1	B nearby	
192	A24	81-045	2	B nearby	
195	A25	81-045	3	B nearby	
197	A26	81-045	4	B nearby	
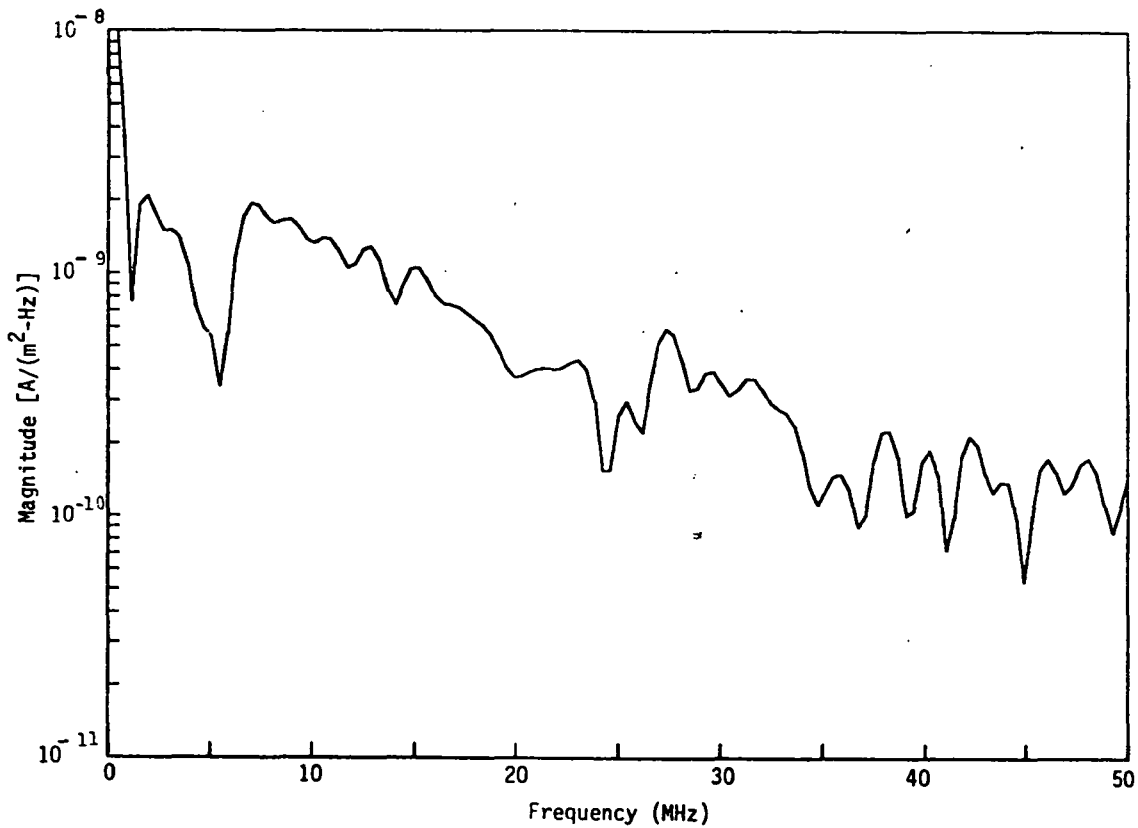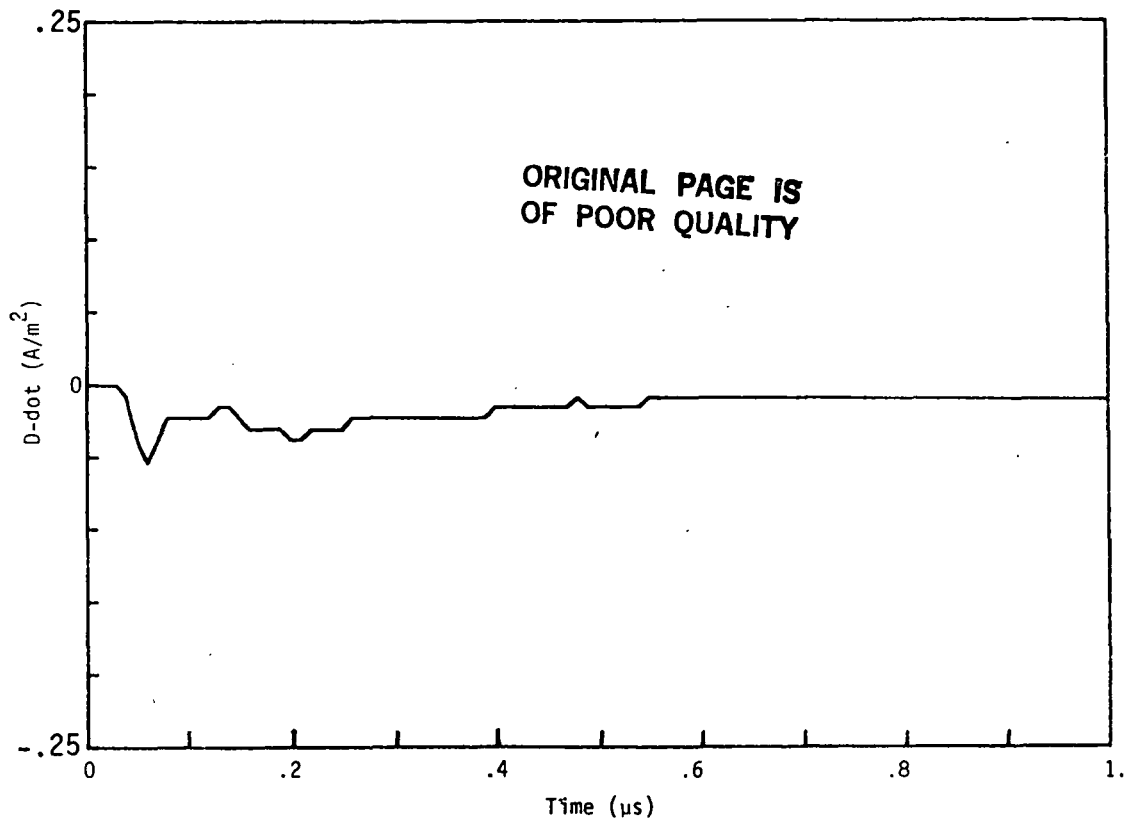
Figure A1.   Measured D-dot Data (a) and Computed Spectral Response (b) for Flight 81-026-01.

P E A K   P I C K
* Relative peak height for this run ---> 5E-03 *
* Bounds set for this run : 2 to 50 Mhz

FILENAME ---> D810261/FRQ
* Min pt ---> 44.92 MHz , 5.36E-04 amplitude

* increasing frequency representation *

* # *	* MHz *	* amplitude *
1	7.03	1.95E-02
2	8.98	1.67E-02
3	10.55	1.40E-02
4	12.89	1.29E-02
5	15.23	1.06E-02
6	21.48	4.06E-03
7	23.05	4.38E-03
8	25.39	2.97E-03
9	27.34	5.91E-03
10	29.69	3.97E-03
11	31.25	3.69E-03

* decreasing amplitude representation *
* the 10 highest peaks *

* # *	* MHz *	* amplitude *	* % *
1	7.03	1.95E-02	100.00
2	8.98	1.67E-02	85.69
3	10.55	1.40E-02	71.63
4	12.89	1.29E-02	66.10
5	15.23	1.06E-02	54.06
6	27.34	5.91E-03	30.27
7	23.05	4.38E-03	22.42
8	21.48	4.06E-03	20.80
9	29.69	3.97E-03	20.33
10	31.25	3.69E-03	18.89

P R O N Y   A N A L Y S I S

* Filename ---> d810261 * dt =0.010 *

** Window 0 * 26 poles * t = .04 to .56 us **

Pole Pair	Prony Pole damp. freq(MHz)		Prony Residue real imag		Residue pole	%
1	-3.86	0.0	-0.776	0.0000	0.201	100.000
2	-11.04	0.0	0.705	0.0000	0.064	31.722
3	-7.94	6.6	-0.085	0.0747	0.003	1.333
4	-26.22	21.4	0.155	0.0832	0.001	0.639
5	-144.96	0.0	-0.162	0.0003	0.001	0.557'
6	-6.74	23.2	-0.023	-0.0284	0.000	0.125
7	-10.66	33.2	0.011	-0.0153	0.000	0.044
8	-6.93	45.0	0.011	0.0013	0.000	0.020
9	-0.79	27.2	0.006	0.0017	0.000	0.019
10	-3.00	41.7	0.000	-0.0048	0.000	0.009

* 9 of 26 poles rejected. *

** Window 0 * 18 poles * t = .04 to .4 us **

Pole Pair	Prony Pole damp. freq(MHz)		Prony Residue real imag		Residue pole	%
1	-1.41	0.0	-0.355	0.000	0.252	100.00
2	-13.00	22.1	0.083	-0.067	0.001	0.30

* 15 of 18 poles rejected. *

** Window 0 * 10 poles * t = .04 to .24 us **

Pole Pair	Prony Pole damp. freq(MHz)		Prony Residue real imag		Residue pole	%
1	-29.88	0.0	-0.827	0.000	0.028	100.00
2	-127.63	0.0	0.727	-0.000	0.006	20.58
3	-24.26	33.3	-0.001	-0.051	0.000	0.88
4	-0.35	19.7	0.022	0.016	0.000	0.78

* 4 of 10 poles rejected. *
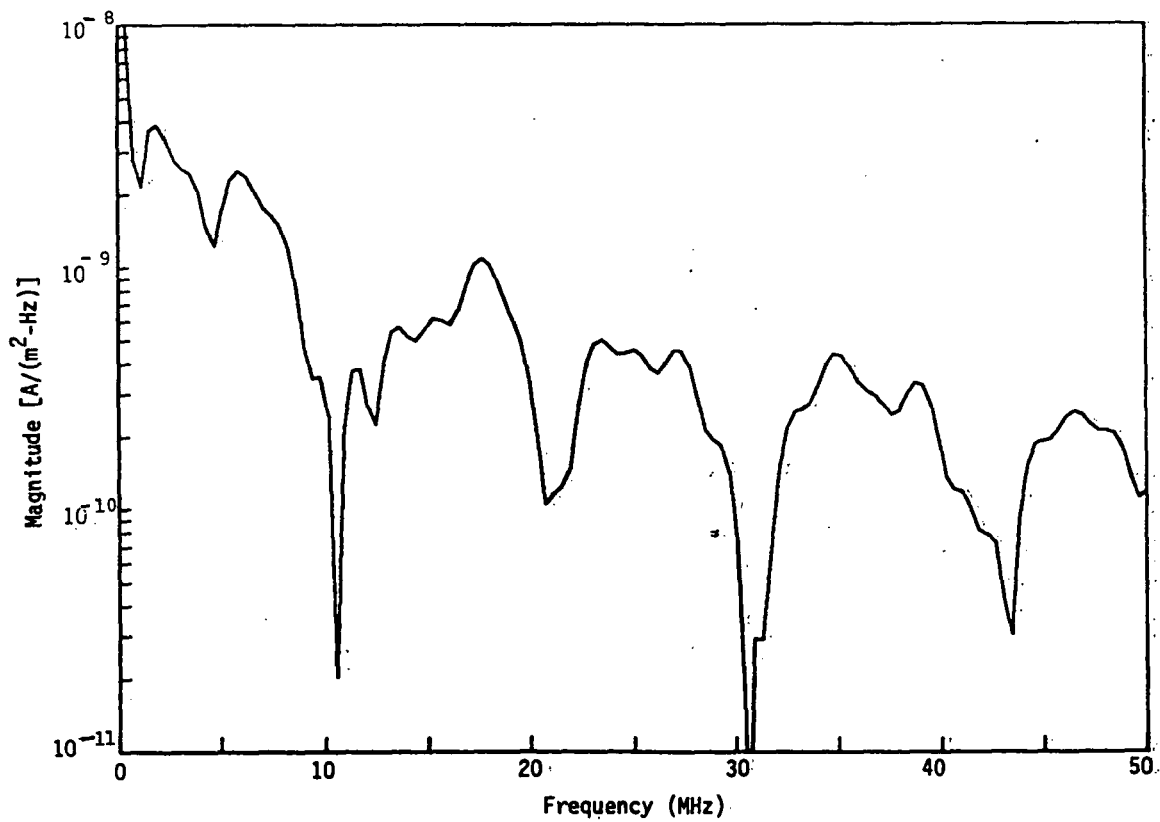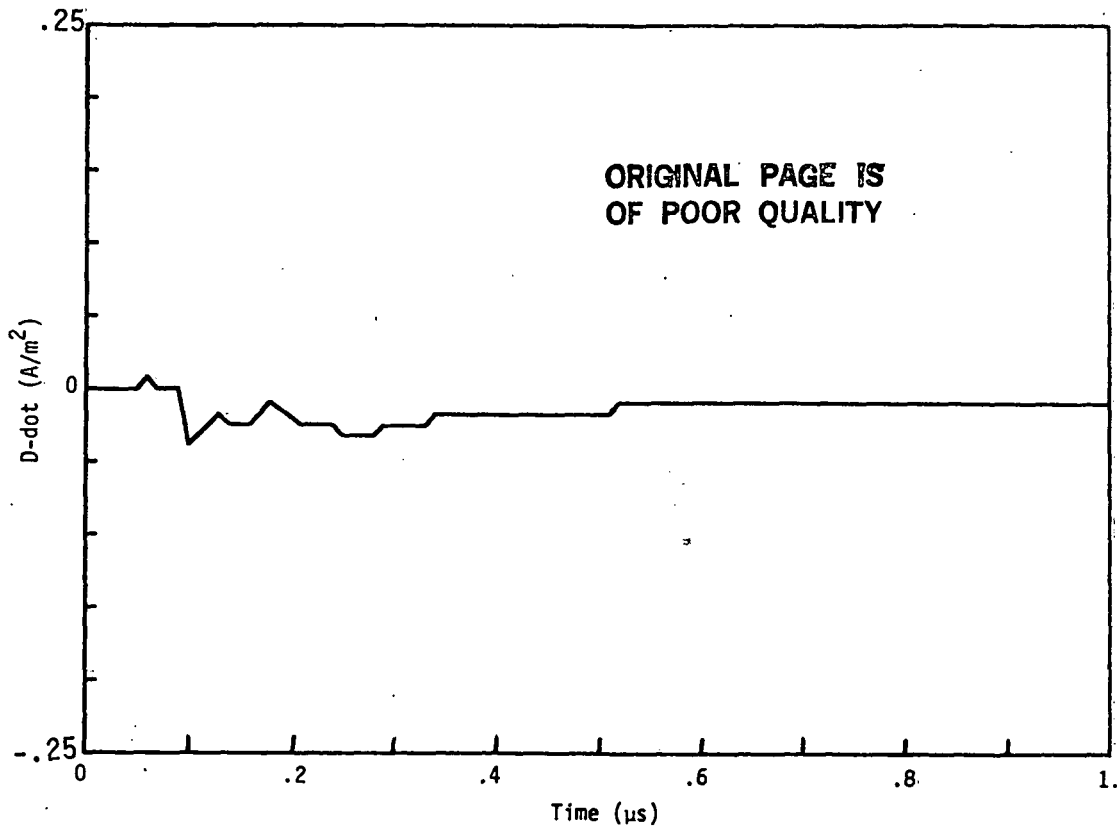
Figure A2.   Measured D-dot Data (a) and Computed Spectral Response (b)
for Flight 81-026-02.

P E A K   P I C K
* Relative peak height for this run --> 5E-03   *
* Bounds set for this run : 2 to 50 Mhz

FILENAME ---> D810262A/FRQ
* Min pt --> 30.47 MHz , 7.63E-05 amplitude

* increasing frequency representation *

* # *	* MHz *	* amplitude *
1	5.86	2.53E-02
2	9.77	3.55E-03
3	11.72	3.83E-03
4	13.67	5.71E-03
5	15.23	6.15E-03
6	17.58	1.09E-02
7	23.44	5.03E-03
8	25.00	4.56E-03
9	26.95	4.55E-03
10	34.77	4.36E-03
11	38.67	3.34E-03

* decreasing amplitude representation *
* the 10 highest peaks *

* # *	* MHz *	* amplitude *	* % *
1	5.86	2.53E-02	100.00
2	17.58	1.09E-02	43.21
3	15.23	6.15E-03	24.32
4	13.67	5.71E-03	22.56
5	23.44	5.03E-03	19.86
6	25.00	4.56E-03	18.02
7	26.95	4.55E-03	17.98
8	34.77	4.36E-03	17.25
9	11.72	3.83E-03	15.16
10	9.77	3.55E-03	14.04

PRONY ANALYSIS

* Filename ---> d810262 * dt =0.010 *

** Window 6 * 30 poles * t = .1 to .7 us **

Pole Pair	Prony damp.	Pole freq(MHz)	Prony real	Residue imag	Residue / pole	%
1	-4.84	0.4	-0.0921	0.4972	0.094	100.00
2	-57.19	0.0	0.0966	-0.0057	0.002	1.81
3	-3.95	5.3	-0.0495	-0.0212	0.002	1.72
4	-6.33	17.7	-0.0379	-0.0168	0.000	0.40
5	-8.76	43.6	-0.0098	-0.0277	0.000	0.11
6	-2.75	38.8	-0.0047	-0.0074	0.000	0.04

* 19 of 30 poles rejected. *

** Window 4 * 30 poles * t = .08 to .68 us **

Pole Pair	Prony damp.	Pole freq(MHz)	Prony real	Residue imag	Residue / pole	%
1	-2.94	0.5	-0.1242	0.1992	0.055	100.00
2	-55.28	0.0	0.5062	-0.0267	0.009	16.76
3	-4.20	17.6	0.0154	0.0237	0.000	0.47

* 25 of 30 poles rejected. *

** Window 2 * 30 poles * t = .06 to .66 us **

Pole Pair	Prony damp.	Pole freq(MHz)	Prony real	Residue imag	Residue / pole	%
1	-3.53	0.0	-0.6230	0.0000	0.177	100.00
2	-12.99	0.0	0.7630	-0.0000	0.059	33.25
3	-2.19	5.7	0.0115	0.0460	0.001	0.75
4	-19.09	20.7	-0.1267	0.0319	0.001	0.56
5	-3.30	7.2	0.0108	0.0284	0.001	0.38
6	-5.51	17.3	0.0306	-0.0178	0.000	0.18
7	-11.27	35.0	0.0277	-0.0230	0.000	0.09
8	-14.45	45.2	0.0110	-0.0362	0.000	0.08
9	-3.84	39.1	0.0106	-0.0016	0.000	0.02

* 14 of 30 poles rejected. *

PRONY   ANALYSIS

* Filename ---> d810262   (continued)   *   dt =0.010 *

** Window 0 * 30 poles * t = .04 to .64 us **

Pole Pair	Prony damp.	Pole freq(MHz)	Prony real	Residue imag	Residue pole	%
1	-3.55	0	-0.6744	0.000	0.190	100.00
2	-12.80	0	0.9779	-0.055	0.076	40.30
3	-204.83	0	-0.8178	-1.014	0.006	3.35

* 27 of 30 poles rejected. *

** Window 0 * 22 poles * t = .04 to .48 us **

Pole Pair	Prony damp.	Pole freq(MHz)	Prony real	Residue imag	Residue pole	%
1	-2.67	0.0	-0.4625	0.0000	0.173	100.000
2	-24.87	0.0	1.5091	-0.0043	0.061	35.045
3	-78.31	0.0	-1.2200	0.0032	0.016	8.998
4	-8.15	5.4	0.0393	0.1890	0.006	3.207
5	-30.29	38.6	0.1995	0.4398	0.002	1.142
6	-1.77	0.0	0.0028	0.0000	0.002	0.917
7	-11.67	18.3	-0.0877	0.1306	0.001	0.786
8	-9.36	36.8	0.0256	-0.0510	0.000	0.142
9	-7.61	42.2	-0.0209	0.0226	0.000	0.067
10	-0.20	27.3	0.0010	-0.0027	0.000	0.010

* 6 of 22 poles rejected. *

** Window 0 * 14 poles * t = .04 to .32 us **

Pole Pair	Prony damp.	Pole freq(MHz)	Prony real	Residue imag	Residue pole	%
1	-0.05	1.5	0.029	0.1319	0.015	100.00
2	-5.83	6.3	0.104	0.0230	0.003	18.09
3	-12.69	19.1	-0.005	0.1399	0.001	7.85
4	-31.15	32.0	-0.158	0.0663	0.001	5.71
5	-8.64	14.5	0.022	0.0069	0.000	1.73
6	-13.87	45.8	0.008	-0.0487	0.000	1.16

* 2 of 14 poles rejected. *

ORIGINAL PAGE IS
OF POOR QUALITY
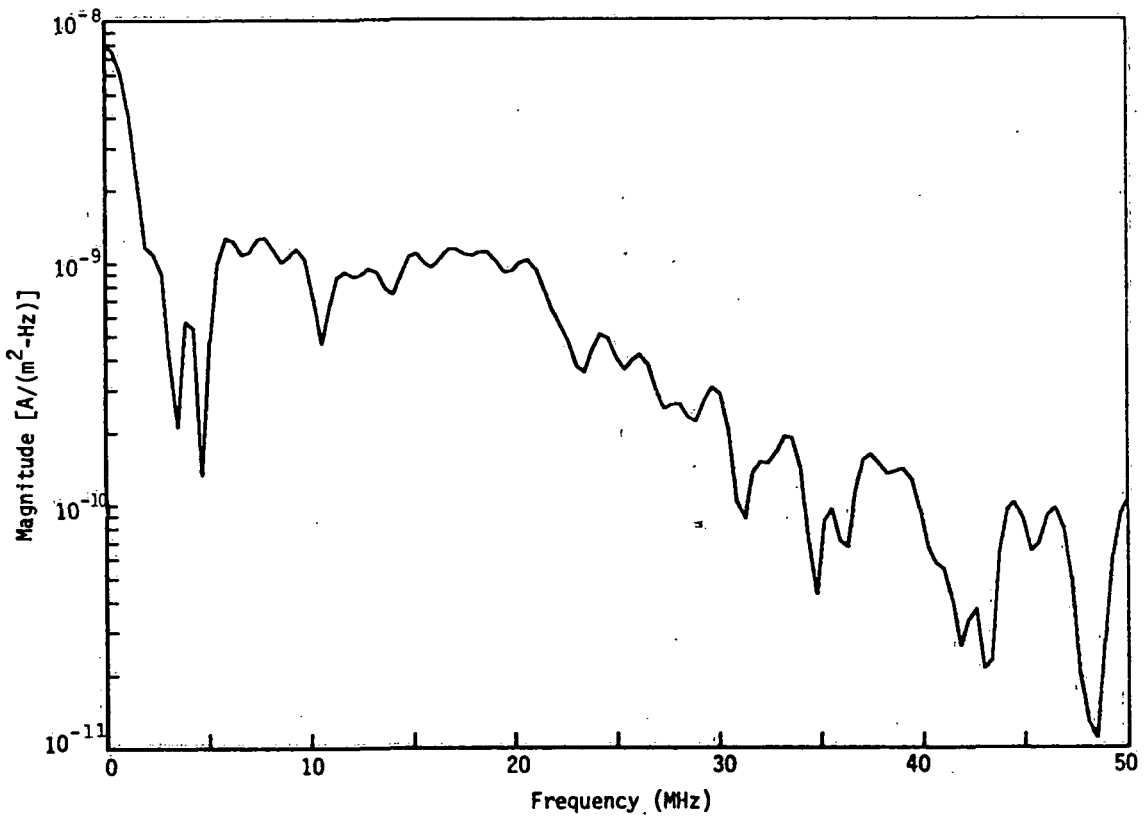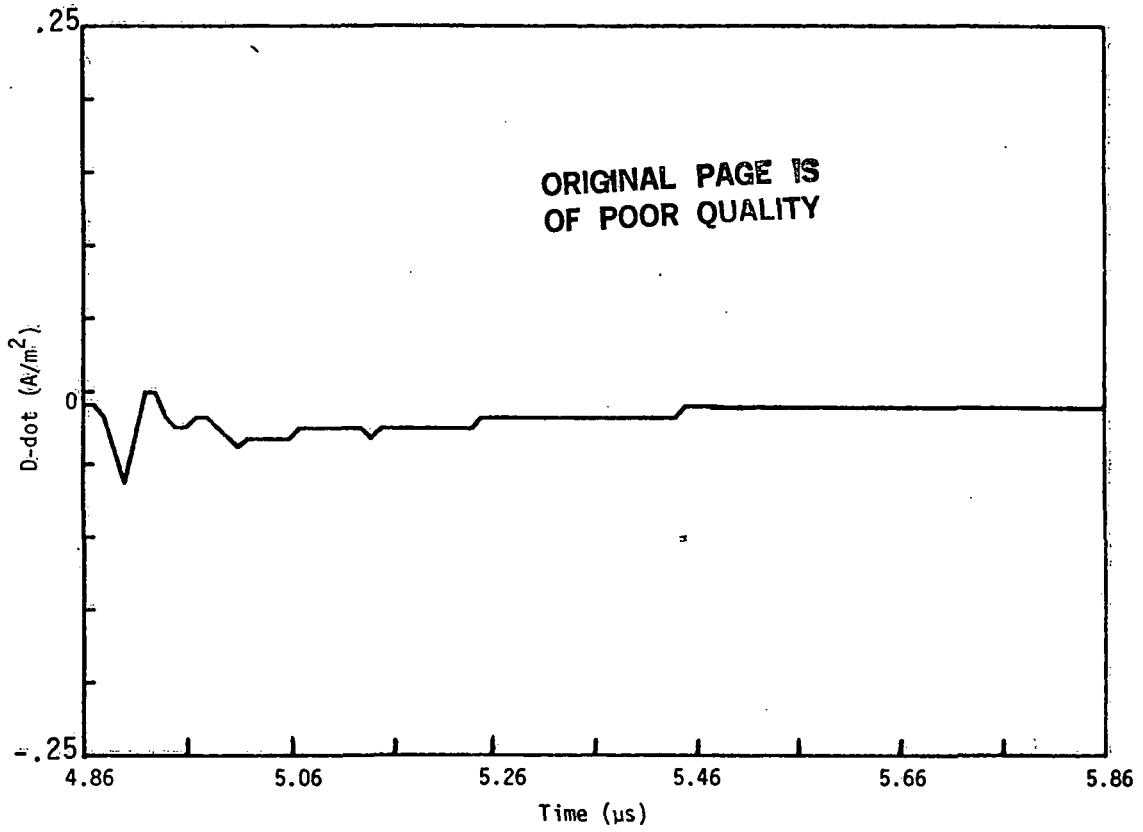
Figure A3.   Measured D-dot Data (a) and Computed Spectral Response (b)
for Flight 81-026-02 (continued).

-116-

P E A K   P I C K
* Relative peak height for this run --> 5E-03   *
* Bounds set for this run : 2 to 50 Mhz

FILENAME   ---> D810262B/FRQ
* Min pt --> 48.44 MHz , 1.09E-04 amplitude

* increasing frequency representation *

* # *	* MHz *	* amplitude *
1	3.91	5.72E-03
2	5.86	1.26E-02
3	7.81	1.27E-02
4	9.38	1.14E-02
5	11.72	9.15E-03
6	12.89	9.44E-03
7	15.23	1.08E-02
8	17.19	1.13E-02
9	18.36	1.10E-02
10	20.70	1.02E-02
11	24.22	5.04E-03
12	26.17	4.17E-03
13	29.69	3.05E-03

* decreasing amplitude representation *
* the 10 highest peaks *

* # *	* MHz *	* amplitude *	* % *
1	7.81	1.27E-02	100.00
2	5.86	1.26E-02	99.27
3	9.38	1.14E-02	90.01
4	17.19	1.13E-02	89.05
5	18.36	1.10E-02	86.80
6	15.23	1.08E-02	85.13
7	20.70	1.02E-02	80.10
8	12.89	9.44E-03	74.25
9	11.72	9.15E-03	71.92
10	3.91	5.72E-03	44.97

Figure A4.   Measured D-dot Data (a) and Computed Spectral Response (b) for Flight 81-026-03.

P E A K   P I C K
* Relative peak height for this run --> 5E-03   *
* Bounds set for this run : 2 to 50 Mhz

FILENAME   ---> D810263/FRQ
* Min pt --> 29.69 MHz , 8.47E-05 amplitude

* increasing frequency representation *

* # *	* MHz *	* amplitude *
1	2.73	2.01E-02
2	4.30	9.69E-03
3	6.25	2.04E-02
4	8.20	2.30E-02
5	11.33	1.29E-02
6	12.89	9.38E-03
7	14.84	7.59E-03
8	20.70	4.03E-03
9	22.66	4.52E-03
10	24.61	4.22E-03
11	26.17	5.53E-03
12	32.42	3.01E-03

* decreasing amplitude representation *
* the 10 highest peaks *

* # *	* MHz *	* amplitude *	* % *
1	8.20	2.30E-02	100.00
2	6.25	2.04E-02	88.57
3	2.73	2.01E-02	87.23
4	11.33	1.29E-02	55.97
5	4.30	9.69E-03	42.09
6	12.89	9.38E-03	40.74
7	14.84	7.59E-03	32.95
8	26.17	5.53E-03	24.04
9	22.66	4.52E-03	19.64
10	24.61	4.22E-03	18.32

PRONY   ANALYSIS

* Filename ---> d810263 *   dt =0.010 *

** Window 0 * 30 poles * t = .04 to .64 us **

Pole Pair	Prony Pole damp. freq(MHz)		Prony Residue real	imag	Residue / pole	%
1	-2.27	0.0	-0.4780	0.000	0.211	100.00
2	-80.02	0.0	1.3138	0.019	0.016	7.80
3	-10.91	5.4	-0.2772	-0.041	0.008	3.74
4	-75.25	0.0	-0.2518	-0.048	0.003	1.62
5	-2.74	0.0	0.0071	-0.001	0.003	1.24
6	-2.03	14.7	0.0059	0.004	0.000	0.04

* 22 of 30 poles rejected. *

** Window 0 * 22 poles * t = .04 to .48 us **

Pole Pair	Prony Pole damp. freq(MHz)		Prony Residue real	imag	Residue / pole	%
1	-1.87	0.0	-0.433	0.000	0.232	100.00
2	-9.84	5.0	-0.162	-0.169	0.007	3.09
3	-19.20	0.0	0.094	-0.000	0.005	2.11
4	-14.79	8.4	0.157	0.045	0.003	1.29
5	-15.53	26.4	0.014	-0.119	0.001	0.31
6	-10.41	22.0	-0.034	-0.041	0.000	0.17
7	-9.37	16.4	0.014	-0.036	0.000	0.16
8	-22.66	45.0	0.087	-0.048	0.000	0.15
9	-17.14	34.3	0.012	-0.068	0.000	0.14

* 6 of 22 poles rejected. *

** Window 0 * 14 poles * t = .04 to .32 us **

Pole Pair	Prony Pole damp. freq(MHz)		Prony Residue real	imag	Residue / pole	%
1	-42.32	16.3	0.1686	-0.136	0.002	100.00
2	-2.23	6.6	-0.0630	0.050	0.002	98.11
3	-3.93	0.0	0.0068	-0.000	0.002	88.44
4	-3.42	42.0	-0.0058	0.005	0.000	1.48

* 7 of 14 poles rejected. *
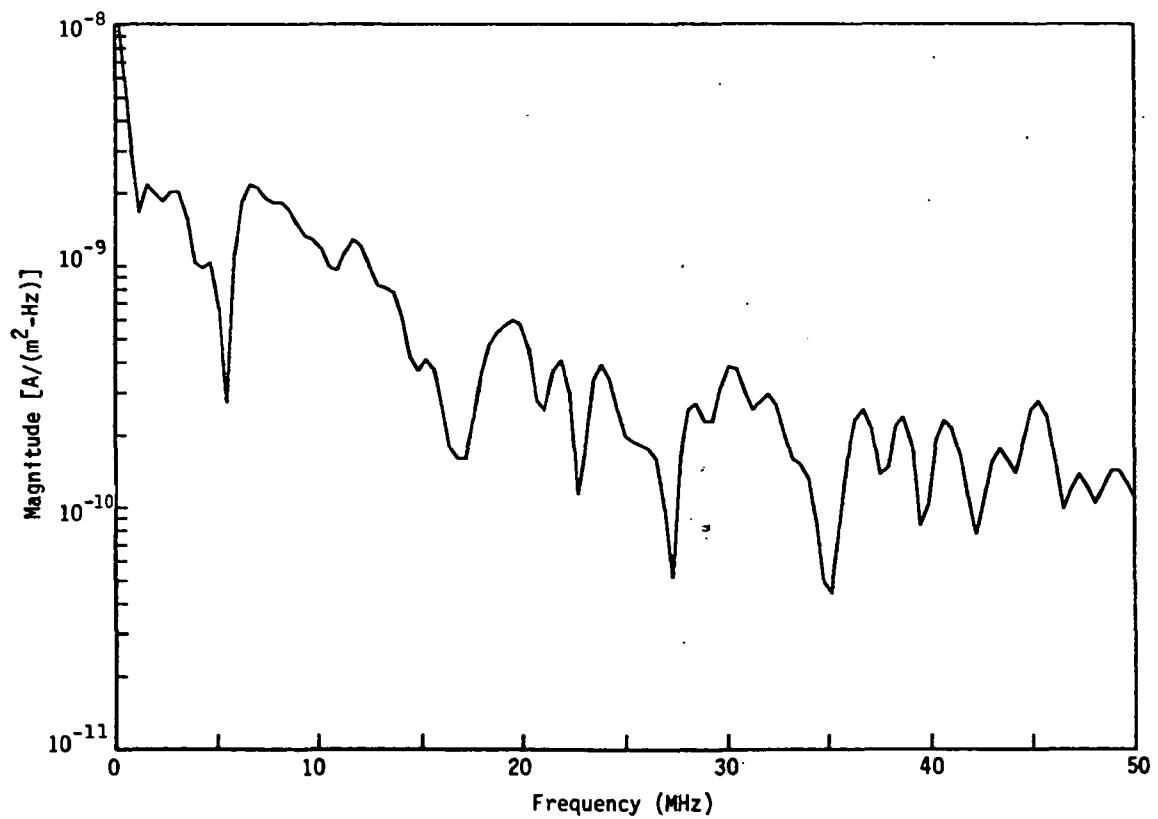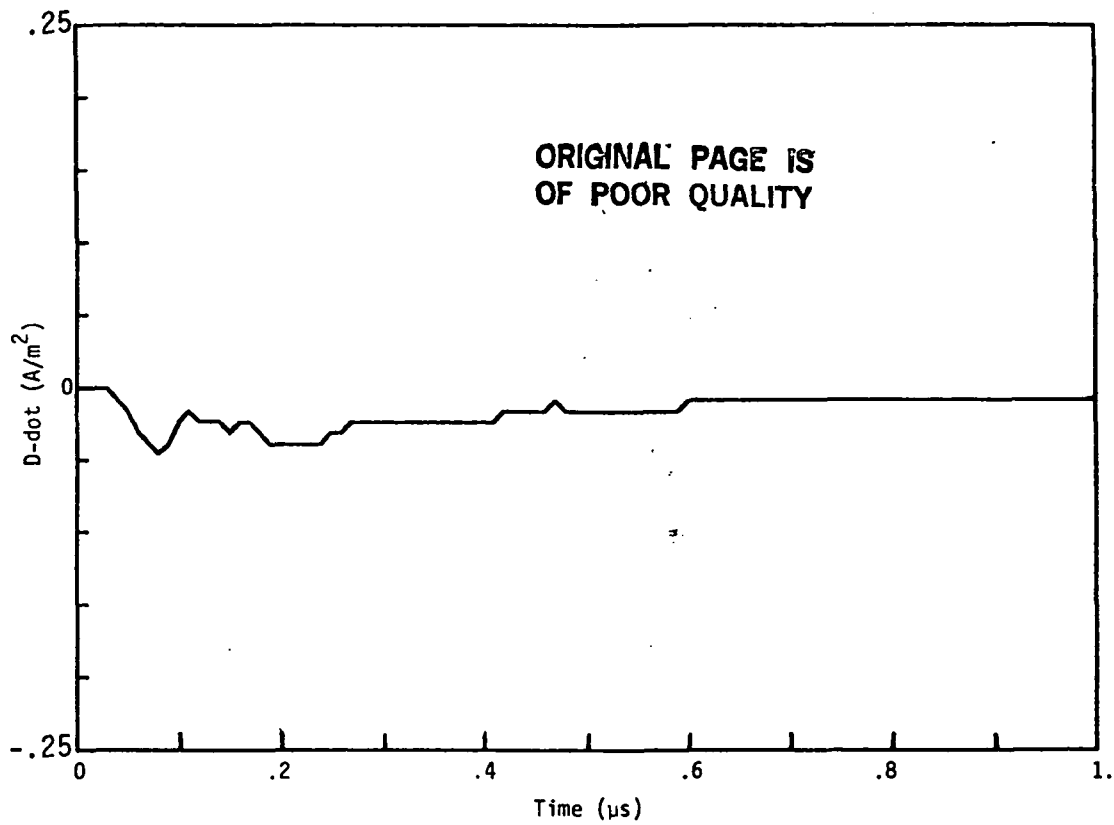
Figure A5. Measured D-dot Data (a) and Computed Spectral Response (b) for Flight 81-026-04.

P E A K   P I C K
* Relative peak height for this run --> 5E-03 *
* Bounds set for this run : 2 to 50 Mhz

FILENAME ---> D810264/FRQ
* Min pt --> 35.16 MHz , 4.44E-04 amplitude

* increasing frequency representation *

* # *	* MHz *	* amplitude *
1	2.73	2.05E-02
2	4.69	1.04E-02
3	6.64	2.19E-02
4	11.72	1.29E-02
5	15.23	4.13E-03
6	19.53	6.03E-03
7	21.88	4.10E-03
8	23.83	3.94E-03
9	30.08	3.87E-03
10	32.03	2.98E-03

* decreasing amplitude representation *
* the 10 highest peaks *

* # *	* MHz *	* amplitude *	* % *
1	6.64	2.19E-02	100.00
2	2.73	2.05E-02	93.60
3	11.72	1.29E-02	59.01
4	4.69	1.04E-02	47.40
5	19.53	6.03E-03	27.58
6	15.23	4.13E-03	18.90
7	21.88	4.10E-03	18.78
8	23.83	3.94E-03	18.02
9	30.08	3.87E-03	17.70
10	32.03	2.98E-03	13.63

P R O N Y   A N A L Y S I S

* Filename ---> d810264 * dt =0.010 *

** Window 0 * 28 poles * t = .04 to .6 us **

Pole Pair	Prony Pole damp. freq(MHz)		Prony Residue real	imag	Residue / pole	%
1	-2.44	0.0	-0.4770	0.0000	0.195	100.00
2	-74.91	0.0	1.0424	0.0013	0.014	7.13
3	-111.84	0.0	-0.4062	0.1605	0.004	2.00
4	-5.83	3.9	-0.0521	-0.0302	0.002	1.24
5	-7.05	19.1	-0.0364	-0.0245	0.000	0.19
6	-14.15	28.1	-0.0224	0.0596	0.000	0.18
7	-4.46	11.3	-0.0194	0.0113	0.000	0.16

* 17 of 28 poles rejected. *

** Window 0 * 20 poles * t = .04 to .44 us **

Pole Pair	Prony Pole damp. freq(MHz)		Prony Residue real	imag	Residue / pole	%
1	-0.03	0.0	-0.3390	0.000	11.113	100.000
2	-88.60	23.7	0.3730	-0.553	0.004	0.035
3	-4.43	5.7	-0.0888	0.012	0.002	0.022
4	-12.88	19.3	-0.0870	-0.032	0.001	0.007
5	-16.87	27.7	-0.0442	0.084	0.001	0.005
6	-1.29	10.7	-0.0127	-0.002	0.000	0.002

* 9 of 20 poles rejected. *

** Window 0 * 12 poles * t = .04 to .28 us **

Pole Pair	Prony Pole damp. freq(MHz)		Prony Residue real	imag	Residue / pole	%
1	-6.06	0.0	-0.569	0.000	0.094	100.00
2	-95.72	0.0	0.520	-0.000	0.005	5.79
3	-12.58	17.5	0.000	-0.087	0.001	0.84
4	-5.11	33.7	0.001	-0.019	0.000	0.10
5	-1.73	44.2	-0.002	-0.007	0.000	0.03

* 4 of 12 poles rejected. *
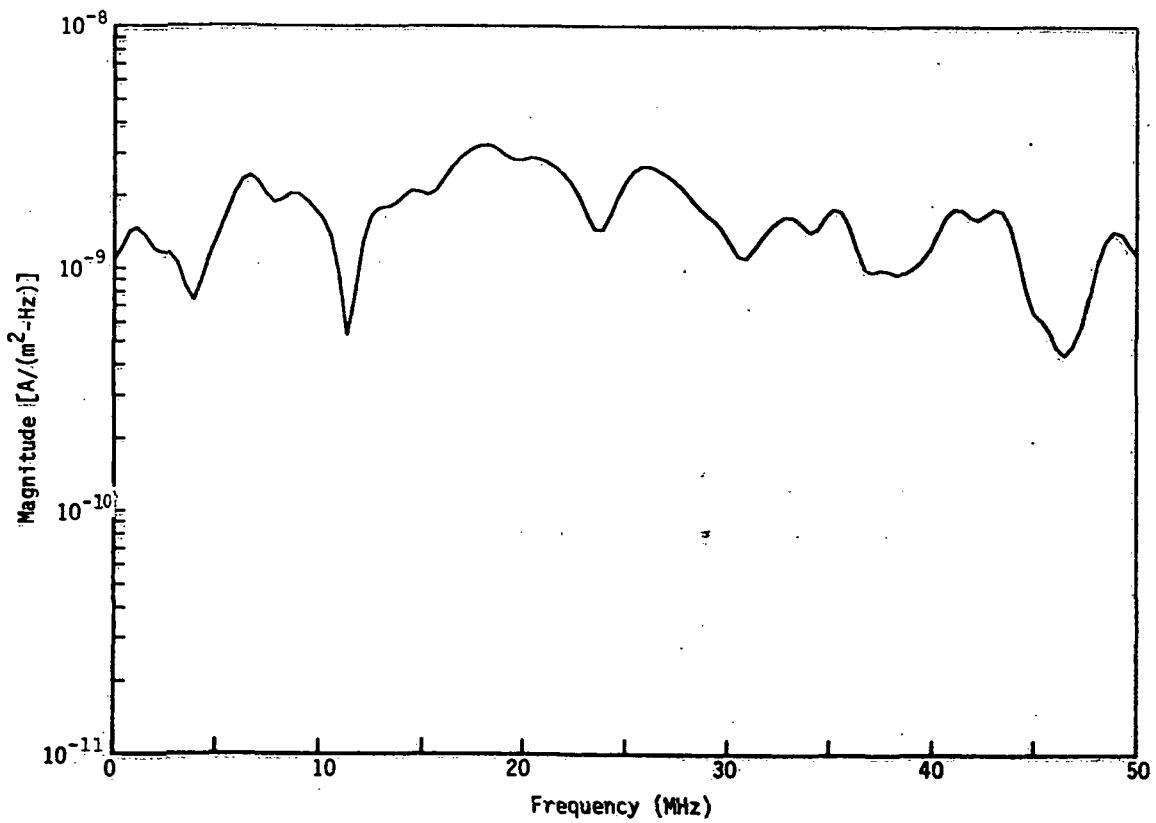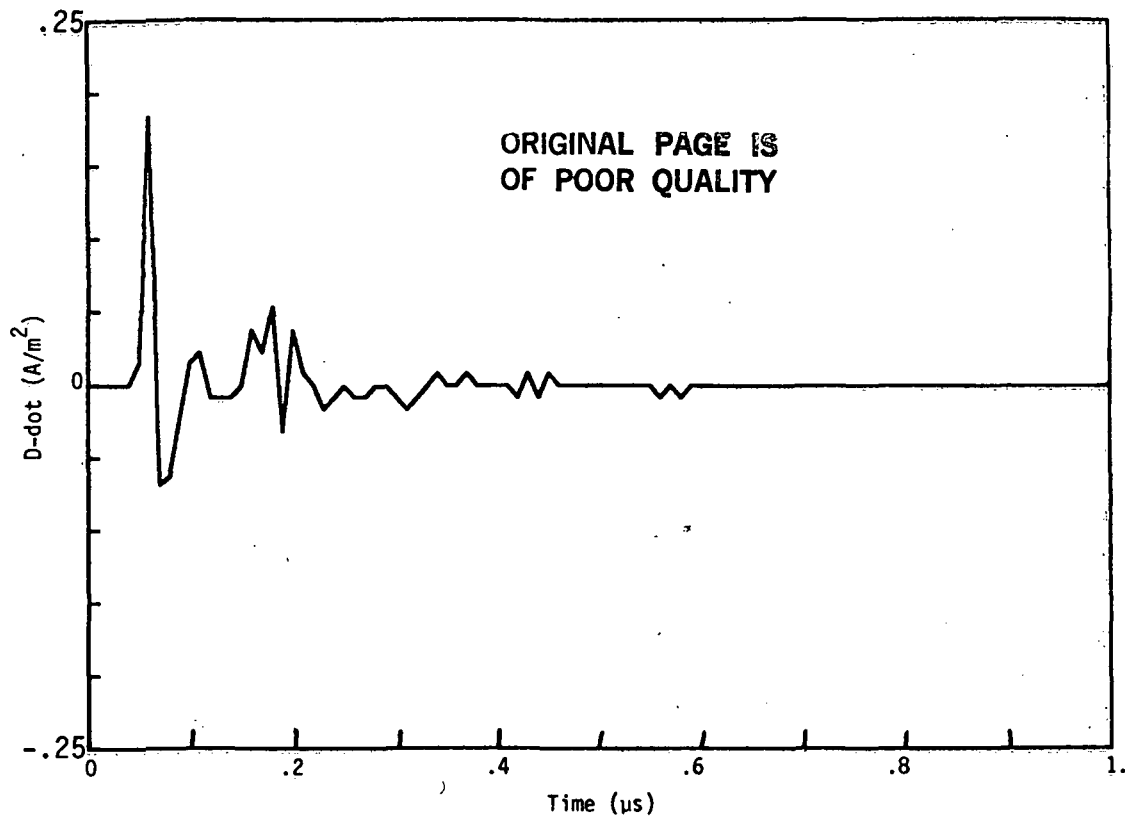
Figure A6.   Measured D-dot Data (a) and Computed Spectral Response (b)
for Flight 81-026-05.

PEAK PICK
* Relative peak height for this run --> .01 *
* Bounds set for this run : 0 to 50 Mhz

FILENAME ---> D810265/FRQ
* Min pt --> 46.48 MHz , 4.43E-03 amplitude

* increasing frequency representation *

* # *	* MHz *	* amplitude *
1	1.17	1.47E-02
2	6.64	2.42E-02
3	8.59	2.05E-02
4	14.45	2.10E-02
5	17.97	3.25E-02
6	20.31	2.87E-02
7	25.78	2.65E-02
8	32.81	1.65E-02
9	35.16	1.78E-02
10	37.50	9.98E-03
11	41.02	1.78E-02
12	42.97	1.78E-02
13	48.83	1.44E-02
14	50.00	1.15E-02

* decreasing amplitude representation *
* the 10 highest peaks *

* # *	* MHz *	* amplitude *	* % *
1	17.97	3.25E-02	100.00
2	20.31	2.87E-02	88.48
3	25.78	2.65E-02	81.68
4	6.64	2.42E-02	74.62
5	14.45	2.10E-02	64.78
6	8.59	2.05E-02	62.98
7	41.02	1.78E-02	54.95
8	42.97	1.78E-02	54.87
9	35.16	1.78E-02	54.81
10	32.81	1.65E-02	50.93

P R O N Y   A N A L Y S I S

* Filename ---> d810265 * dt =0.010 *

** Window 0 * 29 poles * t = .04 to .62 us **

Pole Pair	Prony damp.	Pole freq(MHz)	Prony real	Residue imag	Residue / pole	%
1	-105.54	0.0	3.6711	-0.0000	0.035	100.00
2	-21.70	23.9	-3.2484	1.7183	0.024	69.76
3	-15.77	24.3	1.6880	-1.5656	0.015	43.15
4	-8.50	4.4	-0.2420	0.1430	0.010	28.08
5	-2.34	0.0	-0.0112	0.0000	0.005	13.78
6	-6.36	11.3	-0.0948	0.0746	0.002	4.87
7	-8.93	31.7	-0.0861	-0.0954	0.001	1.85
8	-4.89	16.9	0.0457	-0.0277	0.001	1.44
9	-5.82	40.9	-0.0023	0.0952	0.000	1.06

* 13 of 29 poles rejected. *

** Window 0 * 21 poles * t = .04 to .46 us **

Pole Pair	Prony damp.	Pole freq(MHz)	Prony real	Residue imag	Residue / pole	%
1	-75.16	0.0	3.1785	0.0000	0.042	100.00
2	-8.69	4.7	-0.2058	0.2355	0.010	23.88
3	-5.54	11.5	-0.0565	0.0856	0.001	3.35
4	-7.70	17.4	0.0634	-0.1039	0.001	2.62

* 16 of 21 poles rejected. *

** Window 0 * 13 poles * t = .04 to .3 us **

Pole Pair	Prony damp.	Pole freq(MHz)	Prony real	Residue imag	Residue / pole	%
1	-7.84	0.0	0.2813	0.000	0.036	100.00
2	-21.07	18.8	-0.2428	-0.762	0.007	18.58
3	-7.85	42.8	0.2357	0.102	0.001	2.66
4	-2.87	26.3	-0.0895	-0.036	0.001	1.63
5	-5.24	35.0	0.0047	0.085	0.000	1.08

* 4 of 13 poles rejected. *

P R O N Y   A N A L Y S I S

* Filename ---> d810265 (continued) * dt =0.010 *

** Window 0 * 5 poles * t = .04 to .14 us **

| Pole Pair	Prony damp.	Pole freq(MHz)	Prony real	Residue imag	$\dfrac{\text{Residue}}{\text{pole}}$	%
1	-38.14	19.9	-0.6055	-1.437	0.012	100.00
2	-40.87	0.0	-0.3685	0.000	0.009	75.62
3	-47.96	42.9	0.7898	0.609	0.004	30.60

ORIGINAL PAGE IS
OF POOR QUALITY
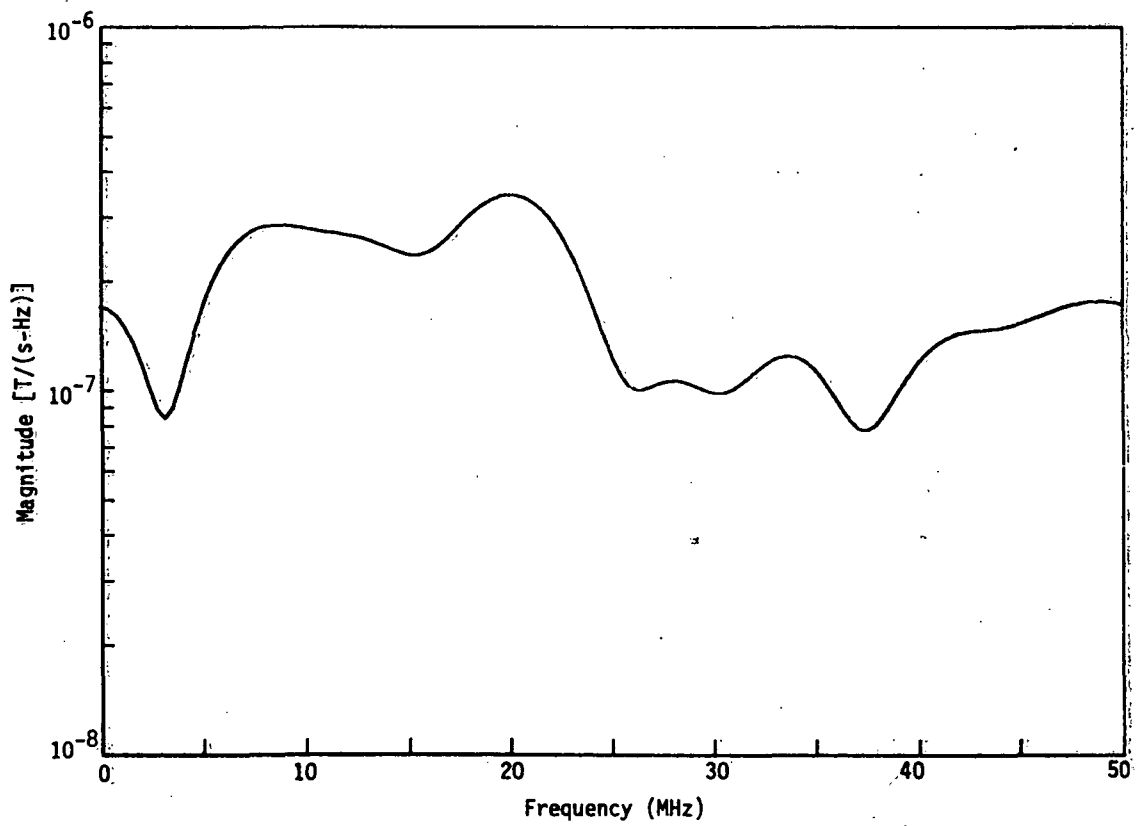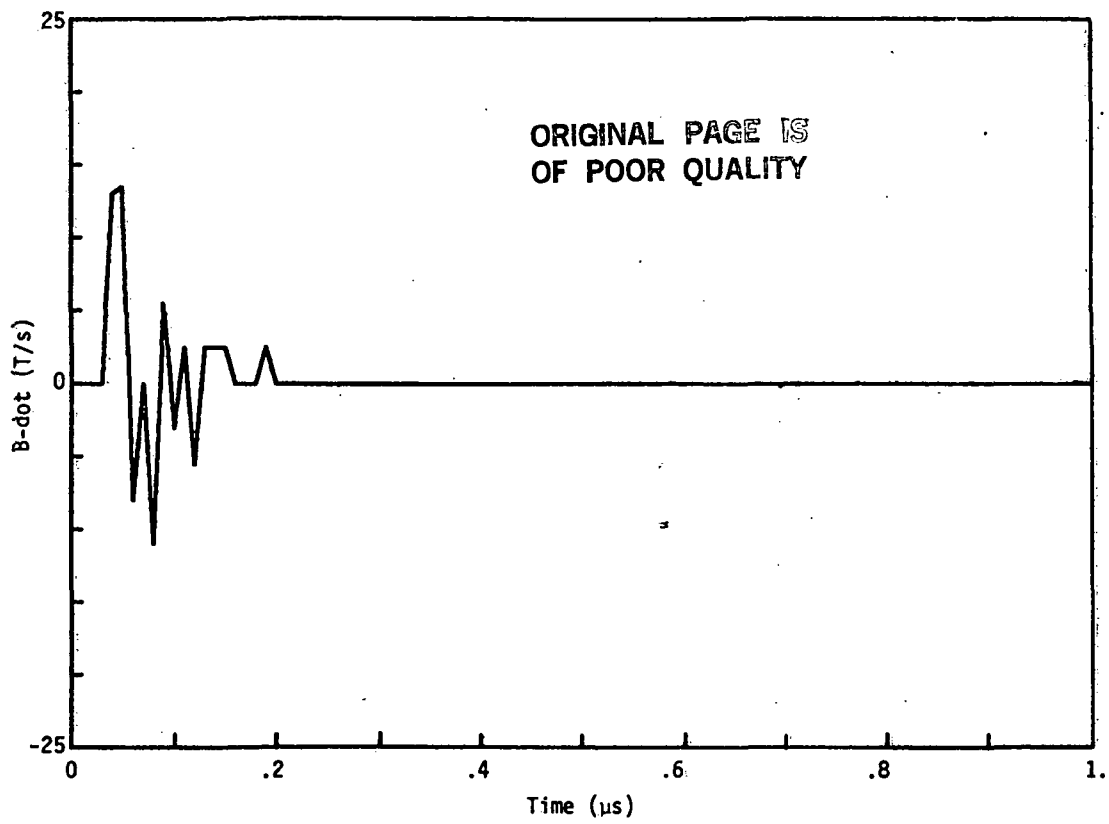
Figure A7.   Measured B-dot Data (a) and Computed Spectral Response (b)
for Flight 81-026-05.

P E A K   P I C K
* Relative peak height for this run --> .01   *
* Bounds set for this run : 0 to 50 Mhz

FILENAME ---> B810265/FRQ
* Min pt --> 37.50 MHz , 7.83E-02 amplitude

* increasing frequency representation *

* # *	* MHz *	* amplitude *
1	0.00	1.70E-01
2	8.59	2.87E-01
3	19.92	3.48E-01
4	28.13	1.07E-01
5	33.59	1.26E-01
6	48.83	1.77E-01
7	50.00	1.73E-01

* decreasing amplitude representation *
* the 10 highest peaks *

* # *	* MHz *	* amplitude *	* % *
1	19.92	3.48E-01	100.00
2	8.59	2.87E-01	82.34
3	48.83	1.77E-01	50.87
4	50.00	1.73E-01	49.77
5	0.00	1.70E-01	48.88
6	33.59	1.26E-01	36.11
7	28.13	1.07E-01	30.80

P R O N Y   A N A L Y S I S

* Filename ---> b810265 * dt = 0.005 *

** Window 0 * 18 poles * t = .04 to .22 us **

Pole Pair	Prony Pole damp. freq(MHz)		Prony Residue real imag		Residue pole	%
1	-13.98	8.1	1.703	1.696	0.046	100.00
2	-31.31	50.0	-14.188	2.058	0.045	99.20
3	-13.25	21.4	1.091	-3.364	0.026	57.30
4	-3.45	36.9	-0.409	0.094	0.002	3.96

* 10 of 18 poles rejected. *

** Window 0 * 15 poles * t = .04 to .19 us **

Pole Pair	Prony Pole damp. freq(MHz)		Prony Residue real imag		Residue pole	%
1	-257.34	0.0	28.6805	0.000	0.111	100.00
2	-8.39	6.5	-0.0290	1.757	0.042	38.00
3	-180.17	0.0	-6.5396	0.000	0.036	32.57
4	-9.86	21.8	0.2417	-2.673	0.020	17.50
5	-15.31	49.4	-4.8899	-0.416	0.016	14.17

* 7 of 15 poles rejected. *

** Window 0 * 12 poles * t = .04 to .16 us **

Pole Pair	Prony Pole damp. freq(MHz)		Prony Residue real imag		Residue pole	%
1	-27.95	9.8	5.0480	2.2449	0.082	100.00
2	-12.20	48.4	-4.0114	-1.3232	0.014	16.99
3	-0.89	20.8	0.9828	-1.2802	0.012	15.09

* 6 of 12 poles rejected. *

** Window 0 * 9 poles * t = .04 to .13 us **

Pole Pair	Prony Pole damp. freq(MHz)		Prony Residue real imag		Residue pole	%
1	-598.58	31.3	16.0783	-187.569	0.299	100.00
2	-30.11	0.0	-6.3797	0.000	0.212	70.92
3	-24.35	22.5	-1.2322	-4.894	0.035	11.79

* 4 of 9 poles rejected. *

P R O N Y   A N A L Y S I S

* Filename ---> b810265 (continued) * dt =0.005 *

** Window 0 * 6 poles * t = .04 to .1 us **

Pole Pair	Prony damp.	Pole freq(MHz)	Prony real	Residue imag	Residue / pole	%
1	−29.70	14.5	8.0668	−0.536	0.084	100.00
2	−40.30	0.0	−0.9479	−0.000	0.024	27.85
3	−239.22	0.0	3.4996	−0.000	0.015	17.32

* 2 of 6 poles rejected. *
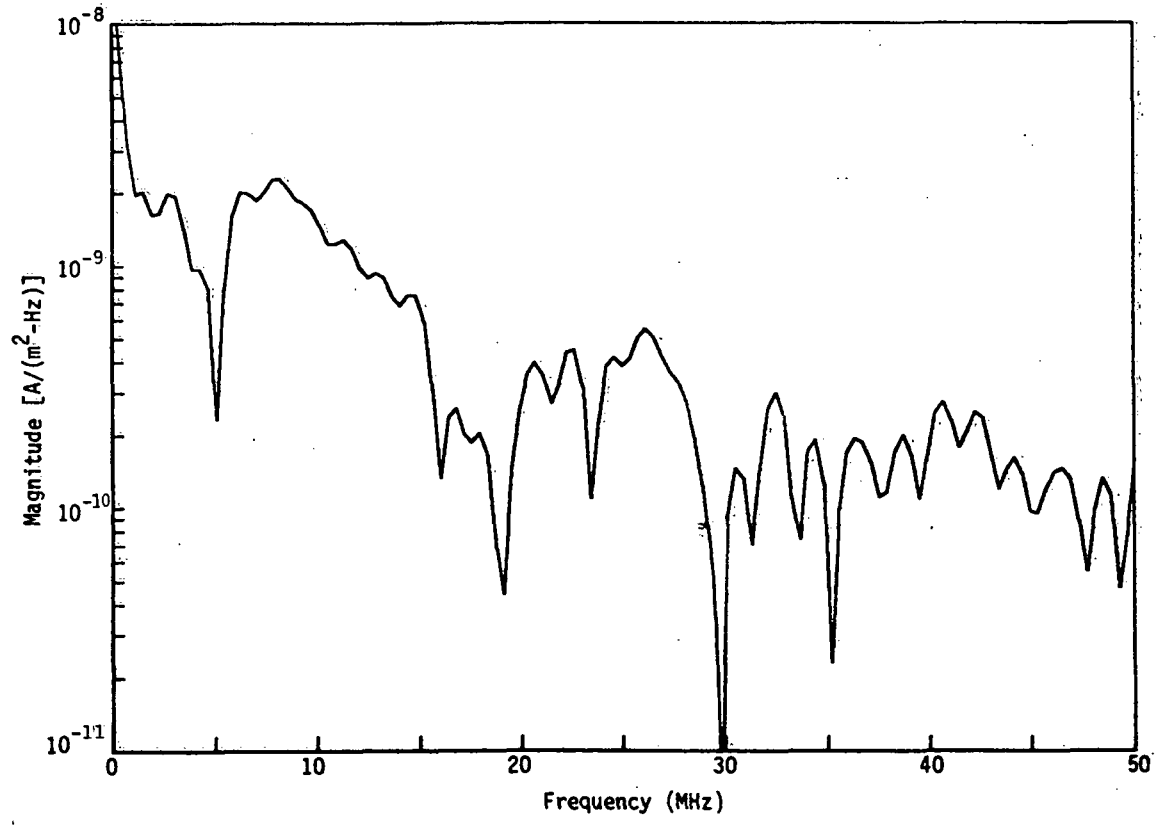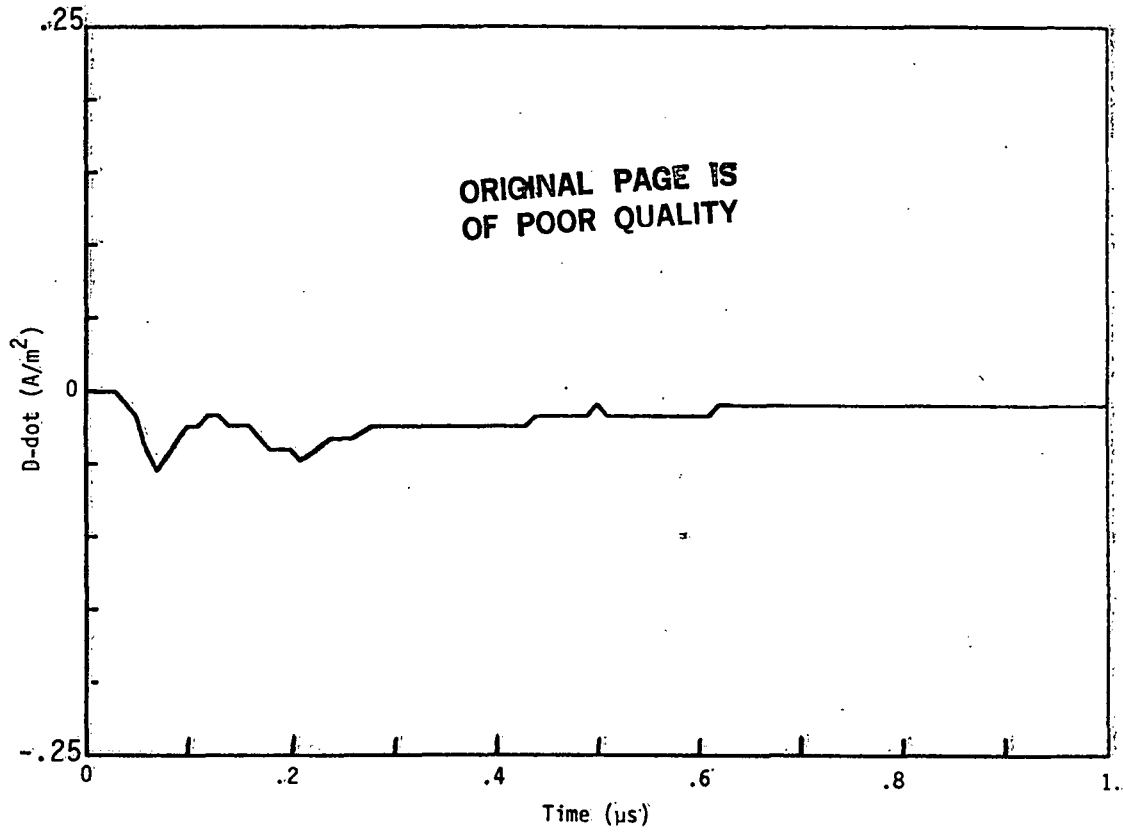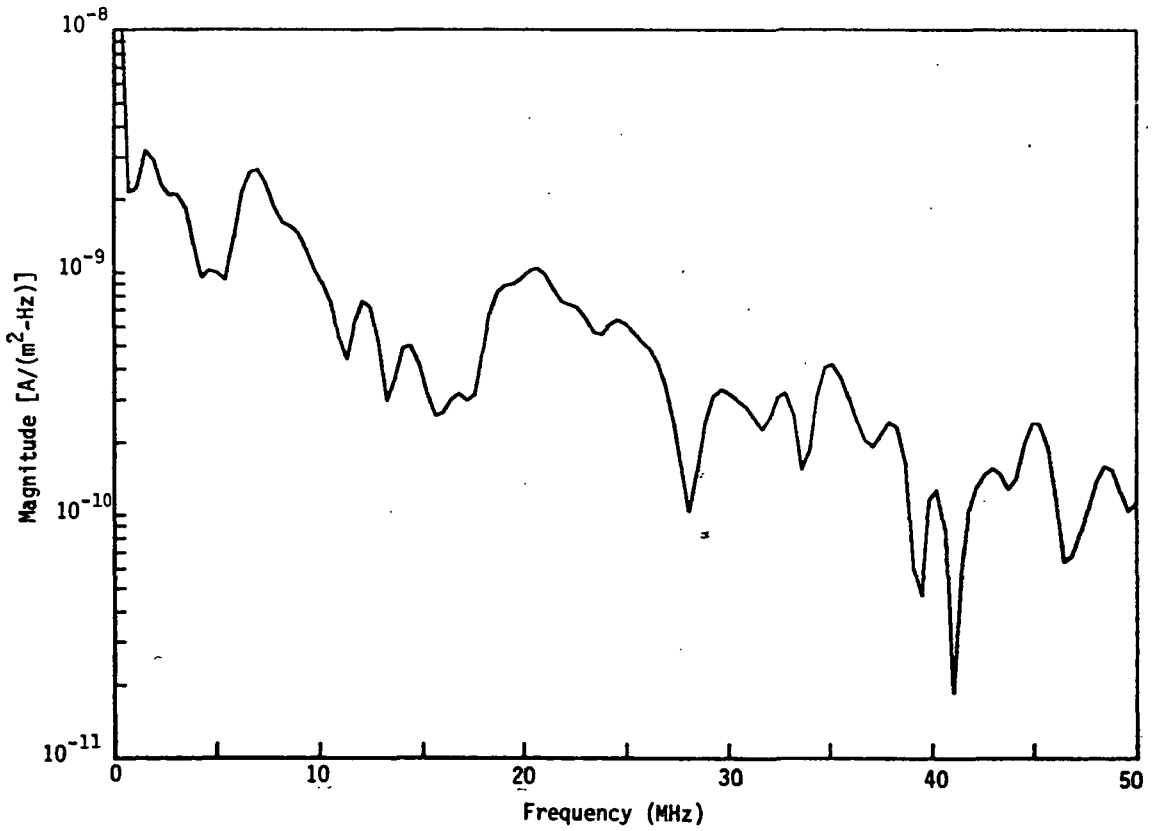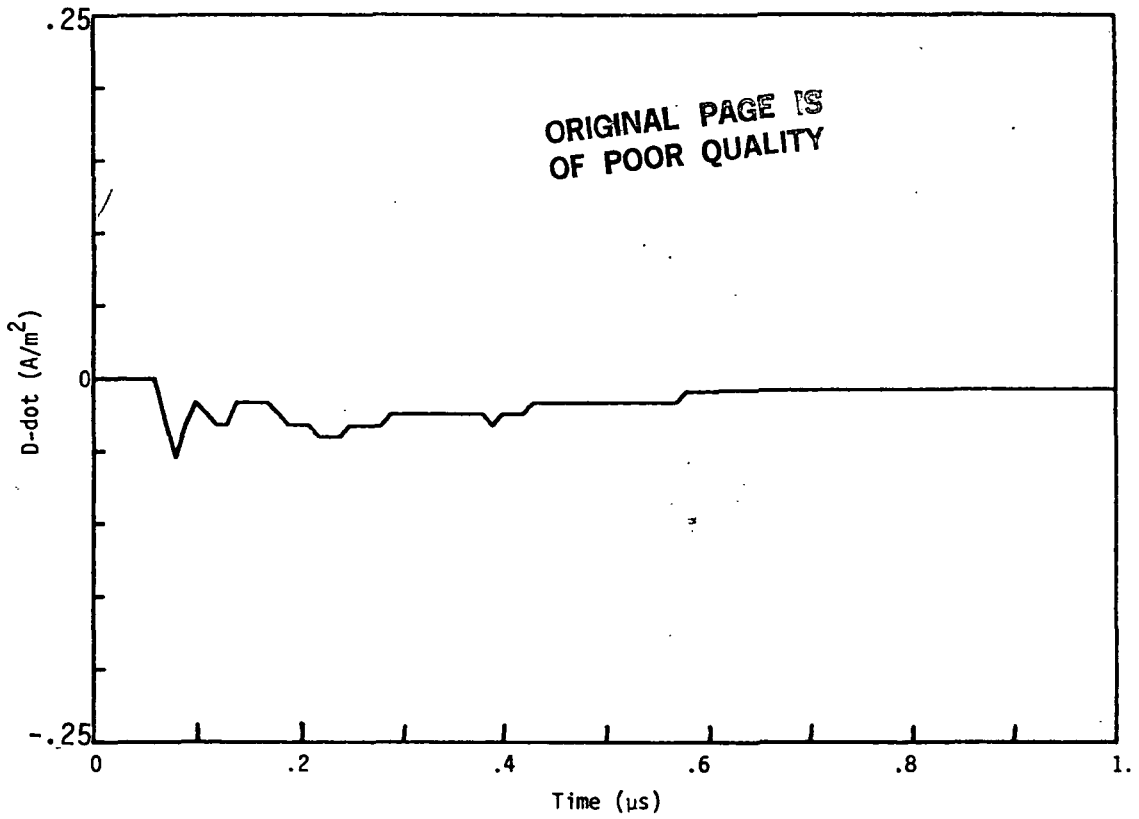
Figure A8. Measured D-dot Data (a) and Computed Spectral Response (b) for Flight 81-026-06.

```
                    P E A K   P I C K
        * Relative peak height for this run --> 5E-03  *
        * Bounds set for this run : 2  to  50  Mhz


    FILENAME  ---> D810266/FRQ
  * Min pt --> 41.02 MHz , 1.87E-04 amplitude

    * increasing frequency representation *

  * # *            * MHz *           * amplitude *
    1               3.13              2.10E-02
    2               4.69              1.02E-02
    3               7.03              2.65E-02
    4              12.11              7.63E-03
    5              14.45              5.01E-03
    6              16.80              3.19E-03
    7              20.70              1.05E-02
    8              24.61              6.42E-03
    9              29.69              3.32E-03
   10              32.81              3.21E-03
   11              35.16              4.20E-03



    * decreasing amplitude representation *
         * the 10 highest peaks *
  * # *            * MHz *           * amplitude *     * % *
    1               7.03              2.65E-02        100.00
    2               3.13              2.10E-02         79.42
    3              20.70              1.05E-02         39.55
    4               4.69              1.02E-02         38.38
    5              12.11              7.63E-03         28.80
    6              24.61              6.42E-03         24.24
    7              14.45              5.01E-03         18.92
    8              35.16              4.20E-03         15.88
    9              29.69              3.32E-03         12.54
   10              32.81              3.21E-03         12.14
```

PRONY   ANALYSIS

* Filename ---> d810266 * dt =0.010 *

** Window 0 * 28 poles * t = .04 to .6 us **

Pole Pair	Prony Pole damp. freq(MHz)		Prony Residue real	imag	Residue/pole	%
1	-2.82	0	-0.740	0.000	0.265	100.00
2	-35.95	0	-0.219	-0.133	0.007	2.69

* 26 of 28 poles rejected. *

** Window 0 * 20 poles * t = .04 to .44 us **

Pole Pair	Prony Pole damp. freq(MHz)		Prony Residue real	imag	Residue/pole	%
1	-1.24	0.0	-0.3723	0.000	0.300	100.00
2	-55.39	20.1	1.2930	-0.910	0.011	3.82
3	-9.70	5.6	-0.2233	0.160	0.008	2.52
4	-25.79	9.6	-0.3453	-0.318	0.007	2.38
5	-65.90	0.0	-0.3611	0.000	0.005	1.83
6	-25.75	24.8	-0.4245	0.375	0.004	1.19
7	-7.89	23.4	0.0799	0.029	0.001	0.19
8	-6.66	34.1	-0.0168	0.004	0.000	0.03
9	-3.33	46.7	0.0035	0.012	0.000	0.01

* 4 of 20 poles rejected. *

** Window 0 * 12 poles * t = .04 to .28 us **

Pole Pair	Prony Pole damp. freq(MHz)		Prony Residue real	imag	Residue/pole	%
1	-1.74	0.0	-0.343	0.000	0.198	100.00
2	-21.83	17.3	0.267	-0.054	0.002	1.25
3	-24.89	44.5	-0.093	-0.012	0.000	0.17
4	-0.45	29.5	0.017	0.006	0.000	0.05

* 5 of 12 poles rejected. *

** Window 0 * 4 poles * t = .04 to .12 us **

| Pole Pair	Prony Pole damp. freq(MHz)		Prony Residue real	imag	Residue/pole	%
1	-25.85	8	0.242	0.7030	0.013	100.00
2	-83.05	0	-0.485	0.0000	0.006	45.34

* 1 of 4 poles rejected. *

-134-

Figure A9. Measured D-dot Data (a) and Computed Spectral Response (b) for Flight 81-026-07.

P E A K   P I C K
* Relative peak height for this run --> 5E-03 *
* Bounds set for this run : 2 to 50 Mhz

FILENAME ---> D810267/FRQ
* Min pt --> 33.59 MHz , 3.11E-04 amplitude

* increasing frequency representation *

* # *	* MHz *	* amplitude *
1	3.13	1.67E-02
2	7.03	2.77E-02
3	10.16	2.00E-02
4	14.06	1.26E-02
5	17.58	7.70E-03
6	21.88	7.99E-03
7	24.22	6.99E-03
8	25.78	5.76E-03
9	27.73	3.81E-03
10	34.77	2.95E-03
11	36.33	3.86E-03

* decreasing amplitude representation *
* the 10 highest peaks *

* # *	* MHz *	* amplitude *	* % *
1	7.03	2.77E-02	100.00
2	10.16	2.00E-02	71.98
3	3.13	1.67E-02	60.29
4	14.06	1.26E-02	45.26
5	21.88	7.99E-03	28.82
6	17.58	7.70E-03	27.77
7	24.22	6.99E-03	25.20
8	25.78	5.76E-03	20.76
9	36.33	3.86E-03	13.92
10	27.73	3.81E-03	13.75

P R O N Y   A N A L Y S I S

*   Filename ---> d810267 *   dt =0.010 *

**   Window 0   *   28 poles   *   t = .04 to .6 us   **

Pole Pair	Prony Pole damp. freq(MHz)		Prony Residue real imag		Residue / pole	%
1	−3.53	0.0	−0.764	0.0000	0.217	100.00
2	−15.10	0.0	0.719	0.0002	0.048	22.00
3	−6.06	6.5	−0.111	0.1005	0.004	1.68
4	−10.18	11.1	0.064	0.0262	0.001	0.46
5	−7.26	14.1	0.008	0.0494	0.001	0.26
6	−12.83	24.3	0.035	−0.0607	0.000	0.21
7	−5.26	21.8	−0.018	−0.0365	0.000	0.14
8	−2.10	17.6	0.013	0.0076	0.000	0.06
9	−7.20	35.6	−0.016	0.0180	0.000	0.05

*   12 of 28 poles rejected.   *

**   Window 0   *   20 poles   *   t = .04 to .44 us   **

Pole Pair	Prony Pole damp. freq(MHz)		Prony Residue real imag		Residue / pole	%
1	−4.18	0.0	−1.078	0.000	0.258	100.00
2	−9.65	0.0	0.875	0.000	0.091	35.15
3	−6.62	6.3	−0.147	0.074	0.004	1.60
4	−3.16	0.0	−0.009	0.000	0.003	1.14
5	−19.37	0.0	0.047	0.000	0.002	0.94
6	−26.89	20.0	0.193	−0.184	0.002	0.80
7	−6.83	35.9	−0.009	0.020	0.000	0.04

*   10 of 20 poles rejected.   *

**   Window 0   *   12 poles   *   t = .04 to .28 us   **

Pole Pair	Prony Pole damp. freq(MHz)		Prony Residue real imag		Residue / pole	%
1	−5.36	7.1	−0.0792	0.1042	0.003	100.00
2	−60.40	0.0	0.1482	0.0000	0.002	84.53
3	−21.61	19.1	0.1723	−0.0755	0.002	53.24
4	−13.11	35.4	−0.0304	0.0284	0.000	6.43
5	−13.96	28.5	−0.0191	−0.0023	0.000	3.69

*   3 of 12 poles rejected.   *

P R O N Y   A N A L Y S I S

* Filename ----> d810267 (continued) * dt =0.010 *

** Window 0 * 4 poles * t = .04 to .12 us **

Pole Pair	Prony damp.	Pole freq(MHz)	Prony real	Residue imag	Residue/pole	%
1	−32.84	0.0	−1.7946	0.000	0.055	100.00
2	−103.95	0.0	2.0602	0.000	0.020	36.27
3	−33.09	26.4	−0.1744	−0.216	0.002	3.01
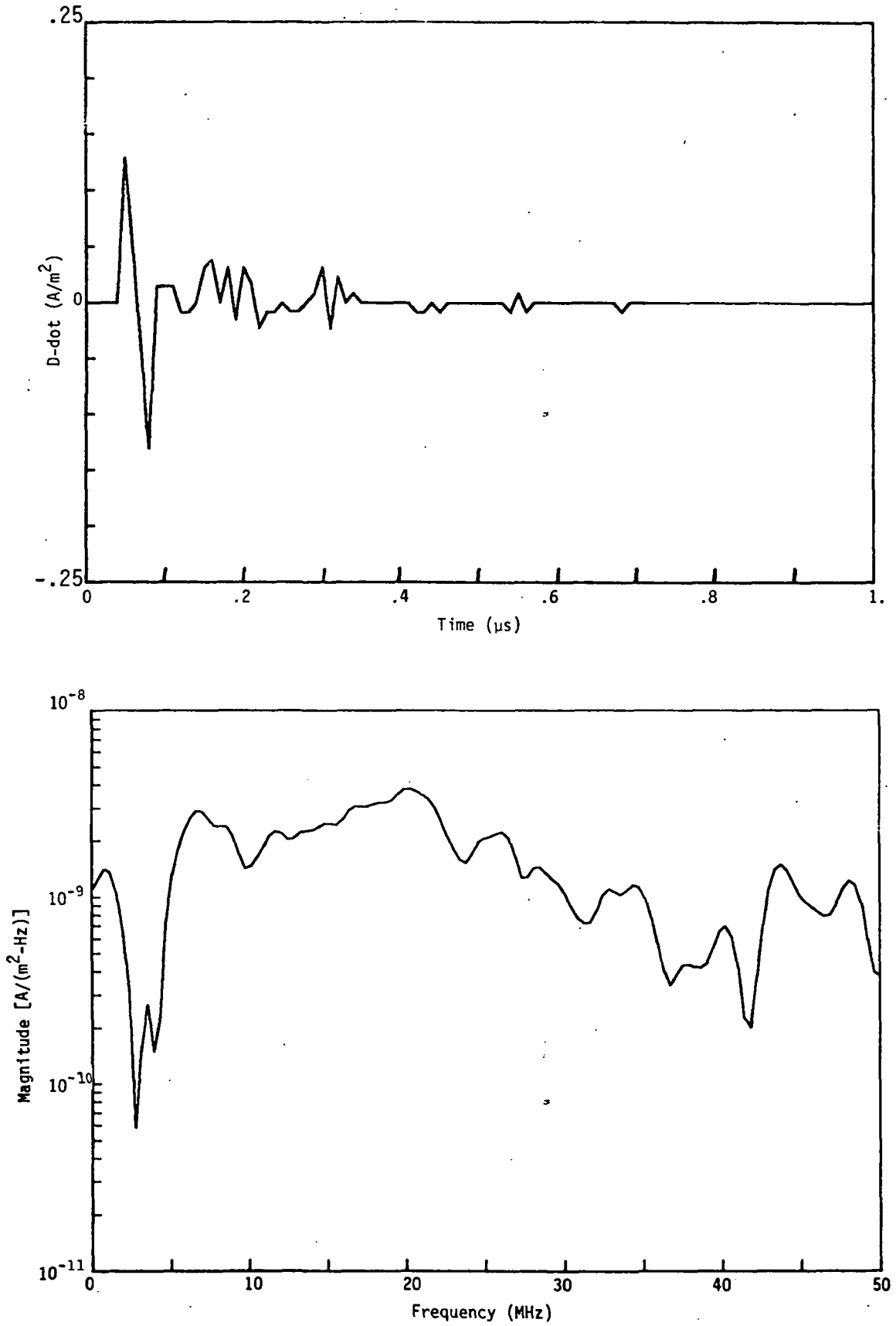
Figure A10.   Measured D-dot Data (a) and Computed Spectral Response (b)
for Flight 81-026-08.

P E A K   P I C K
* Relative peak height for this run --> .01   *
* Bounds set for this run : 0 to 50 Mhz

FILENAME   --> D810268/FRQ
* Min pt --> 2.73 MHz , 5.87E-04 amplitude

* increasing frequency representation *

* # *	* MHz *	* amplitude *
1	0.78	1.41E-02
2	6.64	2.91E-02
3	11.72	2.28E-02
4	14.84	2.49E-02
5	16.80	3.09E-02
6	18.36	3.23E-02
7	20.31	3.83E-02
8	26.17	2.25E-02
9	28.52	1.45E-02
10	32.81	1.11E-02
11	34.38	1.16E-02
12	37.89	4.38E-03
13	40.23	7.05E-03
14	43.75	1.50E-02
15	48.05	1.23E-02
16	50.00	3.81E-03

* decreasing amplitude representation *
* the 10 highest peaks *

* # *	* MHz *	* amplitude *	* % *
1	20.31	3.83E-02	100.00
2	18.36	3.23E-02	84.33
3	16.80	3.09E-02	80.61
4	6.64	2.91E-02	75.91
5	14.84	2.49E-02	64.99
6	11.72	2.28E-02	59.44
7	26.17	2.25E-02	58.60
8	43.75	1.50E-02	39.19
9	28.52	1.45E-02	37.90
10	0.78	1.41E-02	36.88

P R O N Y   A N A L Y S I S

* Filename ---> d810268 * dt =0.010 *

** Window 6 * 30 poles * t = .1 to .7 us **
* 30 of 30 poles rejected. *

** Window 4 * 30 poles * t = .08 to .68 us **

Pole Pair	Prony Pole damp. freq(MHz)		Prony Residue real imag		Residue pole	%
1	-196.25	0.0	3.2070	0.7307	0.017	100.00
2	-5.39	43.3	-0.1201	-0.0837	0.001	3.21
3	-4.29	48.2	-0.0668	0.0437	0.000	1.57

* 25 of 30 poles rejected. *

** Window 2 * 30 poles * t = .06 to .66 us **

Pole Pair	Prony Pole damp. freq(MHz)		Prony Residue real imag		Residue pole	%
1	-49.50	0	0.6370	3.8083	0.078	100.00

* 29 of 30 poles rejected. *

** Window 0 * 30 poles * t = .04 to .64 us **

Pole Pair	Prony Pole damp. freq(MHz)		Prony Residue real imag		Residue pole	%
1	-40.34	0	-3.383	-0.945	0.087	100.00

* 29 of 30 poles rejected. *

P R O N Y   A N A L Y S I S   * dt =0.010 *

* Filename ---> d810268 (continued)

** Window 0 * 22 poles * t = .04 to .48 us **

Pole Pair	Prony Pole damp.	freq(MHz)	Prony Residue real	imag	Residue/pole	%
			0.074	0.000	0.017	100.00
1	-4.37	0.0	-0.226	-0.838	0.007	40.05
2	-17.86	20.3	0.034	0.195	0.005	29.52
3	-6.80	6.3	-0.144	-0.319	0.001	8.14
4	-19.08	40.6	0.216	-0.016	0.001	4.80
5	-5.58	42.6	0.071	-0.082	0.001	4.16
6	-5.48	24.6	0.033	0.074	0.000	2.21
7	-3.09	34.7	-0.017	0.014	0.000	2.02
8	-1.59	10.3				

* 7 of 22 poles rejected. *

** Window 0 * 14 poles * t = .04 to .32 us **

Pole Pair	Prony Pole damp.	freq(MHz)	Prony Residue real	imag	Residue/pole	%
			-0.101	-1.063	0.008	100.00
1	-24.46	20.3	-0.060	0.089	0.003	39.86
2	-0.64	5.2	0.040	-0.156	0.001	7.01
3	-5.82	44.3	0.093	0.005	0.000	4.97
4	-2.37	36.1				

* 6 of 14 poles rejected. *

** Window 0 * 6 poles * t = .04 to .16 us **

Pole Pair	Prony Pole damp.	freq(MHz)	Prony Residue real	imag	Residue/pole	%
			-2.464	0.000	0.033	100.00
1	-73.76	0.0	-0.250	-2.612	0.019	58.22
2	-46.90	20.1	1.482	-1.886	0.009	26.08
3	-60.07	42.8				

* 1 of 6 poles rejected. *
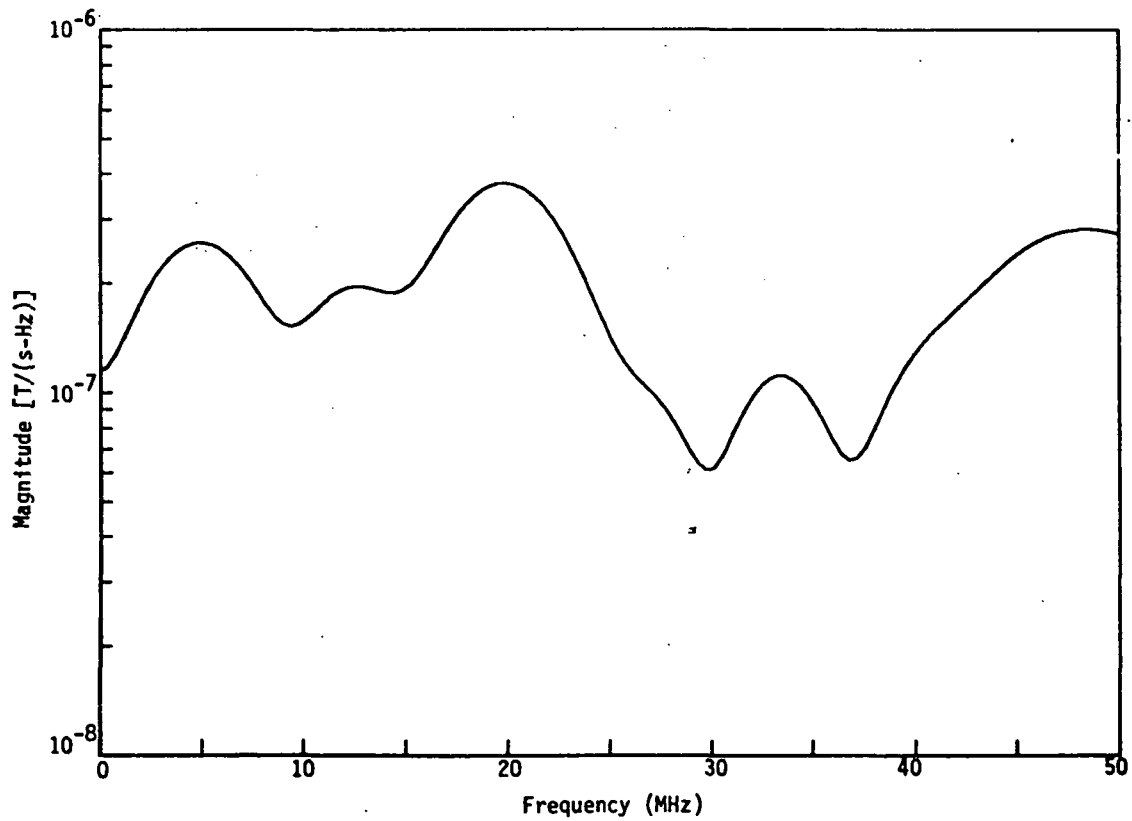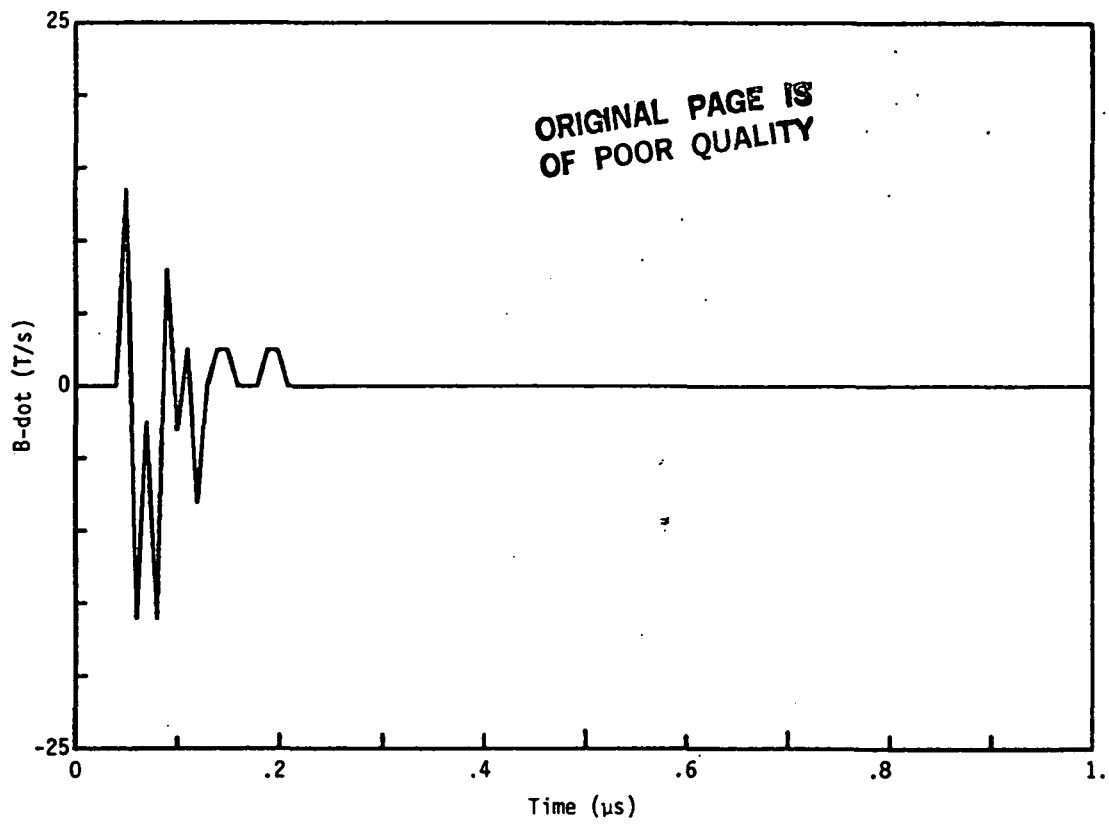
Figure A11.   Measured B-dot Data (a) and Computed Spectral Response (b)
for Flight 81-026-08.

PEAK PICK
* Relative peak height for this run --> .01 *
* Bounds set for this run : 0 to 50 Mhz

FILENAME ---> B810268/FRQ
* Min pt --> 29.69 MHz , 6.13E-02 amplitude

* increasing frequency representation *

* # *	* MHz *	* amplitude *
1	5.08	2.59E-01
2	12.50	1.96E-01
3	19.92	3.78E-01
4	33.20	1.12E-01
5	48.44	2.82E-01
6	50.00	2.73E-01

* decreasing amplitude representation *
* the 10 highest peaks *

* # *	* MHz *	* amplitude *	* % *
1	19.92	3.78E-01	100.00
2	48.44	2.82E-01	74.66
3	50.00	2.73E-01	72.33
4	5.08	2.59E-01	68.43
5	12.50	1.96E-01	51.90
6	33.20	1.12E-01	29.58

PRONY   ANALYSIS

* Filename ---> b810268 * dt =0.005 *

**   Window 0 * 15 poles * t = .04 to .19 us **

Pole Pair	Prony damp.	Pole freq(MHz)	Prony real	Residue imag	Residue/pole	%
1	-10.95	3.4	-2.9648	1.260	0.135	100.00
2	-14.97	20.5	3.1231	-5.066	0.046	33.87
3	-24.24	47.2	-1.7876	-8.997	0.031	22.79
4	-15.24	44.7	-2.0561	-0.451	0.007	5.53
5	-0.92	33.4	-0.0264	-0.327	0.002	1.15

* 5 of 15 poles rejected. *

**   Window 0 * 12 poles * t = .04 to .16 us **

Pole Pair	Prony damp.	Pole freq(MHz)	Prony real	Residue imag	Residue/pole	%
1	-10.30	3.1	-3.173	0.802	0.149	100.00
2	-35.98	46.5	-3.227	-13.665	0.048	32.00
3	-14.66	20.6	2.904	-5.072	0.045	30.15

* 6 of 12 poles rejected. *

**   Window 0 * 9 poles * t = .04 to .13 us **

Pole Pair	Prony damp.	Pole freq(MHz)	Prony real	Residue imag	Residue/pole	%
1	-49.95	5	2.9311	18.1932	0.315	100.00

* 7 of 9 poles rejected. *

**   Window 0 * 6 poles * t = .04 to .1 us **

Pole Pair	Prony damp.	Pole freq(MHz)	Prony real	Residue imag	Residue/pole	%
1	-10.48	46.5	-2.735	-2.315	0.012	100.00

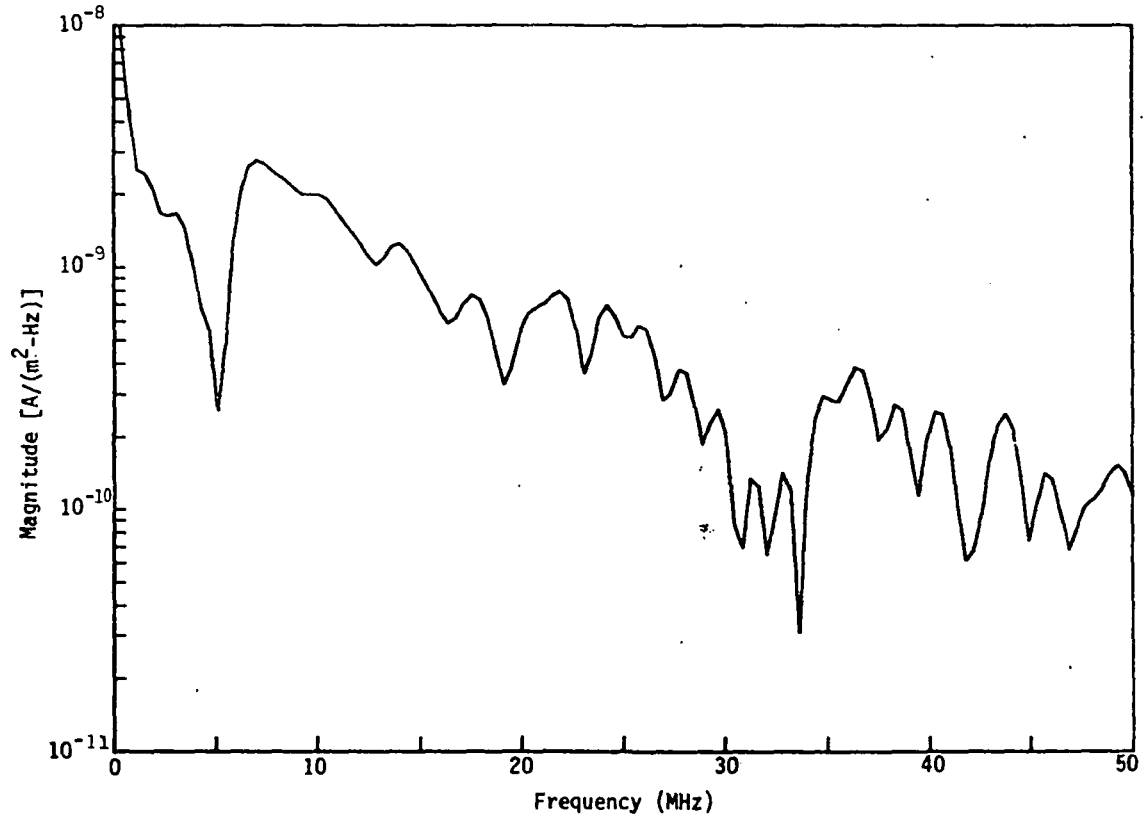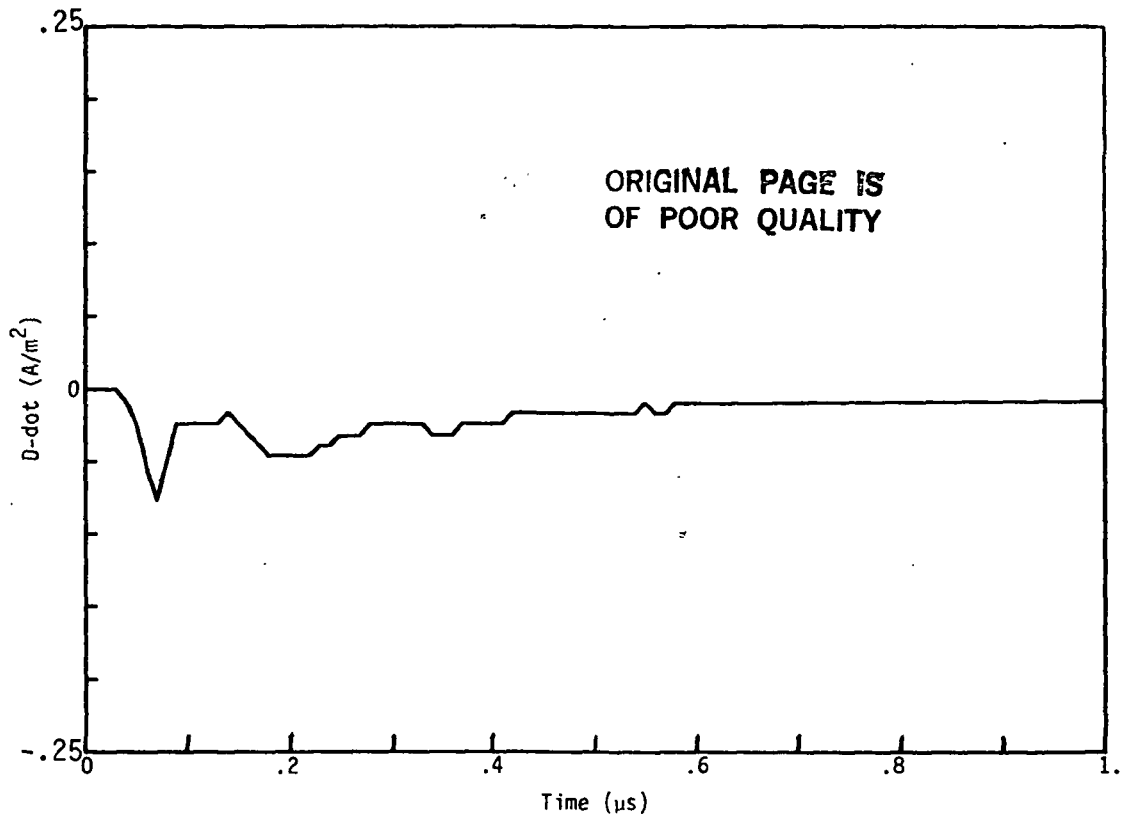*** 4 of 6 poles rejected. ***

ORIGINAL PAGE IS
OF POOR QUALITY
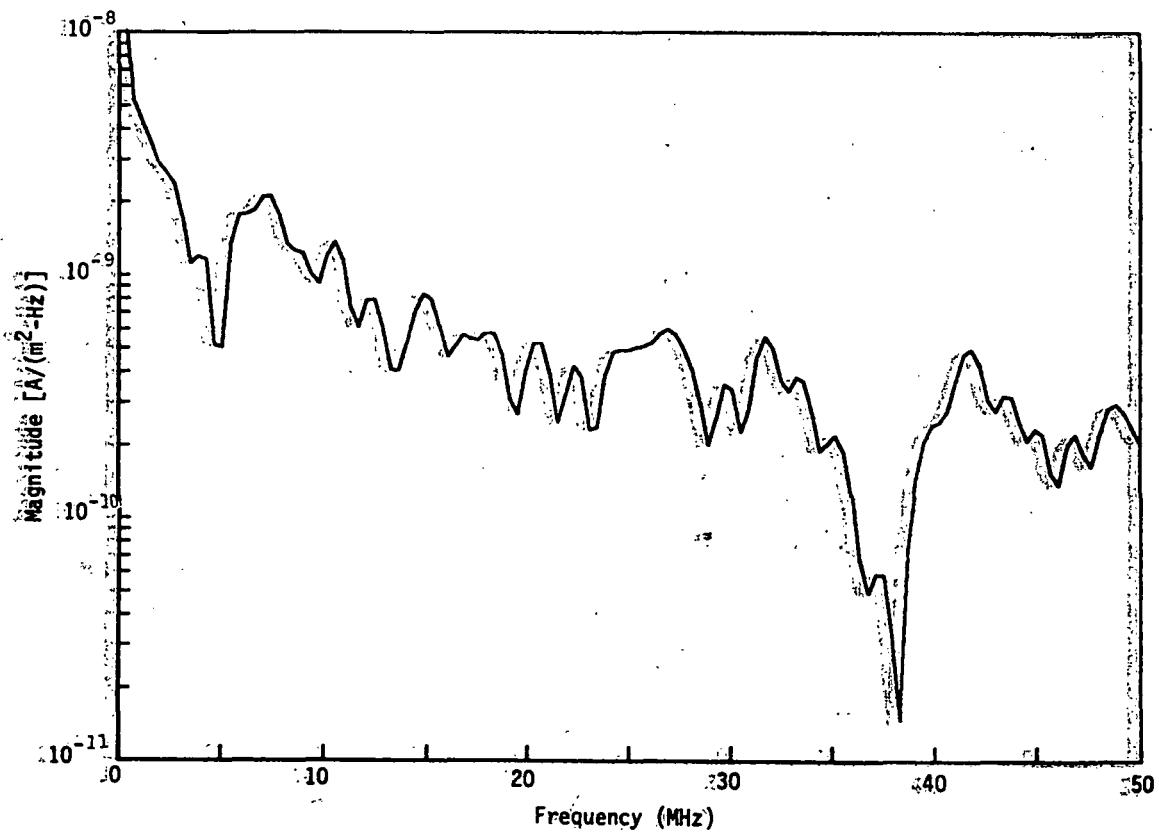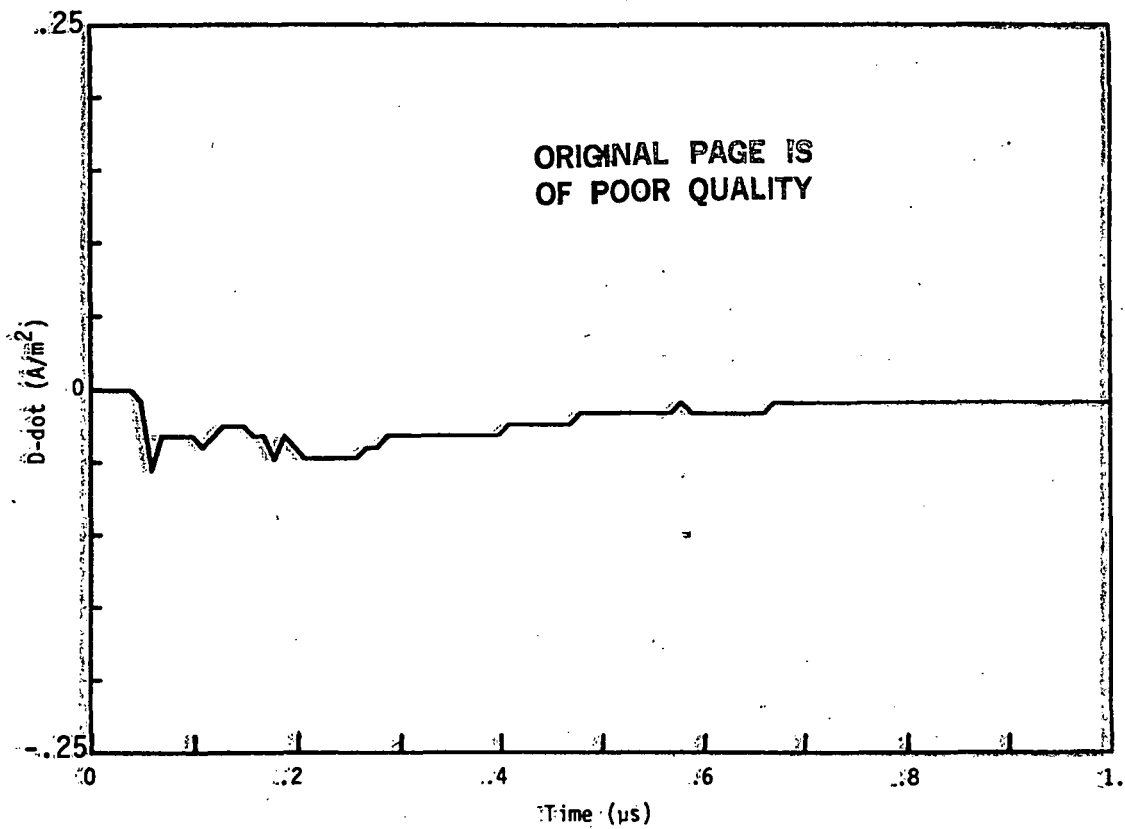
Figure A12.   Measured D-dot Data (a) and Computed Spectral Response (b)
for Flight 81-026-09.

PEAK PICK
* Relative peak height for this run --> 5E-03 *
* Bounds set for this run : 2 to 50 Mhz

FILENAME ---> D810269/FRQ
* Min pt --> 38.28 MHz , 1.48E-04 amplitude

* increasing frequency representation *

* # *	* MHz *	* amplitude *
1	3.91	1.20E-02
2	7.42	2.12E-02
3	10.55	1.37E-02
4	12.50	7.90E-03
5	14.84	8.32E-03
6	16.80	5.68E-03
7	17.97	5.78E-03
8	20.31	5.23E-03
9	22.27	4.23E-03
10	24.61	4.93E-03
11	26.95	6.01E-03
12	29.69	3.54E-03
13	31.64	5.57E-03
14	33.20	3.80E-03
15	41.80	4.97E-03
16	43.36	3.20E-03
17	48.83	2.95E-03

* decreasing amplitude representation *
* the 10 highest peaks *

* # *	* MHz *	* amplitude *	* % *
1	7.42	2.12E-02	100.00
2	10.55	1.37E-02	64.40
3	3.91	1.20E-02	56.73
4	14.84	8.32E-03	39.26
5	12.50	7.90E-03	37.28
6	26.95	6.01E-03	28.32
7	17.97	5.78E-03	27.26
8	16.80	5.68E-03	26.78
9	31.64	5.57E-03	26.25
10	20.31	5.23E-03	24.67

P R O N Y   A N A L Y S I S

* Filename ---> d810269 * dt =0.010 *

** Window 4 * 30 poles * t = .08 to .68 us **

Pole Pair	Prony damp.	Pole freq(MHz)	Prony real	Residue imag	Residue/pole	%
1	-5.42	0.4	-0.1187	0.9527	0.160	100.00
2	-20.26	0.0	-0.2532	-0.0047	0.012	7.81
3	-37.94	0.0	0.4321	0.0110	0.011	7.12
4	-7.19	6.0	-0.0981	-0.0392	0.003	1.71
5	-6.29	28.4	-0.0124	-0.0233	0.000	0.09
6	-9.40	38.3	-0.0155	-0.0291	0.000	0.09
7	-0.51	30.9	-0.0051	-0.0022	0.000	0.02

* 19 of 30 poles rejected. *

** Window 0 * 30 poles * t = .04 to .64 us **

Pole Pair	Prony damp.	Pole freq(MHz)	Prony real	Residue imag	Residue/pole	%
1	-5.40	0.4	-0.0150	1.1488	0.190	100.00
2	-9.22	0.0	-0.0617	-0.0000	0.007	3.52
3	-6.70	6.0	-0.0599	0.1098	0.003	1.72
4	-117.46	0.0	0.3554	-0.0000	0.003	1.59
5	-96.81	0.0	0.2262	-0.0000	0.002	1.23
6	-12.71	18.0	0.0212	0.0795	0.001	0.38
7	-18.69	41.7	-0.1401	-0.0780	0.001	0.32
8	-11.33	37.2	-0.0382	0.0378	0.000	0.12
9	-4.53	22.9	-0.0122	0.0072	0.000	0.05
10	-3.42	31.2	0.0040	0.0118	0.000	0.03

* 13 of 30 poles rejected. *
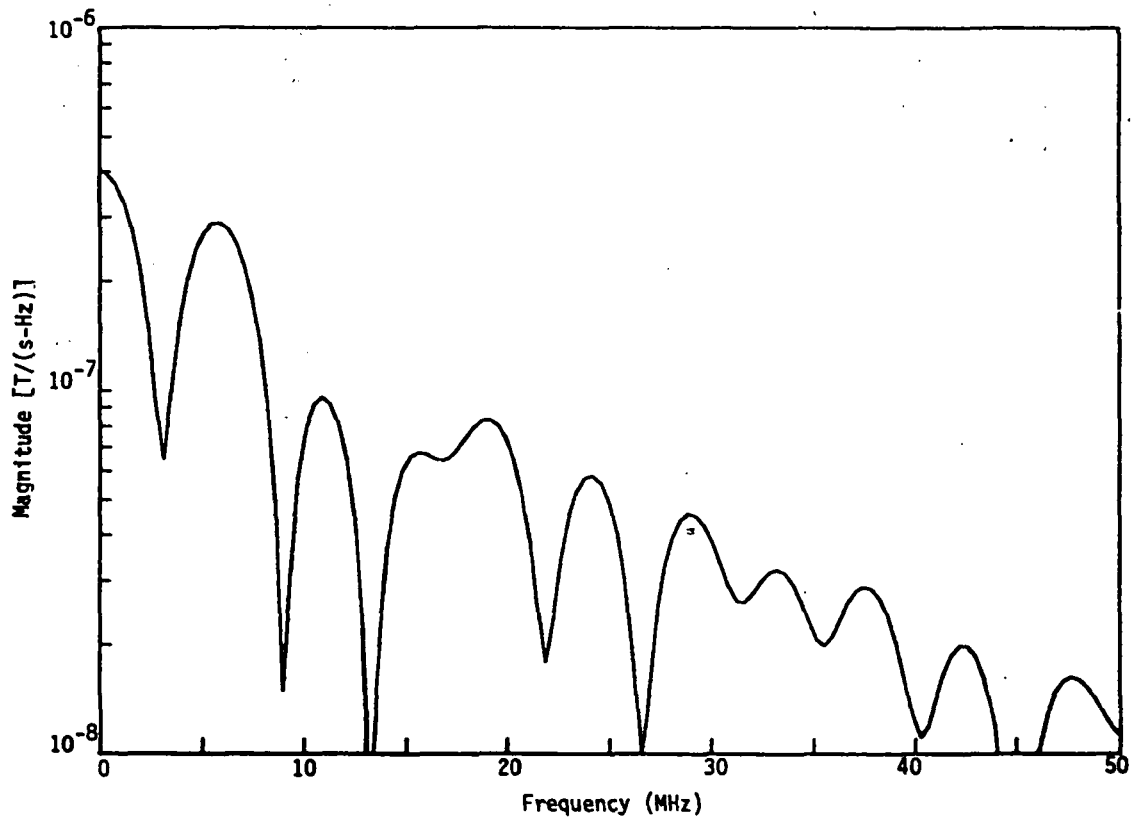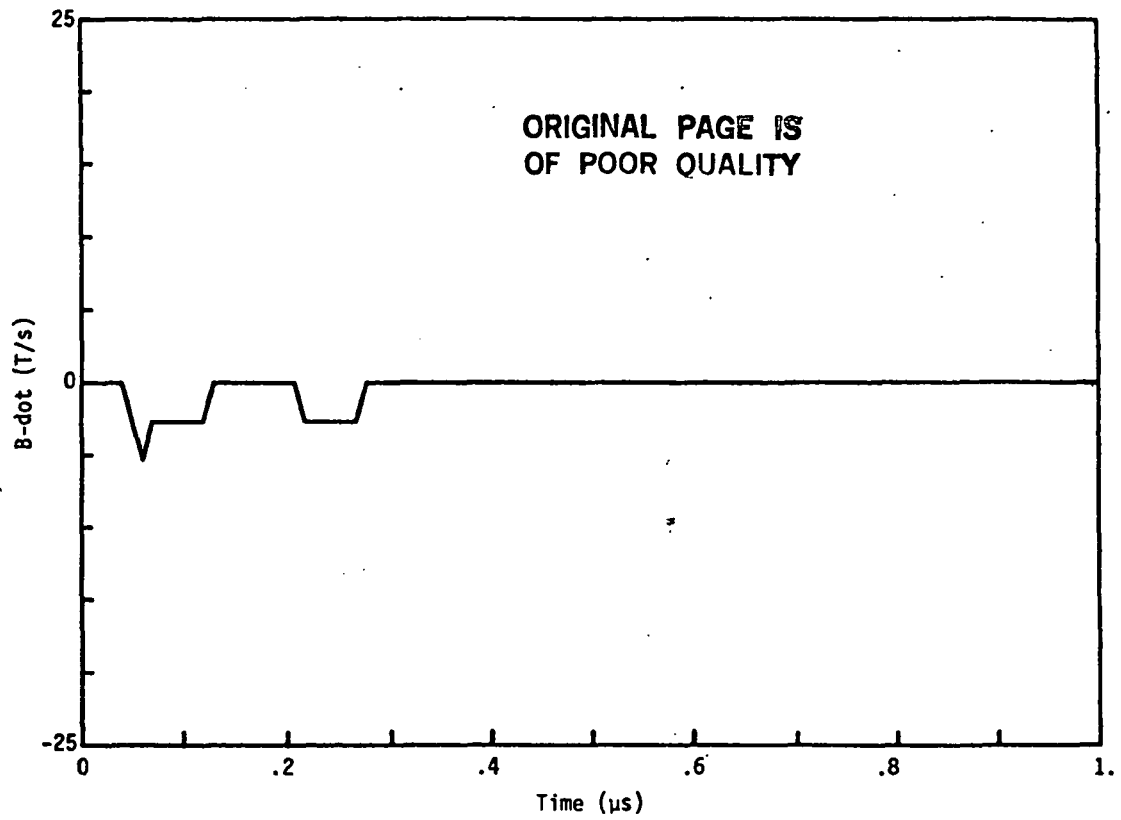
Figure A13.   Measured B-dot Data (a) and Computed Spectral Response (b)
for Flight 81-026-09.

PEAK PICK
* Relative peak height for this run --> 5E-03 *
* Bounds set for this run : 2 to 50 MHz

FILENAME ---> B810269/FRQ
* Min pt --> 44.92 MHz , 1.51E-03 amplitude

* increasing frequency representation *

* # *	* MHz *	* amplitude *
1	5.86	2.90E-01
2	10.94	9.61E-02
3	15.63	6.78E-02
4	19.14	8.34E-02
5	24.22	5.84E-02
6	28.91	4.59E-02
7	33.20	3.21E-02
8	37.50	2.89E-02
9	42.19	1.99E-02
10	47.66	1.63E-02
11	50.00	1.12E-02

* decreasing amplitude representation *
* the 10 highest peaks *

* # *	* MHz *	* amplitude *	* % *
1	5.86	2.90E-01	100.00
2	10.94	9.61E-02	33.19
3	19.14	8.34E-02	28.78
4	15.63	6.78E-02	23.39
5	24.22	5.84E-02	20.15
6	28.91	4.59E-02	15.83
7	33.20	3.21E-02	11.09
8	37.50	2.89E-02	9.97
9	42.19	1.99E-02	6.86
10	47.66	1.63E-02	5.63

P R O N Y   A N A L Y S I S

* Filename ---> b810269 * dt =0.005 *

** Window 0 * 23 poles * t = .04 to .27 us **

Pole Pair	Prony Pole damp. freq(MHz)		Prony Residue real imag		Residue pole	%
1	-6.34	0.0	-2.800	0.000	0.442	100.00
2	-78.81	34.1	0.949	-3.227	0.015	3.33
3	-1.65	16.8	-0.128	0.319	0.003	0.74
4	-1.67	50.0	-0.092	-0.003	0.000	0.07

* 16 of 23 poles rejected. *

** Window 0 * 20 poles * t = .04 to .24 us **

Pole Pair	Prony Pole damp. freq(MHz)		Prony Residue real imag		Residue pole	%
1	-20.11	0.0	-3.416	0.0000	0.170	100.00
2	-17.50	6.2	1.601	2.0103	0.060	35.39
3	-13.67	18.1	0.393	0.9061	0.009	5.09
4	-51.65	0.0	-0.201	-0.0000	0.004	2.29
5	-0.05	35.1	0.102	-0.1816	0.001	0.56
6	-13.33	49.9	-0.292	-0.0003	0.001	0.55

* 10 of 20 poles rejected. *

** Window 0 * 17 poles * t = .04 to .21 us **

Pole Pair	Prony Pole damp. freq(MHz)		Prony Residue real imag		Residue pole	%
1	-39.54	0.0	-17.532	-0.000	0.443	100.00
2	-33.04	9.3	4.064	-5.252	0.099	22.24
3	-29.27	20.2	2.811	-0.068	0.022	4.88
4	-25.18	32.3	1.227	-0.295	0.006	1.39
5	-13.27	43.8	0.250	-0.007	0.001	0.20

* 8 of 17 poles rejected. *

P R O N Y   A N A L Y S I S

* Filename ---> b810269 (continued) * dt =0.005 *

** Window 0 * 14 poles * t = .04 to .18 us **

Pole Pair	Prony damp.	Pole freq(MHz)	Prony real	Residue imag	Residue / pole	%
1	-16.08	4.4	-0.143	3.5967	0.112	100.00
2	-7.59	18.3	0.282	0.6093	0.006	5.18
3	-89.69	0.0	-0.353	-0.0000	0.004	3.50
4	-7.98	34.1	0.200	-0.2904	0.002	1.46
5	-9.01	49.9	-0.224	-0.0029	0.001	0.63

* 5 of 14 poles rejected. *

** Window 0 * 11 poles * t = .04 to .15 us **

Pole Pair	Prony damp.	Pole freq(MHz)	Prony real	Residue imag	Residue / pole	%
1	-8.85	0.0	-4.195	0.000	0.474	100.00
2	-78.32	34.0	0.983	-3.188	0.015	3.09

* 8 of 11 poles rejected. *

ORIGINAL PAGE IS
OF POOR QUALITY
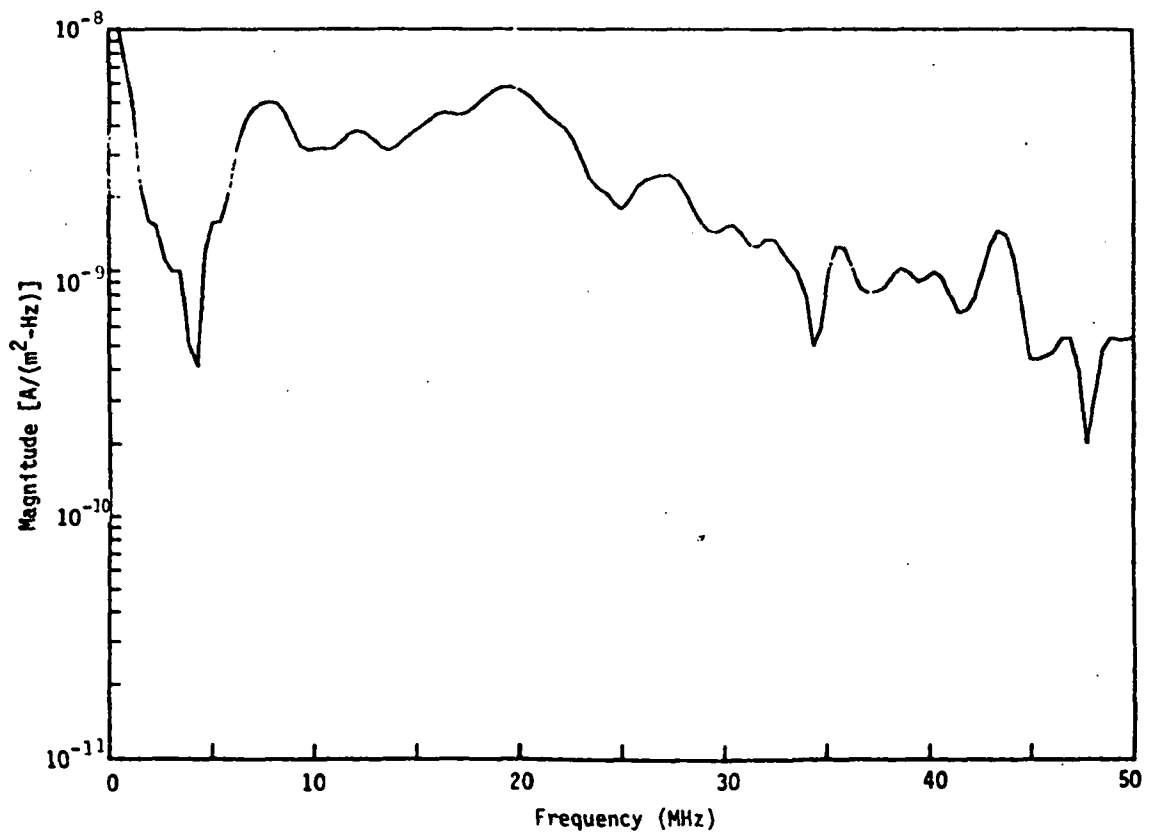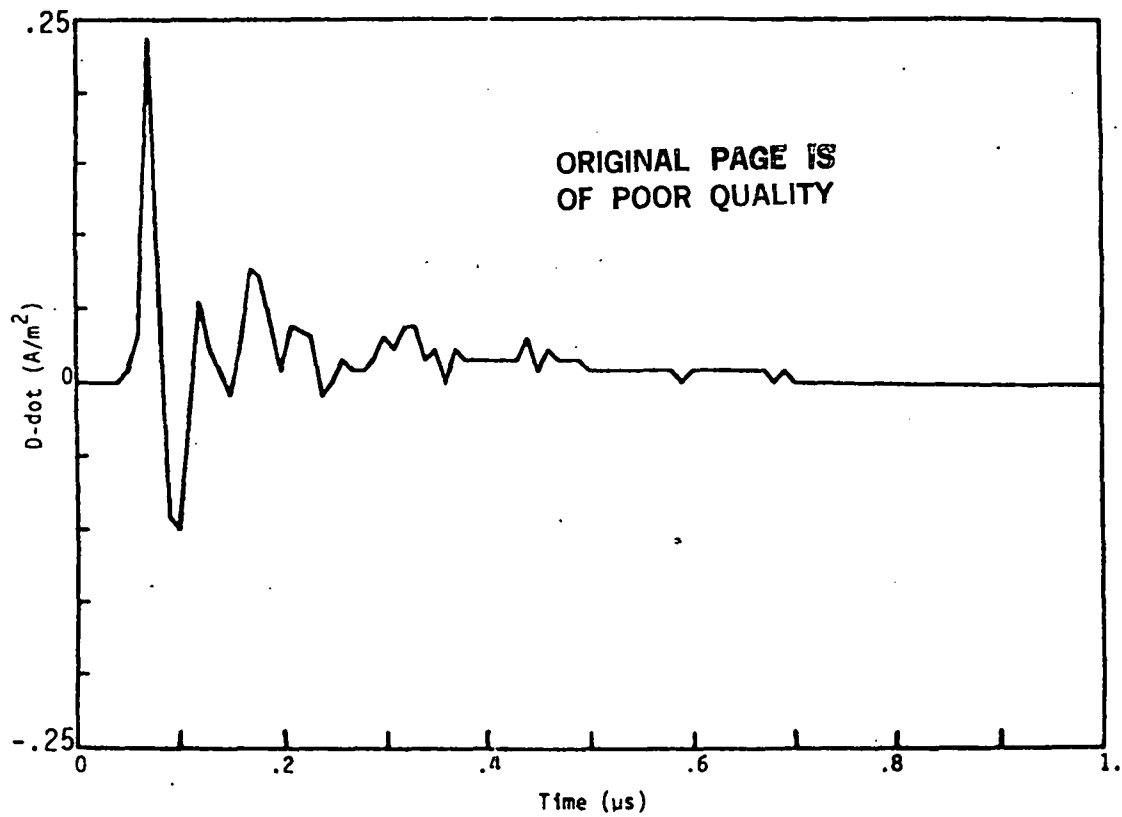
Figure A14. Measured D-dot Data (a) and Computed Spectral Response (b)
for Flight 81-026-10.

P E A K   F I C K
* Relative peak height for this run --> .01   *
* Bounds set for this run : 2   to   50   MHz

FILENAME   ---> D8102610/FRQ
* Min pt --> 47.66 MHz , 2.00E-03 amplitude

* increasing frequency representation *

* # *	* MHz *	* amplitude *
1	3.52	1.00E-02
2	7.81	5.04E-02
3	10.16	3.21E-02
4	12.11	3.81E-02
5	16.41	4.53E-02
6	19.53	5.79E-02
7	27.34	2.49E-02
8	30.47	1.55E-02
9	32.03	1.36E-02
10	35.55	1.28E-02
11	38.67	1.03E-02
12	40.23	9.89E-03
13	43.36	1.45E-02
14	46.88	5.39E-03
15	48.83	5.41E-03
16	50.00	5.43E-03

* decreasing amplitude representation *
* the 10 highest peaks *

* # *	* MHz *	* amplitude *	* % *
1	19.53	5.79E-02	100.00
2	7.81	5.04E-02	87.02
3	16.41	4.53E-02	78.24
4	12.11	3.81E-02	65.78
5	10.16	3.21E-02	55.36
6	27.34	2.49E-02	43.06
7	30.47	1.55E-02	26.73
8	43.36	1.45E-02	25.06
9	32.03	1.36E-02	23.42
10	35.55	1.28E-02	22.05

P R O N Y   A N A L Y S I S

* Filename ---> d8102610 * dt =0.010 *

** Window 5 * 30 poles * t = .09 to .69 us **

Pole Pair	Prony Pole damp. freq(MHz)		Prony Residue real imag		Residue/pole	%
1	-4.95	0.0	0.683	0.0408	0.138	100.00
2	-20.16	20.3	-0.185	0.9953	0.008	5.66
3	-188.36	0.0	-1.017	0.3090	0.006	4.08

* 26 of 30 poles rejected. *

** Window 3 * 30 poles * t = .07 to .67 us **

Pole Pair	Prony Pole damp. freq(MHz)		Prony Residue real imag		Residue/pole	%
1	-1.76	0.0	0.3018	0.0000	0.171	100.00
2	-9.14	7.6	0.3761	0.3162	0.010	5.92
3	-516.34	0.0	1.4134	0.3476	0.003	1.65
4	-4.23	34.2	-0.0537	0.0120	0.000	0.15

* 24 of 30 poles rejected. *

** Window 2 * 30 poles * t = .06 to .66 us **

Pole Pair	Prony Pole damp. freq(MHz)		Prony Residue real imag		Residue/pole	%
1	-2.08	0	0.314	0.0000	0.151	100.00
2	-72.61	0	-1.193	0.3793	0.017	11.42
3	-8.45	7	0.390	0.2191	0.009	6.23

* 26 of 30 poles rejected. *

P R O N Y   A N A L Y S I S

*   Filename ---> d8102610   (continued)   *   dt =0.010 *

** Window 1 * 30 poles * t = .05 to .65 us **

Pole Pair	Prony damp.	Pole freq(MHz)	Prony Residue real	Residue imag	Residue pole	%
1	-1.80	0.0	0.3128	0.000	0.174	100.00
2	-35.20	0.0	0.8543	0.000	0.024	13.95
3	-9.98	7.4	0.6715	0.144	0.014	8.29
4	-14.37	19.5	-0.8199	-0.540	0.008	4.57
5	-12.22	9.0	-0.2969	0.204	0.006	3.56
6	-6.70	16.7	-0.0937	-0.007	0.001	0.51
7	-7.47	26.3	-0.1191	-0.029	0.001	0.43
8	-4.28	12.8	-0.0393	-0.030	0.001	0.35
9	-9.51	41.7	0.0040	-0.142	0.001	0.31

* 14 of 30 poles rejected. *

** Window 0 * 30 poles * t = .04 to .64 us **

Pole Pair	Prony damp.	Pole freq(MHz)	Prony Residue real	Residue imag	Residue pole	%
1	-2.06	0.0	0.341	0.0000	0.166	100.00
2	-19.59	0.0	-0.374	0.0000	0.019	11.51
3	-8.70	7.5	0.476	-0.2885	0.012	7.01
4	-14.87	20.0	-0.593	1.0272	0.009	5.66
5	-16.51	10.4	0.484	0.2070	0.008	4.71
6	-9.46	26.3	-0.028	0.2033	0.001	0.75
7	-12.32	41.2	-0.179	0.0093	0.001	0.42
8	-4.58	13.3	-0.019	0.0538	0.001	0.41
9	-3.99	43.4	-0.077	-0.0778	0.000	0.24

* 14 of 30 poles rejected. *

** Window 0 * 24 poles * t = .04 to .52 us **

Pole Pair	Prony damp.	Pole freq(MHz)	Prony Residue real	Residue imag	Residue pole	%
1	-1.00	0.0	0.265	0.0000	0.265	100.00
2	-27.15	0.0	0.292	-0.0715	0.011	4.18
3	-15.22	20.0	-0.638	1.0059	0.009	3.55

* 20 of 24 poles rejected. *

-156-

PRONY ANALYSIS

* Filename ---> d8102610 (continued) * dt =0.010 *

** Window 0 * 21 poles * t = .04 to .46 us **

Pole Pair	Prony damp.	Pole freq(MHz)	Prony real	Residue imag	Residue/pole	%
1	-0.75	0	0.1852	0.000	0.252	100.00
2	-30.86	0	1.3854	-0.359	0.046	18.43
3	-5.34	0	-0.0223	-0.028	0.007	2.65

* 18 of 21 poles rejected. *

** Window 0 * 18 poles * t = .04 to .4 us **

Pole Pair	Prony damp.	Pole freq(MHz)	Prony real	Residue imag	Residue/pole	%
1	-2.23	0.0	0.358	0.0000	0.161	100.00
2	-16.45	20.1	-0.659	1.1744	0.011	6.57

* 15 of 18 poles rejected. *

** Window 0 * 15 poles * t = .04 to .34 us **

Pole Pair	Prony damp.	Pole freq(MHz)	Prony real	Residue imag	Residue/pole	%
1	-58.86	0.0	-2.556	0.1994	0.044	100.00
2	-42.95	0.0	1.759	-0.1294	0.041	94.28
3	-17.46	19.9	-0.912	1.1369	0.012	26.55
4	-6.05	6.0	0.245	0.2651	0.009	21.59

* 9 of 15 poles rejected. *

** Window 0 * 12 poles * t = .04 to .28 us **

Pole Pair	Prony damp.	Pole freq(MHz)	Prony real	Residue imag	Residue/pole	%
1	-10.84	0.0	0.9868	0.0000	0.091	100.00
2	-11.77	5.7	0.5613	0.5210	0.020	22.15
3	-15.80	19.8	-0.7468	0.9364	0.010	10.51
4	-24.57	43.4	-0.3985	-0.2142	0.002	1.82
5	-7.57	27.8	0.0931	0.0895	0.001	0.81

* 3 of 12 poles rejected. *

P R O N Y   A N A L Y S I S

* Filename ---> d8102610 (continued)   *   dt =0.010 *

** Window 0 * 9 poles * t = .04 to .22 us **

Pole Pair	Prony damp.	Pole freq(MHz)	Prony real	Residue imag	Residue / pole	%
1	−11.97	11.8	−0.3603	−0.479	0.008	100.00
2	−7.31	18.0	−0.6326	−0.139	0.006	71.92
3	−38.10	28.4	1.0190	−0.192	0.006	71.46
4	−17.43	41.2	−0.0314	−0.255	0.001	12.42

* 1 of 9 poles rejected. *

** Window 0 * 6 poles * t = .04 to .16 us **

| Pole Pair	Prony damp.	Pole freq(MHz)	Prony real	Residue imag	Residue / pole	%
1	−30.44	16.4	−2.532	−1.084	0.026	100.00
2	−52.35	26.7	2.433	−0.738	0.014	56.46
3	−14.98	39.5	0.099	−0.194	0.001	3.40
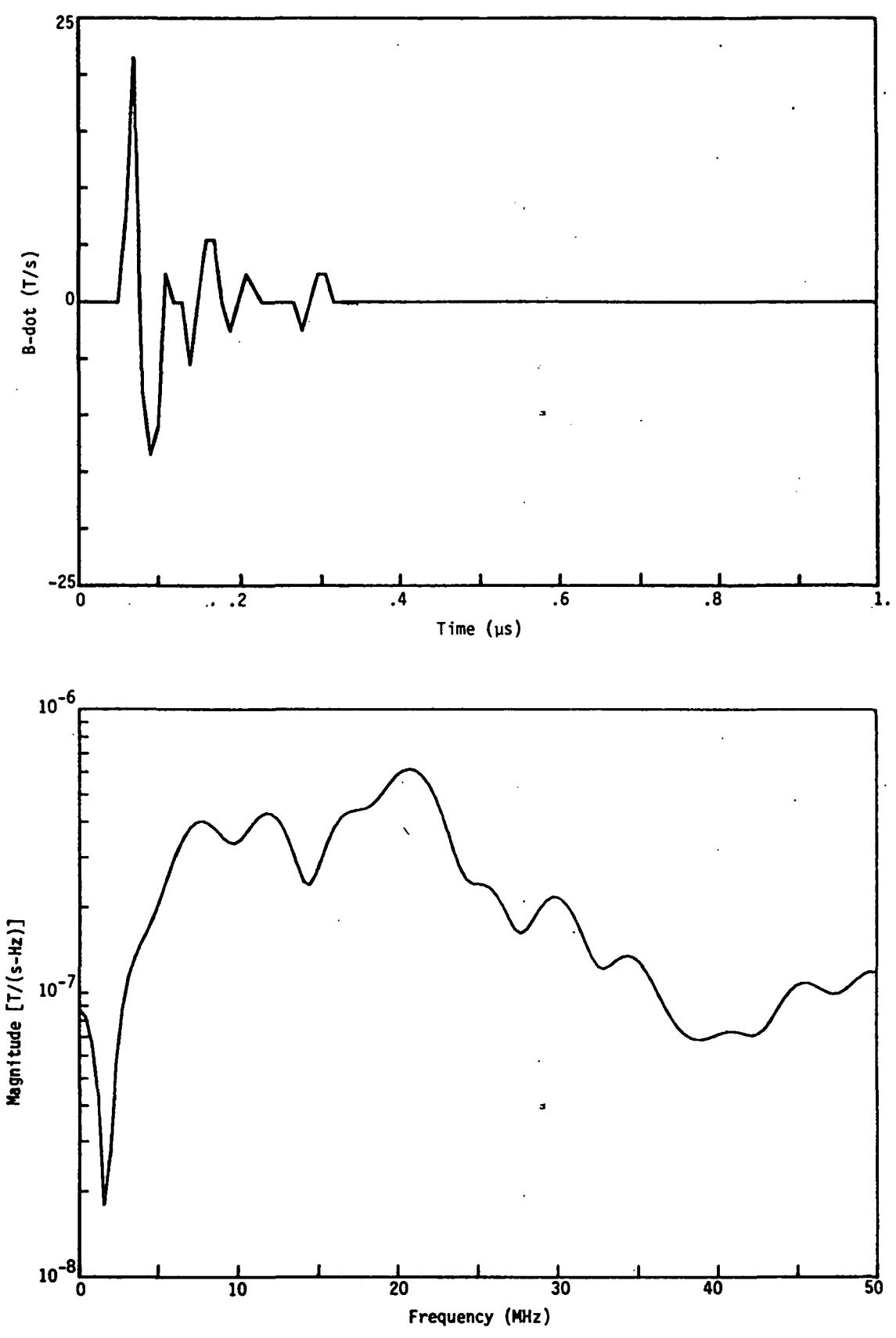
Figure A15.   Measured B-dot Data (a) and Computed Spectral Response (b)
for Flight 81-026-10.

P E A K   P I C K
* Relative peak height for this run --> .01   *
* Bounds set for this run : 0   to   50   Mhz

FILENAME   ---> B8102610/FRQ
* Min pt --> 1.56 MHz , 1.79E-02 amplitude

* increasing frequency representation *

* # *	* MHz *	* amplitude *
1	0.00	8.75E-02
2	7.81	4.03E-01
3	11.72	4.30E-01
4	20.70	6.17E-01
5	29.69	2.18E-01
6	34.38	1.36E-01
7	41.02	7.32E-02
8	45.31	1.09E-01
9	49.61	1.19E-01
10	50.00	1.19E-01

* decreasing amplitude representation *
* the 10 highest peaks *

* # *	* MHz *	* amplitude *	* % *
1	20.70	6.17E-01	100.00
2	11.72	4.30E-01	69.72
3	7.81	4.03E-01	65.39
4	29.69	2.18E-01	35.42
5	34.38	1.36E-01	22.00
6	49.61	1.19E-01	19.35
7	50.00	1.19E-01	19.32
8	45.31	1.09E-01	17.62
9	0.00	8.75E-02	14.19
10	41.02	7.32E-02	11.87

PRONY   ANALYSIS

* Filename ---> b8102610 * dt =0.005 *

** Window 0 * 26 poles * t = .04 to .3 us **

Pole Pair	Prony damp.	Pole freq(MHz)	Prony real	Residue imag	Residue / pole	%
1	-44.65	49.5	-32.031	-11.719	0.109	100.00
2	-14.39	20.3	-9.845	3.017	0.080	73.71
3	-4.38	5.9	1.518	0.980	0.048	44.48
4	-7.50	10.2	1.621	-1.730	0.037	33.88
5	-27.51	37.1	-1.892	-2.599	0.014	12.60
6	-3.69	28.1	-0.364	0.312	0.003	2.50

* 14 of 26 poles rejected. *

** Window 0 * 23 poles * t = .04 to .27 us **
* 23 of 23 poles rejected. *

** Window 0 * 20 poles * t = .04 to .24 us **

Pole Pair	Prony damp.	Pole freq(MHz)	Prony real	Residue imag	Residue / pole	%
1	-16.15	7.9	7.8145	-0.3903	0.150	100.00
2	-11.20	20.7	-6.5100	3.8561	0.058	38.66
3	-25.73	30.3	3.1903	2.9437	0.023	15.08

* 14 of 20 poles rejected. *

** Window 0 * 17 poles * t = .04 to .21 us **

Pole Pair	Prony damp.	Pole freq(MHz)	Prony real	Residue imag	Residue / pole	%
1	-15.03	7.9	7.175	-0.3334	0.139	100.00
2	-12.19	20.6	-7.305	3.7913	0.063	45.60
3	-22.02	31.2	2.866	1.3892	0.016	11.64
4	-7.04	47.5	-1.000	-0.3279	0.004	2.54

* 9 of 17 poles rejected. *

P R O N Y   A N A L Y S I S

*   Filename ---> b8102610   (continued)   *   dt =0.005 *

**   Window 0   *   14 poles   *   t = .04 to .18 us   **

Pole Pair	Prony damp.	Pole freq(MHz)	Prony real	Residue imag	Residue pole	%
1	-14.17	7.7	6.5815	0.2472	0.131	100.00
2	-14.68	20.8	-8.6613	5.0912	0.076	58.46
3	-415.37	0.0	16.4747	0.0000	0.040	30.32
4	-70.13	0.0	-1.7853	-0.0000	0.025	19.46
5	-20.65	49.8	-4.2474	0.0731	0.014	10.35
6	-8.64	31.3	1.0202	0.6942	0.006	4.80

*   4 of 14 poles rejected.   *

**   Window 0   *   11 poles   *   t = .04 to .15 us   **

Pole Pair	Prony damp.	Pole freq(MHz)	Prony real	Residue imag	Residue pole	%
1	-132.42	0.0	115.115	0.0000	0.869	100.00
2	-23.66	0.0	-15.570	-0.0000	0.658	75.68
3	-33.56	20.1	-26.449	12.3019	0.223	25.64
4	-161.51	0.0	-15.343	0.0000	0.095	10.93

*   6 of 11 poles rejected.   *

**   Window 0   *   8 poles   *   t = .04 to .12 us   **

Pole Pair	Prony damp.	Pole freq(MHz)	Prony real	Residue imag	Residue pole	%
1	-1.56	15.6	-4.2391	-5.951	0.074	100.00
2	-26.51	31.9	6.5597	2.122	0.034	45.95

*   4 of 8 poles rejected.   *

**   Window 0   *   5 poles   *   t = .04 to .09 us   **
*   5 of 5 poles rejected.   *
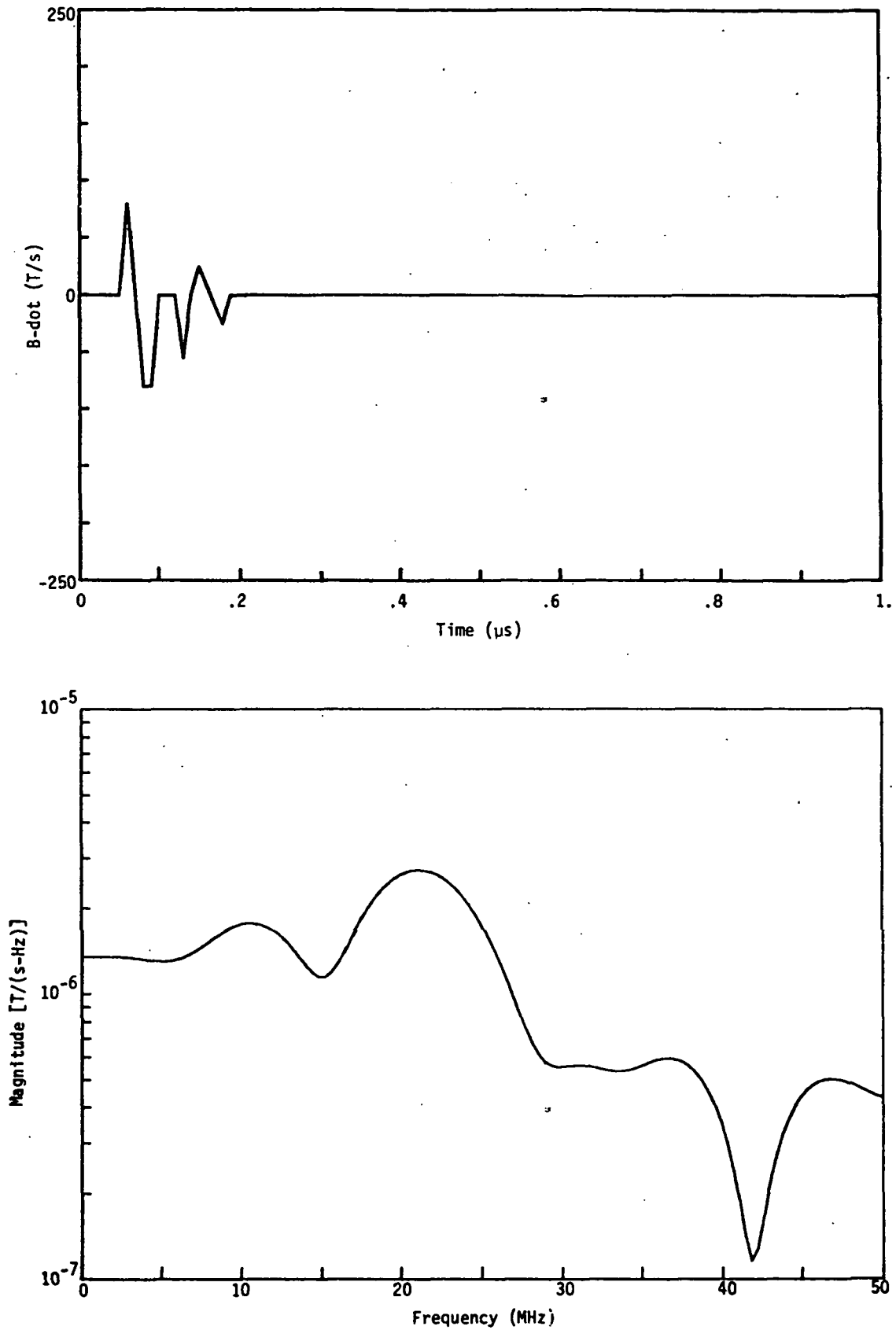
Figure A16.   Measured B-dot Data (a) and Computed Spectral Response (b)
for Flight 81-041-01.

PEAK PICK
* Relative peak height for this run --> .01 *
* Bounds set for this run : 0 to 50 Mhz

FILENAME ---> B810411/FRQ
* Min pt --> 41.80 MHz , 1.16E-01 amplitude

* increasing frequency representation *

* # *	* MHz *	* amplitude *
1	1.56	1.35E+00
2	10.55	1.77E+00
3	21.09	2.72E+00
4	30.86	5.60E-01
5	36.72	5.93E-01
6	46.88	5.02E-01
7	50.00	4.31E-01

* decreasing amplitude representation *
* the 10 highest peaks *

* # *	* MHz *	* amplitude *	* % *
1	21.09	2.72E+00	100.00
2	10.55	1.77E+00	65.16
3	1.56	1.35E+00	49.69
4	36.72	5.93E-01	21.82
5	30.86	5.60E-01	20.59
6	46.88	5.02E-01	18.46
7	50.00	4.31E-01	15.85

P R O N Y   A N A L Y S I S

* Filename ---> b810411 * dt =0.005 *

** Window 0 * 17 poles * t = .04 to .21 us **

Pole Pair	Prony Pole damp.	freq(MHz)	Prony Residue real	imag	Residue/pole	%
1	-19.36	7.1	34.993	27.0373	0.905	100.00
2	-11.45	22.0	-40.572	-2.6931	0.293	32.41
3	-3.01	49.9	6.823	-0.0191	0.022	2.40
4	-1.07	37.8	3.712	0.0557	0.016	1.73

* 9 of 17 poles rejected. *

** Window 0 * 14 poles * t = .04 to .18 us **

Pole Pair	Prony Pole damp.	freq(MHz)	Prony Residue real	imag	Residue/pole	%
1	-27.38	5.7	47.6953	62.4649	1.751	100.00
2	-13.34	22.3	-45.3143	2.9021	0.323	18.43
3	-65.22	0.0	-4.9616	0.0000	0.076	4.34
4	-0.56	49.3	4.6990	1.3225	0.016	0.90

* 7 of 14 poles rejected. *

** Window 0 * 11 poles * t = .04 to .15 us **

Pole Pair	Prony Pole damp.	freq(MHz)	Prony Residue real	imag	Residue/pole	%
1	-14.79	0.0	-60.059	0.000	4.062	100.00
2	-152.58	0.0	273.525	0.000	1.793	44.14
3	-24.43	21.2	-80.880	-17.738	0.613	15.09
4	-160.83	0.0	-37.290	-0.000	0.232	5.71

* 6 of 11 poles rejected. *

** Window 0 * 8 poles * t = .04 to .12 us **

Pole Pair	Prony Pole damp.	freq(MHz)	Prony Residue real	imag	Residue/pole	%
1	-414.93	0	-104.379	0.0000	0.285	100.00

* 7 of 8 poles rejected. *

-165-
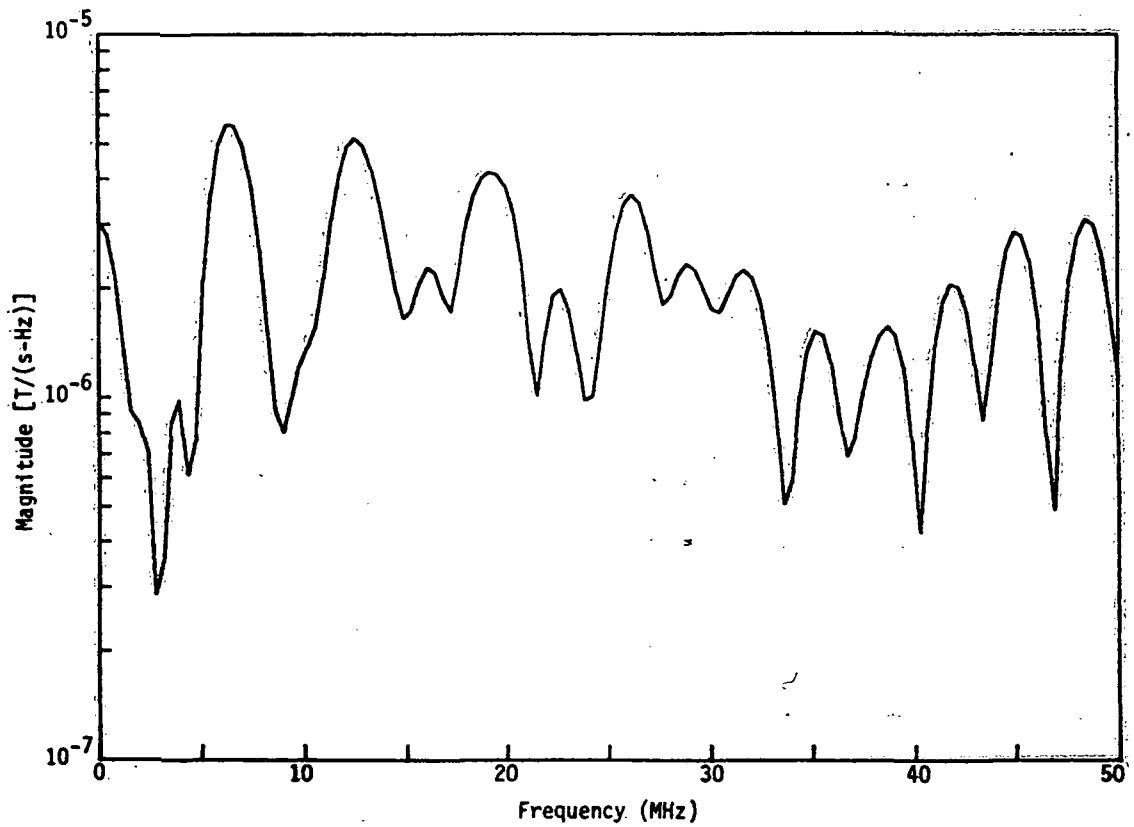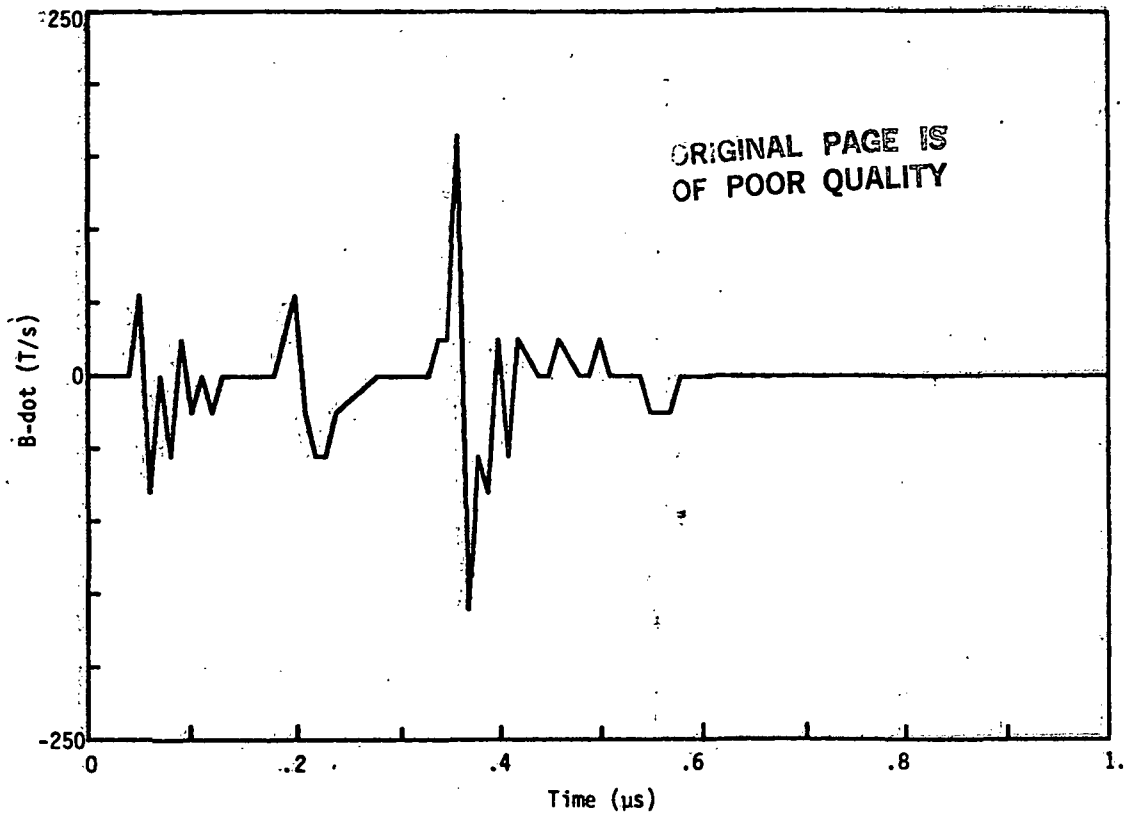
Figure A17.   Measured B-dot Data (a) and Computed Spectral Response (b) for Flight 81-041-02.

P E A K   P I C K
* Relative peak height for this run --> .01   *
* Bounds set for this run : 0 to 50 Mhz

FILENAME   ---> 8810412/FRQ
* Min pt --> 2.73 MHz , 2.87E-01 amplitude

* increasing frequency representation *

* # *	* MHz *	* amplitude *
1	0.00	3.05E+00
2	3.91	9.87E-01
3	6.25	5.64E+00
4	12.50	5.17E+00
5	16.02	2.28E+00
6	19.14	4.18E+00
7	22.66	1.98E+00
8	26.17	3.62E+00
9	28.91	2.33E+00
10	31.64	2.23E+00
11	35.16	1.52E+00
12	38.67	1.56E+00
13	41.80	2.05E+00
14	44.92	2.85E+00
15	48.44	3.09E+00
16	50.00	1.13E+00

* decreasing amplitude representation *
* the 10 highest peaks *

* # *	* MHz *	* amplitude *	* % *
1	6.25	5.64E+00	100.00
2	12.50	5.17E+00	91.70
3	19.14	4.18E+00	74.10
4	26.17	3.62E+00	64.18
5	48.44	3.09E+00	54.86
6	0.00	3.05E+00	54.09
7	44.92	2.85E+00	50.52
8	28.91	2.33E+00	41.23
9	16.02	2.28E+00	40.34
10	31.64	2.23E+00	39.55

PRONY ANALYSIS

* Filename ---> b810412 * dt =0.005 *

** Window 0 * 15 poles * t = .04 to .19 us **

Pole Pair	Prony damp.	Pole freq(MHz)	Prony Residue real	Residue imag	Residue/pole	%
1	-10.06	0.0	-33.121	0.000	3.292	100.00
2	-19.87	20.8	12.538	-11.832	0.131	3.96
3	-9.23	48.3	-19.985	7.266	0.070	2.13
4	-13.15	0.0	0.018	0.000	0.001	0.04

* 9 of 15 poles rejected. *

** Window 0 * 12 poles * t = .04 to .16 us **

Pole Pair	Prony damp.	Pole freq(MHz)	Prony Residue real	Residue imag	Residue/pole	%
1	-41.56	1.6	4.328	139.443	3.265	100.00
2	-17.38	20.1	14.021	-6.887	0.123	3.75
3	-20.09	47.4	-23.597	-12.442	0.089	2.74

* 6 of 12 poles rejected. *

** Window 0 * 9 poles * t = .04 to .13 us **

Pole Pair	Prony damp.	Pole freq(MHz)	Prony Residue real	Residue imag	Residue/pole	%
1	-14.40	0.0	-28.7169	0.000	1.994	100.00
2	-57.52	48.7	86.5492	-90.589	0.402	20.18
3	-29.18	20.7	19.1125	-18.327	0.198	9.94

* 4 of 9 poles rejected. *

** Window 0 * 6 poles * t = .04 to .1 us **

Pole Pair	Prony damp.	Pole freq(MHz)	Prony Residue real	Residue imag	Residue/pole	%
1	-30.60	11.9	32.9191	32.9080	0.578	100.00

* 4 of 6 poles rejected. *

P R O N Y   A N A L Y S I S

* Filename ---> b810412 * dt =0.005 *

** Window 0 * 26 poles * t = .04 to .3 us **

Pole Pair	Prony damp.	Pole freq(MHz)	Prony real	Residue imag	Residue/pole	%
1	-28.90	0.0	418.483	0.000	14.479	100.00
2	-37.66	4.1	75.122	566.659	12.484	86.22
3	-46.87	21.4	-137.660	174.731	1.562	10.79
4	-28.69	50.0	-103.012	14.887	0.330	2.28
5	-9.86	27.4	-13.294	19.860	0.139	0.96
6	-13.11	40.5	7.294	7.341	0.041	0.28

* 15 of 26 poles rejected. *

** Window 0 * 23 poles * t = .04 to .27 us **

Pole Pair	Prony damp.	Pole freq(MHz)	Prony real	Residue imag	Residue/pole	%
1	-35.19	7.4	179.384	79.554	3.351	100.00
2	-38.18	21.7	-69.069	125.198	1.008	30.07
3	-25.33	50.0	-83.369	10.316	0.266	7.95
4	-11.88	27.3	-18.173	26.188	0.185	5.53
5	-10.66	41.3	8.365	1.914	0.033	0.99

* 13 of 23 poles rejected. *

** Window 0 * 14 poles * t = .04 to .18 us **

Pole Pair	Prony damp.	Pole freq(MHz)	Prony real	Residue imag	Residue/pole	%
1	-27.54	7.8	118.972	43.799	2.247	100.00
2	-41.83	21.1	-116.463	71.010	0.980	43.63
3	-28.24	47.5	-59.569	-74.417	0.318	14.16
4	-4.84	29.1	5.733	14.100	0.083	3.71

* 6 of 14 poles rejected. *

P R O N Y   A N A L Y S I S

* Filename ---> b810412 (continued) * dt =0.005 *

** Window 0 * 11 poles * t = .04 to .15 us **

Pole Pair	Prony Pole damp. freq(MHz)		Prony Residue real	imag	Residue / pole	%
1	-172.36	0.0	207.896	-0.000	1.206	100.00
2	-12.17	8.6	58.489	8.317	1.072	88.85
3	-35.12	25.2	-60.209	129.810	0.881	73.07
4	-18.96	50.0	-71.399	5.528	0.228	18.88
5	-45.94	0.0	-8.120	0.000	0.177	14.65

* 3 of 11 poles rejected. *

** Window 0 * 8 poles * t = .04 to .12 us **

Pole Pair	Prony Pole damp. freq(MHz)		Prony Residue real	imag	Residue / pole	%
1	-1.09	34.0	31.3374	12.0021	0.157	100.00

* 6 of 8 poles rejected. *

** Window 0 * 5 poles * t = .04 to .09 us **

| Pole Pair	Prony Pole damp. freq(MHz)		Prony Residue real	imag	Residue / pole	%
1	-545.38	0	72.989	0.0000	0.159	100.00
2	%-1090.05	0	-82.768	0.0000	0.088	55.62

* 3 of 5 poles rejected. *

-170-
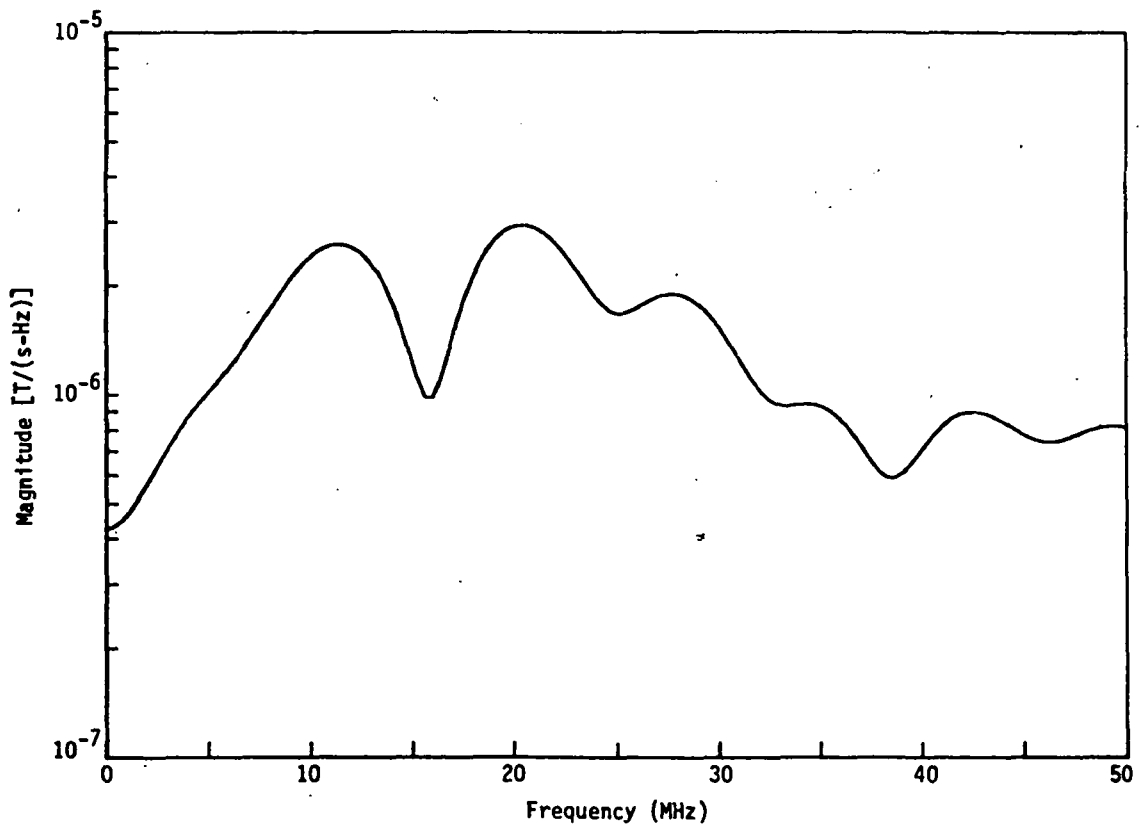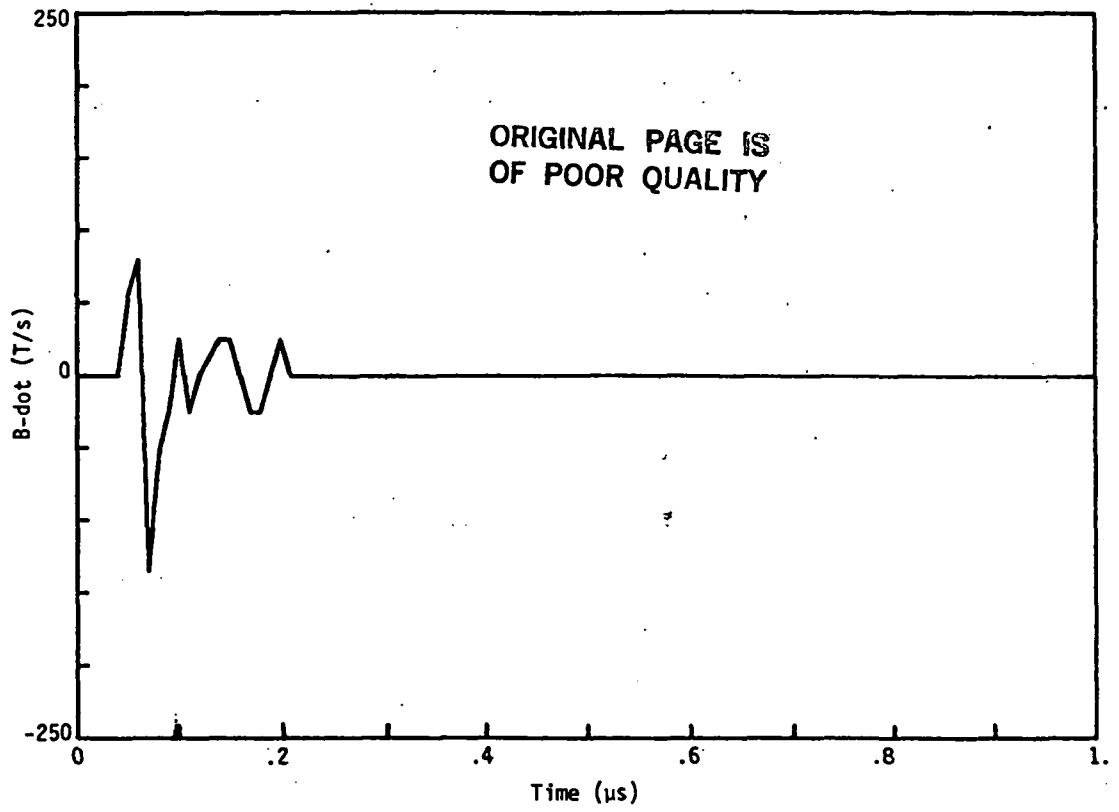
Figure A18.   Measured B-dot Data (a) and Computed Spectral Response (b)
for Flight 81-042.

P E A K   P I C K
* Relative peak height for this run --> .01 *
* Bounds set for this run : 0 to 50 Mhz

FILENAME ---> B81042/FRQ
* Min pt -->   0.00 MHz , 4.25E-01 amplitude

* increasing frequency representation *

* # *	* MHz *	* amplitude *
1	11.33	2.60E+00
2	20.31	2.93E+00
3	27.73	1.89E+00
4	34.38	9.43E-01
5	42.58	8.99E-01
6	49.22	8.21E-01
7	50.00	8.11E-01

* decreasing amplitude representation *
* the 10 highest peaks *

* # *	* MHz *	* amplitude *	* % *
1	20.31	2.93E+00	100.00
2	11.33	2.60E+00	88.53
3	27.73	1.89E+00	64.43
4	34.38	9.43E-01	32.14
5	42.58	8.99E-01	30.63
6	49.22	8.21E-01	27.99
7	50.00	8.11E-01	27.65

P R O N Y   A N A L Y S I S

* Filename ---> b81042 *   dt =0.005 *

** Window 0 * 18 poles * t = .04 to .22 us **

Pole Pair	Prony damp.	Pole freq(MHz)	Prony real	Residue imag	Residue / pole	%
1	-23.47	10.8	79.7344	15.1557	1.135	100.00
2	-33.03	29.9	-37.3003	33.2307	0.262	23.07
3	-43.66	45.5	16.1951	72.6795	0.257	22.67
4	-4.06	18.4	16.7923	2.2793	0.146	12.90

* 10 of 18 poles rejected. *

** Window 0 * 15 poles * t = .04 to .19 us **

Pole Pair	Prony damp.	Pole freq(MHz)	Prony real	Residue imag	Residue / pole	%
1	-96.00	0.0	-303.239	-0.000	3.159	100.00
2	-36.36	19.7	66.733	-136.862	1.182	37.41
3	-3.02	12.1	7.096	-16.188	0.232	7.34
4	-40.57	49.2	68.723	2.374	0.220	6.98
5	-8.64	34.3	4.444	2.892	0.025	0.78

* 6 of 15 poles rejected. *

** Window 0 * 12 poles * t = .04 to .16 us **

Pole Pair	Prony damp.	Pole freq(MHz)	Prony real	Residue imag	Residue / pole	%
1	-11.38	7.0	3.373	29.438	0.648	100.00
2	-32.74	23.4	-44.832	-83.489	0.629	97.06

* 8 of 12 poles rejected. *

** Window 0 * 9 poles * t = .04 to .13 us **

| Pole Pair	Prony damp.	Pole freq(MHz)	Prony real	Residue imag	Residue / pole	%
1	-31.95	23.3	-41.273	-83.513	0.623	100.00
2	-8.39	6.9	1.450	25.988	0.589	94.55
3	-28.08	50.0	40.664	-5.061	0.130	20.87
4	-56.15	0.0	-2.126	-0.000	0.038	6.08

* 2 of 9 poles rejected. *

Figure A19. Measured B-dot Data (a) and Computed Spectral Response (b)
for Flight 81-043-01.

PEAK PICK
* Relative peak height for this run --> 5E-03 *
* Bounds set for this run : 2 to 50 Mhz

FILENAME ---> B810431/FRQ
* Min pt --> 1.95 MHz , 4.94E-01 amplitude

* increasing frequency representation *

* # *	* MHz *	* amplitude *
1	3.52	2.28E+00
2	6.64	5.23E+00
3	10.16	3.23E+00
4	12.50	2.81E+00
5	17.58	2.22E+00
6	21.09	1.43E+00
7	24.22	1.24E+00
8	27.73	1.32E+00
9	31.25	1.35E+00
10	32.42	1.36E+00
11	38.28	1.20E+00
12	41.41	9.61E-01
13	44.14	8.48E-01
14	47.66	8.75E-01
15	50.00	7.71E-01

* decreasing amplitude representation *
* the 10 highest peaks *

* # *	* MHz *	* amplitude *	* % *
1	6.64	5.23E+00	100.00
2	10.16	3.23E+00	61.90
3	12.50	2.81E+00	53.69
4	3.52	2.28E+00	43.67
5	17.58	2.22E+00	42.46
6	21.09	1.43E+00	27.40
7	32.42	1.36E+00	25.96
8	31.25	1.35E+00	25.80
9	27.73	1.32E+00	25.19
10	24.22	1.24E+00	23.69

P R O N Y   A N A L Y S I S

* Filename ---> b810431 * dt = 0.010 *

** Window 0 * 21 poles * t = .04 to .46 us **

Pole Pair	Prony damp.	Pole freq(MHz)	Prony real	Residue imag	Residue/pole	%
1	-20.01	10.3	77.888	-33.085	1.249	100.00
2	-40.15	22.1	52.865	170.137	1.235	98.86
3	-55.04	44.9	-153.321	284.575	1.125	90.02
4	-4.34	6.8	21.506	-0.348	0.498	39.85
5	-4.51	15.8	10.295	-4.144	0.112	8.95
6	-6.25	32.8	-5.050	-2.913	0.028	2.26
7	-6.06	47.2	-3.081	3.743	0.016	1.31

* 7 of 21 poles rejected. *

** Window 0 * 13 poles * t = .04 to .3 us **

Pole Pair	Prony damp.	Pole freq(MHz)	Prony real	Residue imag	Residue/pole	%
1	-24.80	0.0	92.3678	-0.000	3.725	100.00
2	-3.59	0.0	-6.2744	0.000	1.747	46.91
3	-8.79	6.7	34.9667	22.451	0.973	26.12
4	-49.72	31.3	13.9897	-166.842	0.826	22.19
5	-25.51	19.0	-90.9447	25.779	0.773	20.75

* 5 of 13 poles rejected. *

** Window 0 * 5 poles * t = .04 to .14 us **
* 5 of 5 poles rejected. *
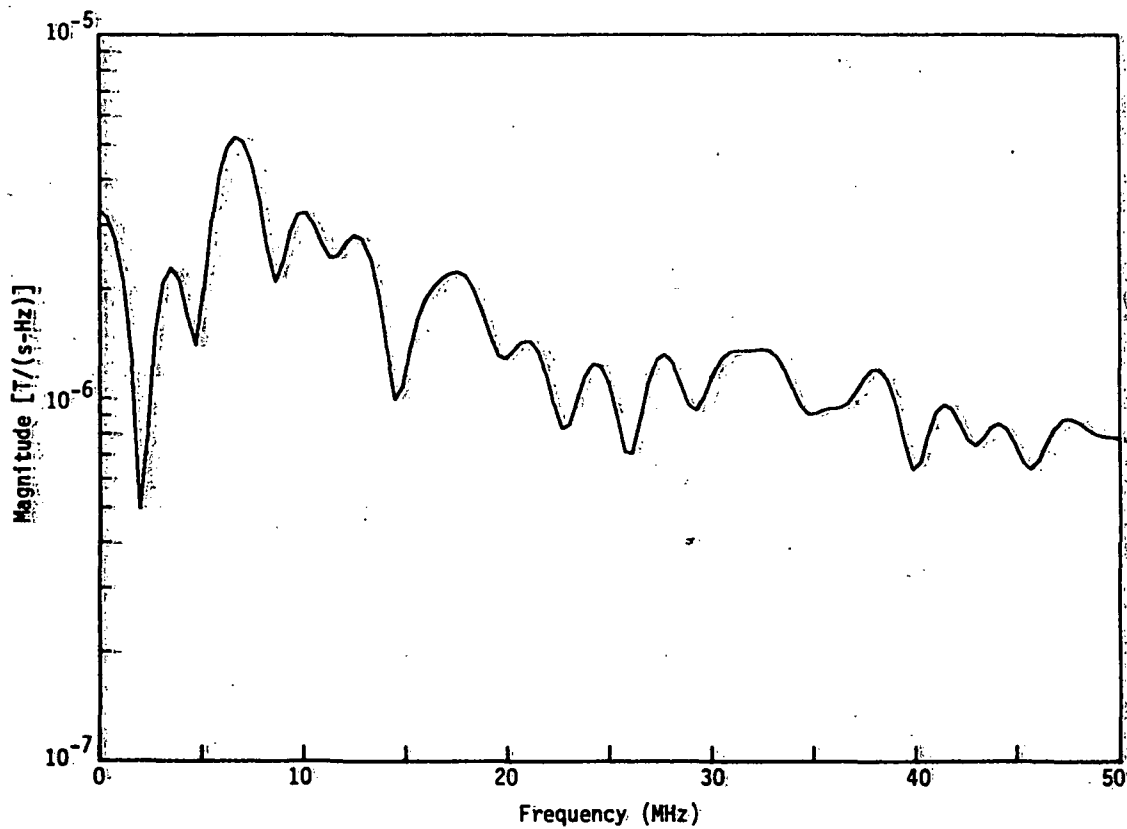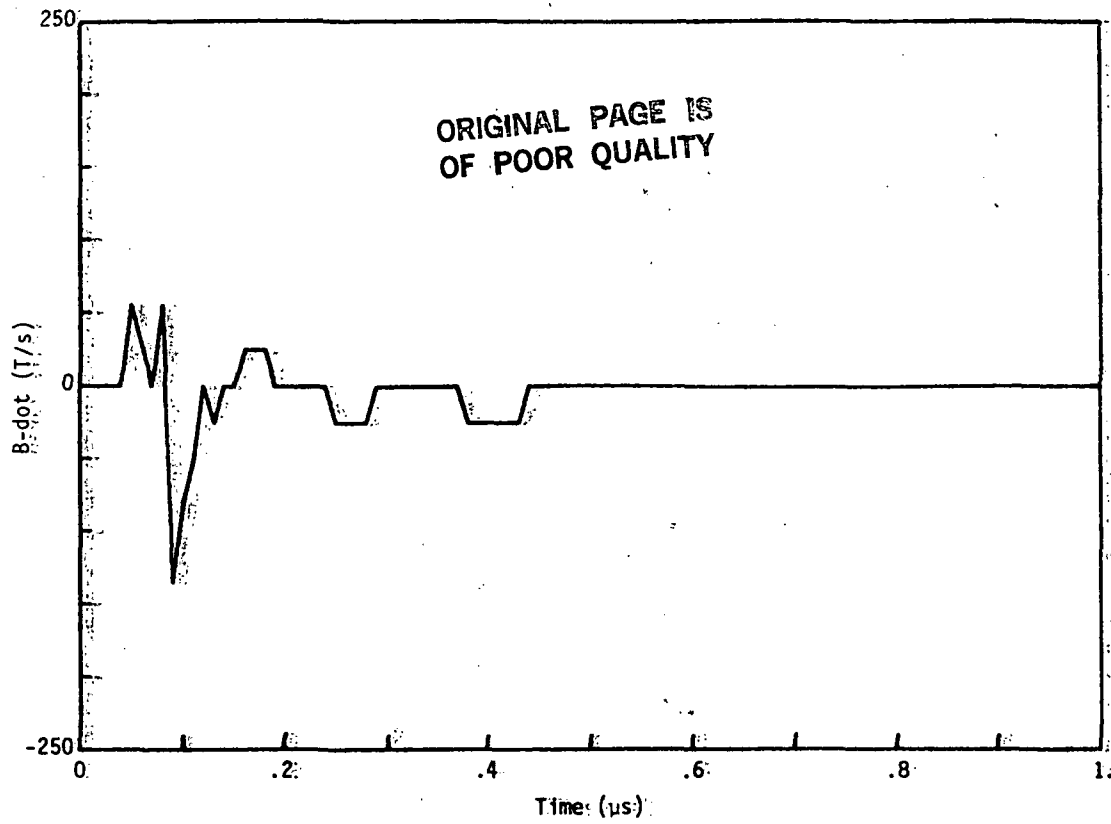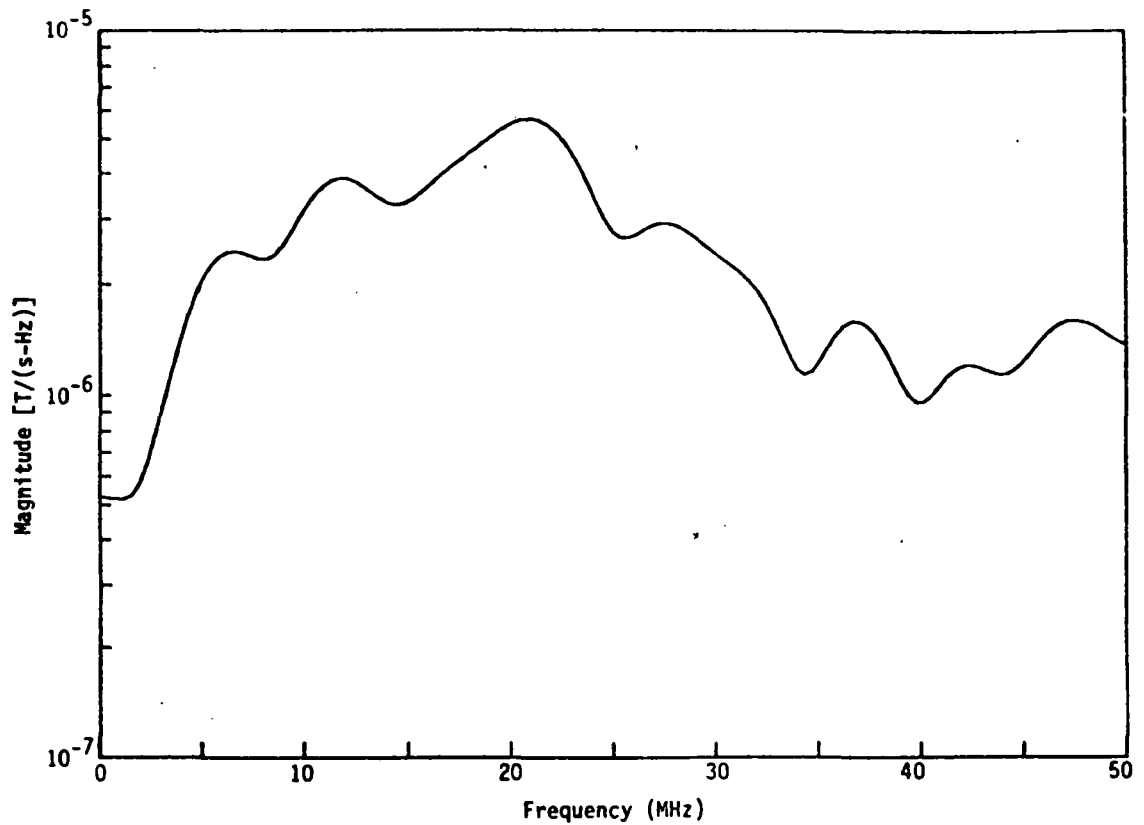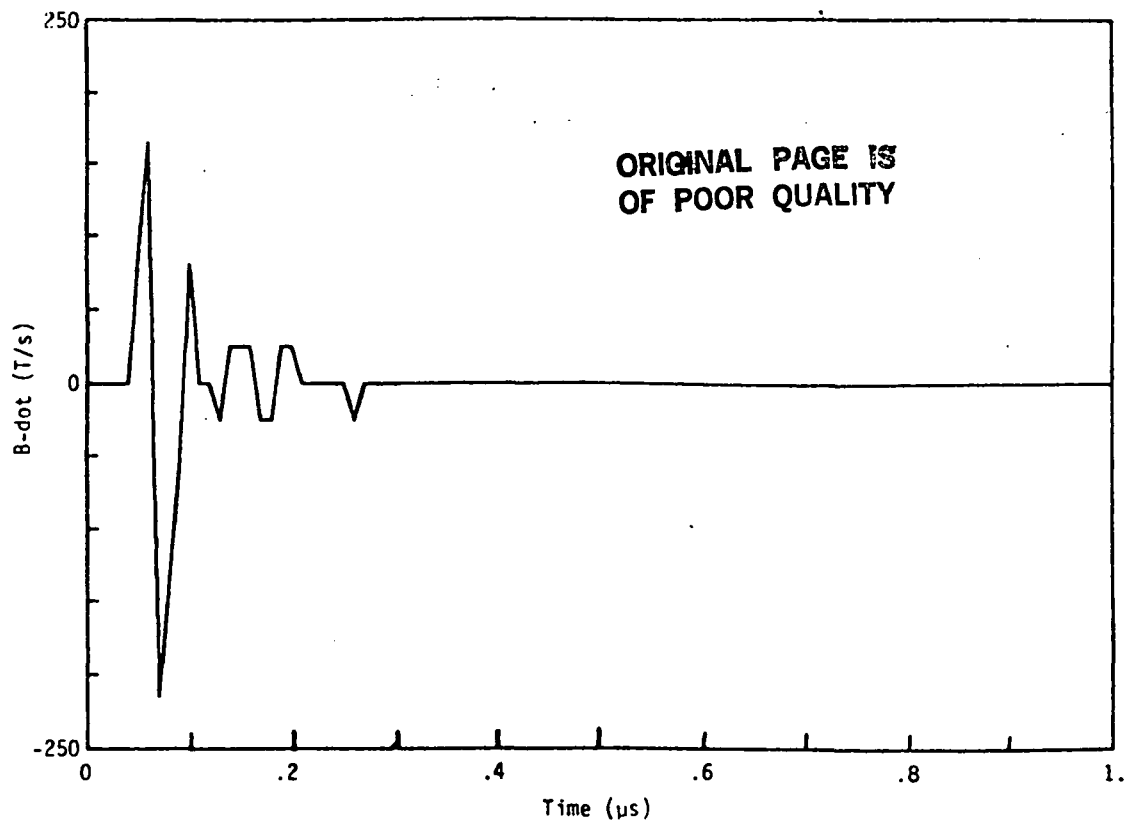
Figure A20.   Measured B-dot Data (a) and Computed Spectral Response (b)
for Flight 81-043-02.

P E A K   P I C K
** Relative peak height for this run --> .01 **
** Bounds set for this run : 0 to 50 MHz

FILENAME ---> B810432/FRQ
** Min pt --> 11.17 MHz , 5.17E-01 amplitude

** increasing frequency representation **

** # **	** MHz **	** amplitude **
1	0.00	5.25E-01
2	6.69	2.46E+00
3	11.72	3.88E+00
4	21.09	5.65E+00
5	27.73	2.93E+00
6	36.72	1.59E+00
7	42.19	1.20E+00
8	47.27	1.59E+00
9	50.00	1.37E+00

** decreasing amplitude representation **
** the 10 highest peaks **

** # **	** MHz **	** amplitude **	** % **
1	21.09	5.65E+00	100.00
2	11.72	3.88E+00	68.68
3	27.73	2.93E+00	51.87
4	6.64	2.46E+00	43.56
5	36.72	1.59E+00	28.17
6	47.27	1.59E+00	28.17
7	50.00	1.37E+00	24.19
8	42.19	1.20E+00	21.20
9	0.00	5.25E-01	9.30

P R O N Y   A N A L Y S I S

* Filename ---> b810432 *   dt =0.010 *

** Window 0 * 13 poles * t = .04 to .3 us **

Pole Pair	Prony damp.	Pole freq(MHz)	Prony real	Residue imag	Residue / pole	%
1	-34.48	0.0	100.820	-0.000	2.924	100.00
2	-27.14	5.8	-19.314	114.907	2.566	87.77
3	-17.26	21.3	-55.921	-99.674	0.847	28.96
4	-13.91	49.1	48.477	-42.336	0.208	7.13
5	-13.62	28.1	-25.078	-17.827	0.174	5.93

* 4 of 13 poles rejected. *

** Window 0 * 5 poles * t = .04 to .14 us **

Pole Pair	Prony damp.	Pole freq(MHz)	Prony real	Residue imag	Residue / pole	%
1	-80.19	9.1	175.994	560.819	5.969	100.00
2	-23.24	0.0	104.238	0.000	4.484	75.12
3	-42.60	21.8	-228.113	-284.529	2.543	42.60
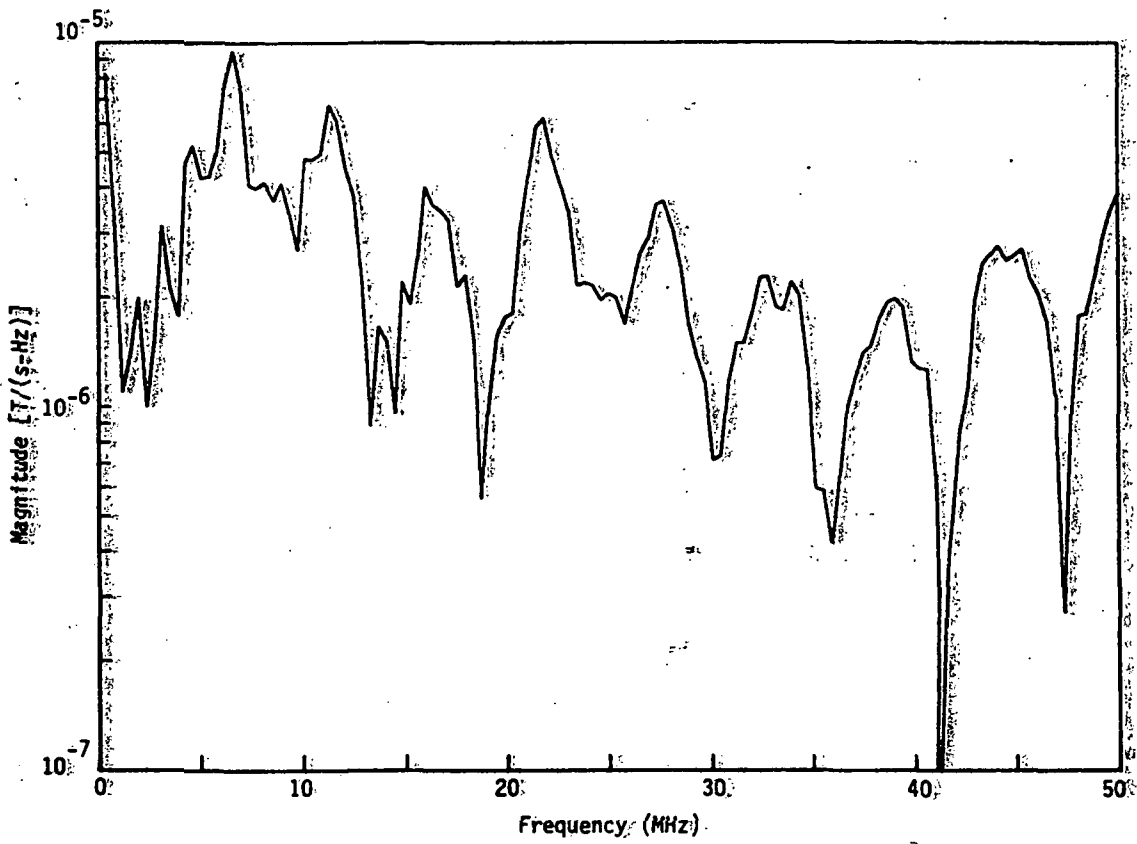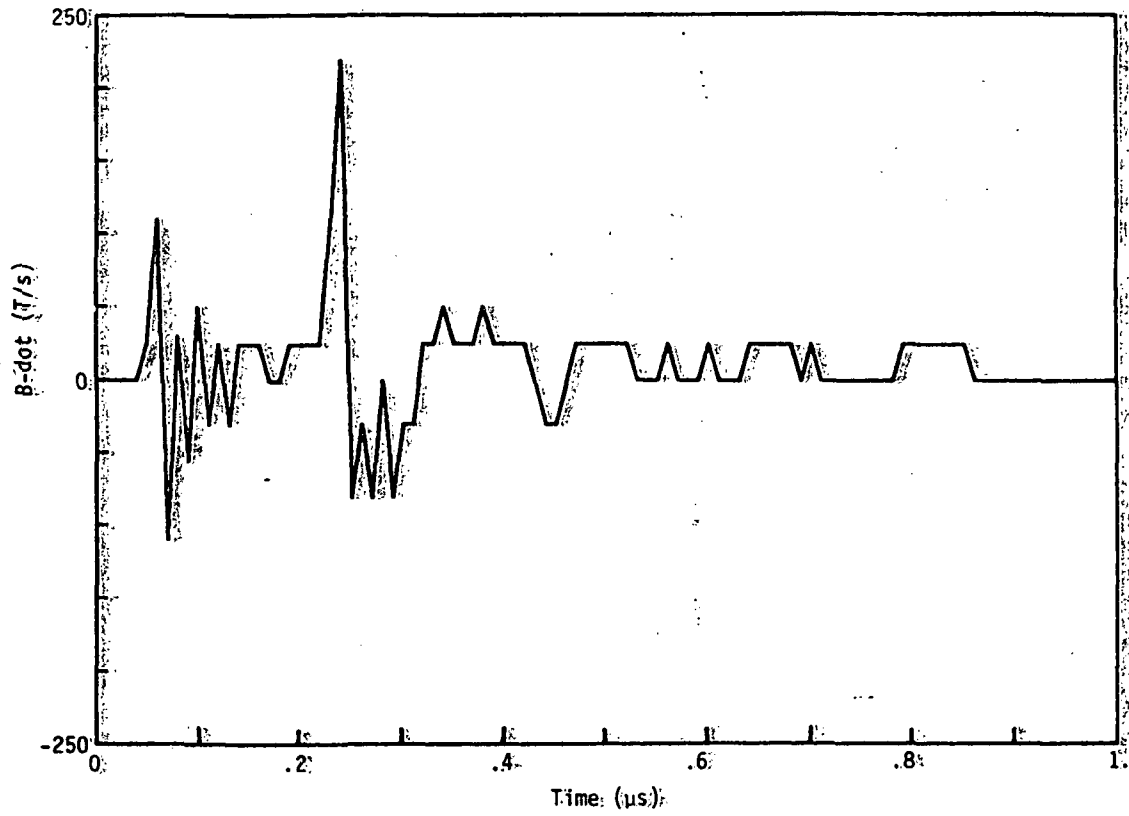
Figure A21. Measured B-dot Data (a) and Computed Spectral Response (b)
for Flight 81-043-03.

P E A K   P I C K
* Relative peak height for this run --> .01   *
* Bounds set for this run : 2 to 50   Mhz

FILENAME   ---> B810433/FRQ
* Min pt ---> 41.41 MHz , 9.52E-02 amplitude

* increasing frequency representation *

* # *	* MHz *	* amplitude *
1	3.13	3.13E+00
2	4.69	5.22E+00
3	6.64	9.49E+00
4	8.20	4.15E+00
5	8.98	4.11E+00
6	10.16	4.82E+00
7	11.33	6.73E+00
8	13.67	1.66E+00
9	14.84	2.19E+00
10	16.02	4.00E+00
11	17.97	2.29E+00
12	21.88	6.22E+00
13	23.83	2.19E+00
14	25.00	2.04E+00
15	27.73	3.68E+00
16	32.81	2.28E+00
17	33.98	2.20E+00
18	39.06	1.98E+00
19	44.14	2.77E+00
20	45.31	2.71E+00
21	50.00	3.88E+00

* decreasing amplitude representation *
* the 10 highest peaks *

* # *	* MHz *	* amplitude *	* % *
1	6.64	9.49E+00	100.00
2	11.33	6.73E+00	70.91
3	21.88	6.22E+00	65.56
4	4.69	5.22E+00	54.99
5	10.16	4.82E+00	50.80
6	8.20	4.15E+00	43.74
7	8.98	4.11E+00	43.32
8	16.02	4.00E+00	42.19
9	50.00	3.88E+00	40.91
10	27.73	3.68E+00	38.76

P R O N Y   A N A L Y S I S

* Filename ---> 6810433 * dt =0.010 *

** Window 6 * 30 poles * t = .1 to .7 us **

Pole Pair	Prony Pole damp.	Pole freq(MHz)	Prony real	Residue imag	Residue pole	%
1	-0.75	0.	585.489	0.0000	810.39	100.00

* 29 of 30 poles rejected. *

** Window 4 * 30 poles * t = .08 to .68 us **

Pole Pair	Prony Pole damp.	Pole freq(MHz)	Prony real	Residue imag	Residue pole	%
1	-0.97	0.0	16.813	0.000	17.392	100.000
2	-3.86	0.0	23.350	0.000	6.057	34.825
3	-64.12	0.0	-269.625	-0.125	4.205	24.180
4	-9.29	4.0	-0.589	-54.790	2.064	11.866
5	-5.44	7.0	69.059	0.054	1.554	8.938
6	-16.63	25.8	183.930	2.148	1.127	6.479
7	-14.88	29.3	-45.634	131.681	0.753	4.332
8	-9.10	21.0	3.164	-69.656	0.527	3.034
9	-4.45	11.8	22.236	28.858	0.489	2.812
10	-14.01	35.3	-65.417	27.834	0.320	1.839
11	-63.80	0.0	0.016	0.016	0.000	0.002

* 12 of 30 poles rejected. *

** Window 2 * 30 poles * t = .06 to .66 us **

Pole Pair	Prony damp.	Pole freq(MHz)	Prony real	Residue imag	Residue pole	%
1	-82.35	0.0	-1694.630	-279.731	20.856	100.00
2	-0.92	0.0	17.063	0.000	18.508	88.74
3	-181.36	0.0	2550.250	58.556	14.066	67.44
4	-4.21	0.0	28.719	0.127	6.823	32.71
5	-9.06	4.0	-30.468	-55.271	2.386	11.44
6	-5.42	7.0	49.698	-58.832	1.735	8.32
7	-16.13	26.1	-229.080	95.518	1.506	7.22
8	-15.68	29.5	-85.028	-182.999	1.086	5.21
9	-8.66	21.1	-30.677	75.722	0.615	2.95
10	-4.45	11.8	32.980	-21.830	0.531	2.54
11	-13.80	35.3	-12.237	-87.923	0.399	1.91

* 12 of 30 poles rejected. *

P R O N Y   A N A L Y S I S

* Filename ---> b810433 (continued) * dt =0.010 *

** Window 0 * 30 poles * t = .04 to .64 us **

Pole Pair	Prony damp.	Pole freq(MHz)	Prony real	Residue imag	Residue / pole	%
1	-6.09	0.0	57.822	0.000	9.496	100.00
2	-197.63	0.0	-479.621	0.000	2.427	25.56
3	-5.99	4.8	-24.078	37.811	1.457	15.34
4	-3.97	7.3	-29.988	-37.941	1.050	11.06
5	-13.12	30.1	115.249	-6.380	0.608	6.40
6	-4.38	11.5	1.970	-42.156	0.582	6.13
7	-9.32	26.5	40.614	-80.745	0.543	5.72
8	-8.51	16.8	10.086	-54.924	0.528	5.56
9	-15.33	39.8	50.503	114.008	0.498	5.24

* 14 of 30 poles rejected. *

** Window 0 * 22 poles * t = .04 to .48 us **

Pole Pair	Prony damp.	Pole freq(MHz)	Prony real	Residue imag	Residue / pole	%
1	-12.93	0.0	369.439	0.000	28.580	100.00
2	-243.10	0.0	-2297.940	0.000	9.453	33.07
3	-8.66	0.0	62.580	-0.000	7.225	25.28
4	-19.35	30.6	231.177	-230.101	1.688	5.91
5	-17.76	46.3	373.578	-254.450	1.549	5.42
6	-11.90	16.7	33.903	-102.810	1.025	3.59
7	-11.71	27.0	-30.462	-161.797	0.970	3.39
8	-15.34	41.7	100.750	-197.322	0.844	2.95
9	-15.83	35.9	154.443	-95.043	0.802	2.81
10	-4.68	11.1	31.270	-41.383	0.742	2.60

* 5 of 22 poles rejected. *

** Window 0 * 14 poles * t = .04 to .32 us **

Pole Pair	Prony damp.	Pole freq(MHz)	Prony real	Residue imag	Residue / pole	%
1	-284.75	0	7593.050	0.0000	27.571	100.00
2	-424.23	0	-8128.470	0.0000	19.832	71.93

* 12 of 14 poles rejected. *

PRONY   ANALYSIS

* Filename ---> b810433 (continued) * dt =0.010 *

** Window 0 * 6 poles * t = .04 to .16 us **

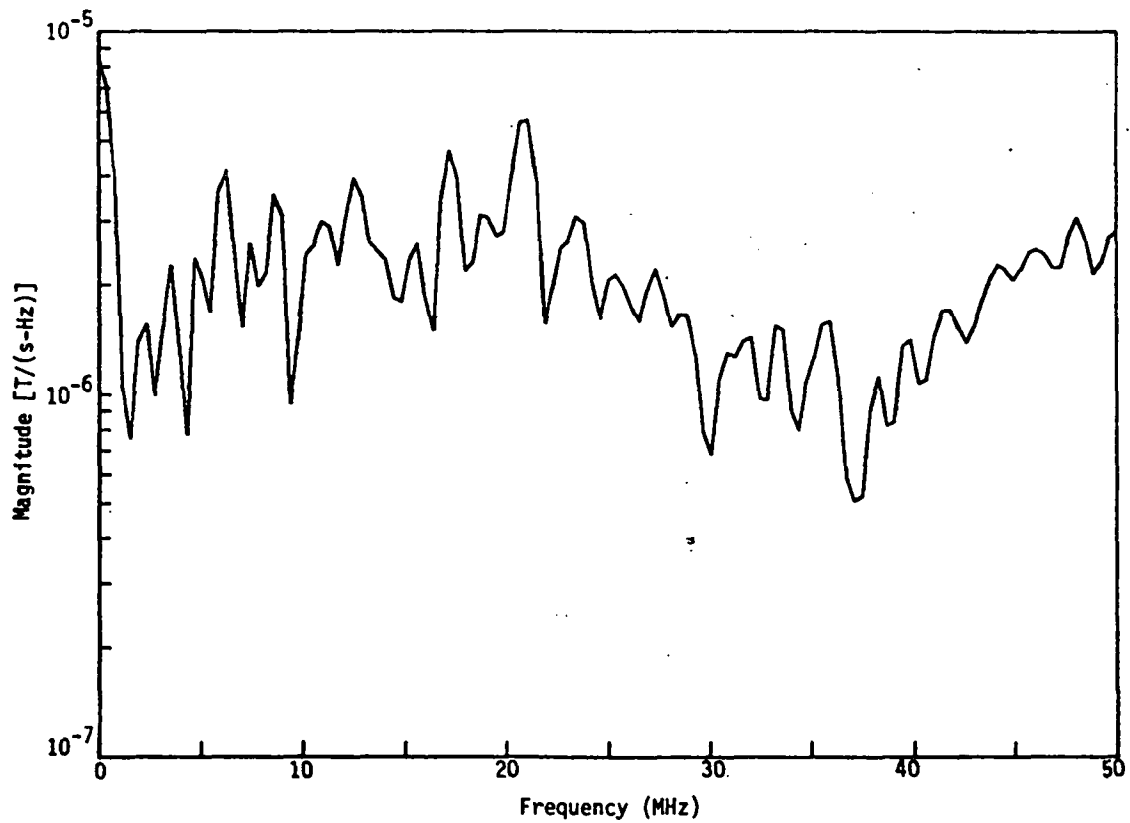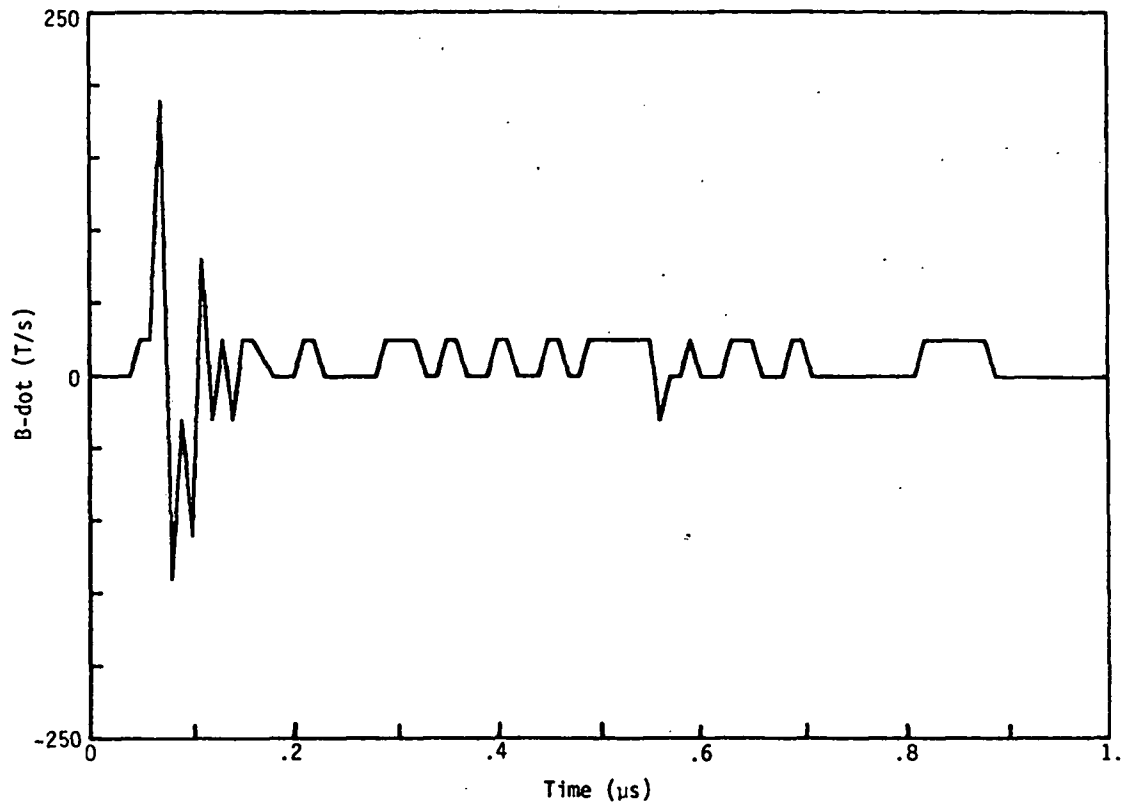| Pole Pair	Prony damp.	Pole freq(MHz)	Prony Residue real	Residue imag	Residue pole	%
1	-18.90	0.0	128.356	-0.000	6.792	100.00
2	-47.35	16.9	72.726	-77.464	0.913	13.44
3	-456.18	0.0	-273.814	-0.000	0.600	8.84

* 2 of 6 poles rejected. *

Figure A22.   Measured B-dot Data (a) and Computed Spectral Response (b)
for Flight 81-043-04.

P E A K   P I C K
* Relative peak height for this run --> .01 *
* Bounds set for this run : 2 to 50 Mhz

FILENAME ---> B810434/FRQ
* Min pt --> 37.11 MHz , 5.03E-01 amplitude

* increasing frequency representation *

* # *	* MHz *	* amplitude *
1	2.34	1.55E+00
2	4.69	2.35E+00
3	6.25	4.11E+00
4	8.59	3.53E+00
5	10.94	2.97E+00
6	12.50	3.92E+00
7	15.63	2.60E+00
8	17.19	4.66E+00
9	18.75	3.09E+00
10	21.09	5.67E+00
11	23.44	3.07E+00
12	25.39	2.13E+00
13	27.34	2.19E+00
14	30.86	1.30E+00
15	33.20	1.54E+00
16	35.94	1.59E+00
17	38.28	1.12E+00
18	39.84	1.41E+00
19	41.80	1.70E+00
20	44.14	2.27E+00
21	46.09	2.51E+00
22	48.05	3.06E+00
23	50.00	2.81E+00

There are 5 additional peaks near these peaks.

* decreasing amplitude representation *
* the 10 highest peaks *

* # *	* MHz *	* amplitude *	* % *
1	21.09	5.67E+00	100.00
2	17.19	4.66E+00	82.05
3	6.25	4.11E+00	72.52
4	12.50	3.92E+00	69.02
5	8.59	3.53E+00	62.21
6	18.75	3.09E+00	54.51
7	23.44	3.07E+00	54.16
8	48.05	3.06E+00	53.92
9	10.94	2.97E+00	52.41
10	50.00	2.81E+00	49.44

P R O N Y   A N A L Y S I S

**   Window 6   *   30 poles   *   t = .1 to .7 us   **

Pole Pair	Prony Pole damp.	Pole freq(MHz)	Prony Residue real	Residue imag	Residue / pole	%
1	-43.15	0.0	-93.294	-0.000	2.162	100.00
2	-28.51	0.0	-10.161	0.000	0.356	16.48
3	-1.49	21.0	-5.047	-6.984	0.065	3.02
4	-3.20	13.3	-3.226	3.912	0.061	2.81
5	-0.41	23.1	1.261	-2.381	0.019	0.86
6	-3.68	36.4	2.453	-3.467	0.019	0.86
7	-2.62	44.4	-1.060	-0.214	0.004	0.18

*   18 of 30 poles rejected.   *

**   Window 4   *   30 poles   *   t = .08 to .68 us   **

Pole Pair	Prony Pole damp.	Pole freq(MHz)	Prony Residue real	Residue imag	Residue / pole	%
1	-0.90	0.0	-1.897	0.000	2.110	100.00
2	-78.63	0.0	-143.243	-0.000	1.822	86.33
3	-36.07	44.4	-8.902	-90.146	0.322	15.27
4	-1.93	21.1	2.556	10.383	0.081	3.82
5	-2.75	13.2	3.719	2.993	0.057	2.72
6	-1.46	22.9	-3.333	2.694	0.030	1.41
7	-7.47	37.1	5.187	-2.019	0.024	1.13
8	-1.76	29.0	3.341	-0.584	0.019	0.88

*   16 of 30 poles rejected.   *

**   Window 2   *   30 poles   *   t = .06 to .66 us   **

Pole Pair	Prony Pole damp.	Pole freq(MHz)	Prony Residue real	Residue imag	Residue / pole	%
1	-56.54	48.0	65.342	-928.214	3.030	100.00
2	-33.58	0.0	-89.536	-0.000	2.666	88.00
3	-30.19	29.2	-17.773	-83.458	0.458	15.13
4	-10.81	22.6	6.640	-32.394	0.232	7.66
5	-4.75	13.0	7.261	-4.594	0.105	3.47
6	-5.55	29.7	-0.060	9.491	0.051	1.68
7	-0.49	36.4	-2.559	0.526	0.011	0.38

*   17 of 30 poles rejected.   *

PRONY   ANALYSIS

* Filename ---> b810434 (continued) *   dt =0.010 *

** Window 0 * 30 poles * t = .04 to .64 us **

Pole Pair	Prony Pole damp. freq(MHz)		Prony Residue real imag		Residue pole	%
1	−25.83	0	−43.072	3.3862	1.673	100.00

* 29 of 30 poles rejected. *

** Window 0 * 22 poles * t = .04 to .48 us **

Pole Pair	Prony Pole damp. freq(MHz)		Prony Residue real imag		Residue pole	%
1	−36.60	46.9	53.9411	−360.178	1.227	100.00
2	−4.88	36.5	−3.9542	−6.341	0.033	2.65

* 18 of 22 poles rejected. *

** Window 0 * 14 poles * t = .04 to .32 us **

Pole Pair	Prony Pole damp. freq(MHz)		Prony Residue real imag		Residue pole	%
1	−33.71	46.6	49.049	−291.852	1.005	100.00
2	−15.10	7.2	34.005	10.943	0.747	74.31
3	−18.41	20.6	−84.615	12.801	0.656	65.24
4	−6.31	36.2	−2.861	−7.093	0.034	3.34

* 6 of 14 poles rejected. *

** Window 0 * 6 poles * t = .04 to .16 us **

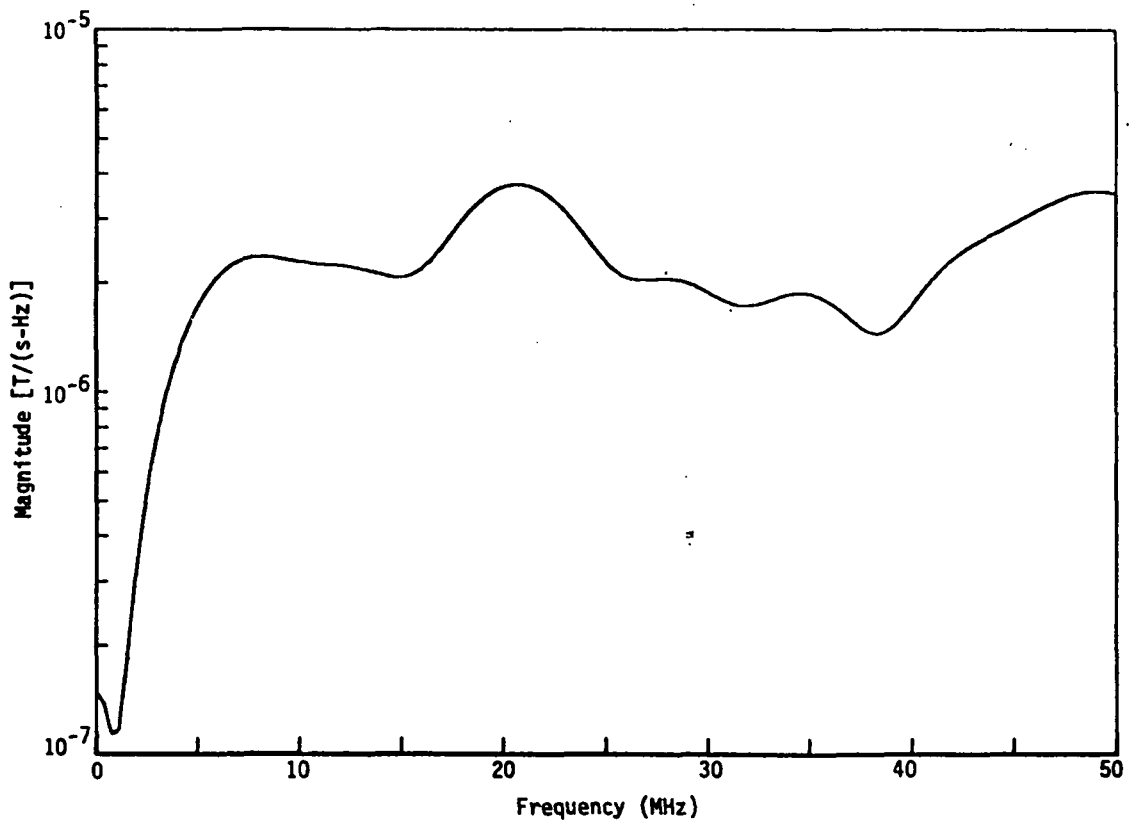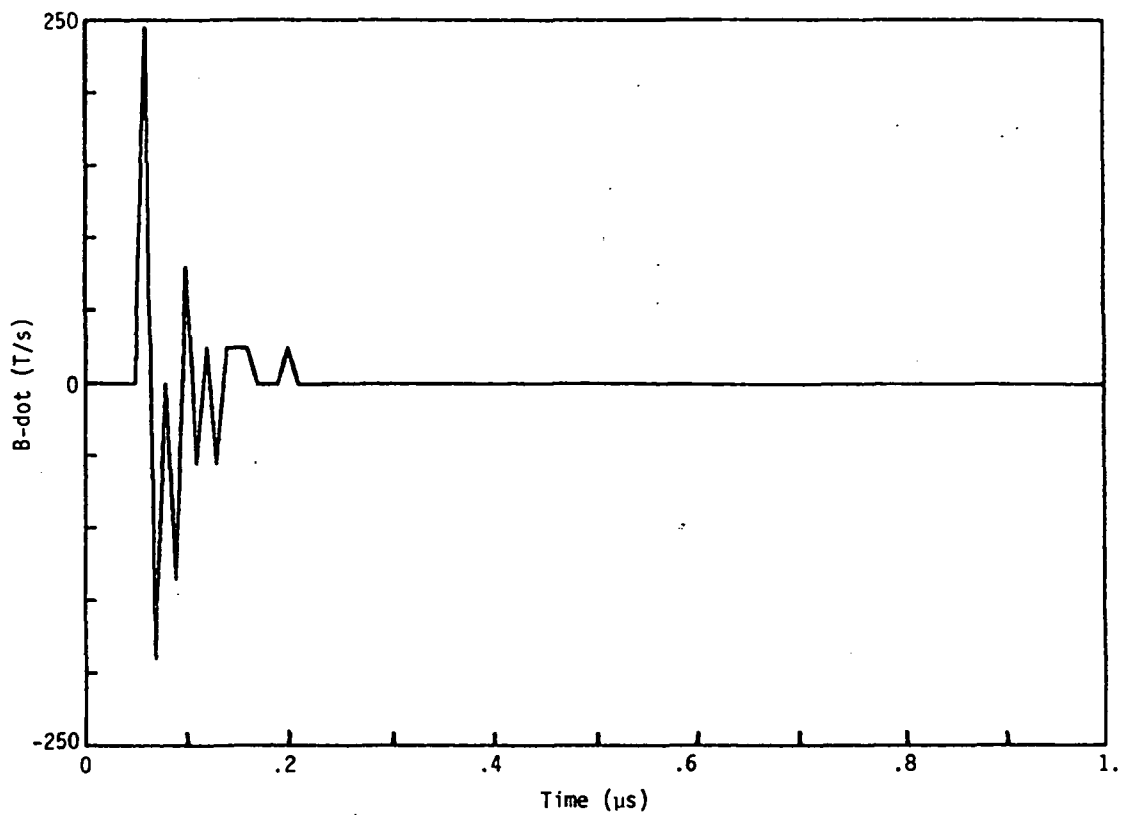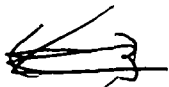| Pole Pair	Prony Pole damp. freq(MHz)		Prony Residue real imag		Residue pole	%
1	−35.96	9.2	127.813	10.646	1.886	100.00
2	−30.12	22.3	−106.793	109.410	1.068	56.63
3	−18.51	46.6	−20.982	−102.200	0.356	18.86

Figure A23.   Measured B-dot Data (a) and Computed Spectral Response (b)
for Flight 81-045-01.

P E A K   P I C K
* Relative peak height for this run --> .01 *
* Bounds set for this run : 0 to 50 Mhz

FILENAME ---> B810451/FRQ
* Min pt -->   0.78 MHz , 1.14E-01 amplitude

* increasing frequency representation *

* # *	* MHz *	* amplitude *
1	0.00	1.50E-01
2	8.20	2.36E+00
3	20.70	3.74E+00
4	27.73	2.05E+00
5	34.38	1.87E+00
6	49.22	3.59E+00
7	50.00	3.53E+00

* decreasing amplitude representation *
* the 10 highest peaks *

* # *	* MHz *	* amplitude *	* % *
1	20.70	3.74E+00	100.00
2	49.22	3.59E+00	95.90
3	50.00	3.53E+00	94.35
4	8.20	2.36E+00	63.10
5	27.73	2.05E+00	54.83
6	34.38	1.87E+00	50.08
7	0.00	1.50E-01	4.01

C-3

P R O N Y   A N A L Y S I S

* Filename ---> b810451 * dt =0.005 *

** Window 0 * 18 poles * t = .04 to .22 us **

Pole Pair	Prony Pole damp. freq(MHz)		Prony Residue real imag		Residue pole	%
1	−30.62	0.0	251.564	0.000	8.216	100.00
2	−30.57	5.0	35.131	225.021	5.175	62.99
3	−241.96	49.5	−329.968	496.717	1.514	18.43
4	−29.17	50.0	179.145	−26.879	0.574	6.98
5	−13.54	20.3	−9.549	−41.386	0.332	4.04
6	−9.06	39.5	0.710	−9.069	0.037	0.45

* 7 of 18 poles rejected. *

** Window 0 * 15 poles * t = .04 to .19 us **

Pole Pair	Prony Pole damp. freq(MHz)		Prony Residue real imag		Residue pole	%
1	−72.48	0.0	−315.569	−0.000	4.354	100.00
2	−26.63	17.8	75.475	−151.952	1.480	33.98
3	−13.71	12.3	−25.331	−53.433	0.753	17.29
4	−15.05	49.3	93.185	−2.786	0.301	6.91

* 8 of 15 poles rejected. *

** Window 0 * 9 poles * t = .04 to .13 us **

Pole Pair	Prony Pole damp. freq(MHz)		Prony Residue real imag		Residue pole	%
1	−15.34	0.0	−53.135	0.000	3.463	100.00
2	−38.98	19.8	−63.410	−159.567	1.318	38.05
3	−13.42	47.8	53.916	16.122	0.187	5.40

* 4 of 9 poles rejected. *

** Window 0 * 6 poles * t = .04 to .1 us **
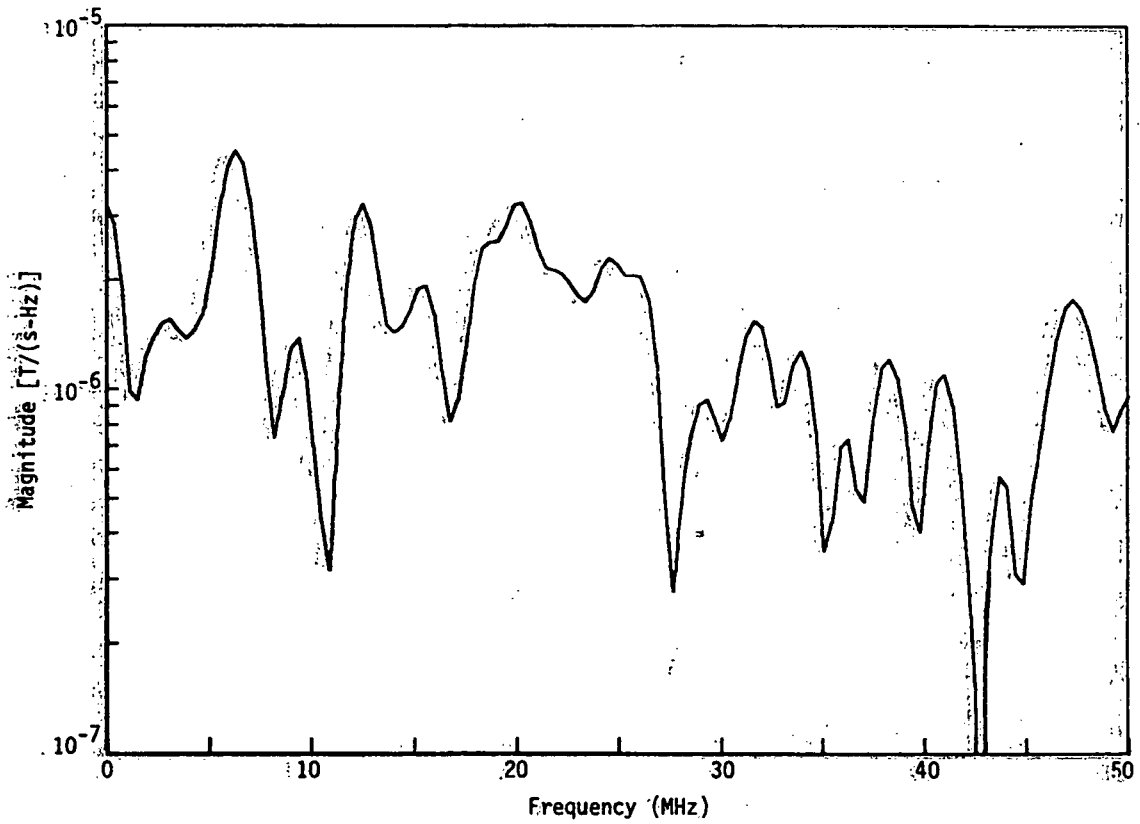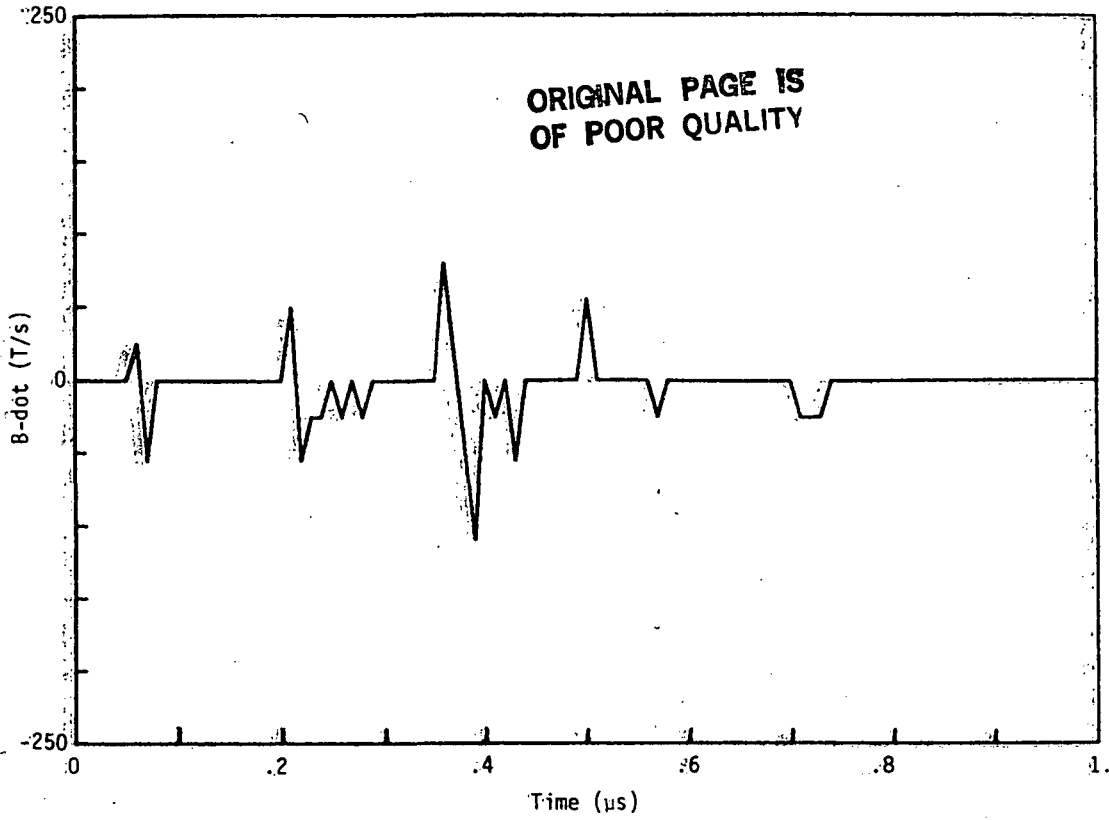* 6 of 6 poles rejected. *

-191-

Figure A24. Measured B-dot Data (a) and Computed Spectral Response (b) for Flight 81-045-02.

P E A K   P I C K
* Relative peak height for this run --> .01 *
* Bounds set for this run : 2 to 50 Mhz

FILENAME ---> B810452/FRQ
* Min pt --> 42.97 MHz , 9.58E-02 amplitude

* increasing frequency representation *

* # *	* MHz *	* amplitude *
1	3.13	1.54E+00
2	6.25	4.50E+00
3	9.38	1.38E+00
4	12.50	3.23E+00
5	15.63	1.91E+00
6	20.31	3.25E+00
7	24.61	2.28E+00
8	25.78	2.04E+00
9	29.30	9.45E-01
10	31.64	1.55E+00
11	33.98	1.28E+00
12	36.33	7.30E-01
13	38.28	1.22E+00
14	41.02	1.10E+00
15	43.75	5.76E-01
16	47.27	1.77E+00
17	50.00	9.63E-01

* decreasing amplitude representation *
* the 10 highest peaks *

* # *	* MHz *	* amplitude *	* % *
1	6.25	4.50E+00	100.00
2	20.31	3.25E+00	72.22
3	12.50	3.23E+00	71.88
4	24.61	2.28E+00	50.62
5	25.78	2.04E+00	45.30
6	15.63	1.91E+00	42.49
7	47.27	1.77E+00	39.38
8	31.64	1.55E+00	34.44
9	3.13	1.54E+00	34.27
10	9.38	1.38E+00	30.77

P R O N Y   A N A L Y S I S

* Filename ---> b810452 * dt =0.010 *

** Window 6 * 30 poles * t = .1 to .7 us **
* 30 of 30 poles rejected. *

** Window 4 * 30 poles * t = .08 to .68 us **
* 30 of 30 poles rejected. *

** Window 2 * 30 poles * t = .06 to .66 us **

Pole Pair	Prony Pole damp. freq(MHz)		Prony Residue real imag		Residue pole	%
1	−2.66	33.3	6.0469	1.4409	0.030	100.00
2	−0.20	40.5	3.3427	2.0873	0.015	52.18

* 26 of 30 poles rejected. *

** Window 0 * 30 poles * t = .04 to .64 us **
* 30 of 30 poles rejected. *

** Window 0 * 22 poles * t = .04 to .48 us **

Pole Pair	Prony Pole damp. freq(MHz)		Prony Residue real imag		Residue pole	%
1	−1.10	12.6	3.549	1.9436	0.051	100.00
2	−1.83	32.3	−7.211	−2.6898	0.038	74.46
3	−6.32	28.2	−5.512	1.6128	0.032	63.63
4	−5.33	40.9	4.850	4.7450	0.026	51.78
5	−2.15	37.3	−1.767	−2.8908	0.014	28.39

* 12 of 22 poles rejected. *

** Window 0 * 14 poles * t = .04 to .32 us **

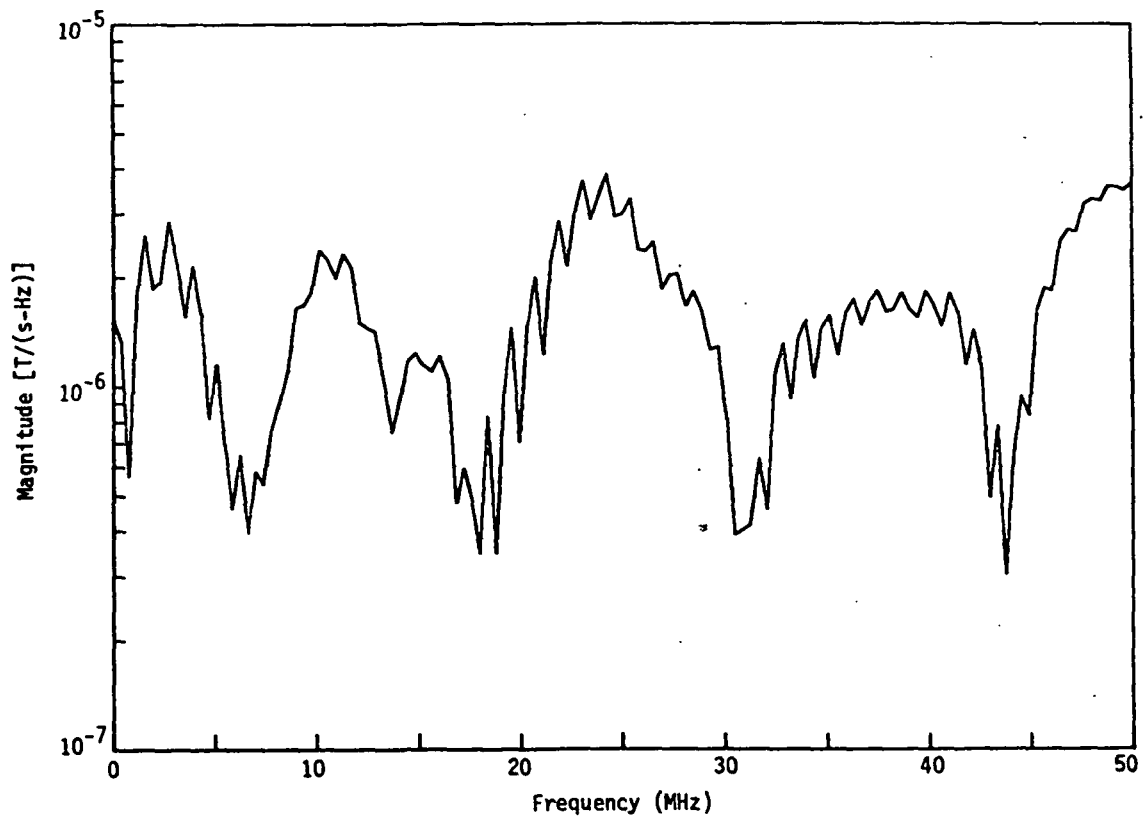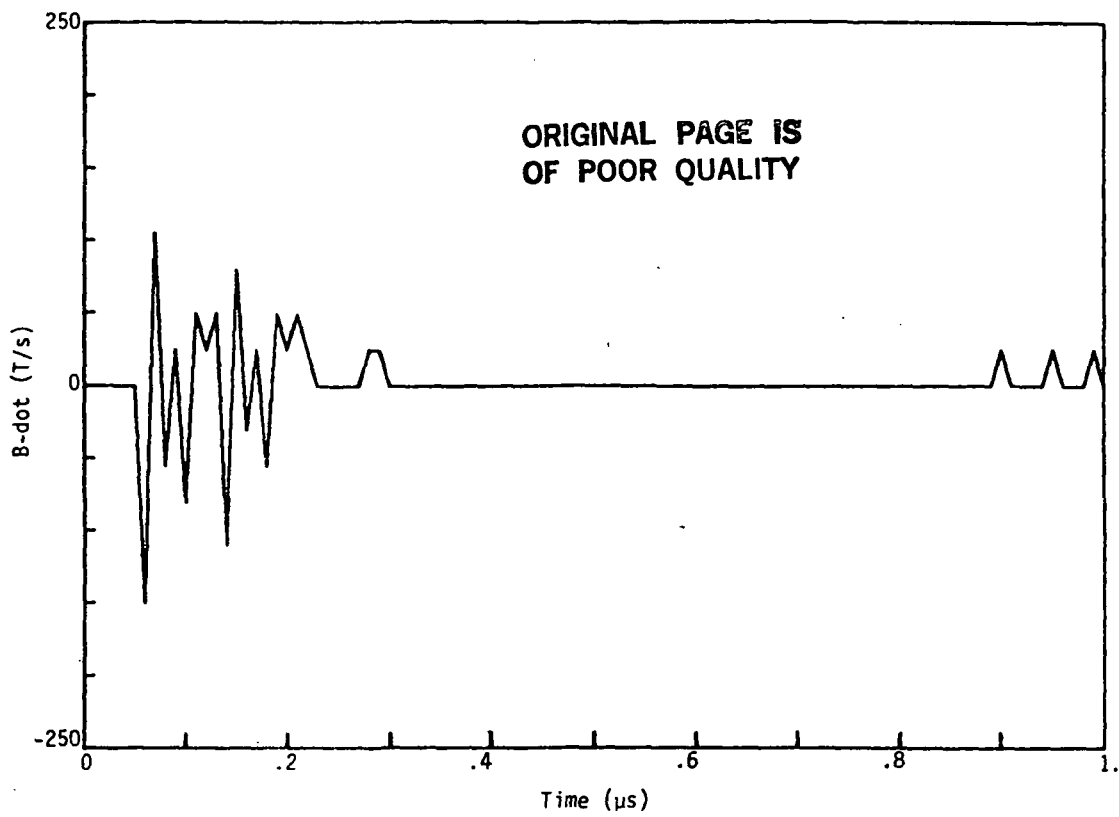| Pole Pair	Prony Pole damp. freq(MHz)		Prony Residue real imag		Residue pole	%
1	−119.54	12.4	342.797	284.383	3.123	100.00
2	−118.41	37.4	−342.797	401.959	2.006	64.24

* 10 of 14 poles rejected. *

Figure A25.   Measured B-dot Data (a) and Computed Spectral Response (b)
for Flight 81-045-03.

P E A K   P I C K
* Relative peak height for this run --> .01 *
* Bounds set for this run : 0 to 50 Mhz

FILENAME ---> B810453/FRQ
* Min pt --> 43.75 MHz , 3.05E-01 amplitude

* increasing frequency representation *

* # *	* MHz *	* amplitude *
1	0.00	1.55E+00
2	2.73	2.86E+00
3	5.08	1.16E+00
4	10.16	2.38E+00
5	14.84	1.24E+00
6	17.19	5.95E-01
7	19.53	1.45E+00
8	21.88	2.87E+00
9	24.22	3.86E+00
10	26.56	2.51E+00
11	29.69	1.29E+00
12	32.81	1.32E+00
13	35.16	1.58E+00
14	37.50	1.84E+00
15	39.84	1.83E+00
16	42.19	1.44E+00
17	44.53	9.41E-01
18	46.88	2.72E+00
19	50.00	3.64E+00

There are 22 additional peaks near these peaks.

* decreasing amplitude representation *
* the 10 highest peaks *

* # *	* MHz *	* amplitude *	* % *
1	24.22	3.86E+00	100.00
2	50.00	3.64E+00	94.33
3	21.88	2.87E+00	74.31
4	2.73	2.86E+00	74.22
5	46.88	2.72E+00	70.39
6	26.56	2.51E+00	65.01
7	10.16	2.38E+00	61.80
8	37.50	1.84E+00	47.73
9	39.84	1.83E+00	47.52
10	35.16	1.58E+00	40.91

ORIGINAL PAGE IS
OF POOR QUALITY
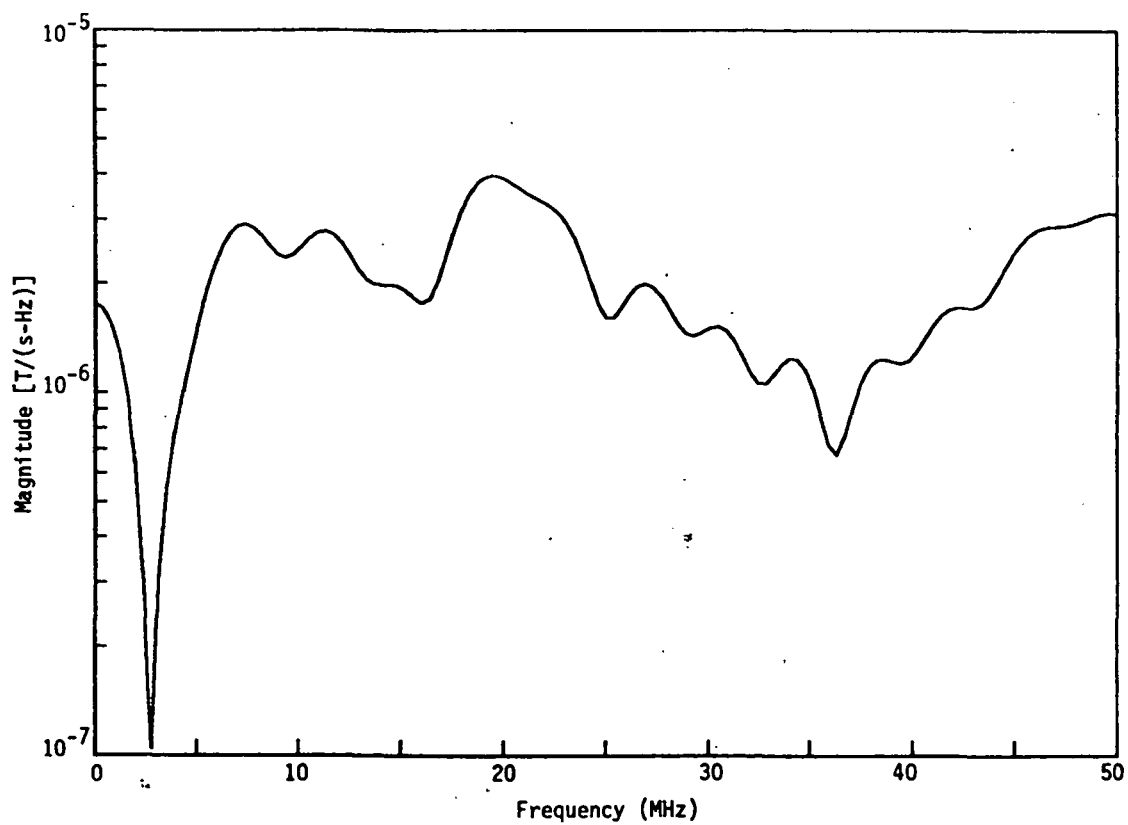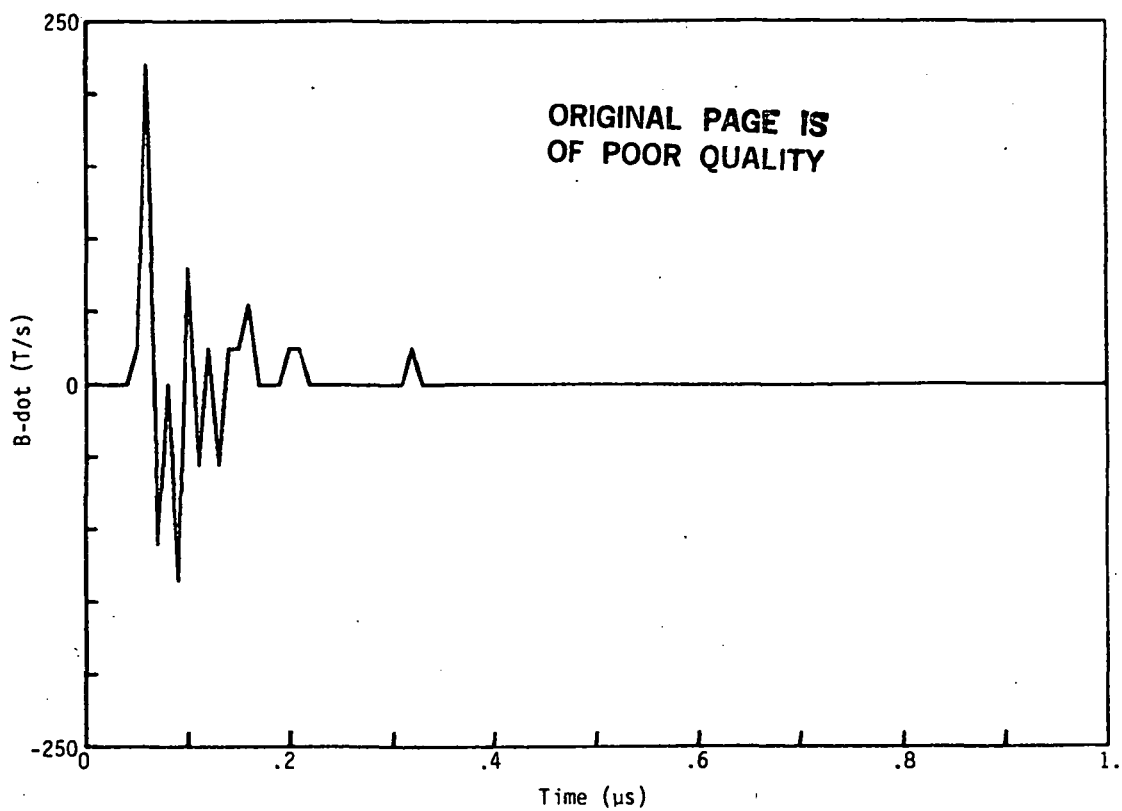
Figure A26. Measured B-dot Data (a) and Computed Spectral Response (b)
for Flight 81-045-04.

P E A K   P I C K
* Relative peak height for this run --> .01   *
* Bounds set for this run : 2 to 50 Mhz

FILENAME   ---> B810454/FRQ
* Min pt --->   2.73 MHz , 1.05E-01 amplitude

* increasing frequency representation *

* # *	* MHz *	* amplitude *
1	7.42	2.91E+00
2	11.33	2.78E+00
3	14.45	1.98E+00
4	19.53	3.97E+00
5	26.95	1.99E+00
6	30.47	1.52E+00
7	33.98	1.25E+00
8	38.67	1.24E+00
9	42.19	1.72E+00
10	49.61	3.13E+00
11	50.00	3.11E+00

* decreasing amplitude representation *
* the 10 highest peaks *

* # *	* MHz *	* amplitude *	* % *
1	19.53	3.97E+00	100.00
2	49.61	3.13E+00	78.70
3	50.00	3.11E+00	78.22
4	7.42	2.91E+00	73.16
5	11.33	2.78E+00	70.10
6	26.95	1.99E+00	50.22
7	14.45	1.98E+00	49.89
8	42.19	1.72E+00	43.23
9	30.47	1.52E+00	38.33
10	33.98	1.25E+00	31.43

P R O N Y   A N A L Y S I S

*   Filename ---> b810454   *   dt =0.005 *

**   Window 0   *   27 poles   *   t = .04 to .31 us   **

Pole Pair	Prony Pole damp. freq(MHz)		Prony Residue real imag		Residue pole	%
1	-9.78	0.0	17.934	1.201	1.838	100.00
2	-18.15	19.9	-38.759	-89.652	0.773	42.05

*   24 of 27 poles rejected.   *

**   Window 0   *   24 poles   *   t = .04 to .28 us   **

Pole Pair	Prony Pole damp. freq(MHz)		Prony Residue real imag		Residue pole	%
1	-30.00	12.5	-37.285	-82.487	1.075	100.00
2	-8.17	4.0	-23.509	12.210	1.004	93.37
3	-14.83	0.0	-9.453	8.224	0.845	78.57
4	-14.24	19.5	-3.529	-62.792	0.510	47.46
5	-21.82	47.3	31.651	60.779	0.230	21.38
6	-8.70	36.7	2.668	-3.586	0.019	1.80

*   13 of 24 poles rejected.   *

1. Report No. NASA CR-172127	2. Government Accession No.	3. Recipient's Catalog No.
4. Title and Subtitle ANALYSIS OF DIRECT AND NEARBY LIGHTNING STRIKE DATA FOR AIRCRAFT		5. Report Date June 1983
		6. Performing Organization Code
7. Author(s) D.V. Giri, R.S. Noss, D.B. Phuoc and F.M. Tesche		8. Performing Organization Report No.
		10. Work Unit No.
9. Performing Organization Name and Address LuTech, Inc. 3516 Breakwater Court Hayward, CA 94545		11. Contract or Grant No. NAS1-16893
		13. Type of Report and Period Covered Contractor Report
12. Sponsoring Agency Name and Address National Aeronautics and Space Administration Washington, DC 20546		
		14. Sponsoring Agency Code

15. Supplementary Notes

Langley Technical Monitor: K.P. Zaepfel
Final Report

16. Abstract

This report discusses a method for interpreting direct strike and nearby strike lightning data on aircraft. The theoretical basis for the interpretation involves a transmission line model for the aircraft, and is discussed in Section II. Results of applying this model to the F-106 aircraft are presented in Section III where the natural resonances are computed for several different electrical representations of the aircraft. In Section IV, the signal processing techniques useful for extracting pole (resonance) information from experimental data are discussed, and the use of these techniques on the measured lightning data is illustrated. Finally, in Section V, the results of a related ground-based lightning experiment are discussed and data are presented. The purpose of this test was to gain additional understanding of the resonance properties of the F-106 aircraft.

17. Key Words (Suggested by Author(s)) Lightning Data Prony analysis Stick model of aircraft Data analysis	18. Distribution Statement

19. Security Classif. (of this report) Unclassified	20. Security Classif. (of this page) Unclassified	21. No. of Pages 204	22. Price